BEILSTEIN JOURNAL OF ORGANIC CHEMISTRY

N-Heterocyclic carbenes

Edited by Steven P. Nolan

Imprint

Beilstein Journal of Organic Chemistry
www.bjoc.org
ISSN 1860-5397
Email: journals-support@beilstein-institut.de

The *Beilstein Journal of Organic Chemistry* is published by the Beilstein-Institut zur Förderung der Chemischen Wissenschaften.

Beilstein-Institut zur Förderung der Chemischen Wissenschaften
Trakehner Straße 7–9
60487 Frankfurt am Main
Germany
www.beilstein-institut.de

BEILSTEIN JOURNAL OF ORGANIC CHEMISTRY

N-Heterocyclic carbenes

Steven P. Nolan

Editorial

Open Access

Address:
Chemistry Department, College of Science, King Saud University, Riyadh 11451, Saudi Arabia

Email:
Steven P. Nolan - stevenpnolan@gmail.com

Beilstein J. Org. Chem. **2015,** *11,* 2474–2475.
doi:10.3762/bjoc.11.268

Received: 12 November 2015
Accepted: 19 November 2015
Published: 07 December 2015

This article is part of the Thematic Series "N-Heterocyclic carbenes".

Guest Editor: S. P. Nolan

The N-heterocyclic carbenes (NHC) now hold a preferred-ligand status in organic and organometallic chemistry. Their role in catalysis continues to grow. When the editorial staff at the Beilstein Journal of Organic Chemistry contacted me to act as a guest editor for the thematic series “N-Heterocyclic carbenes”, I was more than happy to accept what appeared to me to be a simple and exciting endeavor. Indeed, the job was made simple as the number of research groups focusing on this topic continues to grow and today the literature is flooded with one use or another of these fascinating, stabilizing ligands.

To state here what a great influence these ligands have had on modern synthetic chemistry in providing unique catalytic tools (but also in view of their stabilizing effects due to their steric and electronic tunable properties) might be unnecessary. The use of these ligands now extends to numerous fields spanning from fine chemicals to polymer synthesis. The area of main group chemistry has also benefited from these ligands as stabilizing entities.

Since the seminal work of Bertrand [1] and Arduengo [2] (and mostly post-1994–1995) the field has underwent fantastic advances. Carbenes such as 1,3-dimesityl-1,3-dihydro-2*H*-imidazol-2-ylidene (IMes) and the 2,6-diisopropylphenyl analogue (IPr) have become commonplace, replacing tertiary phosphanes as modifying ligands on metals.

The field continues to experience tremendous development, with a considerable number of publications still reporting new reactions that are catalyzed and controlled by the carbenes as ligands or as organocatalysts. The action of state-of-the-art catalysts are nowadays better understood through detailed mechanistic work, which permits the design of ever-better performing catalytic systems. This design/mechanistic study/redesign cycle will ensure the continued evolution of the field. The area of NHC-based research is a worldwide effort, as exemplified by contributions in this NHC-focused Thematic Series.

This compendium again highlights the diversity of fields that are affected and enhanced by NHCs. It is my hope that such a collection of contributions will inspire readers in novel and exciting directions. I never tire of being amazed at the ingenuity of researchers in using these entities as building blocks for progress.

Steven P. Nolan

Riyadh, November 2015

References

1. Igau, A.; Baceiredo, A.; Trinquier, G.; Betrand, G. *Angew. Chem., Int. Ed. Engl.* **1989,** *28,* 621–622. doi:10.1002/anie.198906211
2. Arduengo, A. J., III; Harlow, R. L.; Kline, M. *J. Am. Chem. Soc.* **1991,** *113,* 361–363. doi:10.1021/ja00001a054

License and Terms

BEILSTEIN JOURNAL OF ORGANIC CHEMISTRY

Synthesis and structures of ruthenium–NHC complexes and their catalysis in hydrogen transfer reaction

Chao Chen[1], Chunxin Lu[2], Qing Zheng[1], Shengliang Ni*[1], Min Zhang[3] and Wanzhi Chen*[3]

Full Research Paper

Open Access

Address:
[1]College of Life Sciences, Huzhou University, Huzhou 313000, China, [2]College of Biological, Chemical Sciences and Engineering, Jiaxing University, Jiaxing 314001, China and [3]Department of Chemistry, Zhejiang University, Hangzhou 310007, China

Email:
Shengliang Ni* - shengliangni@163.com;
Wanzhi Chen* - chenwzz@zju.edu.cn

* Corresponding author

Keywords:
N-heterocyclic carbene; ruthenium; transfer hydrogenation

Beilstein J. Org. Chem. **2015,** *11,* 1786–1795.
doi:10.3762/bjoc.11.194

Received: 04 July 2015
Accepted: 09 September 2015
Published: 30 September 2015

This article is part of the Thematic Series "N-Heterocyclic carbenes".

Guest Editor: S. P. Nolan

Abstract

Ruthenium complexes $[Ru(L1)_2(CH_3CN)_2](PF_6)_2$ (**1**), $[RuL1(CH_3CN)_4](PF_6)_2$ (**2**) and $[RuL2(CH_3CN)_3](PF_6)_2$ (**3**) (L1= 3-methyl-1-(pyrimidine-2-yl)imidazolylidene, L2 = 1,3-bis(pyridin-2-ylmethyl)benzimidazolylidene) were obtained through a transmetallation reaction of the corresponding nickel–NHC complexes with $[Ru(p\text{-cymene})_2Cl_2]_2$ in refluxing acetonitrile solution. The crystal structures of three complexes determined by X-ray analyses show that the central Ru(II) atoms are coordinated by pyrimidine- or pyridine-functionalized N-heterocyclic carbene and acetonitrile ligands displaying the typical octahedral geometry. The reaction of $[RuL1(CH_3CN)_4](PF_6)_2$ with triphenylphosphine and 1,10-phenanthroline resulted in the substitution of one and two coordinated acetonitrile ligands and afforded $[RuL1(PPh_3)(CH_3CN)_3](PF_6)_2$ (**4**) and $[RuL1(phen)(CH_3CN)_2](PF_6)_2$ (**5**), respectively. The molecular structures of the complexes **4** and **5** were also studied by X-ray diffraction analysis. These ruthenium complexes have proven to be efficient catalysts for transfer hydrogenation of various ketones.

Introduction

N-Heterocyclic carbenes (NHCs) have been recognized as a class of strong donating ligands which can stabilize various metal complexes of catalytic importance. Transition metal complexes bearing NHCs are more stable to air, moisture, heat, and tolerant toward oxidation compared to phosphine ligands [1-7]. Among NHCs, functionalized NHC ligands have been extensively studied in recent years because of their intriguing structural diversities and potential applications in coordination chemistry and homogenous catalysis. NHC ligands containing additional phosphine, nitrogen, oxygen, and sulfur donating groups [8-16] have been reported.

In the family of metal complexes supported by functionalized NHCs, ruthenium complexes have long been a research focus

on various applications such as catalysis and photochemistry [17-26]. However, the majority of such ruthenium complexes often contain coordinated aromatic carbocycles [27-29]. In contrast, only a few examples Ru(II) complexes of functionalized NHCs containing easily dissociating acetonitrile ligands have been studied [30-32]. We have reported the synthesis of some pyridine- and phenanthrolin-functionalized Ru(II)–NHC complexes containing acetonitrile ligands [33,34]. The most notable example is the acetonitrile-coordinated dinuclear Ru(II)–NHC complex derived from 3,6-bis(*N*-(pyridylmethyl)imidazolylidenyl)pyridazine, which is a very efficient catalyst for the oxidation of alkenes [35]. In continuation of our studies on functionalized Ru(II)–NHC complexes containing acetonitrile ligands, we herein report the synthesis and characterization of three pyrimidine- and pyridine-functionalized NHC–ruthenium complexes containing two, four, and three acetonitrile ligands, respectively. These complexes show good catalytic activity in the transfer hydrogenation of ketones. The reaction of acetonitrile-coordinated Ru–NHC complex **2** with other donors such as triphenylphosphine and 1,10-phenanthroline was also studied.

Results and Discussion

Synthesis and characterization of $[Ru(L1)_2(CH_3CN)_2](PF_6)_2$ (**1**), $[RuL1(CH_3CN)_4](PF_6)_2$ (**2**) and $[RuL2(CH_3CN)_3](PF_6)_2$ (**3**)

The ruthenium–NHC complexes **1** and **2** were synthesized by using the corresponding nickel–NHC complexes as the carbene transfer agent [36]. The reaction of imidazolium salt $HL1(PF_6)$ (L1 = 3-methyl-1-(pyrimidine-2-yl)imidazolylidene) with Raney nickel afforded the nickel–NHC complexes which were not isolated [30]. The subsequent reaction of the generated nickel–NHC complexes with a quarter equivalent of $[Ru(p\text{-cymene})Cl_2]_2$ in refluxing acetonitrile solution afforded bis-NHC complex $[Ru(L1)_2(CH_3CN)_2](PF_6)_2$ (**1**) in a yield of 76% (Scheme 1). When a half equivalent of $[Ru(p\text{-cymene})Cl_2]_2$ and an excess of NH_4PF_6 were employed under the same conditions, the reaction afforded the mono-NHC complex $[RuL1(CH_3CN)_4](PF_6)_2$ (**2**) in 53% yield. It is worth noting that most of the structurally characterized acetonitrile complexes are obtained through the reaction of halides with silver complexes ($AgPF_6$ or $AgBF_4$) in acetonitrile solution [20]. The reaction in refluxing acetonitrile is more convenient than the above mentioned procedure. The formulations of complexes **1** and **2** were first characterized by NMR measurements and further confirmed by elemental analysis and X-ray diffraction. In the ^{1}H NMR spectra of complexes **1** and **2**, disappearance of the resonances assigned to the imidazolium acidic CH and *p*-cymene protons were observed. The acetonitrile protons of complex **1** were found at 2.41 ppm as a singlet. However, the protons of acetonitrile ligands of complex **2** were found at 2.52, 2.12, and 1.96 ppm as three singlets. This illustrates that the three acetonitrile ligands in complex **2** are magnetic unequivalent. The ^{13}C NMR spectra of **1** and **2** exhibit resonance signals at 193.1 and 193.0 ppm ascribed to the carbenic carbons.

The ruthenium–NHC complexes **1** and **2** are stable in air and under light irradiation. Single crystals suitable for X-ray diffraction could be obtained by slow diffusion of Et_2O into CH_3CN solutions and the detailed structure of **1** is depicted in Figure 1. In complex **1**, the central ruthenium ion is hexacoordinated by two bidentate NHC ligands and two acetonitrile ligands in an

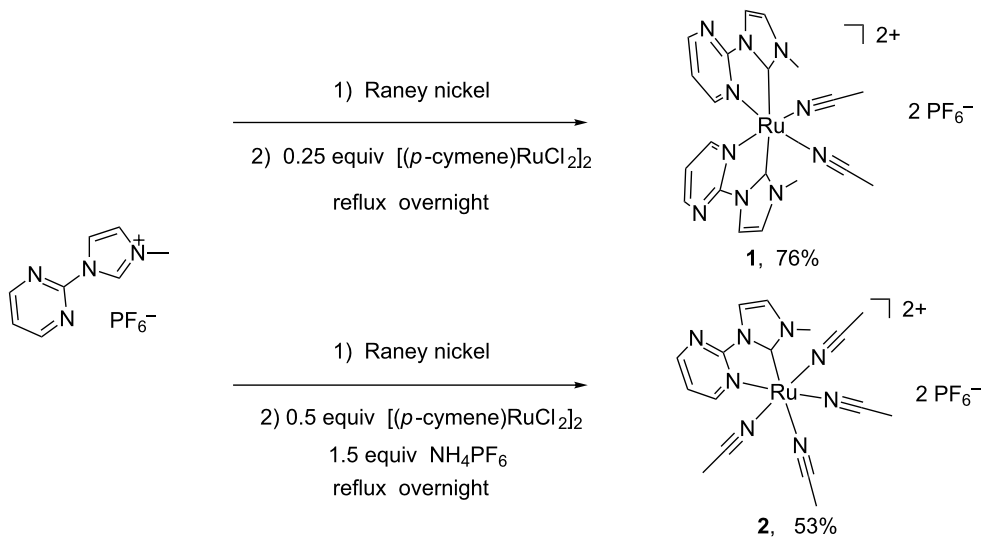

Scheme 1: Synthesis of complexes **1** and **2**.

octahedral geometry. One NHC ligand, one acetonitrile ligand and one carbon atom of the other NHC ligand occupy the equatorial plane in which two carbon atoms of two NHC ligands are mutually *trans*-arranged. The remaining acetonitrile ligand and one nitrogen atom of the NHC ligand lie on the axial positions. The angles (N–Ru–N) of adjacent nitrogen atoms and Ru(II) ion are in the range of 83.9 to 94.0°. The Ru–C distance (2.066 Å) is consistent with the reported values in known Ru–NHC complexes [17-29]. The Ru–$N_{pyrimidine}$ distance (2.081 Å) is slightly longer than Ru–$N_{acetonitrile}$ (2.033 Å).

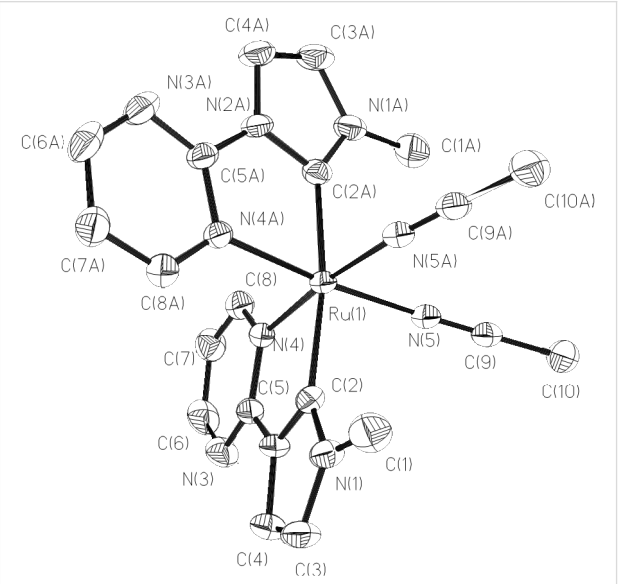

Figure 1: Structural view of **1** showing 30% thermal ellipsoids. All hydrogen atoms and PF_6^- were omitted for clarity. Selected bond lengths (Å) and angles (deg): Ru(1)–N(5) 2.033(4), Ru(1)–C(2) 2.066(5), Ru(1)–N(4) 2.081(4), N(5)#1–Ru(1)–N(5) 83.9(2), N(5)–Ru(1)–C(2) 87.87(16), C(2)#1–Ru(1)–C(2) 171.2(3), N(5)–Ru(1)–N(4) 91.12(16), C(2)#1–Ru(1)–N(4) 95.88(17), N(5)–Ru(1)–N(4)#1 174.20(14). Symmetry code: #1 −x, y, −z+1/2.

The cationic structure of **2** is shown in Figure 2. The central Ru(II) ion is surrounded by one pyrimidine-functionalized NHC ligand and four acetonitrile ligands also in a typical octahedral geometry. The Ru ion lies on a twofold axis. The bidentate NHC ligand and two *cis*-arranged acetonitrile molecules form a $Ru(L1)(CH_3CN)_2$ plane, whereas the other two acetonitrile molecules occupy the axial positions. The bond length of Ru–C_{NHC} is 1.989 Å, which is slightly shorter than those found in Ru–NHC complexes [12-18] and in complex **1**. The bond distance of Ru–$N_{acetonitrile}$ (2.113 Å) at the *trans*-position of the carbene ligand is longer than the other three Ru–$N_{acetonitrile}$ bonds (2.023–2.033 Å) and the Ru–$N_{pyrimidine}$ (2.064 Å).

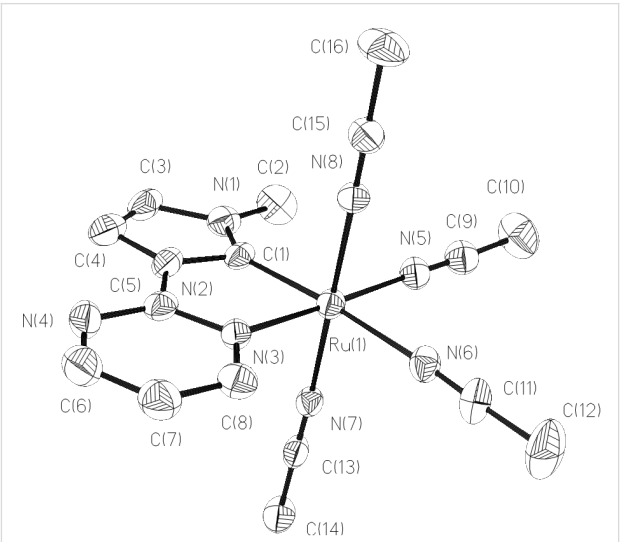

Figure 2: Structural view of **2** showing 30% thermal ellipsoids. All hydrogen atoms and PF_6^- were omitted for clarity. Selected bond lengths (Å) and angles (deg): Ru(1)–C(2) 1.989(7), Ru(1)–N(5) 2.023(5), Ru(1)–N(8) 2.027(5), Ru(1)–N(7) 2.033(6), Ru(1)–N(4) 2.064(5), Ru(1)–N(6) 2.113(6), C(2)–Ru(1)–N(5) 88.3(2), C(2)–Ru(1)–N(8) 91.2(2), N(5)–Ru(1)–N(8) 179.3(2), C(2)–Ru(1)–N(7) 99.8(3).

Similarly, the reaction of the in situ generated nickel–NHC complex from imidazolium salt HL2(PF_6) (L2 = 1,3-bis(pyridin-2-ylmethyl)benzimidazolylidene) with a half equivalent of [Ru(*p*-cymene)Cl_2]$_2$ and an excess of NH_4PF_6 in a refluxing acetonitrile solution afforded the tri-acetonitrile coordinated Ru(II)–NHC complex [RuL2$(CH_3CN)_3$]$(PF_6)_2$ (**3**) in a yield of 61% (Scheme 2). The formation of **3** was also confirmed by the ^{1}H NMR and ^{13}C NMR spectra. The ^{1}H NMR spectrum of **3** shows characteristic resonance signals due to the

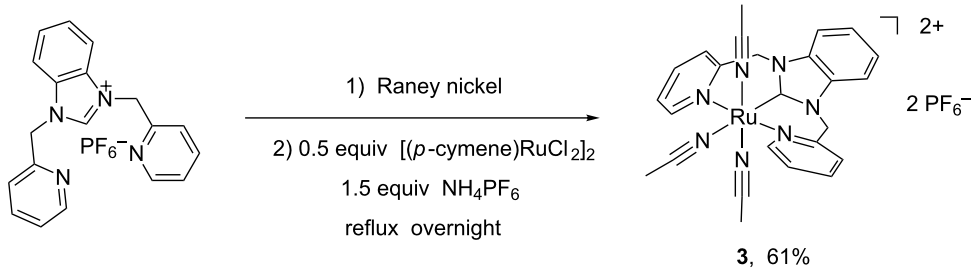

Scheme 2: Synthesis of **3**.

pyridyl, methylene, benzimidazolylidene and acetonitrile groups. The absence of a benzimidazole acidic C2-H proton illustrates the formation of the Ru–C bond. The acetonitrile protons appear at 2.35 and 2.08 ppm as two singlets. The ^{13}C NMR spectrum of **3** exhibits a resonance peak at 190 ppm, which is ascribed to the carbenic carbon atom. Complex **3** has been further identified by X-ray crystallography and the cationic structure of molecular **3** is depicted in Figure 3. The ruthenium ion is coordinated by a tridentate pincer NHC ligand and three acetonitrile ligands also in an octahedral geometry. The symmetrical pincer-type NCN ligand and an acetonitrile ligand occupy the equatorial plane and the remaining two acetonitrile ligands are located at the axial positions. The N–Ru–N angles of the three acetonitrile ligands and the Ru(II) ion are 86.03, 89.12 and 174.99°, respectively. Similar to complex **2**, the bond distance of Ru–$N_{acetonitrile}$ (2.130 Å) at the *trans*-position of the carbene ligand is slightly longer than the other bond distances of Ru–$N_{acetonitrile}$ (2.030 and 2.028 Å) and the Ru–C (1.947 Å) is shorter than that of many known Ru–$C_{carbene}$ distances [17-29].

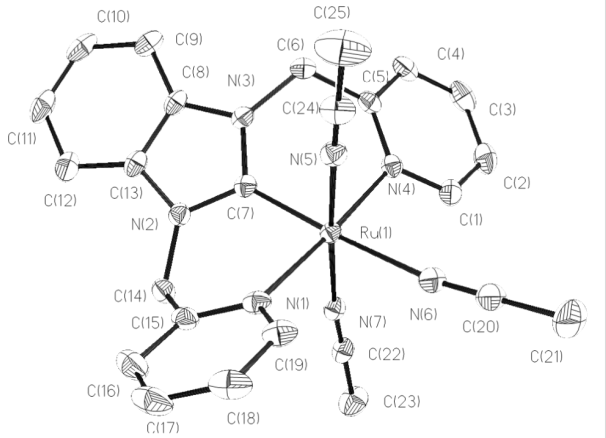

Figure 3: Structural view of **3** showing 50% thermal ellipsoids. All hydrogen atoms and PF_6^- were omitted for clarity. Selected bond lengths (Å) and angles (deg): Ru(1)–C(7) 1.947(3), Ru(1)–N(7) 2.028(2), Ru(1)–N(5) 2.030(2), Ru(1)–N(4) 2.104(2), Ru(1)–N(1) 2.105(2), Ru(1)–N(6) 2.130(2), C(7)–Ru(1)–N(7) 94.33(10), C(7)–Ru(1)–N(5) 90.55(10), N(7)–Ru(1)–N(5) 174.99(9), C(7)–Ru(1)–N(4) 87.72(10).

Catalytic transfer hydrogenation reaction

Ruthenium–NHC complexes are known to be efficient catalysts for transfer hydrogenation reactions [23,37-39]. The ruthenium–NHC complexes presented above are stabilized by strong Ru–carbene bonds and contain 2–4 easily dissociating acetonitrile molecules, and are thus ideal catalysts. We tested their catalytic activities for transfer hydrogenation of ketones. Firstly, acetophenone was selected as the model substrate to evaluate the catalytic activities of complexes **1**–**3**. The standard experiment was carried out at 80 °C with varied Ru loadings from 1 to 0.01 mol % and the results are summarized in Table 1. The reaction profiles show that acetophenone could be reduced to 1-phenylethanol in 89–99% yield within 0.5 h using

Table 1: Catalytic activities of **1**–**3** in transfer hydrogenation of acetophenone.[a]

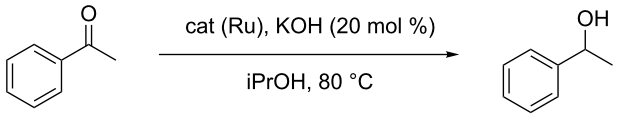

Entry	Catalyst	Catalyst (mol %)	Time (h)	Yield (%)[b]	TON/TOF (h^{-1})
1	**1**	1	0.5	89	89/172
2		0.1	0.5	79	790/1580
3		0.1	1	92	920/920
4		0.01	3	90	9000/3000
5	**2**	1	0.5	99	99/198
6		0.1	0.5	86	860/1720
7		0.1	1	99	990/990
8		0.01	3	97	9700/3233
9	**3**	1	0.5	99	99/198
10		0.1	0.5	89	890/1780
11		0.1	1	99	990/990
12		0.01	3	96	9600/3200

[a]Conditions: acetophenone (1.00 mmol), KOH (20 mol %), and catalyst (1–0.01 mol %) in 3 mL of iPrOH at 80 °C. [b]The yields of products were detected by GC.

1 mol % of the Ru catalysts (Table 1, entries 1, 5 and 9). When the amount of catalysts is decreased to 0.1 mol %, the corresponding conversion still reached 79–89% (Table 1, entries 2, 6 and 10). 1-Phenylethanol could also be obtained in excellent yields using 0.1 mol % and 0.01 mol % Ru catalysts when the reaction time was extended to 1 and 3 h, respectively (Table 1, entries 3, 7, 11 and 4, 8, 12). At catalyst loadings of 0.01 mol %, TOF of **1**–**3** are 3000, 3233, and 3200 h^{-1} for transfer hydrogenation of acetophenone which are nearly identical to that of $[Ru(^{Me}CC^{meth})_2(CH_3CN)_2](BF_4)_2$ ($^{Me}CC^{meth}$ = 1,1'-dimethyl-3,3'-methylene-diimidazol-2,2'-diylidene) [40]. Ruthenium picolyl–NHC complex $[(\eta^5\text{-}C_5Me_5)\text{-}Ru(L)(CH_3CN)][PF_6]$ (L = 3-methyl-1-(2-picolyl)imidazol-2-ylidene) is so far one of the most efficient catalyst for transfer hydrogenation of acetophenone which gave 1-phenylethanol in a conversion of 93% with a catalyst loading of 0.1 mol % [20,41]. When the same amount of complexes **1**–**3** was used, the reaction gave 1-phenylethanol in 89%, 99% and 99% yields, respectively. These data illustrate that complexes **1**–**3** are all quite active catalysts for transfer hydrogenation reactions. It seems that complexes **2** and **3** are a bit better than **1** for this transformation. The *trans*-effect of carbene ligand may promote the substitution of *trans*-positioned acetonitrile ligand by other substrates in the catalytic reaction.

Since complexes **2** and **3** are found to be the efficient catalysts for transfer hydrogenation of acetophenone, we further explored their catalytic potential in the reduction of other aromatic and aliphatic ketones. The reaction conditions are similar as those described in the transfer hydrogenation of acetophenone and 0.1 mol % of Ru catalyst is utilized. The obtained results are given in Table 2. Complexes **2** and **3** are found to be very active in transfer hydrogenation of cyclohexanone, and cyclohexanol are almost quantitatively yielded within 0.5 h (Table 2, entries 1 and 2). The catalyst systems are also found to be good for the reduction of aromatic ketones bearing electron-withdrawing substituents (Table 2, entries 3–8) and electron-donating groups (Table 2, entries 9 and 10), and the target product could be obtained in excellent yields (90–99%). Bulkier aromatic ketone benzophenone is also tested in this reaction with 92% and 94% conversion after 3 h (Table 2, entries 11 and 12). In addition, it is worth mentioning that the two ruthenium complexes exhibited a high tolerance towards sulfur species, 2-acetylthiophene is efficiently hydrogenated (Table 2, entries 13 and 14) with an increased reaction time of 3 h.

Table 2: Transfer hydrogenation using complexes **2** and **3**.[a]

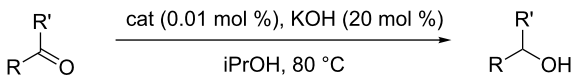

Entry	Substrate	Catalyst	Time (h)	Yield (%)[b]
1	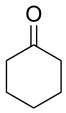	2	0.5	99
2		3	0.5	99
3	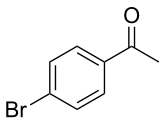	2	1	99
4		3	1	98
5	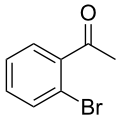	2	1	99
6		3	1	97
7	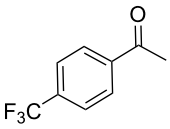	2	1	96
8		3	1	90
9	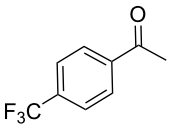	2	1	93
10		3	1	92
11	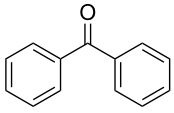	2	3	92
12		3	3	94
13	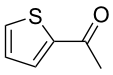	2	3	83
14		3	3	80

[a]Conditions: substrate (1.00 mmol), KOH (20 mol %), catalyst (0.1 mol %) in 3 mL of iPrOH at 80 °C. [b]The yields of products were detected by GC.

Reactions of tetra-acetonitrile Ru(II)–NHC complex **2** with triphenylphosphine and 1,10-phenanthroline

The coordinated acetonitrile ligands could be easily replaced by various *N*- and *P*-donors [22]. The reactions of the acetonitrile-coordinated Ru–NHC complexes with other ligands were studied. The reaction of complex **2** with an excess of triphenylphosphine and 1,10-phenanthroline in heat acetonitrile solution afforded **4** and **5**, respectively. Even excess triphenylphosphine and 1,10-phenanthroline were used, only one and two coordinated acetonitrile ligands were substituted in complexes **4** and **5**. Crystallization by slow diffusion of diethyl ether into their acetonitrile solutions gave **4** as a yellow solid in 40% yield and **5** as an orange yellow solid in 63% yield (Scheme 3). The yields of complexes **4** and **5** are relatively lower than complexes **1**–**3**, but

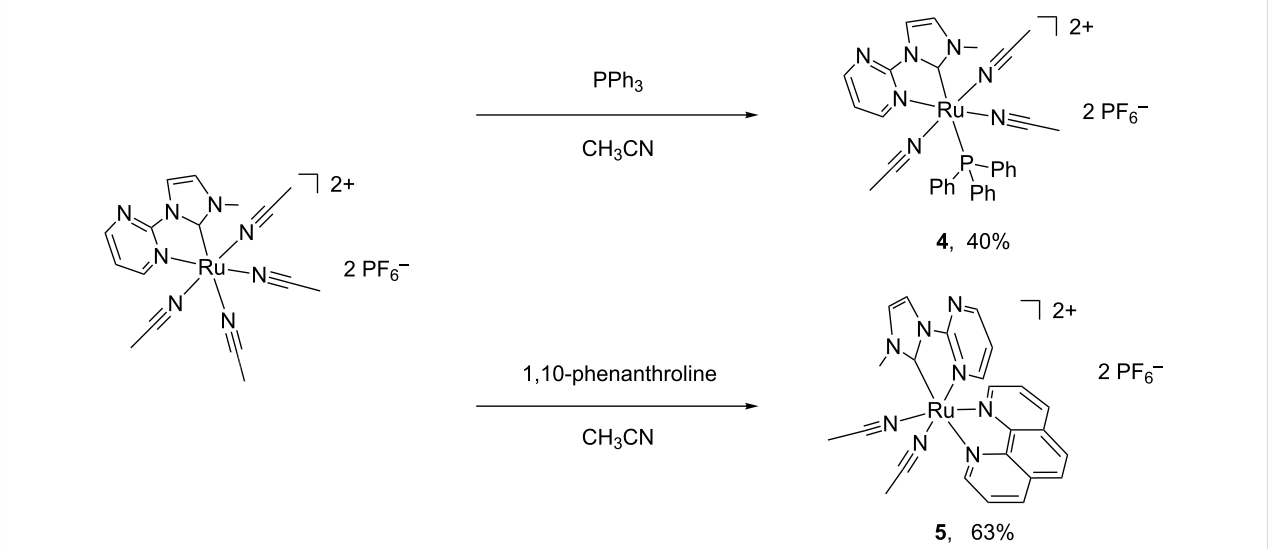

Scheme 3: Synthesis of complexes **4** and **5**.

still in the normal range as compared with the similar reaction [33]. In the ^{1}H NMR of **4**, singlets at 2.14 and 2.07 ppm are ascribed to three CH_3CN ligands, and the rest peaks are belonged to NHC and triphenylphosphine ligand. ^{1}H NMR investigation of **5** suggests that complex **5** contains one NHC ligand, one phenanthroline ligand and two acetonitrile ligands. The CH_3CN protons of **5** are founded at 2.53 and 2.28 ppm. In the ^{13}C NMR, the carbene carbons of complexes **4** and **5** are found at 190 and 200 ppm, respectively.

The structures of **4** and **5** determined by X-ray diffraction analysis are shown in Figure 4 and Figure 5. In the cationic structure of **4**, the acetonitrile ligand at the *trans*-position of the NHC is substituted by a triphenylphosphine ligand. The CNPN atoms form the equatorial plane. The other two acetonitrile ligands are still *trans*-arranged at the axial positions. The P–Ru–N angles of three acetonitrile ligands and pyrimidine are 92.91, 92.06, 88.91, and 98.34°. The Ru–C bond distances being 2.039 Å is slightly longer than those of **2** and **3**, but similar to complex **1**. The Ru–P bond distance is 2.4080 Å, which are no difference from those of reported Ru(II) complexes [3,4]. In complex **5**, the central Ru ion is coordinated by one NHC ligand, one 1,10-phenanthroline ligand and two acetonitrile molecules. The NHC ligand, one acetonitrile ligand and one nitrogen atom of phenanthroline occupy the equatorial plane in which the carbon atom of NHC ligand is *trans* to the nitrogen atom of phenanthroline with the C(2)–Ru(1)–N(6) angle of 169.08°, the acetonitrile molecule is *trans* to the pyrimidine group with the N(8)–Ru(1)–N(1) angle of 176.42°. The rest coordination nitrogen atoms of acetonitrile and phenanthroline lie on the axial positions with the N(7)–Ru(1)–N(5) angle of 173.74°.

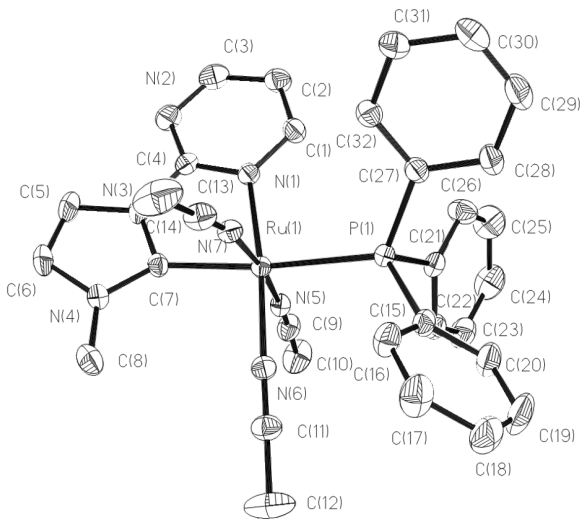

Figure 4: Structural view of **4** showing 30% thermal ellipsoids. All hydrogen atoms and PF_6^- were omitted for clarity. Selected bond lengths (Å) and angles (deg): Ru(1)–N(5) 2.012(4), Ru(1)–N(7) 2.020(4), Ru(1)–N(6) 2.025(4), Ru(1)–C(7) 2.039(4), Ru(1)–N(1) 2.120(4), Ru(1)–P(1) 2.4080(11), N(5)–Ru(1)–N(7) 173.83(16), N(5)–Ru(1)–N(6) 87.01(16), N(7)–Ru(1)–N(6) 89.42(15), N(5)–Ru(1)–C(7) 92.27(17), N(5)–Ru(1)–P(1) 92.91(11), C(7)–Ru(1)–P(1) 173.12(16).

Conclusion

In summary, Ru–NHC complexes bearing pyrimidine- and pyridine-functionalized NHC ligands have been prepared through a carbene transfer reaction using nickel–NHC as the carbene source. Their structures have been definitely determined by X-ray crystallography. The catalytic behavior of di-, tetra- and

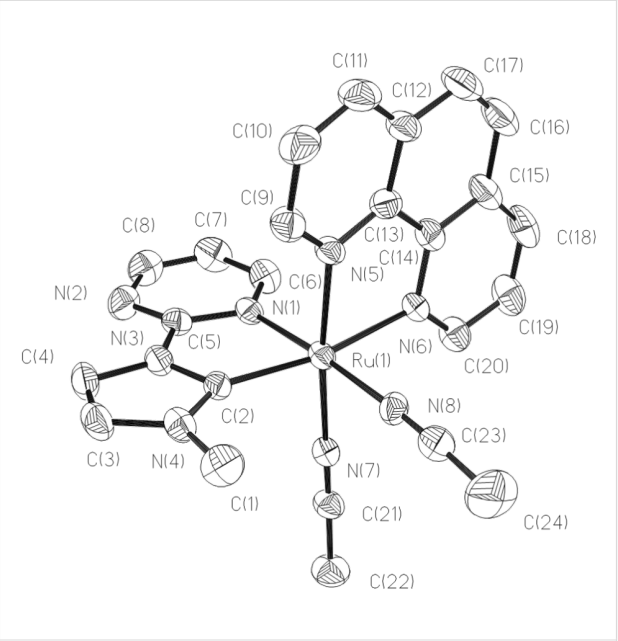

Figure 5: Structural view of **5** showing 30% thermal ellipsoids. All hydrogen atoms and PF_6^- were omitted for clarity. Selected bond lengths (Å) and angles (deg): Ru(1)–C(2) 2.007(5), Ru(1)–N(8) 2.022(4) Ru(1)–N(7) 2.049(4), Ru(1)–N(5) 2.063(4), Ru(1)–N(1) 2.077(4), Ru(1)–N(6) 2.126(4), C(2)–Ru(1)–N(8) 99.06(18), C(2)–Ru(1)–N(7) 91.10(17), N(8)–Ru(1)–N(7) 87.76(16), C(2)–Ru(1)–N(5) 95.03(17), N(8)–Ru(1)–N(5) 90.05(16), N(7)–Ru(1)–N(5) 173.74(16). Symmetry code: #1 x, −y+3/2, z.

tri-acetonitrile-coordinated ruthenium complexes in transfer hydrogenation reactions was studied. These ruthenium complexes were found to be highly efficient catalysts for transfer hydrogenation of ketones. The catalytic properties of the ruthenium complexes in other organic transformation will be further studied.

Experimental

All chemicals were obtained from commercial suppliers in reagent grade quality and were used as received. $HL1PF_6$ and $HL2PF_6$ were synthesized according to the reported method [42,43]. ^1H and ^{13}C NMR spectra were recorded on a Bruker Avance-400 (400 MHz) spectrometer operating at 400 MHz for ^1H and at 100 MHz for ^{13}C. Chemical shifts (δ) were expressed in ppm downfield to TMS at δ = 0 ppm and coupling constants (*J*) were expressed in Hz. Elemental analyses were performed by a Flash EA 1112 ThermoFinnigan analyzer.

Synthesis of $[Ru(L1)_2(CH_3CN)_2](PF_6)_2$ (1). A mixture of $HL1(PF_6)$ (306 mg, 1.0 mmol), excess Raney nickel (500 mg) in 10 mL MeCN was stirred at 80 °C for 24 h. After it was cooled to room temperature, the solution was filtered through Celite. Then $[Ru(p\text{-cymene})Cl_2]_2$ (153 mg, 0.25 mmol) was added to the solution and stirred at reflux for 12 h. After filtration through a plug of Celite, the mixture was concentrated and poured into Et_2O (30 mL) to precipitate the product. Compound **1** was obtained as a yellow solid. Yield: 307 mg, 76%. Anal. calcd for $C_{20}H_{22}F_{12}N_{10}P_2Ru$: C, 30.27; H, 2.79; N, 17.65; found: C, 30.19; H, 2.82; N, 17.55; ^1H NMR (400 MHz, DMSO-d_6) δ 8.77 (d, *J* = 4.8 Hz, $C_4H_3N_2$, 2H), 8.31 (d, *J* = 2.0 Hz, $C_3H_2N_2$, 2H), 8.09 (d, *J* = 4.8 Hz, $C_4H_3N_2$, 2H), 7.90 (d, *J* = 2.0 Hz, $C_4H_3N_2$, 2H), 7.27 (t, *J* = 4.8 Hz, $C_4H_3N_2$, 2H), 4.17 (s, CH_3, 3H), 2.41 (s, CH_3CN, 6H); ^{13}C NMR (100 MHz, DMSO-d_6) δ 193.1 (Ru-*C*), 166.2, 159.8, 158.7, 128.6, 127.0, 120.0, 117.9, 37.7, 4.17.

Synthesis of $[RuL1(CH_3CN)_4](PF_6)_2$ (2). A mixture of $HL1(PF_6)$ (153 mg, 0.5 mmol), excess Raney nickel (300 mg) in 10 mL MeCN was stirred at 80 °C for 24 h. After it was cooled to room temperature, the solution was filtered through Celite. Then $[Ru(p\text{-cymene})Cl_2]_2$ (153 mg, 0.25 mmol) and NH_4PF_6 (163 mg, 1.0 mmol) was added to the filtrate and stirred at reflux for 12 h. The mixture was filtered through Celite to remove precipitated $NiCl_2$ and all volatiles were evaporated under reduced pressure. The residue was washed with water and dried in vacuo. The yellow residue was dissolved in MeCN and concentrated to about 2 mL. The addition of Et_2O induced precipitation of the product as a yellow solid. Yield: 190 mg, 53%. Anal. calcd for $C_{16}H_{20}F_{12}N_8P_2Ru$: C, 26.86; H, 2.82; N, 15.66; found: C, 26.70; H, 2.90; N, 15.58; ^1H NMR (400 MHz, DMSO-d_6) δ 9.12 (d, *J* = 4.8 Hz, $C_4H_3N_2$, 1H), 8.85 (d, *J* = 4.8 Hz, $C_4H_3N_2$, 1H), 8.00 (d, *J* = 2.4 Hz, $C_3H_2N_2$, 1H), 7.48 (t, *J* = 2.4 Hz, $C_4H_3N_2$, 1H), 7.36 (d, *J* = 2.4 Hz, $C_3H_2N_2$, 1H), 4.04 (s, CH_3, 3H), 2.52, (s, CH_3CN, 3H), 2.12, (s, CH_3CN, 6H), 1.96, (s, CH_3CN, 3H); ^{13}C NMR (100 MHz, DMSO-d_6) δ 193.0 (Ru-*C*), 180.9, 166.6, 158.4, 158.3, 157.4, 128.7, 125.7, 125.6, 117.7, 116.2, 35.8, 2.64, 2.20, 1.77.

Synthesis of $[RuL2(CH_3CN)_3](PF_6)_2$ (3). According to the same procedure as described for **2**, complex **3** was obtained as a yellow soild. Yield: 249 mg, 61%. Anal. calcd for $C_{29}H_{31}F_{12}N_9P_2Ru$ ($[RuL2(CH_3CN)_3](PF_6)_2)\cdot 2CH_3CN$: C, 38.85; H, 3.48; N, 14.06; found: C, 38.70; H, 3.60; N, 14.08; ^1H NMR (400 MHz, DMSO-d_6) δ 8.90 (d, *J* = 4.4 Hz, C_5H_4N, 2H), 8.11 (t, *J* = 6.4 Hz, C_5H_4N, 2H), 7.95–7.92 (m, C_6H_4, 4H), 7.64 (t, *J* = 5.2 Hz, C_5H_4N, 2H), 7.41–7.40 (m, C_5H_4N, 2H), 5.85 (s, CH_2, 4H), 2.35, (s, CH_3CN, 6H), 2.08 (s, CH_3CN, 3H); ^{13}C NMR (100 MHz, DMSO-d_6) δ 192.0 (Ru-*C*), 154.1, 148.2, 140.5, 134.7, 125.5, 125.3, 125.0, 117.2, 116.6, 111.4, 50.5, 2.80, 2.15.

Synthesis of $[RuL1(PPh_3)(CH_3CN)_3](PF_6)_2$ (4). A mixture of **2** (142 mg, 0.2 mmol) and triphenylphosphine (262 mg, 1.0 mmol) in 5 mL CH_3CN was stirred at 80 °C for 6 h. Then the mixture was filtered through Celite and all volatiles were

evaporated under reduced pressure. The residue was washed with ethyl acetate and dried in vacuo. The yellow residue was dissolved in CH_3CN and crystallization by slow diffusion of Et_2O into the CH_3CN solution gave **4** as yellow solid. Yield: 75 mg, 40%. Anal. calcd for $C_{32}H_{32}F_{12}N_7P_3Ru$: C, 41.04; H, 3.44; N, 10.47; found: C, 41.10; H, 3.40; N, 10.58; ^{1}H NMR (DMSO-d_6) δ 8.99 (s, 1H), 8.46 (s, 1H), 8.38 (s, 1H), 7.87 (s, 1H), 7.57(s, 13H), 7.42 (s, 2H), 7.25 (s, 1H), 4.11 (s, 3H), 2.14 (s, 6H), 2.07 (s, 3H); ^{13}C NMR (DMSO-d_6) δ 192.2 (Ru-C), 183.8, 182.8, 163.4, 158.6, 157.9, 132.0, 131.9, 131.7, 131.5, 129.0, 128.7, 127.9, 127.6, 127.5, 127.4, 127.2, 127.1, 126.3, 125.5, 117.9, 116.4, 116.3, 35.8, 2.15, 1.72.

Synthesis of [RuL1(Phen)(CH$_3$CN)$_2$](PF$_6$)$_2$ (5). A mixture of **2** (142 mg, 0.2 mmol) and 1,10-phenanthroline·1H$_2$O (198 mg, 1.0 mmol) in 5 mL CH_3CN was stirred at 80 °C for 6 h. Then the mixture was filtered through Celite to afford a yellow solution. Crystallization by slow diffusion of Et_2O into the CH_3CN solution gave **5** as an orange yellow solid. Yield: 103 mg, 63%. Anal. calcd for $C_{24}H_{22}F_{12}N_8P_2Ru$: C, 35.43; H, 2.73; N, 13.77; found: C, 35.50; H, 2.90; N, 13.80; ^{1}H NMR (DMSO-d_6) δ 9.77 (dd, J = 1.2 and 4.0 Hz, 1H), 9.08 (dd, J = 0.8 and 6.4 Hz, 1H), 8.75 (dd, J = 1.6 and 4.0 Hz, 1H), 8.44–8.38 (m, 3H), 8.32–8.29 (m, 2H), 7.94 (d, J = 1.6 Hz, 1H), 7.73 (dd, J = 4.4 and 6.4 Hz, 1H), 7.68 (dd, J = 1.6 and 6.4 Hz, 1H), 7.11 (dd, J = 4.0 and 4.4 Hz, 1H), 4.23 (s, 3H), 4.22 (s, 3H), 2.53, 2.28 (s, CH_3CN, each 3H); ^{13}C NMR (DMSO-d_6) δ 192.3 (Ru-C), 161.9, 159.9, 159.0, 157.5, 152.5, 148.0, 146.6, 138.8, 137.4, 130.9, 130.6, 128.3, 128.2, 127.4, 127.2, 127.1, 126.4, 119.5, 118.5, 37.1, 4.56, 3.83, 1.62.

Typical procedure for catalytic transfer hydrogenation reaction

The ketone (1.0 mmol), KOH (0.2 mmol) and 2 mL of iPrOH were placed in a Schlenk tube. Anisole (0.25 mmol) was added as an internal GC standard. The mixture was heated at 80 °C and then catalyst solution (0.01 mmol, 0.001 mmol, or 0.0001 mol of ruthenium complexes in iPrOH (1 mL) was injected. Aliquots (0.2 mL) were taken at fixed time intervals, quenched with 1 mL of H_2O and extracted with 3 mL of Et_2O. The product yields were determined by GC analysis.

X-ray diffraction analysis

Single-crystal X-ray diffraction data were collected at 298(2) K on a Siemens Smart-CCD area-detector diffractometer with a MoKα radiation (λ = 0.71073 Å) by using a ω-2θ scan mode. Unit-cell dimensions were obtained with least-squares refinement. Data collection and reduction were performed using the Oxford Diffraction CrysAlisPro software [44]. All structures were solved by direct methods, and the non-hydrogen atoms were subjected to anisotropic refinement by full-matrix least squares on F^2 using the SHELXTXL package [45]. Hydrogen atom positions for all of the structures were calculated and allowed to ride on their respective C atoms with C–H distances of 0.93–0.97 Å and U_{iso}(H) = −1.2–1.5U_{eq}(C). Details of the X-ray experiments and crystals data are summarized in Table 3.

Table 3: Crystallographic data for complexes **1**–**5**.

	1	**2**	**3**·2CH$_3$CN	**4**·CH$_3$CN	**5**
CCDC number	1407422	1407423	1407424	1407425	1407426
Formula	$C_{20}H_{22}F_{12}N_{10}P_2Ru$	$C_{16}H_{20}F_{12}N_8P_2Ru$	$C_{29}H_{31}F_{12}N_9P_2Ru$	$C_{34}H_{35}F_{12}N_8P_3Ru$	$C_{24}H_{22}F_{12}N_8P_2Ru$
Fw	793.49	715.41	896.64	977.68	813.51
crystal system	Monoclinic	Monoclinic	Triclinic	Triclinic	Monoclinic,
space group	*C*2/*c*	*P*2/*n*	*P*−1	*P*−1	*P*2$_1$/*m*
a, Å	23.240(3)	11.2914(5)	11.4695(12)	9.9130(16)	10.9570(8)
b, Å	10.3410(5)	12.7244(6)	13.1322(14)	12.665(2)	22.2567(16)
c, Å	16.060(4)	21.4357(11)	13.7721(14)	2 18.222(3)	16.8706(11)
α, deg	90	90	97.7010	90	90
β, deg	130.19(3)	102.469(4)	103.2130	90	97.384(6)
γ, deg	90	90	94.0570	66.96	90
V, Å^3	2948.4(8)	3007.2(2)	1990.1(4)	2105.2(6)	4080.1(5)
Z	4	4	2	2	4
D_{calcd}, Mg/m^3	1.788	1.580	1.496	1.542	1.324
Reflections collected	5571	10931	15882	7390	15951
Reflections independent (R_{int})	2597 (0.0289)	5299 (0.0492)	7002 (0.0129)	7390 (0.0000)	7385 (0.0278)
Goodness-of-fit on F^2	1.059	1.064	1.053	1.050	1.083
R (*I* > 2σ*I*)	0.0539, 0.1465	0.0712, 0.2121	0.0373, 0.0973	0.0418, 0.1020	0.0604, 0.1788
R (all data)	0.0617, 0.1558	0.0913, 0.2322	0.0389, 0.0984	0.0455, 0.1049	0.0794, 0.1904

Supporting Information

Supporting Information File:

Supporting Information File 1

X-ray crystallographic data CCDC 1407422–1407426.
[http://www.beilstein-journals.org/bjoc/content/supplementary/1860-5397-11-194-S1.cif]

Acknowledgements

This work was financially supported by the National Natural Science Foundation of Zhejiang Province (LQ14B020003).

References

1. Poyatos, M.; Mata, J. A.; Peris, E. *Chem. Rev.* **2009,** *109,* 3677–3707. doi:10.1021/cr800501s
2. Díez-González, S.; Marion, N.; Nolan, S. P. *Chem. Rev.* **2009,** *109,* 3612–3676. doi:10.1021/cr900074m
3. Hahn, F. E.; Jahnke, M. C. *Angew. Chem., Int. Ed.* **2008,** *47,* 3122–3172. doi:10.1002/anie.200703883
4. Edwards, P. G.; Hahn, F. E. *Dalton Trans.* **2011,** *40,* 10278–10288. doi:10.1039/c1dt10864f
5. Hock, S. J.; Schaper, L.-A.; Herrmann, W. A.; Kühn, F. E. *Chem. Soc. Rev.* **2013,** *42,* 5073–5089. doi:10.1039/c3cs60019j
6. Schaper, L.-A.; Hock, S. J.; Herrmann, W. A.; Kühn, F. E. *Angew. Chem., Int. Ed.* **2013,** *52,* 270–289. doi:10.1002/anie.201205119
7. Hopkinson, M. N.; Richter, C.; Schedler, M.; Glorius, F. *Nature* **2014,** *510,* 485–496. doi:10.1038/nature13384
8. Gradert, C.; Krahmer, J.; Sönnichsen, F. D.; Näther, C.; Tuczek, F. *J. Organomet. Chem.* **2014,** *770,* 61–68. doi:10.1016/j.jorganchem.2014.08.010
9. Galan, B. R.; Wiedner, E. S.; Helm, M. L.; Linehan, J. C.; Appel, A. M. *Organometallics* **2014,** *33,* 2287–2294. doi:10.1021/om500206e
10. Liu, B.; Pan, S.; Liu, B.; Chen, W. *Inorg. Chem.* **2014,** *53,* 10485–10497. doi:10.1021/ic501544d
11. Liu, B.; Liu, B.; Zhou, Y.; Chen, W. *Organometallics* **2010,** *29,* 1457–1464. doi:10.1021/om100009u
12. Chen, C.; Qiu, H.; Chen, W. *Inorg. Chem.* **2011,** *50,* 8671–8678. doi:10.1021/ic2012233
13. Zhang, M.; Ni, X.; Shen, Z. *Organometallics* **2014,** *33,* 6861–6867. doi:10.1021/om500930m
14. Dang, L.; Guo, J.; Song, H.; Liu, B.; Wang, B. *Dalton Trans.* **2014,** *43,* 17177–17183. doi:10.1039/C4DT02198C
15. Borré, E.; Dahm, G.; Aliprandi, A.; Mauro, M.; Dagorne, S.; Bellemin-Laponnaz, S. *Organometallics* **2014,** *33,* 4374–4384. doi:10.1021/om5003446
16. Bierenstiel, M.; Cross, E. D. *Coord. Chem. Rev.* **2011,** *255,* 574–590. doi:10.1016/j.ccr.2010.10.040
17. Saha, B.; Sengupta, G.; Sarbajna, A.; Dutta, I.; Bera, J. K. *J. Organomet. Chem.* **2014,** *771,* 124–130. doi:10.1016/j.jorganchem.2013.12.051
18. Dakkach, M.; Fontrodona, X.; Parella, T.; Atlamsani, A.; Romero, I.; Rodríguez, M. *Dalton Trans.* **2014,** *43,* 9916–9923. doi:10.1039/C4DT00698D
19. Chung, L.-H.; Cho, K.-S.; England, J.; Chan, S.-C.; Wieghardt, K.; Wong, C.-Y. *Inorg. Chem.* **2013,** *52,* 9885–9896. doi:10.1021/ic4010196
20. Fernández, F. E.; Puerta, M. C.; Valerga, P. *Organometallics* **2011,** *30,* 5793–5802. doi:10.1021/om200665f
21. Corberán, R.; Mas-Marzá, E.; Peris, E. *Eur. J. Inorg. Chem.* **2009,** 1700–1716. doi:10.1002/ejic.200801095
22. Normand, A. T.; Cavell, K. J. *Eur. J. Inorg. Chem.* **2008,** 2781–2800. doi:10.1002/ejic.200800323
23. Horn, S.; Gandolfi, C.; Albrecht, M. *Eur. J. Inorg. Chem.* **2011,** 2863–2868. doi:10.1002/ejic.201100143
24. DePasquale, J.; Kumar, M.; Zeller, M.; Papish, E. T. *Organometallics* **2013,** *32,* 966–979. doi:10.1021/om300547f
25. Yang, D.; Tang, Y.; Song, H.; Wang, B. *Organometallics* **2015,** *34,* 2012–2017. doi:10.1021/acs.organomet.5b00256
26. Chen, C.; Zhang, Y.; Hong, S. H. *J. Org. Chem.* **2011,** *76,* 10005–10010. doi:10.1021/jo201756z
27. Semwal, S.; Ghorai, D.; Choudhury, J. *Organometallics* **2014,** *33,* 7118–7124. doi:10.1021/om500876k
28. Su, G.; Huo, X.-K.; Jin, G.-X. *J. Organomet. Chem.* **2012,** *696,* 533–538. doi:10.1016/j.jorganchem.2010.09.018
29. Wylie, W. N. O.; Lough, A. J.; Morris, R. H. *Organometallics* **2012,** *31,* 2137–2151. doi:10.1021/om300108p
30. Naziruddin, A. R.; Huang, Z.-J.; Lai, W.-C.; Lin, W.-J.; Hwang, W.-S. *Dalton Trans.* **2013,** *42,* 13161–13171. doi:10.1039/C3DT51161H
31. Naziruddin, A. R.; Zhuang, C.-S.; Lin, W.-J.; Hwang, W.-S. *Dalton Trans.* **2014,** *43,* 5335–5342. doi:10.1039/C3DT53125B
32. Bernet, L.; Lalrempuia, R.; Ghattas, W.; Mueller-Bunz, H.; Vigara, L.; Llobet, A.; Albrecht, M. *Chem. Commun.* **2011,** *47,* 8058–8060. doi:10.1039/C1CC12615F
33. Liu, X.; Chen, W. *Dalton Trans.* **2012,** *41,* 599–608. doi:10.1039/C1DT11356A
34. Gu, S.; Liu, B.; Chen, J.; Wu, H.; Chen, W. *Dalton Trans.* **2012,** *41,* 962–970. doi:10.1039/C1DT11269D
35. Liu, X.; Chen, W. *Organometallics* **2012,** *31,* 6614–6622. doi:10.1021/om300644h
36. Liu, B.; Liu, X.; Chen, C.; Chen, C.; Chen, W. *Organometallics* **2012,** *31,* 282–288. doi:10.1021/om200881s
37. Wang, D.; Astruc, D. *Chem. Rev.* **2015,** *115,* 6621–6686. doi:10.1021/acs.chemrev.5b00203
38. Enthaler, S.; Jackstell, R.; Hagemann, B.; Junge, K.; Erre, G.; Beller, M. *J. Organomet. Chem.* **2006,** *691,* 4652–4659. doi:10.1016/j.jorganchem.2006.07.013
39. Danopoulos, A. A.; Winston, S.; Motherwell, W. B. *Chem. Commun.* **2002,** 1376–1377. doi:10.1039/B202814J
40. Lai, Y.-B.; Lee, C.-S.; Lin, W.-J.; Naziruddin, A. R.; Hwang, W.-S. *Polyhedron* **2013,** *53,* 243–248. doi:10.1016/j.poly.2013.01.042
41. Fernández, F. E.; Puerta, M. C.; Valerga, P. *Organometallics* **2012,** *31,* 6868–6879. doi:10.1021/om300692a
42. Zhang, X.; Liu, B.; Liu, A.; Xie, W.; Chen, W. *Organometallics* **2009,** *28,* 1336–1349. doi:10.1021/om800982r
43. Chen, C.; Qiu, H.; Chen, W. *J. Organomet. Chem.* **2012,** *696,* 4166–4172. doi:10.1016/j.jorganchem.2011.09.008
44. *CrysAlisPro;* Oxford Diffraction Ltd: Oxford, UK, 2008.
45. Sheldrick, G. M. *SHELXS-97 and SHELXL-97, Program for X-ray crystal structure refinement,* University of Göttingen: Göttingen, Germany, 1997.

BEILSTEIN JOURNAL OF ORGANIC CHEMISTRY

Influence of bulky yet flexible *N*-heterocyclic carbene ligands in gold catalysis

Alba Collado[1], Scott R. Patrick[1], Danila Gasperini[1], Sebastien Meiries[1] and Steven P. Nolan[*2]

Full Research Paper

Open Access

Address:
[1]EaStCHEM School of Chemistry, University of St Andrews, St Andrews, KY16 9ST, UK and [2]Chemistry Department, College of Science, King Saud University, Riyadh 11451, Saudi Arabia

Email:
Steven P. Nolan[*] - stevenpnolan@gmail.com

* Corresponding author

Keywords:
catalysis; flexible and bulky ligands; gold; ligand design; N-heterocyclic carbenes

Beilstein J. Org. Chem. **2015,** *11,* 1809–1814.
doi:10.3762/bjoc.11.196

Received: 28 July 2015
Accepted: 04 September 2015
Published: 02 October 2015

This article is part of the Thematic Series "N-Heterocyclic carbenes".

Associate Editor: J. P. Wolfe

Abstract

Three new Au(I) complexes of the formula [Au(NHC)(NTf_2)] (NHC = *N*-heterocyclic carbene) bearing bulky and flexible ligands have been synthesised. The ligands studied are IPent, IHept and INon which belong to the 'ITent' ('Tent' for 'tentacular') family of NHC derivatives. The effect of these ligands in gold-promoted transformations has been investigated.

Introduction

Homogeneous gold catalysis has witnessed an exponential growth in the last 15 years [1-12]. Gold complexes have been shown to be efficient catalysts in a wide variety of transformations [1-12]. *N*-heterocyclic carbenes (NHC) have attracted particular attention as ancillary ligands due to their donating properties and steric hindrance [13-20]. These can be easily tuned by modifying the architecture of the imidazole ring, typically, by changing the *N*-substituents or the backbone [13-20]. One of our research interests is the study of the electronic and steric properties of new *N*-heterocyclic carbenes and their influence in catalysis upon coordination to a metal centre. We have recently reported the synthesis of the 'ITent' family ('Tent' stands for 'tentacular') of NHC carbenes [21] which comprises IPent, first utilised by Organ, IHept, and INon (Figure 1). IPr [22], which is one of the most commonly used NHC derivatives, can be considered as the simplest congener of the ITent family (Figure 1). These ligands belong to the class of NHC with 'flexible sterics', i.e., ligands capable of adjusting their steric hindrance towards incoming substrates and, at the same time, stabilising low-valent species. This concept, first proposed by Glorius [23-26], has been applied by a number of research groups to metal-catalysed transformations, leading to improvements in catalytic activity over other known systems [27-41]. The ITent ligands have been successfully used in challenging Pd cross-coupling reactions and other Pd-promoted transformations [21-41].

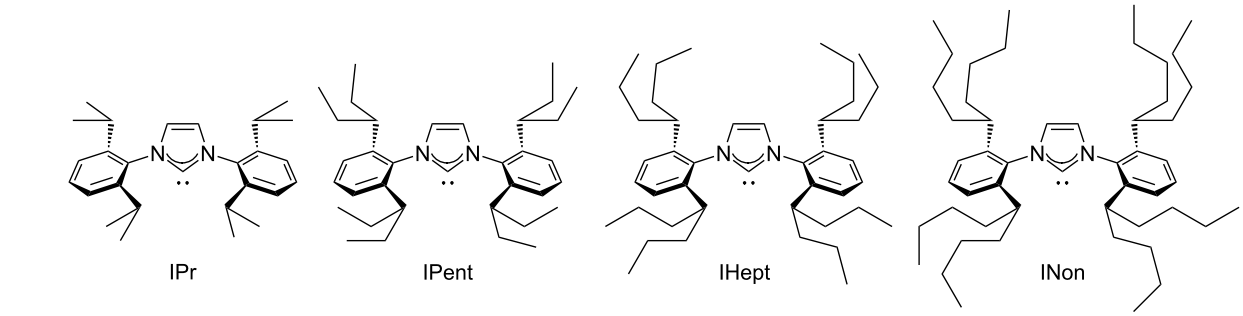

	IPr	IPent	IHept	INon
% V_{bur}	44.5%	I) 49.0% II) 48.6%	51.5%	51.3%
TEP_{DCM}	2051.5 cm^{-1}	2049.3 cm^{-1}	2048.6 cm^{-1}	2048.5 cm^{-1}
TEP_{hex}	2055.1 cm^{-1}	2053.1 cm^{-1}	2052.5 cm^{-1}	2052.1 cm^{-1}

Figure 1: 'ITent' family of ligands, including IPr. First row: percentage buried volume (% V_{bur}) calculated in [Au(ITent)Cl] complexes using the Samb*V*ca software [42-45]. Second and third row: Tolman Electronic Parameter (TEP) calculated from IR measurements in solution of the [Ni(ITent)CO_3] complexes [21,42].

The electronic and steric properties of the ITent family have been determined [21,42,45] and compared to the parent ligand IPr. The observed trend for both electronic and steric properties is as follows: IPr << IPent < IHept ≈ INon showing that an increase in the length of the chain translates into an increase of the donating properties and the steric hindrance. The limit of this increment was found to lie between IHept and INon, where the additional carbon atoms did not have a significant impact on the properties of the ligands.

Herein we report the catalytic activity of gold complexes containing the ITent ligands.

Results and Discussion

Synthesis of complexes

We have recently reported the synthesis of [Au(ITent)Cl] and [Au(ITent)(OH)] derivatives following the synthetic protocol shown in Scheme 1 [45].

In order to study the impact of the ITent ligands in gold catalysis, we sought to synthesise the corresponding Gagosz-type derivatives [46,47]. These complexes, bearing a labile NTf_2 group, do not require additives to promote catalytic transformations. Gagosz-type species have been typically prepared by reacting the corresponding [Au(L)Cl] derivative (L = PR_3, NHC) with $AgNTf_2$ [46,47]. Alternative protocols that avoid the use of silver salts involve the treatment of gold-hydroxide [48] or gold-acetonyl [49] complexes with trifluoromethanesulfonimide. Following this silver-free procedure, [Au(ITent)(OH)] complexes **4**–**6** were reacted with $HNTf_2$ to obtain the corresponding [Au(ITent)(NTf_2)] species **7**–**9** which were isolated as white solids in good to excellent yields (Scheme 2).

Complexes **7**–**9** were characterised by ^1H, $^{13}C\{^1H\}$, and $^{19}F\{^1H\}$ NMR spectroscopies and elemental analysis. The $^{13}C\{^1H\}$ NMR spectra of all the complexes showed a singlet in

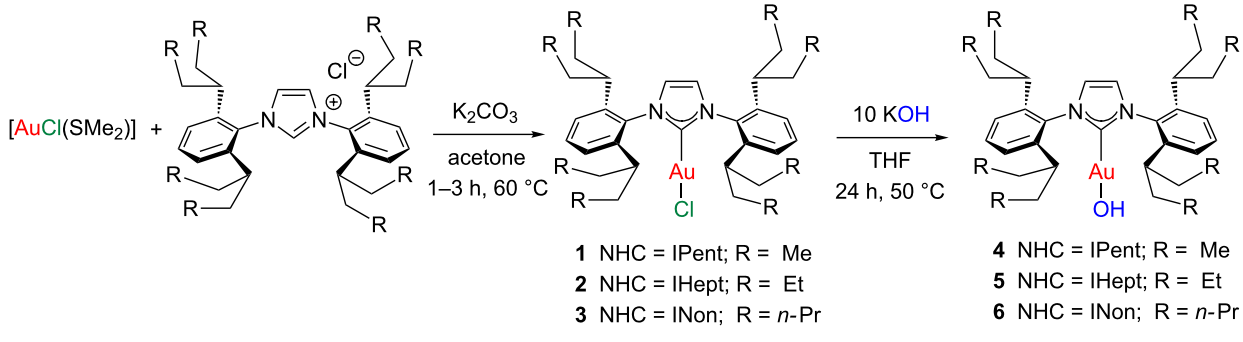

Scheme 1: Synthesis of gold complexes bearing the ITent ligands.

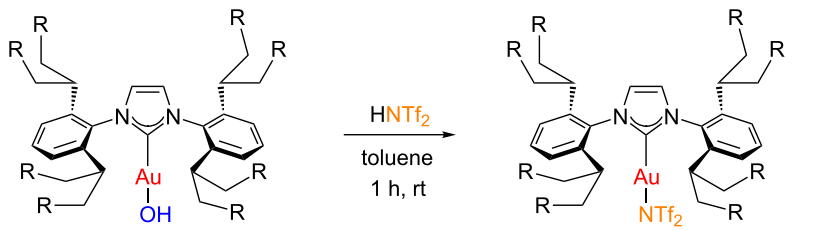

4 NHC = IPent; R = Me
5 NHC = IHept; R = Et
6 NHC = INon; R = *n*-Pr

7 NHC = IPent; R = Me 68%
8 NHC = IHept; R = Et 97%
9 NHC = INon; R = *n*-Pr 99%

Scheme 2: Silver-free synthesis of [Au(ITent)(NTf_2)] complexes.

the low field region of the spectra corresponding to the carbenic carbon atom of the molecule. These signals appear at 167.5–167.8 ppm, in agreement with other [Au(NHC)(NTf_2)] complexes bearing unsaturated NHC ligands [46,50]. Each $^{19}F\{^1H\}$ NMR spectrum contains a singlet at ca. −76 ppm, in agreement with the presence of an inner-sphere NTf_2 ligand [50].

Catalytic transformations

Once fully characterised, the catalytic activity of the new complexes was investigated. To this end, three model reactions were selected: alkyne hydration, nitrile hydration, and the synthesis of homoallylic ketones. To place these results into context, [Au(IPr)(NTf_2)] (**10**) [46] was also tested under the same conditions.

Alkyne hydration

Alkyne hydration is an attractive transformation to generate ketones from alkynes with high atom economy. A number of gold complexes have been shown to be active in this transformation [51-58]. Much effort has been devoted to the development of more sustainable gold-promoted protocols and several advances have been made in this field, e.g., very low catalyst loadings (10–1000 ppm) [51-53,56] have been achieved and the transformation has been successfully performed in aqueous media [54,57]. Due to its relevance and importance, the hydration of phenylacetylene was selected as a model transformation to explore the different activity of complexes **7**–**9**.

The reactions were performed under the reported optimised conditions for this transformation: using a 2:1 mixture of 1,4-dioxane/water at 80 °C [56]. All complexes showed excellent catalytic activity at 0.5 mol % catalyst loading, after 3 hours, and full conversion to the ketone was observed in all cases (Table 1, entries 1–4). In order to determine the influence of the ligands in the catalytic activity, the catalyst loading was reduced.

Table 1: Influence of the ITent ligands in gold-catalysed alkyne hydration.[a]

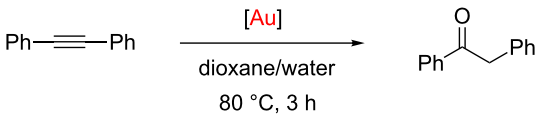

entry	complex	[Au] (mol %)	time (h)	conversion (%)[b]
1	[Au(IPr)(NTf_2)] (**10**)	0.5	3	>99
2	[Au(IPent)(NTf_2)] (**7**)	0.5	3	>99
3	[Au(IHept)(NTf_2)] (**8**)	0.5	3	>99
4	[Au(INon)(NTf_2)] (**9**)	0.5	3	>99
5	[Au(IPr)(NTf_2)] (**10**)	0.25	3	87
6	[Au(IPent)(NTf_2)] (**7**)	0.25	3	68
7	[Au(IHept)(NTf_2)] (**8**)	0.25	3	77
8	[Au(INon)(NTf_2)] (**9**)	0.25	3	70

[a]Reaction conditions: [Au(NHC)(NTf_2)] (0.5 mol %), phenylacetylene (0.5 mmol), 1,4-dioxane/water (2:1, 1 mL), or [Au(NHC)(NTf_2)] (0.25 mol %), phenylacetylene (1.0 mmol), 1,4-dioxane/water (2:1, 2 mL). [b]GC conversion, average of at least two runs.

When the catalyst loading was reduced to 0.25 mol % and the reactions were analysed after 3 h, the differences between the ligands became evident. Good conversions were obtained in all cases (Table 1, entries 5–8). However, the best conversion was observed when complex **10** bearing the IPr ligand was used (Table 1, entry 5). Complexes **7**–**9** afforded lower conversions, with [Au(IHept)(NTf_2)] (**8**) being the most efficient amongst them (Table 1, entries 6–9).

Nitrile hydration

Once it was shown that the use of the ITent ligands in the gold-catalysed hydration of phenylacetylene did not improve upon the performance of the parent IPr ligand, we explored the behaviour of the [Au(ITent)(NTf_2)] complexes in the hydration of nitriles. Mono- and digold complexes have been shown to be efficient catalysts in this transformation [52,59,60] which proceeds with 100% atom economy. In addition, previous findings showed that the digold complex, [{Au(NHC)}$_2$(μ-OH)][BF_4], bearing IPent was more efficient than the IPr analogue in this reaction [52]. This result encouraged us to test the influence of the ITent ligands in the hydration of nitriles promoted by monogold species.

The reactions were conducted in a 1:1 mixture THF/water and heated at 140 °C under microwave irradiation [60]. Low catalyst loadings were employed in order to observe the differences between the four catalysts studied. At 1 mol %, the complexes showed poor to good catalytic activity depending on the ligand (Table 2). As we observed for the hydration of alkynes, the ITent series were found to be less active than complex **10**, which afforded the desired product in 56% conversion (Table 2, entry 1). However, in this case, the gold complex bearing IPent (**7**) was more efficient than the IHept (**8**) and INon (**9**) derivatives (Table 2, entries 2–4).

Synthesis of homoallylic ketones

After the observed trend in hydration transformations, we focused our attention on non-water inclusive reactions and decided to explore the catalytic activity of complexes **7**–**9** in the synthesis of homoallylic ketones via hydroalkoxylation/Claisen rearrangement [61,62]. [Au(NHC)(NTf_2)] complexes have proven to be efficient catalysts for this transformation, promoting the reaction under neat conditions and low catalyst loadings [61].

The reactions were conducted under the reported optimised conditions [61] and were analysed after 20 min. An inverse trend was observed in this case: the increase in the length of the alkyl chain resulted in lower conversions (Table 3). Complex **10** (Table 3, entry 1) was also found to be more efficient than complexes **7**–**9** for this transformation (Table 3, entries 2–4). Complex **7**, containing the IPent ligand, was the most active catalyst among the ITent series (Table 3, entry 2).

Conclusion

In conclusion, three new gold complexes bearing the ITent ligands (IPent, IHept, and INon) have been synthesised and fully characterised. The impact of varying the length of the alkyl chain of the ligands in gold-promoted transformations has been explored. All gold complexes were shown to be active in water inclusive reactions (alkyne and nitrile hydration) and in the synthesis of homoallylic ketones from allylic alcohols and alkynes. [Au(IHept)(NTf_2)] was the most efficient complex of the series in the hydration of alkynes while the [Au(IPent)(NTf_2)] analogue was found to be superior in the hydration of nitriles and in the synthesis of homoallylic ketones. However, when the performance of the catalysts was compared to that of the parent [Au(IPr)(NTf_2)] complex, this appeared to be more active than the remaining complexes, showing that an

Table 2: Influence of the ITent ligands in gold-catalysed nitrile hydration.[a]

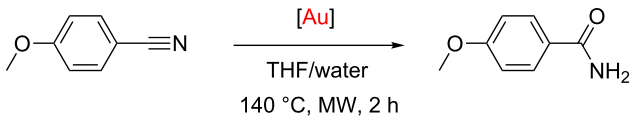

entry	complex	[Au] (mol %)	time (h)	conversion (%)[b]
1	[Au(IPr)(NTf_2)] (**10**)	1.0	2	56
2	[Au(IPent)(NTf_2)] (**7**)	1.0	2	38
3	[Au(IHept)(NTf_2)] (**8**)	1.0	2	13
4	[Au(INon)(NTf_2)] (**9**)	1.0	2	16

[a]Reaction conditions: [Au(NHC)(NTf_2)] (1.0 mol %), 4-methoxybenzonitrile (0.5 mmol), THF (0.5 mL), water (0.5 mL). [b]^{1}H NMR conversion, average of at least two runs.

Table 3: Influence of the ITent ligands in the gold-catalysed synthesis of homoallylic ketones.[a]

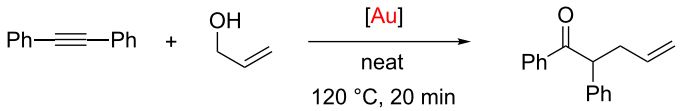

entry	complex	[Au] (mol %)	conversion (%)[b]
1	[Au(IPr)(NTf_2)] (**10**)	0.2	98
2	[Au(IPent)(NTf_2)] (**7**)	0.2	81
3	[Au(IHept)(NTf_2)] (**8**)	0.2	73
4	[Au(INon)(NTf_2)] (**9**)	0.2	56

[a]Reaction conditions: [Au(NHC)(NTf_2)] (0.2 mol %), diphenylacetylene (1.0 mmol), allylic alcohol (3 equiv). [b]GC conversion, average of 3 runs.

increase of the alkyl chain length of the ligands has a detrimental effect in the gold-mediated transformations selected in this study. Further studies on the catalytic activity of the ITent ligands with different metals are currently ongoing.

Supporting Information

Supporting Information File 1

Experimental information and full characterisation of the complexes including a copy of the NMR spectra.
[http://www.beilstein-journals.org/bjoc/content/supplementary/1860-5397-11-196-S1.pdf]

Acknowledgements

The ERC (Advanced Investigator Award-FUNCAT) and Syngenta are gratefully acknowledged for support. Umicore AG is acknowledged for their generous gift of materials.

References

1. Gagosz, F. Organogold Catalysis: Homogeneous Gold-Catalyzed Transformations for a Golden Jubilee. In *Advances in Organometallic Chemistry and Catalysis;* Pombeiro, A. J. L., Ed.; John Wiley & Sons, Inc: Hoboken, 2013. doi:10.1002/9781118742952.ch16
2. Krause, N. Organogold Chemistry. In *Organometallics in Synthesis;* Lipshutz, B. H., Ed.; John Wiley & Sons, Inc., 2013. doi:10.1002/9781118651421.ch4
3. Nolan, S. P. *Acc. Chem. Res.* **2011,** *44,* 91. doi:10.1021/ar1000764
4. Rudolph, M.; Hashmi, A. S. K. *Chem. Commun.* **2011,** *47,* 6536. doi:10.1039/c1cc10780a
5. Li, Z.; Brouwer, C.; He, C. *Chem. Rev.* **2008,** *108,* 3239. doi:10.1021/cr068434l
6. Hashmi, A. S. K. *Chem. Rev.* **2007,** *107,* 3180. doi:10.1021/cr000436x
7. Hashmi, A. S. K.; Hutchings, G. J. *Angew. Chem., Int. Ed.* **2006,** *45,* 7896. doi:10.1002/anie.200602454
8. Hashmi, A. S. K.; Schwarz, L.; Choi, J.-H.; Frost, T. M. *Angew. Chem., Int. Ed.* **2000,** *39,* 2285. doi:10.1002/1521-3773(20000703)39:13<2285::AID-ANIE2285>3.0.CO;2-F
9. Hashmi, A. S. K.; Frost, T. M.; Bats, J. W. *J. Am. Chem. Soc.* **2000,** *122,* 11553. doi:10.1021/ja005570d
10. Riedel, D.; Wurm, T.; Graf, K.; Rudolph, M.; Rominger, F.; Hashmi, A. S. K. *Adv. Synth. Catal.* **2015,** *357,* 1515. doi:10.1002/adsc.201401131
11. Hashmi, A. S. K.; Lothschütz, C.; Graf, K.; Häffner, T.; Schuster, A.; Rominger, F. *Adv. Synth. Catal.* **2011,** *353,* 1407. doi:10.1002/adsc.201100183
12. Hashmi, A. S. K.; Lothschütz, C.; Böhling, C.; Hengst, T.; Hubbert, C.; Rominger, F. *Adv. Synth. Catal.* **2010,** *352,* 3001. doi:10.1002/adsc.201000472
13. Nolan, S. P., Ed. *N-Heterocyclic Carbenes: Effective Tools for Organometallic Synthesis;* Wiley-VCH Verlag GmbH & Co. KGaA: Weinheim, 2014.
14. Hopkinson, M. N.; Richter, C.; Schedler, M.; Glorius, F. *Nature* **2014,** *510,* 485. doi:10.1038/nature13384
15. Nelson, D. J.; Nolan, S. P. *Chem. Soc. Rev.* **2013,** *42,* 6723. doi:10.1039/c3cs60146c
16. Diez-Gonzalez, S., Ed. *N-Heterocyclic Carbenes: From Laboratory Curiosities to Efficient Synthetic Tools;* The Royal Society of Chemistry: Cambridge, 2011.
17. Clavier, H.; Nolan, S. P. *Chem. Commun.* **2010,** *46,* 841. doi:10.1039/b922984a
18. Dröge, T.; Glorius, F. *Angew. Chem., Int. Ed.* **2010,** *49,* 6940. doi:10.1002/anie.201001865
19. Díez-González, S.; Marion, N.; Nolan, S. P. *Chem. Rev.* **2009,** *109,* 3612. doi:10.1021/cr900074m
20. Glorius, F., Ed. *N-Heterocyclic Carbenes in Transition Metal Catalysis;* Springer: Berlin, Heidelberg, 2007.
21. Meiries, S.; Le Duc, G.; Chartoire, A.; Collado, A.; Speck, K.; Arachchige, K. S. A.; Slawin, A. M. Z.; Nolan, S. P. *Chem. – Eur. J.* **2013,** *19,* 17358. doi:10.1002/chem.201302471
22. Jafarpour, L.; Stevens, E. D.; Nolan, S. P. *J. Organomet. Chem.* **2000,** *606,* 49. doi:10.1016/S0022-328X(00)00260-6
23. Würtz, S.; Lohre, C.; Fröhlich, R.; Bergander, K.; Glorius, F. *J. Am. Chem. Soc.* **2009,** *131,* 8344. doi:10.1021/ja901018g
24. Würtz, S.; Glorius, F. *Acc. Chem. Res.* **2008,** *41,* 1523. doi:10.1021/ar8000876

25. Altenhoff, G.; Goddard, R.; Lehmann, C. W.; Glorius, F. *J. Am. Chem. Soc.* **2004,** *126,* 15195. doi:10.1021/ja045349r
26. Altenhoff, G.; Goddard, R.; Lehmann, C. W.; Glorius, F. *Angew. Chem., Int. Ed.* **2003,** *42,* 3690. doi:10.1002/anie.200351325
27. Soleilhavoup, M.; Bertrand, G. *Acc. Chem. Res.* **2015,** *48,* 256. doi:10.1021/ar5003494
28. Chartoire, A.; Lesieur, M.; Falivene, L.; Slawin, A. M. Z.; Cavallo, L.; Cazin, C. S. J.; Nolan, S. P. *Chem. – Eur. J.* **2012,** *18,* 4517. doi:10.1002/chem.201104009
29. Chartoire, A.; Frogneux, X.; Nolan, S. P. *Adv. Synth. Catal.* **2012,** *354,* 1897. doi:10.1002/adsc.201200207
30. Berthon-Gelloz, G.; Siegler, M. A.; Spek, A. L.; Tinant, B.; Reek, J. N. H.; Markó, I. E. *Dalton Trans.* **2010,** *39,* 1444. doi:10.1039/B921894G
31. Lavallo, V.; Canac, Y.; Präsang, C.; Donnadieu, B.; Bertrand, G. *Angew. Chem., Int. Ed.* **2005,** *44,* 5705. doi:10.1002/anie.200501841
32. Groombridge, B. J.; Goldup, S. M.; Larrosa, I. *Chem. Commun.* **2015,** *51,* 3832. doi:10.1039/C4CC08920K
33. Sharif, S.; Rucker, R. P.; Chandrasoma, N.; Mitchell, D.; Rodriguez, M. J.; Froese, R. D. J.; Organ, M. G. *Angew. Chem., Int. Ed.* **2015,** *54,* 9507–9511. doi:10.1002/anie.201502822
34. Marelli, E.; Corpet, M.; Davies, S. R.; Nolan, S. P. *Chem. – Eur. J.* **2014,** *20,* 17272. doi:10.1002/chem.201404900
35. Pompeo, M.; Farmer, J. L.; Froese, R. D. J.; Organ, M. G. *Angew. Chem., Int. Ed.* **2014,** *53,* 3223. doi:10.1002/anie.201310457
36. Suzuki, Y.; Fukui, N.; Murakami, K.; Yorimitsu, H.; Osuka, A. *Asian J. Org. Chem.* **2013,** *2,* 1066. doi:10.1002/ajoc.201300162
37. Hoi, K. H.; Coggan, J. A.; Organ, M. G. *Chem. – Eur. J.* **2013,** *19,* 843. doi:10.1002/chem.201203379
38. Le Duc, G.; Meiries, S.; Nolan, S. P. *Organometallics* **2013,** *32,* 7547. doi:10.1021/om4010143
39. Valente, C.; Çalimsiz, S.; Hoi, K. H.; Mallik, D.; Sayah, M.; Organ, M. G. *Angew. Chem., Int. Ed.* **2012,** *51,* 3314. doi:10.1002/anie.201106131
And references therein.
40. Organ, M. G.; Çalimsiz, S.; Sayah, M.; Hoi, K. H.; Lough, A. J. *Angew. Chem., Int. Ed.* **2009,** *48,* 2383. doi:10.1002/anie.200805661
41. Çalimsiz, S.; Sayah, M.; Mallik, D.; Organ, M. G. *Angew. Chem., Int. Ed.* **2010,** *49,* 2014. doi:10.1002/anie.200906811
42. Collado, A.; Balogh, J.; Meiries, S.; Slawin, A. M. Z.; Falivene, L.; Cavallo, L.; Nolan, S. P. *Organometallics* **2013,** *32,* 3249. doi:10.1021/om400168b
43. Poater, A.; Cosenza, B.; Correa, A.; Giudice, S.; Ragone, F.; Scarano, V.; Cavallo, L. *Eur. J. Inorg. Chem.* **2009,** 1759. doi:10.1002/ejic.200801160
44. This software is available free of charge at http://www.molnac.unisa.it/OMtools.php.
45. Patrick, S. R.; Collado, A.; Meiries, S.; Slawin, A. M. Z.; Nolan, S. P. *J. Organomet. Chem.* **2015,** *775,* 152. doi:10.1016/j.jorganchem.2014.04.022
46. Ricard, L.; Gagosz, F. *Organometallics* **2007,** *26,* 4704. doi:10.1021/om7006002
47. Mézailles, N.; Ricard, L.; Gagosz, F. *Org. Lett.* **2005,** *7,* 4133. doi:10.1021/ol0515917
48. Gaillard, S.; Slawin, A. M. Z.; Nolan, S. P. *Chem. Commun.* **2010,** *46,* 2742. doi:10.1039/c0cc00018c
49. Gasperini, D.; Collado, A.; Goméz-Suárez, A.; Cordes, D. B.; Slawin, A. M. Z.; Nolan, S. P. *Chem. – Eur. J.* **2015,** *21,* 5403. doi:10.1002/chem.201406543
50. Gómez-Suárez, A.; Ramón, R. S.; Songis, O.; Slawin, A. M. Z.; Cazin, C. S. J.; Nolan, S. P. *Organometallics* **2011,** *30,* 5463. doi:10.1021/om200705y
51. Wang, Y.; Wang, Z.; Li, Y.; Wu, G.; Cao, Z.; Zhang, L. *Nat. Commun.* **2014,** *5,* 3470. doi:10.1038/ncomms4470
52. Gómez-Suárez, A.; Oonishi, Y.; Meiries, S.; Nolan, S. P. *Organometallics* **2013,** *32,* 1106. doi:10.1021/om301249r
53. Nun, P.; Ramón, R. S.; Gaillard, S.; Nolan, S. P. *J. Organomet. Chem.* **2011,** *696,* 7. doi:10.1016/j.jorganchem.2010.08.052
54. Czégéni, C. E.; Papp, G.; Kathó, Á.; Joó, F. *J. Mol. Catal. A: Chem.* **2011,** *340,* 1. doi:10.1016/j.molcata.2011.03.009
55. Leyva, A.; Corma, A. *J. Org. Chem.* **2009,** *74,* 2067. doi:10.1021/jo802558e
56. Marion, N.; Ramón, R. S.; Nolan, S. P. *J. Am. Chem. Soc.* **2008,** *131,* 448. doi:10.1021/ja809403e
57. Sanz, S.; Jones, L. A.; Mohr, F.; Laguna, M. *Organometallics* **2007,** *26,* 952. doi:10.1021/om060821y
58. Mizushima, E.; Sato, K.; Hayashi, T.; Tanaka, M. *Angew. Chem., Int. Ed.* **2002,** *41,* 4563. doi:10.1002/1521-3773(20021202)41:23<4563::AID-ANIE4563>3.0.CO;2-U
59. Ramón, R. S.; Gaillard, S.; Poater, A.; Cavallo, L.; Slawin, A. M. Z.; Nolan, S. P. *Chem. – Eur. J.* **2011,** *17,* 1238. doi:10.1002/chem.201002607
60. Ramón, R. S.; Marion, N.; Nolan, S. P. *Chem. – Eur. J.* **2009,** *15,* 8695. doi:10.1002/chem.200901231
61. Gómez-Suárez, A.; Gasperini, D.; Vummaleti, S. V. C.; Poater, A.; Cavallo, L.; Nolan, S. P. *ACS Catal.* **2014,** *4,* 2701. doi:10.1021/cs500806m
62. Ketcham, J. M.; Biannic, B.; Aponick, A. *Chem. Commun.* **2013,** *49,* 4157. doi:10.1039/C2CC37166A

License and Terms

BEILSTEIN JOURNAL OF ORGANIC CHEMISTRY

Half-sandwich nickel(II) complexes bearing 1,3-di(cycloalkyl)imidazol-2-ylidene ligands

Johnathon Yau, Kaarel E. Hunt, Laura McDougall, Alan R. Kennedy and David J. Nelson*

Full Research Paper

Open Access

Address:
WestCHEM Department of Pure and Applied Chemistry, University of Strathclyde, Thomas Graham Building, 295 Cathedral Street, Glasgow G1 1XL, UK

Email:
David J. Nelson* - david.nelson@strath.ac.uk

* Corresponding author

Keywords:
catalysis; cross-coupling; *N*-heterocyclic carbenes; nickel

Beilstein J. Org. Chem. **2015,** *11,* 2171–2178.
doi:10.3762/bjoc.11.235

Received: 07 September 2015
Accepted: 27 October 2015
Published: 12 November 2015

This article is part of the Thematic Series "N-Heterocyclic carbenes".

Guest Editor: S. P. Nolan

Abstract

Two new nickel catalysts have been prepared using a convenient procedure where nickelocene, the NHC·HBF_4 salts, and $[Et_4N]Cl$ were heated in THF using microwave irradiation. The resulting [NiCl(Cp)(NHC)] complexes are air- and moisture stable in the solid state, and represent two new members of this valuable and practical class of nickel catalysts. The new species were fully characterised using methods including NMR spectroscopy and X-ray crystallography. When tested in model Suzuki–Miyaura cross-coupling reactions, these complexes were found to be active for the cross-coupling of aryl bromides and aryl chlorides.

Introduction

Nickel catalysis is currently an area of great interest, due to the potential for nickel to replace palladium in some catalytic processes, as well as its ability to perform a much wider range of reactions [1]. Nickel complexes bearing N-heterocyclic carbenes (NHCs) [2] are an interesting class of catalysts [3,4], due to the fascinating characteristics of NHC ligands, which can be designed to have a wide range of steric and electronic properties [5-7]. Nickel catalysts of the form [Ni(Cp)X(NHC)] have been shown to be versatile and relatively easy-to-handle nickel pre-catalysts for a range of transformations; these species are typically stable to air and moisture in the solid state and are therefore practical and accessible catalysts for a range of researchers [8]. Initial complexes of this motif were disclosed by Cowley and Jones, who prepared [Ni(η^1-Cp)(η^5-Cp)(IMes)] (**1**) from the reaction of the free carbene with nickelocene (IMes = 1,3-bis(2,4,6-trimethylphenyl)imidazol-2-ylidene) (Scheme 1a) [9]. Complexes of the form [NiCl(Cp)(NHC)], such as complex **2**, are typically prepared by simply heating nickelocene with the corresponding NHC·HCl salt, rendering these species highly accessible (Scheme 1b) [10]. After the initial work by Cowley and Jones, various other researchers have disclosed complexes of this form and tested them in cross-coupling reactions such as Buchwald–Hartwig amination [11], Suzuki–Miyaura cross-coupling [12], and ketone α-arylation [3,13]. These species can also catalyse hydrosilylation reactions [14].

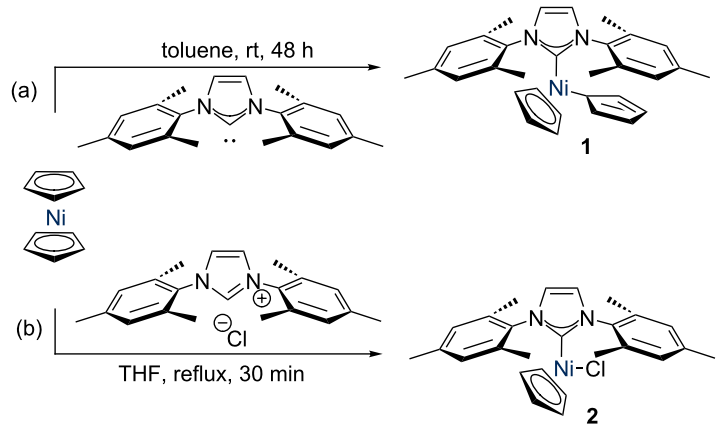

Scheme 1: Synthesis of [Ni(η^1-Cp)(η^5-Cp)(IMes)] (**1**) and [NiCl(Cp)(IMes)] (**2**).

Chatani and co-workers have recently reported that ICy (ICy = 1,3-dicyclohexylimidazol-2-ylidene) is a superior ligand for the cross-coupling of aryl and benzyl methyl ethers with aryl-boronic acid esters, when used as the HCl or HBF_4 salt combined with [Ni(COD)$_2$] [15-17]. In addition, a [Ni(OAc)$_2$]/ICy·HCl system was found to allow the cross-coupling of Grignard reagents with aryl ethers [18].

However, the identity of the active catalyst, which is formed in situ in these reactions, is as yet unknown, and might be a mono- or bis-NHC complex. We therefore decided to prepare and test [NiCl(Cp)(ICy)] (**3**) (closely related to [NiCl(Cp)(IDD)] (**4**)) in some model catalytic reactions, to discover whether the favourable properties of ICy in cross-coupling catalysis could be combined with the ease of synthesis and handling of the nickel half-sandwich motif. Advantages to the use of well-defined catalytic species include that the catalyst and ligand are delivered in a specific and known ratio (in this case 1:1), and that there is no need for a 'pre-reaction' to combine ligand and metal which are both typically added in relatively low concentrations.

Results and Discussion

Catalyst synthesis

Nolan reported that the ICy and I*t*-Bu complexes could not be prepared by heating nickelocene with NHC·HCl salts (I*t*-Bu = 1,3-di-*tert*-butylimidazol-2-ylidene) [19]. In addition, these salts are highly hygroscopic, and therefore difficult to prepare and purify. The tetrafluoroborate salts can be prepared in a one-pot procedure and are easy-to-handle non-hygroscopic white powders, so our first aim was to synthesise the target complexes from NHC·HBF_4 and nickelocene. We were pleased to find that we could prepare [NiCl(Cp)(ICy)] (**3**) by adding [Et$_4$N]Cl to a suspension of ICy·HBF_4 and [Ni(Cp)$_2$] in THF and heating the suspension at reflux for 6 h under an argon atmosphere (Scheme 2), in a manner analogous to that recently reported by Albrecht for the synthesis of triazolylidene-based complexes [20]. However, the yield was rather poor (ca. 20%), so a better route was desired. Changing the solvent to refluxing anhydrous 1,4-dioxane did not improve yields, nor did increased reaction times, or the use of a slight excess of nickelocene. We suspected that the product might be thermally unstable in solution, and that competing decomposition might be reducing the yield. To test this, a purified sample of **3** was subjected to [Et$_4$N]Cl in refluxing anhydrous 1,4-dioxane for 6 h; the deep red solution turned pale and yielded a black precipitate, confirming this hypothesis.

Navarro reported that [NiCl(Cp)(NHC)] complexes can be prepared in much shorter reaction times by using microwave heating [21]. As the microwave apparatus heats the solvent directly, rather than applying heat to the outer walls of a glass vessel, it was proposed that this might allow for better yields. Optimisation of the reaction conditions (20 min at 110 °C in

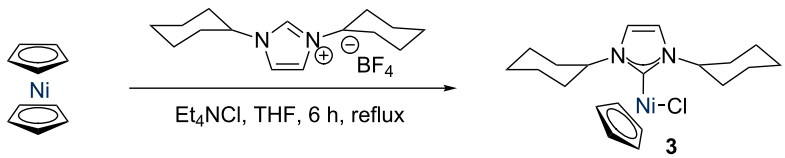

Scheme 2: Synthesis of [NiCl(Cp)(ICy)] using conventional heating.

THF with 1.5 equiv nickelocene) allowed complex **3** to be isolated after work-up in analytically pure form, in 66% yield (Scheme 3a). Slightly lower yields were obtained when less nickelocene was added (43% yield, 1.1 equiv), while a further increase in stoichiometry to 2 equiv did not improve the yield.

With this new complex in hand, structurally similar examples were approached using the same methodology. IDD is a larger analogue of ICy (IDD = 1,3-dicyclododecylimidazol-2-ylidene) [22]; while it typically presents a similar steric profile to ICy in calculations of percent buried volume (% V_{bur}) using solid state structures [6], it is much larger and more flexible. I*t*-Bu possesses significant steric bulk close to the metal centre, and has been known to allow the isolation of the interesting 16 electron three-coordinated [Ni(CO)$_2$(I*t*-Bu)] complex (I*t*-Bu = 1,3-di-*tert*-butylimidazol-2-ylidene) [23]. It has also been reported to trigger spontaneous C–H activation upon coordination to Rh(I) and Ir(I) complexes, leading to 14 electron Rh(III) and Ir(III) species [24,25]. While the methodology applied to ICy worked for IDD (Scheme 3b), repeated attempts to isolate the I*t*-Bu analogue were unsuccessful. Similarly, attempts to first prepare [Ni(η^1-Cp)(η^5-Cp)(I*t*-Bu)] by the reaction of free I*t*-Bu with [NiCp$_2$] (analogous to Cowley's method) [9], envisaging subsequent replacement of the Cp ligand with chloride, were not successful.

The two new complexes were characterised by ^{1}H and ^{13}C{^{1}H} NMR spectroscopy, elemental analysis and X-ray crystallography (Figure 1). Selected crystallographic data can be found in Table 1, and some key bond lengths in Table 2. X-ray quality crystals were obtained by slow diffusion of pentane into a DCM solution of each complex.

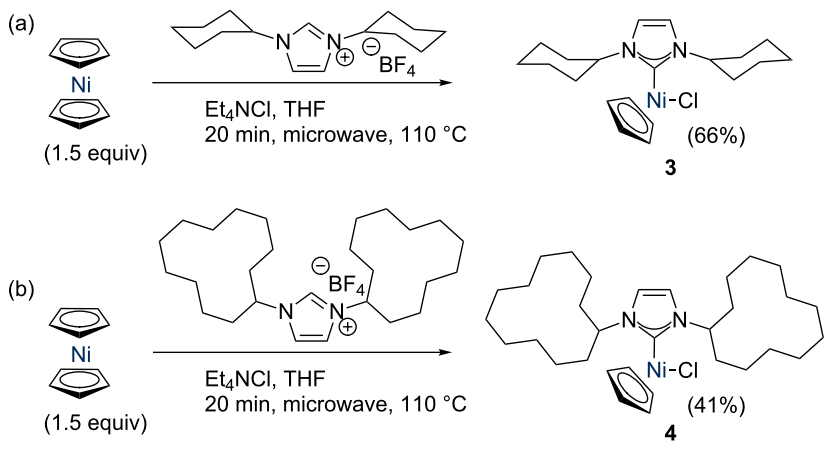

Scheme 3: Synthesis of (a) [NiCl(Cp)(ICy)] (**3**) and (b) [NiCl(Cp)(IDD)] (**4**) with microwave heating.

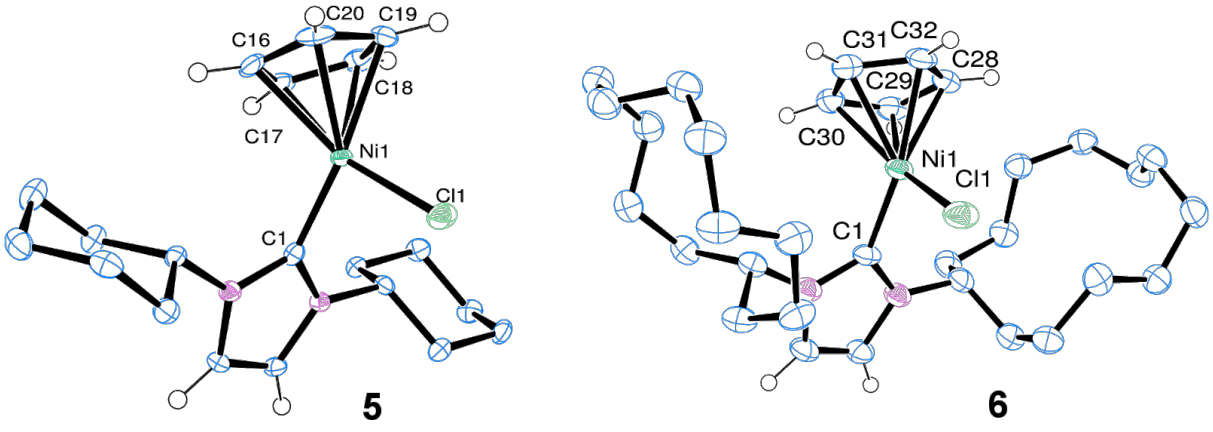

Figure 1: Molecular structures of complexes [NiCl(Cp)(ICy)] (**3**) (left) and [NiCl(Cp)(IDD)] (**4**) (right) as determined by single crystal X-ray diffraction. Displacement ellipsoids are drawn at 50% probability. Most H atoms are excluded for clarity.

Table 1: Experimental data for single-crystal X-ray diffraction analyses of [NiCl(Cp)(ICy)] and [NiCl(Cp)(IDD)].

Structure	[NiCl(Cp)(ICy)] (**3**)	[NiCl(Cp)(IDD)] (**4**)
CCDC ref.	1049879	1049880
Formula	$C_{20}H_{29}ClN_2Ni$	$C_{32}H_{53}ClN_2Ni$
Formula wt	391.61 g mol^{-1}	559.92 g mol^{-1}
Crystal system	orthorhombic	monoclinic
a	16.3306(3) Å	8.5685(2) Å
b	10.2549(2) Å	13.9639(3) Å
c	11.1879(2) Å	25.1631(6) Å
β	90°	97.719(2)°
V	1873.62(6) Å^3	2983.48(12) Å^3
Space group	$Pca2_1$	$P2_1/n$
Z	4	4
μ	1.182 mm^{-1}	1.912 mm^{-1}
Reflns collected	8979	11638
Reflns unique	4499	5828
Reflns observed	4029	4521
R_{int}	0.0316	0.0313
Goodness of fit	1.021	1.036
R1 ($I > 2\sigma(I)$)	0.0336	0.0427
wR2	0.0683	0.1145

Table 2: Selected bond distances (units Å).

[NiCl(Cp)(ICy)] (**3**)		[NiCl(Cp)(IDD)] (**4**)	
Ni(1)–Cl(1)	2.1884(7)	Ni(1)–Cl(1)	2.1833(7)
Ni(1)–C(16)	2.136(3)	Ni(1)–C(28)	2.181(2)
Ni(1)–C(17)	2.056(3)	Ni(1)–C(29)	2.095(2)
Ni(1)–C(18)	2.160(3)	Ni(1)–C(30)	2.091(2)
Ni(1)–C(19)	2.137(3)	Ni(1)–C(31)	2.181(2)
Ni(1)–C(20)	2.192(3)	Ni(1)–C(32)	2.142(2)

The ^{1}H NMR spectra show the expected features; a sharp singlet for the cyclopentadienyl ligand in each complex suggests that this ligand rotates faster than the NMR timescale, while a sharp singlet was also observed for the imidazol-2-ylidene backbone protons. The cycloalkyl nature of the N-substituents results in most of the proton signals for these species appearing as broad multiplets, even at high fields. The methine signal for the cycloalkyl substituents is discrete, appearing at δ_H = 6.01 ppm for ICy and δ_H = 6.28 ppm for IDD as a triplet of triplets and an apparent quintet, respectively. In the carbon NMR spectra, the imidazol-2-ylidene C2 signals resonate at δ_C = 157.0 ppm (ICy) or 158.0 ppm (IDD), compared to ca. 200 ppm for complexes of saturated *N*,*N*-diarylimidazol-2-ylidenes and ca. 170 ppm for their unsaturated counterparts [19]. This difference in δ_C might result from the larger net electron-donating ability of ICy and IDD, as inferred from their lower TEP compared to IPr, IMes, and IPr*, for example [7,26,27].

The crystal structure data for [NiCl(Cp)(ICy)] (**3**) reveal five different Ni–C distances between the nickel centre and the cyclopentadienyl ligand, spanning a range of ca. 0.14 Å. These bond lengths are indicative of distortion from ideal η^5-geometry towards η^1,η^4-geometry (Table 2) [28]. In [NiCl(Cp)(IDD)] (**4**), the distances span a smaller range (ca. 0.09 Å). In both cases, the Cl–Ni–C1 angle is ca. 93–94°. The cyclohexyl rings adopt a chair conformation, while the cyclododecyl rings droop down around the metal centre, with the shortest Cl–H distance being ca. 2.9 Å, approximately the sum of van der Waals radii of the two atoms.

Assessment of catalytic activity

With these new complexes in hand, their activity in some model cross-coupling reactions was examined. Ritleng and Chetcuti have deployed [Ni(Cp)(X)(NHC)] complexes in Suzuki–Miyaura cross-coupling reactions of 4'-bromoacetophenone and 4'-chloroacetophenone with phenylboronic acid (Scheme 4) [12]. It was therefore decided to study these reactions as part of our preliminary evaluation of these new complexes as potential pre-catalysts for cross-coupling reactions. The reactions were conducted in duplicate, and were analysed by ^{1}H NMR methods to calculate conversion. The new ICy- and IDD-bearing complexes were benchmarked against [NiCl(Cp)(IPr)] (**5**) due to the ubiquity of this carbene in transition metal-mediated catalysis [29,30], and [NiCl(Cp)(IPr*)] (**6**) and [NiCl(Cp)(IPr*^{OMe})] (**7**) due to their demonstrated competence as catalysts for the arylation of anilines [11].

The results from the cross-coupling reactions with 4'-bromo- and 4'-chloroacetophenone are summarised in Table 3; running the latter reaction for more than 2 h did not lead to significant increases in conversion.

Unfortunately, we were unable to reproduce the literature conversion with [NiCl(Cp)(IPr)] (87%) despite multiple attempts by different chemists. Different batches of toluene and base (with different water content) were screened, but we consistently achieved much lower conversions. Nevertheless, this provided a platform from which we could assess the new catalysts.

Surprisingly, the IPr* and IPr*^{OMe}-bearing complexes performed rather poorly under these conditions. It was noted that in the Suzuki–Miyaura reactions, the catalysts bearing ICy or IDD changed colour (pink to orange-brown) more quickly, which may be suggestive of faster initiation.

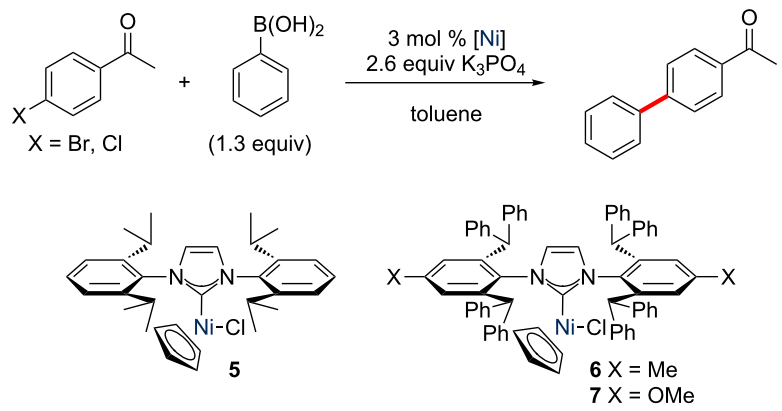

Scheme 4: Model Suzuki–Miyaura reaction for the evaluation of the new complexes as cross-coupling pre-catalysts.

Table 3: Results of test reactions with 4'-bromo- and 4'-chloroacetophenone, conducted using the conditions detailed in Scheme 4.[a]

Complex	X = Br	X = Cl		
	90 °C, 0.5 h	110 °C, 0.5 h	110 °C, 2 h	110 °C, 4 h
[NiCl(Cp)(IPr)] (**5**)	41%	39%	39%	39%
[NiCl(Cp)(ICy)] (**3**)	69%	38%	49%	65%
[NiCl(Cp)(IDD)] (**4**)	40%	43%	53%	54%
[NiCl(Cp)(IPr*)] (**6**)	22%	20%	27%	ND[b]
[NiCl(Cp)(IPr*^{OMe})] (**7**)	32%	ND[b]	ND[b]	ND[b]

[a]All reactions conducted with 3 mol % of pre-catalyst. The conversion to the cross-coupling product was determined in each case by integration of the ^{1}H NMR spectrum of the reaction mixture. Quoted results are an average of at least two independent experiments. [b]Not determined.

Intrigued as to whether the more electron-donating nature of ICy and IDD, as inferred from their lower TEP [22,31], might influence their oxidative addition reactivity, the cross-coupling of 4'-chloroacetophenone and phenylboronic acid was investigated. These experiments suggest that the ICy and IDD complexes are indeed slightly better catalysts for the cross-coupling of more challenging electrophiles. However, extension of these studies to 4-chloroanisole which is a challenging and electron-rich aryl chloride substrate, led to disappointing conversions (ca. 15% with [NiCl(Cp)(ICy)] (**3**)). This may be due to the thermal sensitivity of these complexes, or may suggest that the active species in Chatani's work is in fact a bis(NHC) complex. Further work is underway in our laboratory to understand the effect of NHC structure on cross-coupling reactivity, and to prepare and evaluate bis(ICy) complexes in catalysis.

Conclusion

We have prepared two new half-sandwich Ni(II) complexes, which until recently had been missing relatives in this practical and useful family of pre-catalysts. X-ray crystallographic analyses suggest a tendency towards η^1,η^4-coordination of the cyclopentadienyl ligand.

Preliminary catalyst testing in model Suzuki–Miyaura reactions suggest that these more electron-donating ligands yield complexes that are slightly more active for the cross-coupling of aryl chlorides but less thermally stable. Further studies to fully explore and apply the reactivity of the new complexes are presently underway in our laboratory.

Experimental

General. ICy·HBF$_4$ and I*t*-Bu·HBF$_4$ were prepared according to literature procedures [22,25]. Complexes [NiCl(Cp)(IPr)], [NiCl(Cp)(IPr*)] and [NiCl(Cp)(IPr*^{OMe})] were prepared according to literature procedures [11,19]. Nickelocene was purchased from Strem or Alfa Aesar and stored at −40 °C in the glovebox freezer. Anhydrous, oxygen-free THF and toluene were obtained from an Innovative Technologies PureSolv system (<10 ppm H_2O, as measured by regular Karl Fischer analyses). Anhydrous 1,4-dioxane was obtained from Sigma-Aldrich and sparged with argon before use. [Et$_4$N]Cl was

purchased from Alfa Aesar and dried by heating under vacuum. Reactions under microwave irradiation were carried out using a Biotage apparatus in crimp-cap microwave vials equipped with magnetic stirrer bars.

NMR spectra were acquired using Bruker AV3-400, AV-400, AV3-500HD and AVII-600 spectrometers at 300 K. ^{1}H NMR chemical shifts are reported in ppm referenced to residual solvent signals, while ^{13}C{^{1}H} NMR chemical shifts are reported referenced to deuterated solvent signals [32]. 2D experiments such as [^{1}H,^{1}H] COSY, [^{1}H,^{13}C] HSQC and [^{1}H,^{13}C] HMBC were used where necessary to assign chemical shifts. Elemental analyses were conducted using a Perkin Elmer 2400 Series II instrument. X-ray crystallographic analyses were undertaken with samples mounted in oil at 123(2) K using an Oxford Diffraction diffractometer equipped with a CCD detector. All structures were refined against F^2 and to convergence using all unique reflections and the program Shelxl-97 [33].

IDD·HBF$_4$. Paraformaldehyde (411 mg, 13.7 mmol) was suspended in toluene (25 mL) and cyclododecylamine (2.51 g, 13.7 mmol) was added. The reaction was stirred at room temperature for 3 h, and then cooled to 0 °C in an ice bath. A further portion of cyclododecylamine (2.48 g, 13.5 mmol) was added, followed by the careful addition of aqueous HBF_4 solution (48 wt %, 2 mL, 1.34 g, 15.3 mmol). After the reaction was warmed to room temperature, aqueous glyoxal solution (40 wt %, 2 mL, 1.01 g, 17.4 mmol) was added and the reaction was heated to 40 °C and stirred vigorously overnight. The reaction was quenched with sat. aqueous $NaHCO_3$ solution and filtered on a sintered frit. The resulting solid was washed on the frit with diethyl ether until the solid was white. Drying in a vacuum oven overnight at 50 °C yielded the title compound as a free-flowing white solid. Yield: 6.32 g (12.9 mmol, 95%). ^{1}H NMR ($CDCl_3$, 400 MHz) δ_H 9.13 (s, 1H, NCHN), 7.30 (s, 2H, N(CH)$_2$N), 4.58 (quint., $^3J_{HH}$ = 5.6 Hz, 2H, NCHR$_2$), 2.16–2.00 (m, 4H, CH$_2$), 1.82–1.71 (m, 4H, CH$_2$), 1.56–1.24 (m, 36H, CH$_2$); ^{13}C{^{1}H} NMR ($CDCl_3$, 151 MHz) δ_C 134.5 (NCN), 120.9 (N(CH)$_2$N), 59.0 (NCHR$_2$), 30.4 (CH$_2$), 23.6 (CH$_2$), 23.5 (CH$_2$), 23.4 (CH$_2$), 21.5 (CH$_2$). Even at high field (14.1 T), not all CH$_2$ signals could be successfully resolved. Anal. calcd. for $C_{27}H_{49}BF_4N_2$: C, 66.39; H, 10.11; N, 5.73; found: C, 65.96; H, 10.47; N, 5.76;

[NiCl(Cp)(ICy)]. In the glovebox, a microwave vial with stir bar was charged with nickelocene (75.1 mg, 0.398 mmol, 1.5 equiv), ICy·HBF_4 (84.6 mg, 0.263 mmol, 1 equiv) and [Et_4N]Cl (43.7 mg, 0.264 mmol, 1 equiv) and the cap was secured with parafilm. Outside the glovebox, under a flow of argon, anhydrous THF (3 mL) was added and the vial was sealed with a crimp cap. The reaction was heated to 110 °C for 20 min in the microwave, during which time the solution changed the colour from green to red/purple. The THF was removed and the residue was taken up in hot toluene and filtered. The volume was reduced to ca. 1 mL, and then hexane was added to precipitate the product. The green solution was decanted, and the solid was washed with hexane and dried under high vacuum to yield the product as a pink powder. Yield: 68.6 mg (0.175 mmol, 66%). ^{1}H NMR ($CDCl_3$, 400 MHz) δ_H 6.94 (s, 2H, N(CH)$_2$N), 6.01 (tt, $^3J_{HH}$ = 12, 3.9 Hz, 2H, NCHR$_2$), 5.20 (s, 5H, CpH), 2.49–2.36 (m, 2H, Cy CH$_2$), 2.10–1.92 (m, 6H, Cy CH$_2$), 1.92–1.83 (m, 2H, Cy CH$_2$), 1.81–1.47 (m, 8H, Cy CH$_2$), 1.38–1.22 (2H, m, Cy CH$_2$); ^{13}C{^{1}H} NMR ($CDCl_3$, 101 MHz) δ_C 157.0 (NCN), 118.9 (N(CH)$_2$N), 91.6 (Cp CH), 61.1 (NCHR$_2$), 34.4 (Cy CH$_2$), 34.1 (Cy CH$_2$), 26.0 (Cy CH$_2$), 25.8 (Cy CH$_2$), 25.5 (Cy CH$_2$); Anal. calcd. for $C_{20}H_{29}ClN_2Ni$: C, 61.34; H, 7.46; N, 7.15; found: C, 61.10; H, 7.41; N, 6.84.

[NiCl(Cp)(IDD)]. In the glovebox, a microwave vial with stir bar was charged with nickelocene (100.0 mg, 0.529 mmol, 1.5 equiv), IDD·HBF_4 (172.6 mg, 0.353 mmol, 1 equiv) and [Et_4N]Cl (58.4 mg, 0.352 mmol, 1 equiv) and the cap was secured with parafilm. Outside the glovebox, under a flow of argon, anhydrous THF (5 mL) was added and the vial was sealed with a crimp cap. The reaction was heated to 110 °C for 20 min in the microwave, during which time the solution changed the colour from green to red. The solvent was removed and the residue was taken up in hot toluene and filtered. The volume was reduced to ca. 1 mL, and then hexane was added to precipitate the product. The green solution was decanted, and the solid was washed with hexane and dried under high vacuum, to yield the product as a pink powder. Yield: 81.9 mg (0.146 mmol, 41%). ^{1}H NMR ($CDCl_3$, 400 MHz) δ_H 6.95 (s, 2H, N(CH)$_2$N), 6.28 (app. quint., $^2J_{HH}$ = 5.9 Hz, 2H, NCHR$_2$), 5.21 (s, 5H, CpH), 2.09–1.91 (m, 4H, CH$_2$), 1.91–1.73 (m, 6H, CH$_2$), 1.73–1.39 (m, 34H, CH$_2$); ^{13}C{^{1}H} NMR ($CDCl_3$, 150 MHz) δ_C 158.0 (NCN), 119.6 (N(CH)$_2$N), 91.8 (Cp CH), 59.2 (NCHR$_2$), 31.4 (CDD CH$_2$), 31.2 (CDD CH$_2$), 24.3 (CDD CH$_2$), 24.1 (CDD CH$_2$), 23.9 (CDD CH$_2$), 23.81 (CDD CH$_2$), 23.78 (CDD CH$_2$), 23.5 (CDD CH$_2$), 22.5 (CDD CH$_2$), 22.1 (CDD CH$_2$); Anal. calcd. for $C_{32}H_{53}ClN_2Ni$: C, 68.64; H, 9.54; N, 5.00; found: C, 68.54; H, 9.64; N, 4.88.

General procedure for Suzuki–Miyaura reactions. A reaction tube or Schlenk flask was charged with 4'-bromoacetophenone or 4'-chloroacetophenone (1 mmol), $PhB(OH)_2$ (1.3 mmol, 1.3 equiv), nickel complex and K_3PO_4 (2.6 mmol, 2.6 equiv) and closed with a septum. Anhydrous toluene (3 mL) was added via syringe, and the vial was inserted into a preheated oil bath and stirred vigorously. The septum was removed

and the reaction mixture was filtered through celite and stripped of solvent. A sample of this was then taken up in chloroform-*d* for ^{1}H NMR spectroscopic analysis. Conversion was assessed from the relative integrals of the resonances corresponding to the product at δ_H = 2.63 ppm (4'-phenylacetophenone) and the starting material at δ_H = 2.56 ppm (4'-bromoacetophenone) or δ_H = 2.58 ppm (4'-chloroacetophenone). Slightly lower (by ca. 5%) conversions were obtained in Schlenk flasks versus sealed tubes.

Supporting Information

Supporting Information File 1

Crystal structure data for new complexes.
[http://www.beilstein-journals.org/bjoc/content/supplementary/1860-5397-11-235-S1.cif]

Supporting Information File 2

NMR spectra for compounds and complexes.
[http://www.beilstein-journals.org/bjoc/content/supplementary/1860-5397-11-235-S2.pdf]

Acknowledgements

We thank the University of Strathclyde for funding a Chancellor's Fellowship for DJN, and the Carnegie Trust for funding an Undergraduate Vacation Scholarship for LM. We are grateful to the following specialists and technical staff for their assistance: Mr Craig Irving, Dr John Parkinson (NMR spectroscopy), Mr Alexander Clunie (elemental analyses), Ms Patricia Keating (GC and GC–MS), and Mr Gavin Bain (solvent purification system). We thank Professors Peter Skabara and Nicholas Tomkinson for allowing us to use their microwave equipment, and Professors Jonathan Percy and William Kerr for affording us access to their laboratory apparatus.

References

1. Tasker, S. Z.; Standley, E. A.; Jamison, T. F. *Nature* **2014,** *509,* 299–309. doi:10.1038/nature13274
2. Hopkinson, M. N.; Richter, C.; Schedler, M.; Glorius, F. *Nature* **2014,** *510,* 485–496. doi:10.1038/nature13384
3. Prakasham, A. P.; Ghosh, P. *Inorg. Chim. Acta* **2014,** *431,* 61–100. doi:10.1016/j.ica.2014.11.005
4. Henrion, M.; Ritleng, V.; Chetcuti, M. J. *ACS Catal.* **2015,** *5,* 1283–1302. doi:10.1021/cs5014927
5. Dröge, T.; Glorius, F. *Angew. Chem., Int. Ed.* **2010,** *49,* 6940–6952. doi:10.1002/anie.201001865
6. Clavier, H.; Nolan, S. P. *Chem. Commun.* **2010,** *46,* 841–861. doi:10.1039/b922984a
7. Nelson, D. J.; Nolan, S. P. *Chem. Soc. Rev.* **2013,** *42,* 6723–6753. doi:10.1039/c3cs60146c
8. Nelson, D. J. *Eur. J. Inorg. Chem.* **2015,** 2012–2027. doi:10.1002/ejic.201500061
9. Abernethy, C. D.; Clyburne, J. A. C.; Cowley, A. H.; Jones, R. A. *J. Am. Chem. Soc.* **1999,** *121,* 2329–2330. doi:10.1021/ja983772s
10. Abernethy, C. D.; Cowley, A. H.; Jones, R. A. *J. Organomet. Chem.* **2000,** *596,* 3–5. doi:10.1016/S0022-328X(99)00557-4
11. Martin, A. R.; Makida, Y.; Meiries, S.; Slawin, A. M. Z.; Nolan, S. P. *Organometallics* **2013,** *32,* 6265–6270. doi:10.1021/om4004863
12. Ritleng, V.; Oertel, A. M.; Chetcuti, M. J. *Dalton Trans.* **2010,** *39,* 8153–8160. doi:10.1039/c0dt00021c
13. Henrion, M.; Chetcuti, M. J.; Ritleng, V. *Chem. Commun.* **2014,** *50,* 4624–4627. doi:10.1039/c4cc00959b
14. Postigo, L.; Royo, B. *Adv. Synth. Catal.* **2012,** *354,* 2613–2618. doi:10.1002/adsc.201200389
15. Tobisu, M.; Takahira, T.; Ohtsuki, A.; Chatani, N. *Org. Lett.* **2015,** *17,* 680–683. doi:10.1021/ol503707m
16. Furukawa, T.; Tobisu, M.; Chatani, N. *Chem. Commun.* **2015,** *51,* 6508–6511. doi:10.1039/C5CC01378J
17. Tobisu, M.; Yasutome, A.; Kinuta, H.; Nakamura, K.; Chatani, N. *Org. Lett.* **2014,** *16,* 5572–5575. doi:10.1021/ol502583h
18. Tobisu, M.; Takahira, T.; Chatani, N. *Org. Lett.* **2015,** *17,* 4352–4355. doi:10.1021/acs.orglett.5b02200
19. Kelly, R. A., III; Scott, N. M.; Díez-González, S.; Stevens, E. D.; Nolan, S. P. *Organometallics* **2005,** *24,* 3442–3447. doi:10.1021/om0501879
20. Wei, Y.; Petronilho, A.; Mueller-Bunz, H.; Albrecht, M. *Organometallics* **2014,** *33,* 5834–5844. doi:10.1021/om500593s
21. Landers, B.; Navarro, O. *Inorg. Chim. Acta* **2012,** *380,* 350–353. doi:10.1016/j.ica.2011.09.055
22. Fortman, G. C.; Slawin, A. M. Z.; Nolan, S. P. *Dalton Trans.* **2010,** *39,* 3923–3930. doi:10.1039/c003214j
23. Dorta, R.; Stevens, E. D.; Hoff, C. D.; Nolan, S. P. *J. Am. Chem. Soc.* **2003,** *125,* 10490–10491. doi:10.1021/ja0362151
24. Dorta, R.; Stevens, E. D.; Nolan, S. P. *J. Am. Chem. Soc.* **2004,** *126,* 5054–5055. doi:10.1021/ja049545+
25. Scott, N. M.; Dorta, R.; Stevens, E. D.; Correa, A.; Cavallo, L.; Nolan, S. P. *J. Am. Chem. Soc.* **2005,** *127,* 3516–3526. doi:10.1021/ja043249f
26. Dorta, R.; Stevens, E. D.; Scott, N. M.; Costabile, C.; Cavallo, L.; Hoff, C. D.; Nolan, S. P. *J. Am. Chem. Soc.* **2005,** *127,* 2485–2495. doi:10.1021/ja0438821
27. Balogh, J.; Slawin, A. M. Z.; Nolan, S. P. *Organometallics* **2012,** *31,* 3259–3263. doi:10.1021/om300104j
28. Cross, R. J.; Hoyle, R. W.; Kennedy, A. R.; Manojlović-Muir, L.; Muir, K. W. *J. Organomet. Chem.* **1994,** *468,* 265–271. doi:10.1016/0022-328X(94)80059-6
29. Huang, J.; Nolan, S. P. *J. Am. Chem. Soc.* **1999,** *121,* 9889–9890. doi:10.1021/ja991703n
30. Arduengo, A. J., III; Krafczyk, R.; Schmutzler, R.; Craig, H. A.; Goerlich, J. R.; Marshall, W. J.; Unverzagt, M. *Tetrahedron* **1999,** *55,* 14523–14534. doi:10.1016/S0040-4020(99)00927-8
31. Kelly, R. A., III; Clavier, H.; Giudice, S.; Scott, N. M.; Stevens, E. D.; Bordner, J.; Samardjiev, I.; Hoff, C. D.; Cavallo, L.; Nolan, S. P. *Organometallics* **2008,** *27,* 202–210. doi:10.1021/om701001g
32. Fulmer, G. R.; Miller, A. J. M.; Sherden, N. H.; Gottlieb, H. E.; Nudelman, A.; Stoltz, B. M.; Bercaw, J. E.; Goldberg, K. I. *Organometallics* **2010,** *29,* 2176–2179. doi:10.1021/om100106e
33. Sheldrick, G. M. *Acta Crystallogr., Sect. A* **2008,** *64,* 112–122. doi:10.1107/S0108767307043930

BEILSTEIN JOURNAL OF ORGANIC CHEMISTRY

Evidencing an inner-sphere mechanism for NHC-Au(I)-catalyzed carbene-transfer reactions from ethyl diazoacetate

Manuel R. Fructos, Juan Urbano, M. Mar Díaz-Requejo* and Pedro J. Pérez*

Full Research Paper

Open Access

Address:
Laboratorio de Catálisis Homogénea, Unidad Asociada al CSIC, CIQSO-Centro de Investigación en Química Sostenible and Departamento de Química, Universidad de Huelva, Campus de El Carmen, 21007 Huelva, Spain

Email:
M. Mar Díaz-Requejo* - mmdiaz@dqcm.uhu.es; Pedro J. Pérez* - perez@dqcm.uhu.es

* Corresponding author

Keywords:
carbene transfer; inner sphere; gold catalysis; O–H functionalization; olefin cyclopropanation

Beilstein J. Org. Chem. **2015,** *11,* 2254–2260.
doi:10.3762/bjoc.11.245

Received: 11 September 2015
Accepted: 03 November 2015
Published: 20 November 2015

This article is part of the Thematic Series "N-Heterocyclic carbenes".

Guest Editor: S. P. Nolan

Abstract

Kinetic experiments based on the measurement of nitrogen evolution in the reaction of ethyl diazoacetate (N_2CHCO_2Et, EDA) and styrene or methanol catalyzed by the $[IPrAu]^+$ core (IPr = 1,3-bis(diisopropylphenyl)imidazole-2-ylidene) have provided evidence that the transfer of the carbene group $CHCO_2Et$ to the substrate (styrene or methanol) takes place in the coordination sphere of Au(I) by means of an inner-sphere mechanism, in contrast to the generally accepted proposal of outer-sphere mechanisms for Au(I)-catalyzed reactions.

Introduction

The discovery of the catalytic capabilities of soluble gold(I) species toward the hydration of alkynes by Teles and co-workers [1] is considered as the rising of the golden era for the use of this metal in homogeneous catalysis [2,3]. A number of transformations have been reported to date [4-13], most of them based on a particular feature of gold: a singular carbophilicity that enhances the electrophilic activation of multiple bonds upon coordination followed by subsequent inter- or intramolecular reaction with nucleophiles. Most of the reported systems contain an unsaturated fragment that is activated upon coordination to the gold center, thus triggering further transformations, the formation of very reactive gold–carbene intermediates being proposed [4-14]. As a representative example, the skeletal rearrangement of the [2 + 2] cycloaddition of 1,6-enynes [4] is shown in Scheme 1, where three different gold–carbene intermediates are involved in the possible transformations.

A different reaction in which the formation of gold–carbene intermediates has been proposed arises from the interaction of a gold(I) source and a diazo compound. It was not until 2005 that the first example of this transformation was reported by our

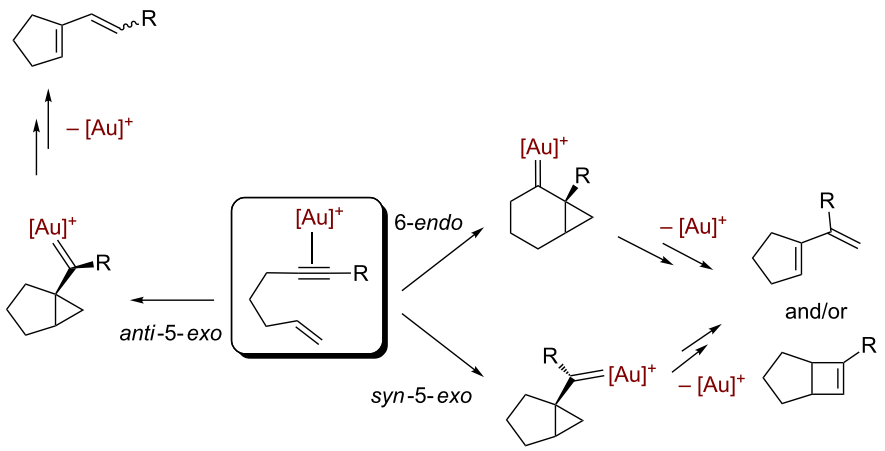

Scheme 1: The Au(I)-catalyzed skeletal rearrangement of the [2 + 2] cycloaddition of 1,6-enynes that involves gold–carbene intermediates.

group [15,16], when the complex IPrAuCl (**1**) (IPr = 1,3-bis(diisopropylphenyl)imidazole-2-ylidene), in the presence of $NaBAr^F_4$ ($BAr^F_4{}^-$ = tetrakis(3,5-bis(trifluoromethyl)phenyl)borate) as a halide scavenger, induced the incorporation of the :$CHCO_2Et$ group from N_2CHCO_2Et to styrene (Scheme 2a) or methanol (Scheme 2b), among others. With the former, in addition to the formation of the expected cyclopropanes, a second type of product was observed, derived from the incorporation of the carbene :$CHCO_2Et$ unit to the C(sp^2)–H bonds. For methanol as the reactant, the ether derived from the functionalization of the O–H bond was obtained.

A transformation related to this contribution is the reaction published by Echavarren (Scheme 3). In this reaction, the complex [LAu(NCR)]SbF_6 (L = tertiary phosphine ligand) abstracted the carbene group :CHPh from a tropilium derivative, and further transferred the gold-bonded carbene group to an olefin [17,18]. This contribution constituted a breakthrough in gold-mediated carbene-transfer reactions since the carbene source lacks of the well-known instability of some of the diazo reagents.

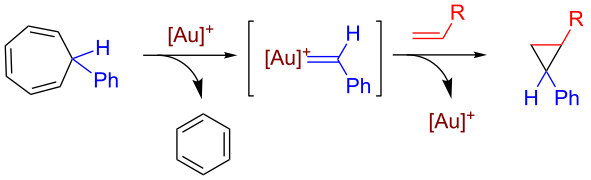

Scheme 3: The gold-promoted decarbenation reaction described by Echavarren and co-workers.

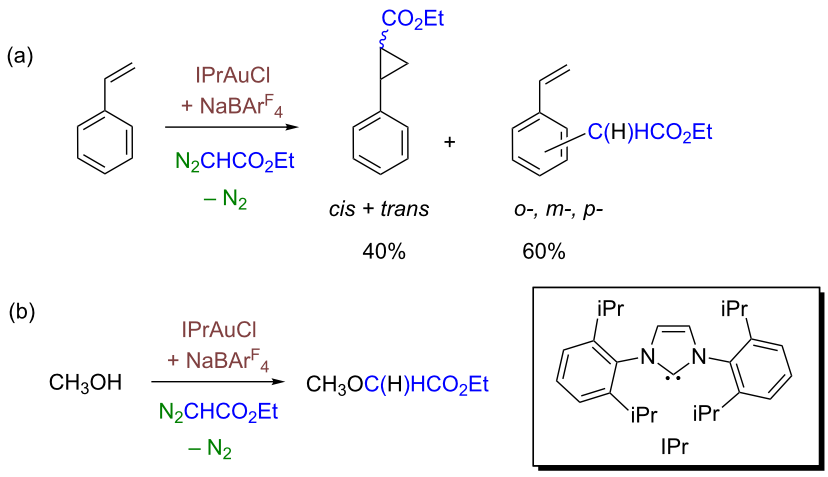

Scheme 2: The catalytic activity of IPrAuCl + $NaBAr^F_4$ in the carbene-transfer reaction to styrene or methanol.

The reactions shown in Scheme 2 and Scheme 3 have been explained through the appearance of a $[LAu{=}CR^1R^2]^+$ intermediate, not detected nor isolated, that further reacts with a non-coordinated nucleophile (i.e., by means of an outer-sphere mechanism). Those intermediates are quite reactive, in contrast to similar but low reactive gold–carbene complexes recently and independently described by the groups of Fürstner [19] and Straub [20]. Scheme 4a shows a generally accepted mechanism for the metal-catalyzed carbene transfer from diazo compounds to nucleophiles [21-27], where the formation of C–C or C–X bonds takes place throughout a transition state in which no interaction of the substrate and the metal center exists (styrene is shown as an example). In many cases, a non-desired side reaction is also observed, in which two molecules of the diazo compound convert into an olefin and/or an azine (Scheme 4b), the second acting as a nucleophile attacking the metallocarbene intermediate [28]. However, our previous studies have shown that this gold-based catalytic system does not induce such non-desired carbene homocoupling [15,16].

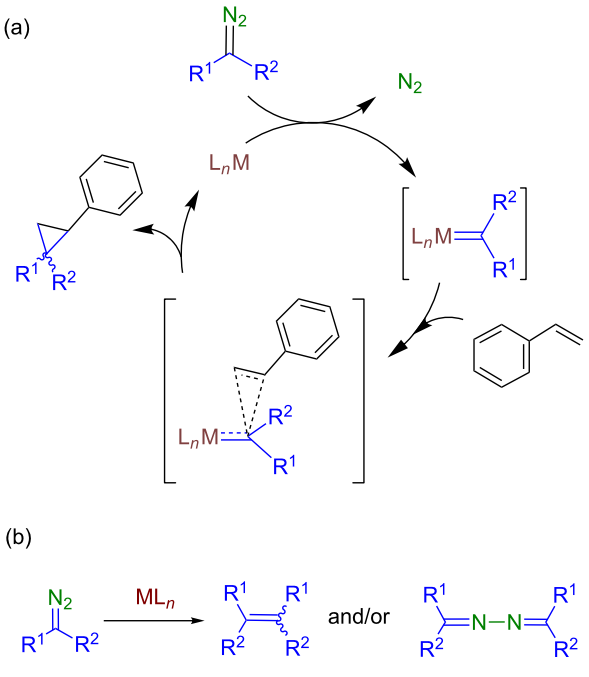

Scheme 4: (a) General representation of the metal-catalyzed carbene-transfer reaction (olefin cyclopropanation). (b) Side-reactions of carbene or diazo coupling commonly observed.

In this contribution we report the results obtained from a kinetic study carried out with the IPrAuCl complex that allows proposing a plausible inner-sphere mechanism in which the substrate (styrene or methanol) seems to remain coordinated to the gold center, a feature that could be extended to many of the reported catalytic systems involving Au(I) complexes.

Results and Discussion

The probe reactions

As mentioned above, we have already described the potential of the system IPrAuCl + $NaBAr^F_4$ to promote the catalytic decomposition of ethyl diazoacetate (N_2CHCO_2Et, EDA) and functionalize styrene or methanol (see Scheme 2). Since molecular nitrogen is evolved in these transformations, we have monitored the pressure above the reaction mixtures of EDA and styrene or methanol in the presence of catalytic amounts (5 mol %) of IPrAuCl + $NaBAr^F_4$. It is worth noting that the catalyst precursors were dissolved in the neat substrate (5 mL) and stirred for 30 min to ensure halide abstraction prior to EDA addition. The experiments have been carried out using a flask connected to a pressure gauge that provides the variation in the increase of the internal pressure (see Experimental). Figure 1 shows the plots of the N_2 concentration (mmol) vs time, from which k_{obs} for N_2 liberation have been obtained as $2.17(0.05) \times 10^{-3}$ s^{-1} and $1.34(0.01) \times 10^{-3}$ s^{-1} for styrene and methanol, respectively. Thus, both reactions decomposed EDA with similar rates within the same order of magnitude. Given the experimental fact that this catalytic system does not promote the carbene coupling side reaction, the amount of measured N_2 exclusively corresponds to that evolved from the formation of the gold–carbene intermediate in the path to the products.

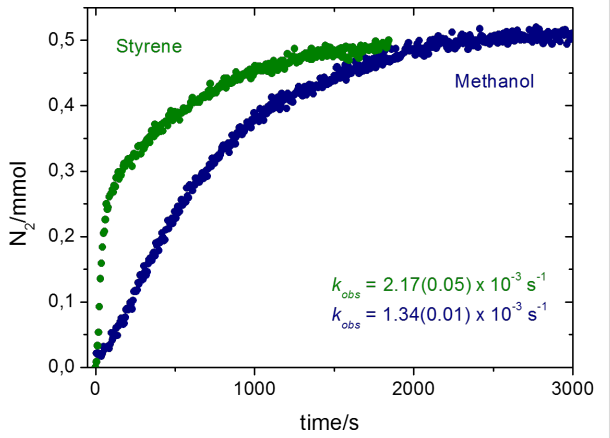

Figure 1: Plot of evolved nitrogen with time for the reactions of EDA with styrene or methanol.

The effect of substrate concentration

A second set of experiments has been performed varying the catalyst to substrate ratio, but maintaining the concentration of the catalyst as a constant. Thus, 100:0, 80:20 and 60:40 v/v mixtures of styrene and cyclohexane, respectively, have been reacted with EDA (0.285 mmol) with the same catalyst precursor (see Experimental). Under these conditions, cyclohexane is much less reactive than styrene and acts as an inert solvent [29]. The kinetic curves for these three experiments are

shown in Figure 2. The plot of k_{obs} vs substrate concentration evidences a direct correlation between styrene concentration and k_{obs}. The same effect is observed in an array of experiments carried out with mixtures of methanol and methylene chloride (Figure 2). These results unambiguously indicate that the release of nitrogen takes place at a faster rate when increasing the amount of the reactant, styrene or methanol.

It is worth mentioning that the addition of 5 equiv of $NaBAr^F{}_4$ did not induce any change in the reaction rate compared with that of one equiv, assessing that the halide-free catalytically-active gold species is available in the latter case. Also, the fact that the same behavior regarding the "dilution effect" shown in Figure 2 is observed with cyclohexane or dichloromethane as dilution agents must be interpreted as the result of their independent behavior in the process, not being involved in any effect relative to polarity or solubility issues.

Mechanistic interpretation

It has been reported by several authors that the use of LAuX (X = halide) as catalyst precursor requires the addition of a halide scavenger with a weekly coordinating ligand (such as NTf_2, $BAr^F{}_4$, SbF_6) [30,31]. Cationic complexes of type $[LAu(NCR)]^+$ have also been isolated previously [32,33]. One way or the other, the incorporation of the reactant has been proposed to be associative in most cases, the reaction then being triggered from there, usually through an outer-sphere mechanism. To the best of our knowledge, there are no evidences which support the alternative route, the inner-sphere mechanism.

The kinetic data available from the previous section have provided the following statements: (i) there is only a slight effect of the nature of the substrate, styrene or methanol, in the rate of evolution of N_2, and (ii) the reaction rate is affected by the relative substrate:catalyst ratio, both magnitudes being directly correlated. Scheme 5 displays a feasible catalytic cycle for these transformations. The mixture of IPrAuCl and $NaBAr^F{}_4$ in styrene or methanol ensures the formation of the cationic species $[IPrAu(sty)]BAr^F{}_4$ (**2**) or $[IPrAu(MeOH)]BAr^F{}_4$ (**3**) similar to structurally characterized $[IPrAu(NCMe)]BF_4$ [32,33]. The addition of EDA originates the immediate evolution of N_2, the gold–carbene intermediate must form from **2** or **3**. Also, this must be the rate determining

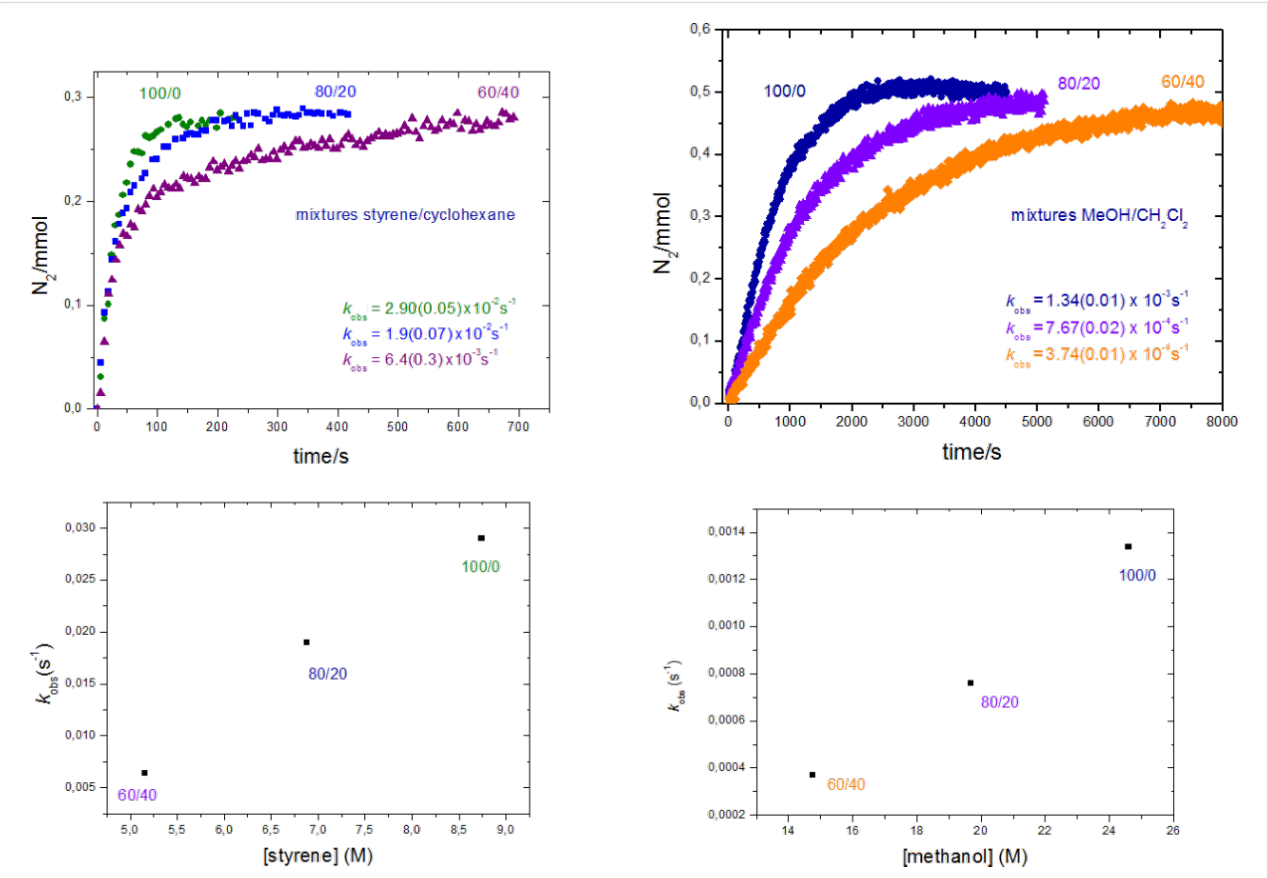

Figure 2: Top: Plots of evolved nitrogen with time for the reactions of EDA with styrene (left) or methanol (right) varying the relative substrate:catalyst ratio, at a constant catalyst value. Bottom: Plots of k_{obs} vs substrate concentration showing a direct correlation between both magnitudes.

step, efforts to detect such intermediates having proven unsuccessful. The commonly accepted pathway (route A, Scheme 5) would suppose an exchange of the substrate ligand with the diazo compound and then evolution of nitrogen. However, that first step of substrate dissociation would be in disagreement with the observation of the enhancement of the reaction rate of nitrogen evolution when increasing the substrate:catalyst ratio, the dissociation of the substrate should be disfavoured at larger substrate concentration. Thus, there is only a plausible explanation for the experimental data (route B, Scheme 5): the substrate remains coordinated while the diazo compound coordinates and eliminates nitrogen, the carbene transfer taking place between two ligands, the carbene and the substrate. This approach would also explain the lack of formation of the olefins derived from carbene coupling with this Au(I)-based system.

Conclusion

The experimental results obtained from the measurement of N_2 evolution in $[IPrAu]^+$-catalyzed carbene transfer from ethyl diazoacetate have allowed proposing that both the carbene and the substrate (styrene or methanol) are bonded to the Au(I) center previously to the corresponding coupling, that is, the functionalization reaction takes place throughout an inner-sphere mechanism. This is not the commonly proposed mechanism for most of the different Au(I)-catalyzed reactions, for which an outer-sphere mechanism has been frequently assumed. We hope that the findings reported herein could be verified for other Au(I)-catalyzed transformations.

Experimental

General methods

All preparations and manipulations were carried out under an oxygen-free nitrogen atmosphere using conventional Schlenk techniques. Solvents were rigorously dried previously to their use. The substrates were purchased from Aldrich. The complex IPrAuCl and $NaBAr^F{}_4$ were prepared according to the literature [34,35]. NMR spectra were performed on Agilent 400 MR and 500 DD2 spectrometers. GC data were collected with a Varian GC-3900 spectrometer with a FID detector.

Kinetic experiments

The kinetic experiments have been carried out similarly to previous procedures from our laboratory [36]. For the sake of clarity, the methodology is briefly described herein. A MinontheMoonTech X201 (http://www.manonthemoontech.com) device consisting of a stainless-steel gas reservoir doubly connected to a pressure transmitter has been employed for the measurement of nitrogen evolution. The variation of the inner pressure inside the reaction flask (Figure 3) is measured with an electronic pressure meter/controller (EL-Press,Bronkhorst HI-TEC).

Figure 3: The experimental device for the measurement of N_2 evolution.

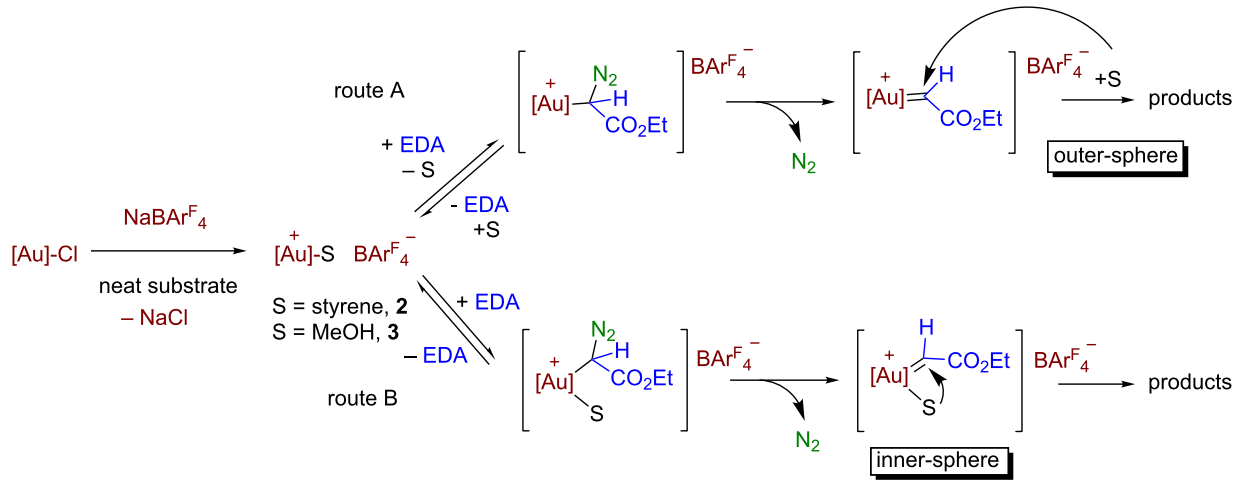

Scheme 5: The outer- and inner-sphere routes for this transformation.

In a typical experiment, the N_2 pressure change was measured after the addition of EDA (0.285 mmol) to a stirred solution of substrate (0. 5 mmol), and a mixture of IPrAuCl and $NaBAr^F{}_4$ (5 mol %) in cyclohexane/CH_2Cl_2 (5 mL) at room temperature. k_{obs} was obtained from experimental curves upon fitting to an exponential growth equation using ORIGIN software.

Acknowledgements

Support for this work was provided by the MINECO (CTQ2014-52769-C3-1-R), and the Junta de Andalucía (P10-FQM-06292).

References

1. Teles, J. H.; Brode, S.; Chabanas, M. *Angew. Chem., Int. Ed.* **1998,** *37,* 1415–1418. doi:10.1002/(SICI)1521-3773(19980605)37:10<1415::AID-ANIE1415>3.0.CO;2-N
2. Norman, R. O. C.; Parr, W. J. E.; Thomas, C. B. *J. Chem. Soc., Perkin Trans. 1* **1976,** 1983–1987. doi:10.1039/p19760001983
3. Fukuda, Y.; Utimoto, K. *J. Org. Chem.* **1991,** *56,* 3729–3731. doi:10.1021/jo00011a058
4. Obradors, C.; Echavarren, A. M. *Chem. Commun.* **2014,** *50,* 16–28. doi:10.1039/C3CC45518A
5. Xie, J.; Pan, C.; Abdukader, A.; Zhu, C. *Chem. Soc. Rev.* **2014,** *43,* 5245–5256. doi:10.1039/C4CS00004H
6. Shapiro, N. D.; Toste, F. D. *Synlett* **2010,** 675–691. doi:10.1055/s-0029-1219369
7. Fürstner, A. *Chem. Soc. Rev.* **2009,** *38,* 3208–3221. doi:10.1039/b816696j
8. Patil, N. T.; Yamamoto, Y. *Chem. Rev.* **2008,** *108,* 3395–3442. doi:10.1021/cr050041j
9. Gorin, D. J.; Sherry, B. D.; Toste, F. D. *Chem. Rev.* **2008,** *108,* 3351–3378. doi:10.1021/cr068430g
10. Jiménez-Núñez, E.; Echavarren, A. M. *Chem. Rev.* **2008,** *108,* 3326–3350. doi:10.1021/cr0684319
11. Jiménez-Núñez, E.; Echavarren, A. M. *Chem. Commun.* **2007,** 333–346. doi:10.1039/B612008C
12. Fürstner, A.; Davies, P. W. *Angew. Chem., Int. Ed.* **2007,** *46,* 3410–3449. doi:10.1002/anie.200604335
13. Hashmi, A. S. K. *Chem. Rev.* **2007,** *107,* 3180–3211. doi:10.1021/cr000436x
14. Lauterbach, T.; Asiri, A. M.; Hashmi, A. S. K. *Adv. Organomet. Chem.* **2014,** *62,* 261–297. doi:10.1016/B978-0-12-800976-5.00005-9
15. Fructos, M. R.; Belderrain, T. R.; de Fremont, P.; Scott, N. M.; Nolan, S. P.; Díaz-Requejo, M. M.; Pérez, P. J. *Angew. Chem., Int. Ed.* **2005,** *44,* 5284–5288. doi:10.1002/anie.200501056
16. Rivilla, I.; Gómez-Emeterio, B. P.; Fructos, M. R.; Díaz-Requejo, M. M.; Pérez, P. J. *Organometallics* **2011,** *30,* 2855–2860. doi:10.1021/om200206m
17. Solorio-Alvarado, C. R.; Wang, Y.; Echavarren, A. M. *J. Am. Chem. Soc.* **2012,** *133,* 11952–11955. doi:10.1021/ja205046h
18. Wang, Y.; McGonigal, P. R.; Herlé, B.; Besora, M.; Echavarren, A. M. *J. Am. Chem. Soc.* **2014,** *136,* 801–809. doi:10.1021/ja411626v
19. Seidel, G.; Fürstner, A. *Angew. Chem., Int. Ed.* **2014,** *53,* 4807–4811. doi:10.1002/anie.201402080
20. Hussong, M. W.; Rominger, F.; Krämer, P.; Straub, B. F. *Angew. Chem., Int. Ed.* **2014,** *53,* 9372–9375. doi:10.1002/anie.201404032
21. Doyle, M. P.; Duffy, R.; Ratnikov, M.; Zhou, L. *Chem. Rev.* **2010,** *110,* 704–724. doi:10.1021/cr900239n
22. Doyle, M. P.; McKervey, M. A.; Ye, T. *Modern Catalytic Methods for Organic Synthesis with Diazo Compounds;* John Wiley & Sons: New York, 1998.
23. Davies, H. M. L.; Dick, A. R. *Top. Curr. Chem.* **2010,** *292,* 303–345. doi:10.1007/128_2009_11
24. Davies, H. M. L.; Manning, J. R. *Nature* **2008,** *451,* 417–424. doi:10.1038/nature06485
25. Díaz-Requejo, M. M.; Pérez, P. J. *Chem. Rev.* **2008,** *108,* 3379–3394. doi:10.1021/cr078364y
26. Díaz-Requejo, M. M.; Belderraín, T. R.; Nicasio, M. C.; Pérez, P. J. *Dalton Trans.* **2006,** 5559–5566. doi:10.1039/b610183f
27. Davies, H. M. L.; Beckwith, R. E. J. *Chem. Rev.* **2003,** *103,* 2861–2904. doi:10.1021/cr0200217
28. Rivilla, I.; Sameera, W. M. C.; Alvarez, E.; Díaz-Requejo, M. M.; Maseras, F.; Pérez, P. J. *Dalton Trans.* **2013,** *42,* 4132–4138. doi:10.1039/c2dt32439c
29. Fructos, M. R.; de Frémont, P.; Nolan, S. P.; Díaz-Requejo, M. M.; Pérez, P. J. *Organometallics* **2006,** *25,* 2237–2241. doi:10.1021/om0507474
    See for the IPrAu-catalyzed alkane functionalization with EDA.
30. Istrate, F. M.; Gagosz, F. *Org. Lett.* **2007,** *9,* 3181–3184. doi:10.1021/ol0713032
31. Qian, J.; Liu, Y.; Cui, J.; Xu, Z. *J. Org. Chem.* **2012,** *77,* 4484–4490. doi:10.1021/jo300543n
32. Nieto-Oberhuber, C.; López, S.; Muñoz, M. P.; Cárdenas, D. J.; Buñuel, E.; Nevado, C.; Echavarren, A. M. *Angew. Chem., Int. Ed.* **2005,** *44,* 6146–6148. doi:10.1002/anie.200501937
33. de Frémont, P.; Stevens, E. D.; Fructos, M. R.; Díaz-Requejo, M. M.; Pérez, P. J.; Nolan, S. P. *Chem. Commun.* **2006,** 2045–2047. doi:10.1039/b601547f
34. de Frémont, P.; Scott, N. M.; Stevens, E. D.; Nolan, S. P. *Organometallics* **2005,** *24,* 2411–2418. doi:10.1021/om050111c
35. Brookhart, M.; Grant, B.; Volpe, A. F., Jr. *Organometallics* **1992,** *11,* 3920–3922. doi:10.1021/om00059a071
36. Pereira, A.; Champouret, Y.; Martín, C.; Álvarez, E.; Etienne, M.; Belderraín, T. R.; Pérez, P. J. *Chem. – Eur. J.* **2015,** *21,* 9769–9775. doi:10.1002/chem.201500776

BEILSTEIN JOURNAL OF ORGANIC CHEMISTRY

Convenient preparation of high molecular weight poly(dimethylsiloxane) using thermally latent NHC-catalysis: a structure-activity correlation

Stefan Naumann[1], Johannes Klein[2], Dongren Wang[1] and Michael R. Buchmeiser[*1,3]

Full Research Paper

Open Access

Address:
[1]Institute for Polymer Chemistry, University of Stuttgart, Pfaffenwaldring 55, D-70569 Stuttgart, Germany, [2]Institut für Chemie und Biochemie, Anorganische Chemie, Freie Universität Berlin, Fabeckstraße 34–36, Berlin, Germany and [3]Institute of Textile Chemistry and Chemical Fibers, Körschtalstrasse 26, D-73770 Denkendorf, Germany

Email:
Michael R. Buchmeiser* - michael.buchmeiser@ipoc.uni-stuttgart.de

* Corresponding author

Keywords:
latency; N-heterocyclic carbenes; ring-opening organocatalysis; polymerization; polysiloxanes

Beilstein J. Org. Chem. **2015,** *11,* 2261–2266.
doi:10.3762/bjoc.11.246

Received: 25 September 2015
Accepted: 04 November 2015
Published: 20 November 2015

This article is part of the Thematic Series "N-Heterocyclic carbenes".

Guest Editor: S. P. Nolan

Abstract

The polymerization of octamethylcyclotetrasiloxane (D_4) is investigated using several five-, six- and seven-membered *N*-heterocyclic carbenes (NHCs). The catalysts are delivered in situ from thermally susceptible CO_2 adducts. It is demonstrated that the polymerization can be triggered from a latent state by mild heating, using the highly nucleophilic 1,3,4,5-tetramethylimidazol-2-ylidene as organocatalyst. This way, high molecular weight PDMS is prepared (up to >400 000 g/mol, $1.6 < Đ_M < 2.5$) in yields >95%, using low catalyst loadings (0.2–0.1 mol %). Furthermore, the results suggest that a nucleophilic, zwitterionic mechanism is in operation, in preference to purely anionic polymerization.

Introduction

N-Heterocyclic carbenes (NHCs) [1-3] have had a resounding impact on organopolymerization [4,5] during the past fifteen years. Considerable research effort has steadily deepened the mechanistic understanding of the polymerization pathways open to NHCs, while the range of accessible monomer structures has grown impressively [6,7]. Nowadays, NHC-mediated polymerization can be applied to prepare polymers of high industrial and commercial importance, such as poly(amide)s [8,9], poly(ether)s [10], poly(urethane)s [11,12] or poly(acrylate)s [13-18]. Likewise, poly(siloxane)s are attractive and versatile macromolecular materials produced on large scale and thus a rewarding field for the development of new catalysts, the more so if the added benefit of metal-free conditions can be implemented [19-21]. In spite of this, few investigations regarding the performance of NHCs in this area have been published. In 2006, Waymouth, Hedrick and co-workers showed that

poly(carbosiloxane)s can be synthesized efficiently from the monomer 2,2,5,5-tetramethyl-1-oxa-2,5-disilacyclopentane in the presence of alcohols as initiators, using two different NHCs [22]. Control over the molecular weight was good ($Đ_M$ < 1.2), but prolonged polymerization led to transetherification. Interestingly, the formation of high molecular weight cyclic poly(carbosiloxane) was observed in the absence of an initiator [23]. Additionally, octamethylcyclotetrasiloxane (D_4) was used to prepare poly(dimethylsiloxane) (PDMS), using three different imidazolium-based free NHCs in combination with benzyl alcohol or methanol as initiator [24]. There, polymerizations were conducted at 80 °C for 16 h to achieve conversions of about 85% (1.5 < $Đ_M$ < 1.7, 0.1% catalyst loading). Notably, it was found that steric hindrance of the NHC shut down polymerization activity. Finally, a report on the polycondensation of α,ω-disilanols describes the efficient polycondensation via NHCs in spite of the generation of water during the reaction, finding that the most basic NHC in the small study delivered the best results [25]. In view of these promising, yet somewhat limited, results, the aim for this study was (a) to investigate a range of structurally diverse NHCs to get more insight into the influence of NHC structure on catalytic activity for the polymerization of D_4, and (b) to generate the NHCs in situ from thermally labile CO_2 adducts. This type of NHC delivery offers the double advantage of improved stability and storability of the NHC adduct and the possibility to generate "on demand" polymerization systems where the catalyst can be activated by heating. This way, a latent, easy-to-handle metal-free process which is more competitive in comparison with other catalytic systems can be realized [26].

Results and Discussion

Several five-, six- and seven-membered NHCs were prepared and reacted with carbon dioxide to receive the corresponding CO_2 adducts (Scheme 1, top), following literature procedures (see Supporting Information File 1). Compounds **7-Neo-CO_2**, **7-iPr-CO_2** and **5_{Cl}-Me-CO_2** have not been described before and full characterization can be found in the experimental part (Supporting Information File 1). In accordance with previous findings [17,27], these NHC-carboxylates were stable at room temperature over long periods of time (observed for up to 2 years) without decomposition, exclusion of humidity provided.

Polymerization experiments with D_4 were conducted solvent-free at elevated temperature (80 °C, 16 h), both in presence and absence of an initiator (benzyl alcohol, BnOH). This immediately revealed sharp differences of reactivity between the individual pre-catalysts (Table 1). When the protected NHC was applied in conjunction with BnOH, only **5_{Me}-Me-CO_2** showed relevant activity, albeit a very high one.

At a catalyst loading of only 0.2 mol %, a molecular weight (M_n) of 70 000 g/mol was achieved at 94% monomer conver-

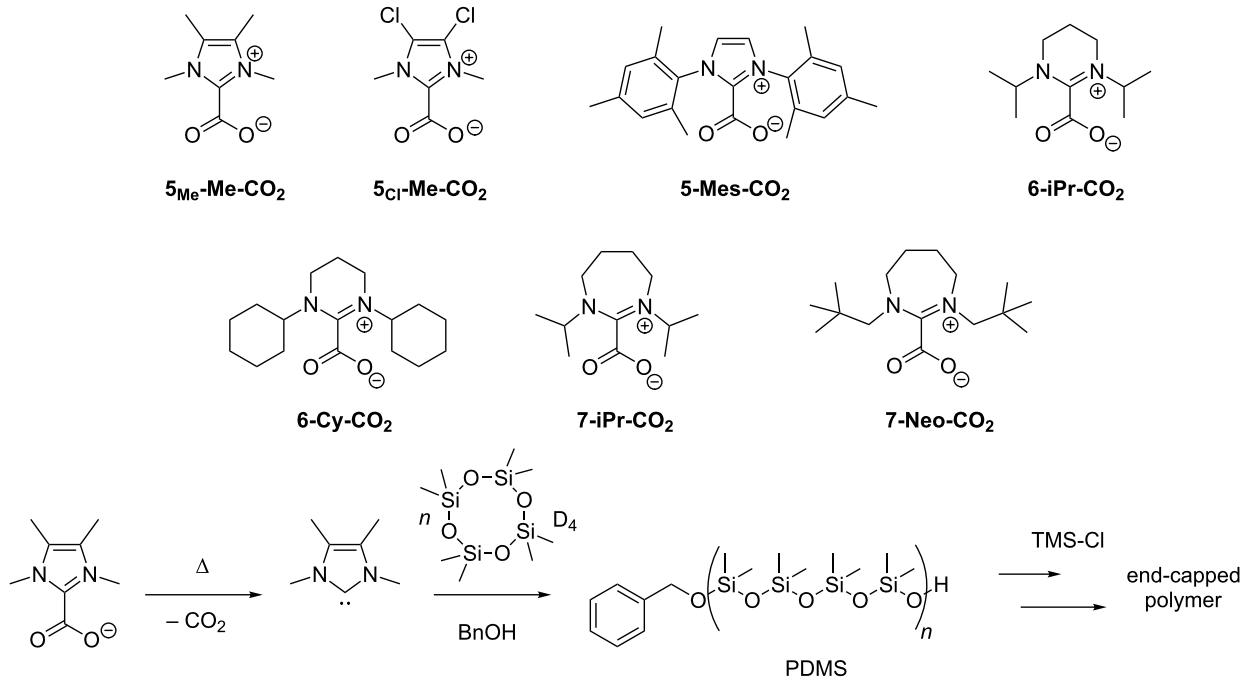

Scheme 1: NHC-carboxylates part of this study (top) and polymerization scheme with initial thermal decarboxylation and final end-capping with TMS-Cl.

Table 1: Polymerization of D_4 in bulk using different protected NHCs (80 °C, 16 h).

Entry	NHC-CO_2	NHC/BnOH/D4	Conversion [%][a]	M_n ×10^3 [g/mol][b]	$Đ_M$
1	**5_{Me}-Me-CO_2**	1:5:500	94	70	1.7
2	**5_{Me}-Me-CO_2**	1:1:100	>95	198	1.9
3	**5_{Me}-Me-CO_2**	1:1:300	>95	288	1.9
4	**5_{Me}-Me-CO_2**	1:1:700	>95	360	2.5
5	**5_{Me}-Me-CO_2**	1:1:1000	>95	424	2.2
6	**5-Mes-CO_2**	1:5:500	7	–	–
7	**5_{Cl}-Me-CO_2**	1:5:500	0	–	–
8	**6-iPr-CO_2**	1:5:500	0	–	–
9	**6-Cy-CO_2**	1:5:500	0	–	–
10	**7-iPr-CO_2**	1:5:500	5	–	–
11	**7-Neo-CO_2**	1:5:500	0	–	–
12	**5_{Me}-Me-CO_2**	1:0:100	92	8	1.3
13	**6-Cy-CO_2**	1:0:100	insoluble	n. d.	–
14	**7-iPr-CO_2**	1:0:100	insoluble	n. d.	–

[a]Determined by ^{1}H NMR spectroscopy; [b]via GPC (THF, PS standards).

sion. Interestingly, some degree of control over the molecular weight is possible by adjusting the initiator to monomer ratio (Table 1, entries 2–5). This way, up to a target degree of polymerization (DP) of 1000, considerable molecular weight can be built up, ranging from 200 000 g/mol to over 400 000 g/mol (M_n). Importantly, in all these cases very high conversion is observed. Matrix-assisted laser desorption/ionization time-of-flight mass spectrometry (MALDI–ToF MS) and NMR experiments clearly show that BnOH is incorporated in the resulting PDMS (S1–S3), underlining the defined structure of the polymer. Contrasting this behaviour of **5_{Me}-Me-CO_2**, its sterically more hindered analogue, **5-Mes-CO_2**, only brought about a low conversion of 7% under identical conditions (Table 1, entry 6), while its electron-poor derivative **5_{Cl}-Me-CO_2** was completely inactive (Table 1, entry 7). More surprisingly, the six- and seven-membered pre-catalysts were all found to deliver very little or no polymer. Differently, in the absence of BnOH (1% catalyst loading, Table 1, entries 12–14), application of both **7-iPr-CO_2** and **6-Cy-CO_2** resulted in an insoluble polymer, most probably because very high molecular weight was generated. Gratifyingly, under the same parameters **5_{Me}-Me-CO_2** effected a conversion of 92% (M_n = 8 100 g/mol). Overall, polymerization with this pre-catalyst proceeds noticeably faster in the presence than in the absence of an initiator (Figure 1). At a polymerization setup of NHC/BnOH/D_4 = 1:5:500, the conversion is practically complete after only 2.5 h.

Above findings obviously render **5_{Me}-Me-CO_2** the most suitable pre-catalyst, but important conclusions with regard to the polymerization mechanism can also be drawn. In part, the results nicely mirror findings by Baceiredo and co-workers [24], who described that steric hindrance eliminates any polymerization activity of the NHC; the same is found here when comparing the performance of **5_{Me}-Me-CO_2** and **5-Mes-CO_2**. Additionally, electron-withdrawing substituents (as present in **5_{Cl}-Me-CO_2**) preclude any activity, emphasizing that nucleophilicity is crucial for successful polymerization. Furthermore, it is interesting to note that the six- and seven-membered NHCs do not show any reactivity here, in spite of being very strong bases. While for a compound like **6-iPr** a p*K*a-value of 28.2 (aqueous solution, 25 °C) was found, the five-membered imidazolium derivative **5-Mes** was determined to have a p*K*a-value of only 20.8 (which compares to 15–19 for typical alcohols; in turn, silanols are even more acidic than the corresponding alcohols) [28-32].

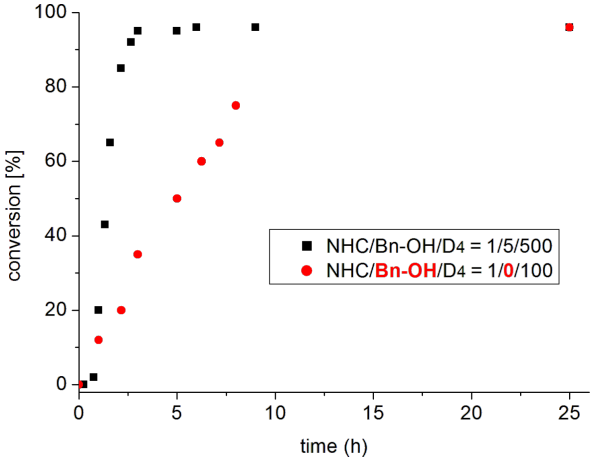

Figure 1: Comparison of conversion over time for D_4 polymerization (80 °C, bulk) using **5_{Me}-Me-CO_2**. Note that the fivefold monomer excess was used in case of BnOH being present.

At the same time, **5_{Me}-Me-CO_2** successfully catalyzed PDMS-formation in the absence of BnOH (see above), and hence a mechanism for direct D_4 polymerization must exist.

Taken together, all above points strongly suggest that nucleophilic ring-opening of the monomer by the NHC is the key step, in agreement with previous proposals [24]. A purely basic (anionic) pathway (Scheme 2), often preferred by the six-membered NHCs [7-9,17], seems clearly disfavoured. In the absence of BnOH, it is therefore reasonable to assume zwitterionic propagation, in analogy to recent findings for NHC-mediated lactone polymerization [33]. The insoluble material received by the action of **7-iPr-CO_2** and **6-Cy-CO_2** could be connected to a low initiation efficiency and consequently low ratio of propagating zwitterions to monomer, resulting in high-molecular weight polymers. In contrast, a sterically uncongested, highly nucleophilic NHC as liberated from **5_{Me}-Me-CO_2** (Table 1, entry 12) is more suitable under these conditions.

Finally, a mixture of **5_{Me}-Me-CO_2**, BnOH and D_4 was tested for thermal latency (Figure 2). Notably, after 72 h at a slightly elevated temperature of 45 °C only negligible conversion was observed. A relatively mild increase to 80 °C, however, triggered a clean jump to near quantitative conversion. Hence, with this catalytic setup it is possible to form one-component, metal-free mixtures which can be activated by mild heating. Polymerization of D_4 is entropically driven [21,34] and thus profits from elevated temperature in any case, rendering the implementation of thermally labile pre-catalysts both practically feasible and advantageous.

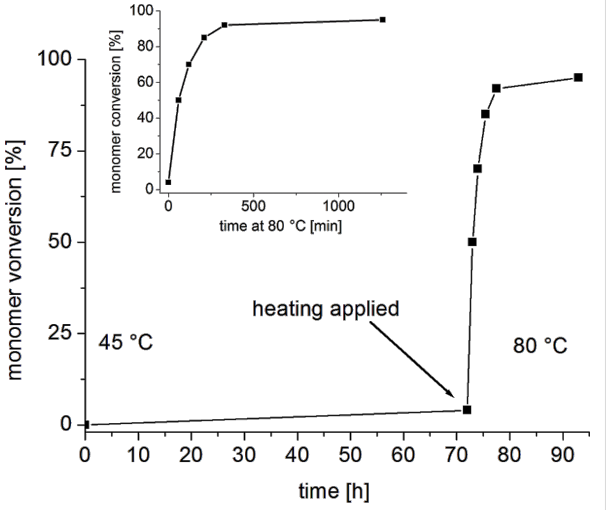

Figure 2: Thermal activation of a **5_{Me}-Me-CO_2**/BnOH/D_4 (1:5:500) composition after a latency period of 72 h.

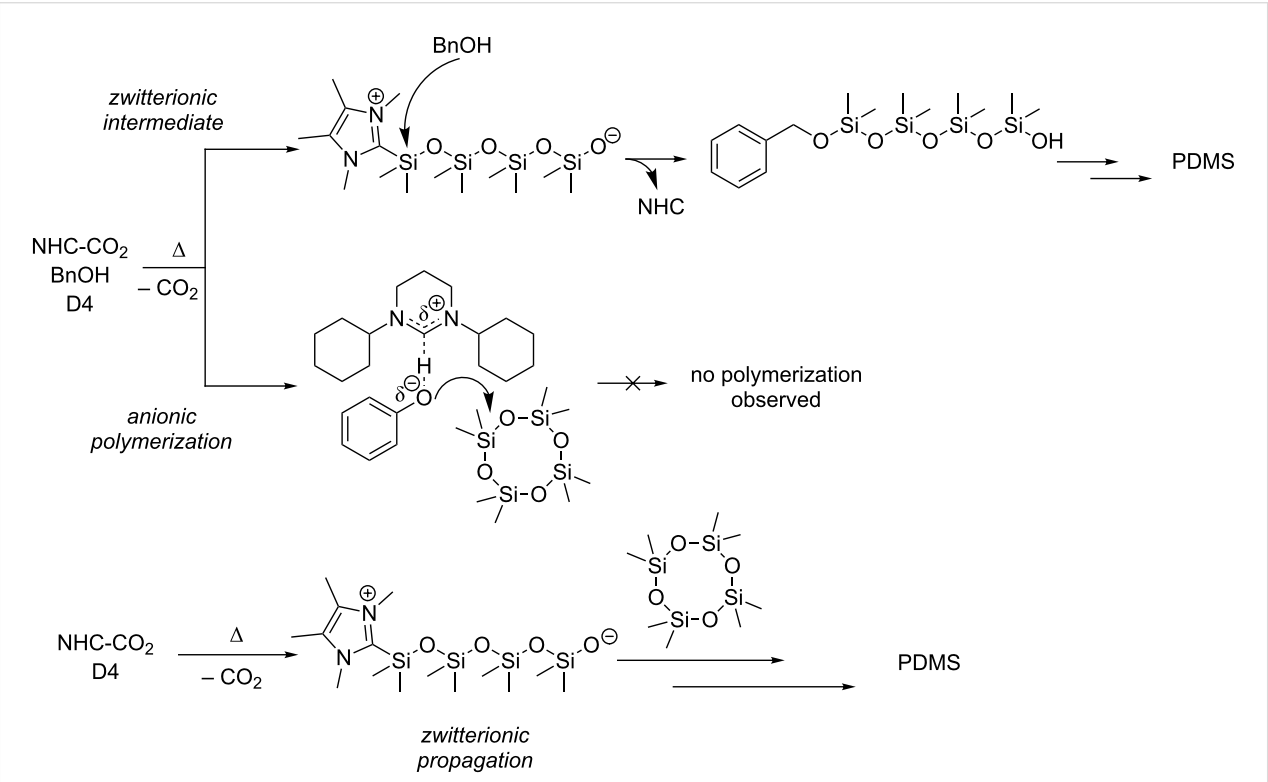

Scheme 2: Discussed mechanisms proposed to operate in NHC-mediated polymerization of D_4 in presence/absence of BnOH.

Conclusion

In conclusion, we have demonstrated the first polymerization of D_4 using NHC-carboxylates. Sterically non-hindered, highly nucleophilic protected NHCs like **5_{Me}-Me-CO_2** offer access to an "on demand", metal-free and effective preparation of PDMS, including high molecular weight polymers. The results of a screening of a range of different NHCs indicate that a nucleophilic action of the organocatalyst is preferred over action as a Brønsted base.

Supporting Information

Supporting Information File 1

Details on the synthesis of NHC-CO_2 and polymerizations.
[http://www.beilstein-journals.org/bjoc/content/supplementary/1860-5397-11-246-S1.pdf]

Acknowledgements

The authors SN, JK and DW all contributed equally to the preparation of the manuscript. M. Sc. Suman Sen is acknowledged for synthetic support.

References

1. Hahn, F. E.; Jahnke, M. C. *Angew. Chem., Int. Ed.* **2008,** *47,* 3122–3172. doi:10.1002/anie.200703883
2. Dröge, T.; Glorius, F. *Angew. Chem., Int. Ed.* **2010,** *49,* 6940–6952. doi:10.1002/anie.201001865
3. Hopkinson, M. N.; Richter, C.; Schedler, M.; Glorius, F. *Nature* **2014,** *510,* 485–496. doi:10.1038/nature13384
4. Kiesewetter, M. K.; Shin, E. J.; Hedrick, J. L.; Waymouth, R. M. *Macromolecules* **2010,** *43,* 2093–2107. doi:10.1021/ma9025948
5. Dove, A. P. *ACS Macro Lett.* **2012,** *1,* 1409–1412. doi:10.1021/mz3005956
6. Fèvre, M.; Pinaud, J.; Gnanou, Y.; Vignolle, J.; Taton, D. *Chem. Soc. Rev.* **2013,** *42,* 2142–2172. doi:10.1039/c2cs35383k
7. Naumann, S.; Dove, A. P. *Polym. Chem.* **2015,** *6,* 3185–3200. doi:10.1039/C5PY00145E
8. Naumann, S.; Epple, S.; Bonten, C.; Buchmeiser, M. R. *ACS Macro Lett.* **2013,** *2,* 609–612. doi:10.1021/mz400199y
9. Naumann, S.; Schmidt, F. G.; Speiser, M.; Böhl, M.; Epple, S.; Bonten, C.; Buchmeiser, M. R. *Macromolecules* **2013,** *46,* 8426–8433. doi:10.1021/ma4018586
10. Raynaud, J.; Absalon, C.; Gnanou, Y.; Taton, D. *J. Am. Chem. Soc.* **2009,** *131,* 3201–3209. doi:10.1021/ja809246f
11. Bantu, B.; Pawar, G. M.; Decker, U.; Wurst, K.; Schmidt, A. M.; Buchmeiser, M. R. *Chem. – Eur. J.* **2009,** *15,* 3103–3109. doi:10.1002/chem.200802670
12. Coutelier, O.; El Ezzi, M.; Destarac, M.; Bonnette, F.; Kato, T.; Baceiredo, A.; Sivasankarapillai, G.; Gnanou, Y.; Taton, D. *Polym. Chem.* **2012,** *3,* 605–608. doi:10.1039/c2py00477a
13. Scholten, M. D.; Hedrick, J. L.; Waymouth, R. M. *Macromolecules* **2008,** *41,* 7399–7404. doi:10.1021/ma801281q
14. Raynaud, J.; Ciolino, A.; Baceiredo, A.; Destarac, M.; Bonnette, F.; Kato, T.; Gnanou, Y.; Taton, D. *Angew. Chem., Int. Ed.* **2008,** *47,* 5390–5393. doi:10.1002/anie.200800490
15. Zhang, Y.; Chen, E. Y.-X. *Angew. Chem., Int. Ed.* **2012,** *51,* 2465–2469. doi:10.1002/anie.201108019
16. Hong, M.; Chen, E. Y.-X. *Angew. Chem., Int. Ed.* **2014,** *53,* 11900–11906. doi:10.1002/anie.201406630
17. Naumann, S.; Schmidt, F. G.; Schowner, R.; Frey, W.; Buchmeiser, M. R. *Polym. Chem.* **2013,** *4,* 2731–2740. doi:10.1039/c3py00073g
18. Matsuoka, S.-i.; Namera, S.; Suzuki, M. *Polym. Chem.* **2015,** *6,* 294–301. doi:10.1039/C4PY01184H
19. Manners, I. *Angew. Chem., Int. Ed. Engl.* **1996,** *35,* 1602–1621. doi:10.1002/anie.199616021
20. Chojnowski, J. *J. Inorg. Organomet. Polym.* **1991,** *1,* 299–323. doi:10.1007/BF00702495
21. Mark, J. E.; Schaefer, D. W.; Lin, G. *The polysiloxanes;* Oxford University Press: New York, NY, 2015.
22. Lohmeijer, B. G. G.; Dubois, G.; Leibfarth, F.; Pratt, R. C.; Nederberg, F.; Nelson, A.; Waymouth, R. M.; Wade, C.; Hedrick, J. L. *Org. Lett.* **2006,** *8,* 4683–4686. doi:10.1021/ol0614166
23. Brown, H. A.; Chang, Y. A.; Waymouth, R. M. *J. Am. Chem. Soc.* **2013,** *135,* 18738–18741. doi:10.1021/ja409843v
24. Rodriguez, M.; Marrot, S.; Kato, T.; Stérin, S.; Fleury, E.; Baceiredo, A. *J. Organomet. Chem.* **2007,** *692,* 705–708. doi:10.1016/j.jorganchem.2006.10.006
25. Marrot, S.; Bonnette, F.; Kato, T.; Saint-Jalmes, L.; Fleury, E.; Baceiredo, A. *J. Organomet. Chem.* **2008,** *693,* 1729–1732. doi:10.1016/j.jorganchem.2008.02.011
26. Naumann, S.; Buchmeiser, M. R. *Catal. Sci. Technol.* **2014,** *4,* 2466–2479. doi:10.1039/c4cy00344f
27. Van Ausdall, B. R.; Glass, J. L.; Wiggins, K. M.; Aarif, A. M.; Louie, J. *J. Org. Chem.* **2009,** *74,* 7935–7942. doi:10.1021/jo901791k
28. Higgins, E. M.; Sherwood, J. A.; Lindsay, A. G.; Armstrong, J.; Massey, R. S.; Alder, R. W.; O'Donoghue, A. C. *Chem. Commun.* **2011,** *47,* 1559–1561. doi:10.1039/C0CC03367G
29. Magill, A. M.; Cavell, K. J.; Yates, B. F. *J. Am. Chem. Soc.* **2004,** *126,* 8717–8724. doi:10.1021/ja038973x
30. Kim, Y.-J.; Streitwieser, A. *J. Am. Chem. Soc.* **2002,** *124,* 5757–5761. doi:10.1021/ja025628j
31. Brown, W. H.; Foote, C. S.; Iverson, B. L.; Anslyn, E. V. *Organic chemistry,* 6th ed.; Brooks/Cole, Cengage Learning: Belmont, CA, 2012.
32. Chandrasekhar, V.; Boomishankar, R.; Nagendran, S. *Chem. Rev.* **2004,** *104,* 5847–5910. doi:10.1021/cr0306135
33. Brown, H. A.; Waymouth, R. M. *Acc. Chem. Res.* **2013,** *46,* 2585–2596. doi:10.1021/ar400072z
34. Odian, G. *Principles of Polymerization,* 4th ed.; John Wiley & Sons: Hoboken, 2004. doi:10.1002/047147875X

BEILSTEIN JOURNAL OF ORGANIC CHEMISTRY

Efficient synthetic protocols for the preparation of common N-heterocyclic carbene precursors

Morgan Hans[1], Jan Lorkowski[1,2], Albert Demonceau[1] and Lionel Delaude[*1]

Full Research Paper

Open Access

Address:
[1]Laboratory of Catalysis, Institut de Chimie (B6a), Allée du six Août 13, Quartier Agora, Université de Liège, 4000 Liège, Belgium and [2]Faculty of Chemistry, Adam Mickiewicz University in Poznań, Umultowska 89b, 61-614 Poznań, Poland

Email:
Lionel Delaude* - l.delaude@ulg.ac.be

* Corresponding author

Keywords:
cyclization; experimental procedure; imidazolinium salt; imidazolium salt; microwave heating

Beilstein J. Org. Chem. **2015,** *11,* 2318–2325.
doi:10.3762/bjoc.11.252

Received: 08 October 2015
Accepted: 13 November 2015
Published: 25 November 2015

This article is part of the Thematic Series "N-Heterocyclic carbenes".

Guest Editor: S. P. Nolan

Abstract

The one-pot condensation of glyoxal, two equivalents of cyclohexylamine, and paraformaldehyde in the presence of aqueous HBF_4 provided a straightforward access to 1,3-dicyclohexylimidazolium tetrafluoroborate (ICy·HBF_4). 1,3-Dibenzylimidazolium tetrafluoroborate (IBn·HBF_4) was obtained along the same lines. To synthesize 1,3-diarylmidazolium salts, it was necessary to isolate the intermediate *N*,*N*′-diarylethylenediimines prior to their cyclization. Although this additional step required more time and reagents, it led to a much more efficient overall process. It also proved very convenient to carry out the synthesis of imidazolinium salts in parallel to their imidazolium counterparts via the reduction of the diimines into diammonium salts. The critical assembly of the C^2 precarbenic unit was best achieved with paraformaldehyde and chlorotrimethylsilane in the case of imidazolium derivatives, whereas the use of triethyl orthoformate under microwave irradiation was most appropriate for the fast and efficient synthesis of imidazolinium salts. This strategy was applied to the synthesis of six common N-heterocyclic carbene precursors, namely, 1,3-dimesitylimidazolium chloride (IMes·HCl), 1,3-dimesitylimidazolium tetrafluoroborate (IMes·HBF_4), 1,3-dimesitylimidazolinium chloride (SIMes·HCl), 1,3-bis(2,6-diisopropylphenyl)imidazolium chloride (IDip·HCl or IPr·HCl), 1,3-bis(2,6-diisopropylphenyl)imidazolinium chloride (SIDip·HCl or SIPr·HCl), and 1,3-bis(2,6-bis(diphenylmethyl)-4-methylphenyl)imidazolium chloride (IDip*·HCl or IPr*·HCl).

Introduction

Since Arduengo and co-workers successfully isolated and characterized the first imidazol-2-ylidene derivative in 1991 [1,2], stable N-heterocyclic carbenes (NHCs) have become a staple of modern synthetic chemistry [3-7]. Over the past twenty five years, they have evolved from laboratory curiosities to ubiquitous ancillary ligands, not only for all the transition metals whether in high or low oxidation state [8-10], but also for lanthanides and actinides [11,12], as well as for main group

elements [12,13]. Countless applications in homogeneous catalysis have already taken advantage of the remarkable stereoelectronic properties and structural diversity of these organometallic species [14-17]. To give just a single example, NHC ligands played a crucial role in the development of highly efficient ruthenium initiators for olefin metathesis and related reactions [18-21]. Lately, these divalent carbon species have also emerged as powerful nucleophilic organocatalysts for polymer chemistry [22,23] and organic synthesis [24-26]. In particular, they were successfully employed for the umpolung of carbonyl compounds, sometimes in an asymmetric fashion [27-29].

Currently, the NHCs most frequently encountered are based on the imidazol-2-ylidene and imidazolin-2-ylidene scaffolds, which are easily accessible via the deprotonation of imidazolium or imidazolinium salts with a strong base (Scheme 1, path A) [26,30]. The reaction is often carried out in situ to avoid the isolation of air- and moisture-sensitive free carbenes. Thus, the mixture of an imidazol(in)ium salt and a base serves de facto as a carbene source for most catalytic and synthetic purposes. Alternative methods to generate NHCs without the intervention of a base, which might lead to unwanted side-reactions, include the facile cleavage of NHC·CO_2 zwitterions (Scheme 1, path B) [31-35], the thermolysis of labile imidazolidine adducts (Scheme 1, path C) [36-38], or the recourse to Ag(I)–NHC complexes as NHC delivery agents (Scheme 1, path D) [39,40]. In many cases, however, these NHC surrogates are obtained from azolium intermediates. Hence, imidazolium and imidazolinium salts are the most common NHC precursors and their synthesis from acyclic starting materials is of utmost practical importance [41].

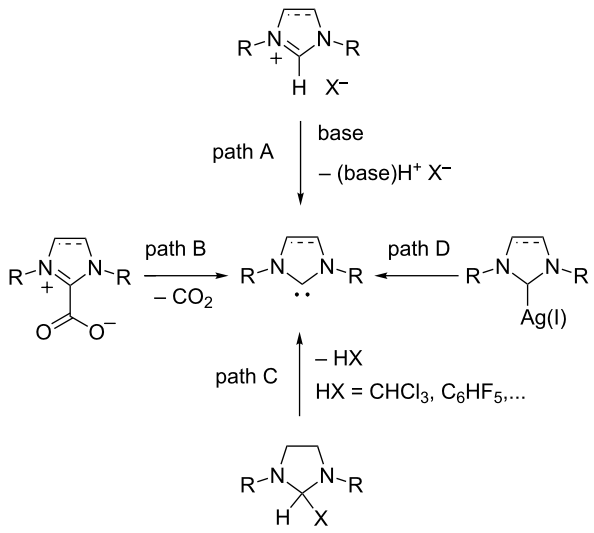

Scheme 1: Various synthetic paths leading to the formation of NHCs.

One of the most atom-economical and straightforward path to elaborate symmetrical imidazolium salts involves the combination of glyoxal, which provides the C^4–C^5 heterocyclic backbone of the NHC, two equivalents of a primary alkylamine or aniline, to introduce the N^1 and N^3 modular units, and a suitable C_1 building block for joining the precarbenic C^2 center (Scheme 2). An additional reduction of the intermediate diimines into diamines is required prior to the assembly of the corresponding imidazolinium derivatives. The first embodiment of this general strategy dates back to 1991 when Arduengo patented the one-pot condensation of glyoxal, two equivalents of an amine, and paraformaldehyde in the presence of hydrochloric acid to afford 1,3-disubstituted imidazolium chlorides [42]. Although this procedure was rather efficient when applied to simple alkylamines, its extension to the synthesis of 1,3-diarylimidazolium salts usually failed due to the formation of dark, tarry ionomer byproducts that could only be painstakingly separated from the desired compounds, thereby leading to low yields of tainted products [43]. This practical complication was very unfortunate because bulky aromatic substituents, such as mesityl (2,4,6-trimethylphenyl) or 2,6-diisopropylphenyl groups, often provide the right balance of electronic donation and steric protection to many NHC-based catalytic systems. Accordingly, it spurred sustained research efforts to improve and optimize experimental conditions leading to imidazol(in)ium salts in both academic [43-45] and industrial laboratories [46]. Because of the incremental nature of these endeavors, a large number of valuable synthetic procedures have been scattered in the literature, often relegated to supporting information, and comparison of their respective merits has become more and more challenging.

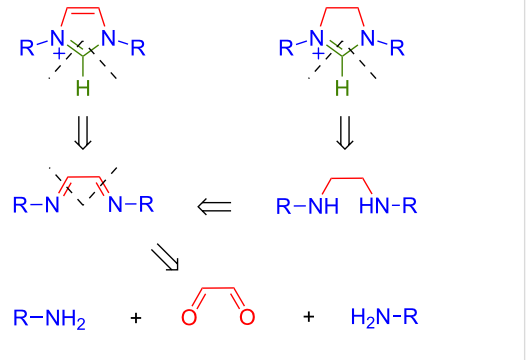

Scheme 2: Retrosynthetic path for the preparation of symmetrical imidazolium and imidazolinium salts from simple acyclic precursors.

In this report, we aimed at collecting a series of efficient synthetic protocols for the preparation of eight common N-heterocyclic carbene precursors differing by the nature of their central core (imidazolium or imidazolinium), the choice of the asso-

ciated counterion (chloride or tetrafluoroborate), or the steric bulk of their nitrogen substituents (ranging from small, flexible cyclohexyl rings to hefty 2,6-bis(diphenylmethyl)-4-methylphenyl groups, Figure 1). For each target compound, we strove to put together the most straightforward, detailed experimental procedure that was checked to afford high yield and purity, and a full characterization by ^{1}H and ^{13}C NMR spectroscopies.

Results and Discussion

Synthesis of 1,3-dicylohexylimidazolium tetrafluoroborate

The one-pot synthesis of 1,3-dicyclohexylimidazolium chloride (ICy·HCl) was first disclosed in the open literature by Herrmann and co-workers in 1996 [47]. The reaction proceeded smoothly and the product did not show any tendency to form an ionic liquid, unlike its lower weight unsymmetrical analogues. It turned out, however, to be highly hygroscopic, which hindered its purification and subsequent reactions with moisture-sensitive bases or organometallic compounds. Other counterions were found to alleviate this tendency. In particular, the replacement of HCl with aqueous HBF_4 in the original procedure allowed us [48] and others [49] to isolate ICy·HBF_4 as a well-behaved, non-hygroscopic solid that could be easily purified by recrystallization from isopropanol. Typical yields were in the 70–80% range (Scheme 3).

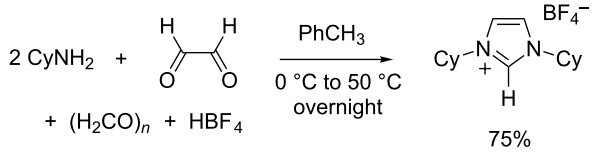

Scheme 3: Synthesis of 1,3-dicyclohexylimidazolium tetrafluoroborate (ICy·HBF_4).

Synthesis of 1,3-dibenzylimidazolium tetrafluoroborate

At first sight, benzyl chloride or benzyl bromide seem to be ideal candidates to prepare 1,3-dibenzylimidazolium salts via a double alkylation of imidazole. Indeed, these primary alkyl halides are highly reactive toward nucleophiles and do not undergo elimination reactions. Accordingly, numerous procedures were reported for the two-step synthesis of 1,3-dibenzylimidazolium halides via the formation of 1-benzylimidazole [50-53]. In our hands, however, the quaternization of this intermediate with benzyl chloride or bromide was often sluggish, which led to incomplete conversions and residues of unpleasant, lachrymatory reagents. We were very pleased to find out that the one-pot procedure described above for 1,3-dicyclohexylimidazolium tetrafluoroborate could be seamlessly translated to the preparation of 1,3-dibenzylimidazolium tetrafluoroborate (IBn·HBF_4) from glyoxal, benzylamine, paraformaldehyde, and tetrafluoroboric acid (Scheme 4). To the best of our knowledge, this superior route had not been explored so far.

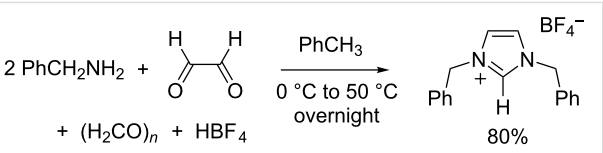

Scheme 4: Synthesis of 1,3-dibenzylimidazolium tetrafluoroborate (IBn·HBF_4).

Synthesis of 1,3-dimesitylimidazolium salts

Although little experimental details were supplied, the preparation of 1,3-dimesitylimidazolium chloride (IMes·HCl) was first disclosed by Arduengo et al. in 1992 using a one-pot procedure [54]. Several research groups noticed that this strategy often led to dark brown molasses out of which a solid product

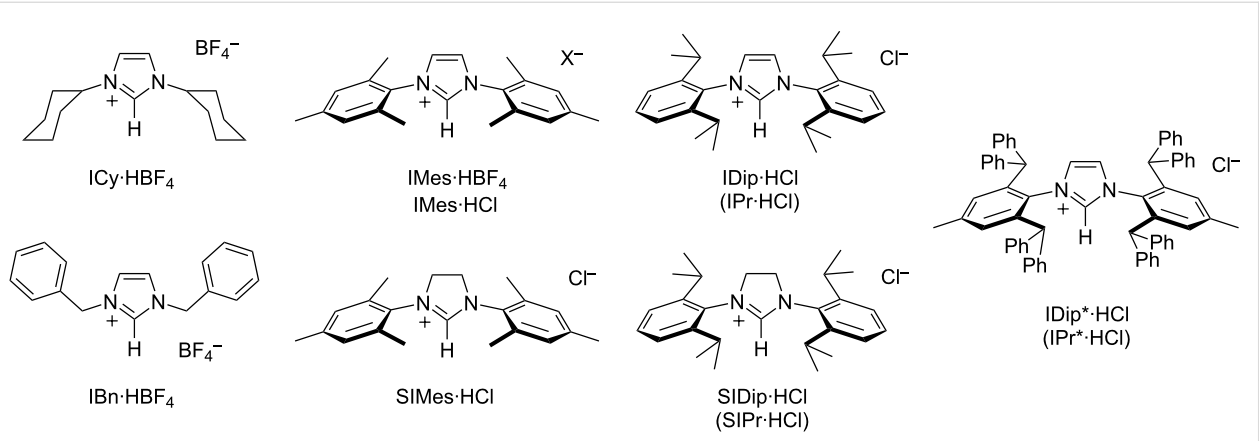

Figure 1: Structures of the imidazolium and imidazolinium salts discussed in this study and their acronyms.

could only be painstakingly extracted after extensive washing, resulting in low yields of rather impure materials [43,55,56]. To circumvent this problem, Arduengo and co-workers devised a two-step protocol involving the isolation of *N,N′*-dimesitylethylenediimine followed by cyclization with chloromethyl ethyl ether, which slowly reacted to afford both the C^2 imidazolium center and the chloride counterion [43]. While this procedure remained low-yielding and time-consuming, it significantly eased the isolation of the final product, which cleanly precipitated from the reaction mixture. Most importantly, this work demonstrated the importance of isolating the intermediate Schiff base prior to its cyclization, a feature that proved crucial to successfully achieve the synthesis of 1,3-diarylimidazolium salts by late introduction of the precarbenic atom moiety. It should be pointed out that Nolan et al. also reached this conclusion when they first optimized the synthesis of 1,3-bis(2,6-diisopropylphenyl)imidazolium chloride in 1999 (vide infra) [57].

Over the years, several variations were reported on the two-step route leading to 1,3-dimesitylimidazolium chloride [41]. Only minor changes concerned the initial condensation between glyoxal and two equivalents of mesitylamine (Scheme 5). The reaction proceeds readily in aqueous/alcoholic mixtures at room temperature and the product begins to separate as a bright yellow solid after a few minutes. Of note, second and even third crops of precipitate are usually obtained upon work-up during the synthesis of diimines. They may be added to the first crop in order to further increase the yield, but their purity needs to be checked beforehand. Formic acid is sometimes added as a catalyst but does not seem to be mandatory, maybe because glyoxal is often contaminated with glyoxylic and oxalic acids, especially upon prolonged storage under aerobic conditions. More significant alterations were brought to the cyclization step. In addition to the use of chloromethyl ethyl ether pioneered by Arduengo et al. [43], mixtures of paraformaldehyde and HCl in anhydrous solvents were investigated by Bantreil and Nolan [45], while Hintermann identified chlorotrimethylsilane as a convenient source of chloride counterions [44]. Furthermore, this last reagent does not lead to the formation of water, which can hydrolyze the starting diimine and has a deleterious influence on the reaction course. Thus, we adopted the experimental procedure carefully optimized by Hintermann to obtain IMes·HCl in ca. 85% yield (Scheme 5).

We were also interested in the preparation of IMes·HBF_4 because imidazolium tetrafluoroborates are usually less hygroscopic and easier to crystallize than chlorides [45]. Moreover, when imidazolium salts are used to generate NHCs in situ, for instance to accomplish organocatalytic transformations, the exact nature of the counterion may influence the solubility and

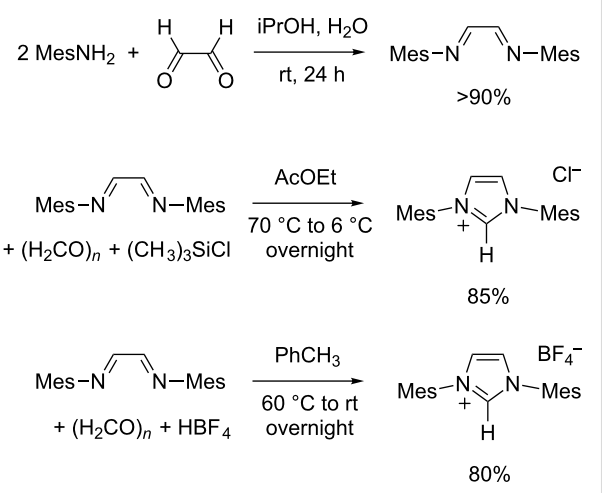

Scheme 5: Synthesis of 1,3-dimesitylimidazolium salts (IMes·HCl and IMes·HBF_4).

the deprotonation rate of the carbene precursor [58]. A report from 2010 had shown that treating *N,N′*-dimesitylethylenediimine with paraformaldehyde and a 48% aqueous solution of tetrafluoroboric acid in warm toluene afforded 1,3-dimesitylimidazolium tetrafluoroborate without any apparent complication [59]. We have further optimized this procedure on the occasion of a mechanistic study of the Staudinger reaction catalyzed by NHC·ketene zwitterions (Scheme 5) [60].

Synthesis of 1,3-dimesitylimidazolinium chloride

The "saturated" analogue of the IMes carbene, 1,3-dimesitylimidazolin-2-ylidene (SIMes), was first isolated in 1995 by Arduengo et al. [61] who later disclosed the experimental details of the synthetic path leading to this stable NHC and its immediate precursor, 1,3-dimesitylimidazolinium chloride (SIMes·HCl) [43]. The latter salt was obtained in three steps starting from widely available, acyclic reagents (Scheme 6). First, the condensation of glyoxal with two equivalents of mesitylamine afforded the corresponding diimine, as described above for the synthesis of IMes·HCl and IMes·HBF_4 (cf. Scheme 5). Next, the diimine was reduced into a diamine with sodium borohydride in THF, followed by an acidic work-up with aqueous hydrochloric acid to quench the excess of hydride and to precipitate *N,N′*-dimesitylethylenediammonium dichloride as a stable white solid. A third step afforded the final heterocyclic product upon ring-closure with triethyl orthoformate in the presence of a catalytic amount of formic acid. In this reaction, the orthoester served both as a solvent and a precarbenic C^2 provider.

Following the seminal contribution of Arduengo and co-workers, several other research groups proposed experi-

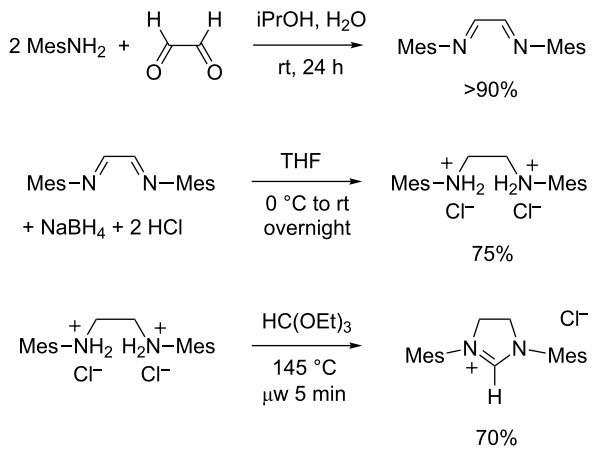

Scheme 6: Synthesis of 1,3-dimesitylimidazolinium chloride (SIMes·HCl).

mental procedures for the preparation of imidazolinium salts from *N*,*N*′-disubstituted 1,2-ethanediamines or their ammonium salts and triethyl orthoformate [62-65]. In most cases, prolonged heating under reflux conditions was necessary to reach satisfactory conversions, even when ethanol was distilled off the reaction mixture to drive the equilibrium toward completion. In 2006, we found that microwave irradiation allowed to dramatically reduce the reaction time from hours to minutes, while affording very high yields of pure products [66]. We have applied this procedure to the synthesis of a wide range of cyclic amidinium salts differing by their ring size, N-substituents, and counterions [67]. In 2010, we have further optimized the microwave-assisted synthesis of SIMes·HCl to turn it into a convenient, laboratory-scale preparation [68]. With the latest implementation of our protocol, which uses an 80 mL glass vessel in a monomodal microwave reactor, it took 5 minutes to perform the cyclization on a 50 mmol batch and the product was isolated in 70% yield after purification (Scheme 6).

Synthesis of 1,3-bis(2,6-diisopropylphenyl)-imidazolium chloride

Huang and Nolan first reported the introduction of 2,6-diisopropylphenyl groups on an imidazolylidene backbone in 1999 while searching for bulky NHC ligands to coordinate onto palladium catalysts for Kumada cross-coupling reactions [57]. The resulting carbene was nicknamed IPr and this designation still persists in the literature, although IDip is a more fitting acronym to avoid any confusion with 1,3-di(isopropyl)-imidazol-2-ylidene. Thus, 1,3-bis(2,6-diisopropylphenyl)imidazolium chloride (IDip·HCl) was obtained following a two-step procedure that first involved the condensation of glyoxal and two equivalents of 2,6-diisopropylaniline into the corresponding diazabutadiene. This intermediate was then cyclized into the final product using paraformaldehyde in toluene as the precarbenic C^2 donor reagent and anhydrous HCl in dioxane as the source of the counterion. Soon thereafter, Arduengo and co-workers described the synthesis of IDip·HCl using chloromethyl ethyl ether as a single provider for the azolium chloride building block [43]. From a practical point of view, both procedures represented a significant breakthrough, because the one-pot strategy was largely inefficient for imidazolium salts bearing bulky aromatic substituents on their nitrogen atoms.

Over the years, minor changes were brought to the original protocols of Nolan and Arduengo in order to improve yields that did not initially pass the 50% threshold [45,69,70]. Yet, the most convenient preparation available to date for IDip·HCl was proposed in 2007 by Hintermann [44]. It involved the reaction of *N*,*N*′-bis(2,6-diisopropylphenyl)ethylenediimine with paraformaldehyde and chlorotrimethylsilane in ethyl acetate (Scheme 7). In our hands, this procedure proved reliable and afforded typical yields of 85%. Its major drawback is the necessity to work under high dilution conditions, which implies the use of large amounts of solvent and hinders scale up.

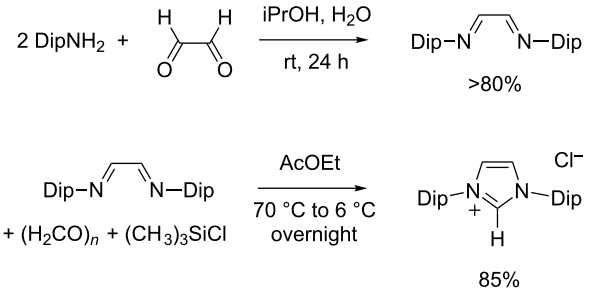

Scheme 7: Synthesis of 1,3-bis(2,6-diisopropylphenyl)-imidazolium chloride (IDip·HCl).

Synthesis of 1,3-bis(2,6-diisopropylphenyl)-imidazolinium chloride

In most cases, experimental procedures leading to 1,3-dimesitylimidazolinium salts could be successfully extended to their 1,3-bis(2,6-diisopropylphenyl) counterparts without any adaptation. Thus, the three-step synthesis of SIDip·HCl (also known as SIPr·HCl) initially reported by Arduengo et al. closely matched the one defined for SIMes·HCl in terms of experimental conditions and yields [43]. Likewise, our microwave-assisted cyclization performed equally well when applied to *N*,*N*′-bis(2,6-diisopropylphenyl)ethylenediammonium chloride instead of the dimesityl intermediate (Scheme 8). In both cases, the desired product was isolated in (70 ± 5)% yield after a very simple work-up that involved filtration and washing.

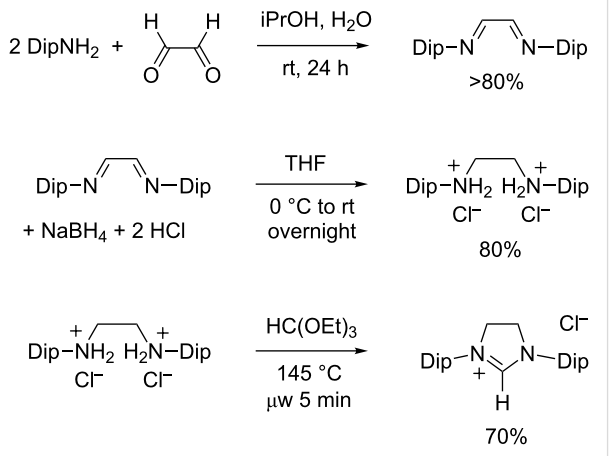

Scheme 8: Synthesis of 1,3-bis(2,6-diisopropylphenyl)-imidazolinium chloride (SIDip·HCl).

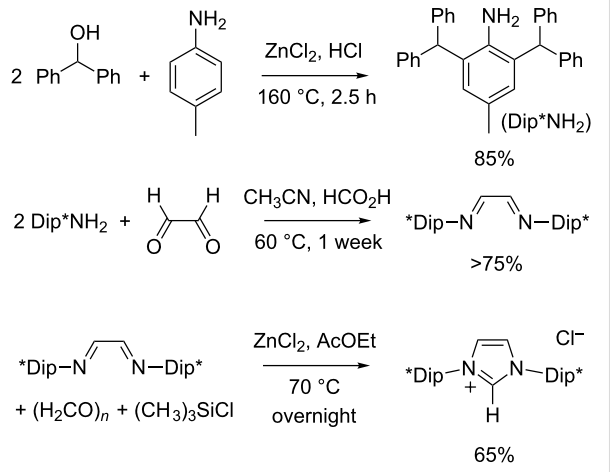

Scheme 9: Synthesis of 1,3-bis(2,6-bis(diphenylmethyl)-4-methylphenyl)imidazolium chloride (IDip*·HCl).

Synthesis of 1,3-bis(2,6-bis(diphenylmethyl)-4-methylphenyl)imidazolium chloride

In 2010, the group of Markó designed a very bulky, yet flexible NHC ligand by replacing the methyl groups of IDip with phenyl rings [71]. This new highly hindered carbene that we shall designate as IDip* (but it is also trivially named IPr*) was readily obtained by deprotonation of 1,3-bis(2,6-bis(diphenylmethyl)-4-methylphenyl)imidazolium chloride (IDip*·HCl). The synthesis of this stable precursor was accomplished in three steps starting from commercially available reagents (Scheme 9). First, *p*-toluidine was dialkylated with diphenylmethanol (benzhydrol) in the presence of stoichiometric amounts of HCl and $ZnCl_2$. This Friedel–Crafts alkylation was carried out under solvent-free conditions and afforded high yields of the bulky aniline needed to follow the Arduengo formylative cyclization path. It was originally performed in a sealed tube under autogeneous pressure at 160 °C. We checked that the reaction could be carried out in an open vessel without any detrimental consequence, thereby leading to a safer experimental procedure. In the second step, 2,6-bis(diphenylmethyl)-4-methylaniline (Dip^*NH_2) was reacted with aqueous glyoxal to form the corresponding ethylenediimine. Markó et al. performed this condensation in dichloromethane containing formic acid as a catalyst and anhydrous magnesium sulfate as a dehydrating agent. We found this procedure difficult to reproduce. Moreover, a rather tedious work-up was required to separate and to purify the product. Inspired by a report from Cole and co-workers on the preparation of another bulky imidazolium salt [72], we found that acetonitrile was a much more convenient solvent than dichloromethane to achieve the condensation of Dip^*NH_2 and glyoxal. Although the reaction was slow and took about a week to reach completion at 60 °C, the desired diazabutadiene cleanly precipitated from the reaction mixture and could be isolated in high yield by simple filtration and washing.

For the critical cyclization step of IDip*·HCl, Markó et al. ingeniously took advantage of the Lewis acidity of zinc chloride to activate paraformaldehyde and of its coordinating ability to maintain the intermediate diimine in the required *s-cis* conformation [71]. Concentrated hydrochloric acid was added as the counterion source and the final imidazolium product was isolated in 50–60% yield. We further improved this procedure through the use of chlorotrimethylsilane as the chloride donor to minimize hydrolysis and other side-reactions of the diimine. The templating effect of $ZnCl_2$ was also maximized by combining this stoichiometric additive with the diimine and paraformaldehyde prior to the addition of Me_3SiCl. Under these revised conditions, IDip*·HCl was isolated in 65% yield after recrystallization.

Conclusion

The one-pot condensation of glyoxal, two equivalents of a primary alkylamine, and paraformaldehyde in the presence of aqueous HBF_4 provided a straightforward access to symmetrical 1,3-dialkylimidazolium tetrafluoroborates. To achieve the preparation of 1,3-diarylimidazolium salts, it was necessary to isolate the intermediate diimines prior to their cyclization. Although this additional step required more time and reagents, it led to a much more efficient overall process. It proved also very convenient to carry out the synthesis of imidazolinium salts in parallel to their imidazolium counterparts via the reduction of the diimines into diamines or diammonium salts. The critical assembly of the C^2 precarbenic unit was best achieved with paraformaldehyde and chlorotrimethylsilane in the case of the imidazolium derivatives, whereas the use of triethyl orthoformate under microwave irradiation was most appropriate for the fast and efficient synthesis of imidazolinium salts.

With the possible exception of a monomodal microwave reactor, all the equipment and glassware needed to carry out the syntheses outlined in this report are widely available in chemical laboratories and do not require any particular skills from the experimenter. Furthermore, the detailed experimental procedures supplied in Supporting Information File 1 of this article are easy to scale up or down according to the particular needs for a given compound. Thus, we hope that they will be helpful to the large community of organic and organometallic chemists working with NHCs.

Supporting Information

Supporting Information File 1

Full experimental section with detailed synthetic procedures and analytical data for all the compounds.
[http://www.beilstein-journals.org/bjoc/content/supplementary/1860-5397-11-252-S1.pdf]

Acknowledgements

The financial support of the "Fonds de la Recherche Scientifique–FNRS", Brussels, is gratefully acknowledged. JL is indebted to the EC for an Erasmus+ fellowship. The authors would like to thank all the trainees and the researchers from the Laboratory of Catalysis who have tested, improved, and checked the procedures reported in this study over the years.

References

1. Arduengo, A. J., III; Harlow, R. L.; Kline, M. *J. Am. Chem. Soc.* **1991,** *113,* 361–363. doi:10.1021/ja00001a054
2. Arduengo, A. J., III. *Acc. Chem. Res.* **1999,** *32,* 913–921. doi:10.1021/ar980126p
3. Glorius, F., Ed. *N-Heterocyclic Carbenes in Transition Metal Catalysis; Topics in Organometallic Chemistry*, Vol. 21; Springer: Berlin, 2007.
4. Díez-González, S., Ed. *N-Heterocyclic Carbenes: From Laboratory Curiosities to Efficient Synthetic Tools; RSC Catalysis Series*, Vol. 6; Royal Society of Chemistry: Cambridge, 2010.
5. Cazin, C. S. J., Ed. *N-Heterocyclic Carbenes in Transition Metal Catalysis and Organocatalysis; Catalysis by Metal Complexes*, Vol. 32; Springer: Dordrecht, 2011.
6. Nolan, S. P., Ed. *N-Heterocyclic Carbenes: Effective Tools for Organometallic Synthesis;* Wiley-VCH: Weinheim, 2014.
7. Hopkinson, M. N.; Richter, C.; Schedler, M.; Glorius, F. *Nature* **2014,** *510,* 485–496. doi:10.1038/nature13384
8. Hahn, F. E.; Jahnke, M. C. *Angew. Chem., Int. Ed.* **2008,** *47,* 3122–3172. doi:10.1002/anie.200703883
9. Lin, J. C. Y.; Huang, R. T. W.; Lee, C. S.; Bhattacharyya, A.; Hwang, W. S.; Lin, I. J. B. *Chem. Rev.* **2009,** *109,* 3561–3598. doi:10.1021/cr8005153
10. Bellemin-Laponnaz, S.; Dagorne, S. *Chem. Rev.* **2014,** *114,* 8747–8774. doi:10.1021/cr500227y
11. Arnold, P. L.; Casely, I. J. *Chem. Rev.* **2009,** *109,* 3599–3611. doi:10.1021/cr8005203
12. Willans, C. E. Non-transition metal N-heterocyclic carbene complexes. In *Organometallic Chemistry;* Fairlamb, I. J. S.; Lynam, J. M., Eds.; Royal Society of Chemistry: Cambridge, 2010; Vol. 36, pp 1–28. doi:10.1039/9781847559616-00001
13. Kuhn, N.; Al-Sheikh, A. *Coord. Chem. Rev.* **2005,** *249,* 829–857. doi:10.1016/j.ccr.2004.10.003
14. Marion, N.; Nolan, S. P. *Chem. Soc. Rev.* **2008,** *37,* 1776–1782. doi:10.1039/b711132k
15. Díez-González, S.; Marion, N.; Nolan, S. P. *Chem. Rev.* **2009,** *109,* 3612–3676. doi:10.1021/cr900074m
16. Poyatos, M.; Mata, J. A.; Peris, E. *Chem. Rev.* **2009,** *109,* 3677–3707. doi:10.1021/cr800501s
17. Ingleson, M. J.; Layfield, R. A. *Chem. Commun.* **2012,** *48,* 3579–3589. doi:10.1039/c2cc18021a
18. Samojłowicz, C.; Bieniek, M.; Grela, K. *Chem. Rev.* **2009,** *109,* 3708–3742. doi:10.1021/cr800524f
19. Vougioukalakis, G. C.; Grubbs, R. H. *Chem. Rev.* **2010,** *110,* 1746–1787. doi:10.1021/cr9002424
20. Delaude, L.; Demonceau, A. *Dalton Trans.* **2012,** *41,* 9257–9268. doi:10.1039/c2dt30293d
21. Hamad, F. B.; Sun, T.; Xiao, S.; Verpoort, F. *Coord. Chem. Rev.* **2013,** *257,* 2274–2292. doi:10.1016/j.ccr.2013.04.015
22. Kamber, N. E.; Jeong, W.; Waymouth, R. M.; Pratt, R. C.; Lohmeijer, B. G. G.; Hedrick, J. L. *Chem. Rev.* **2007,** *107,* 5813–5840. doi:10.1021/cr068415b
23. Fèvre, M.; Pinaud, J.; Gnanou, Y.; Vignolle, J.; Taton, D. *Chem. Soc. Rev.* **2013,** *42,* 2142–2172. doi:10.1039/c2cs35383k
24. Enders, D.; Niemeier, O.; Henseler, A. *Chem. Rev.* **2007,** *107,* 5606–5655. doi:10.1021/cr068372z
25. Marion, N.; Díez-González, S.; Nolan, S. P. *Angew. Chem., Int. Ed.* **2007,** *46,* 2988–3000. doi:10.1002/anie.200603380
26. Flanigan, D. M.; Romanov-Michailidis, F.; White, N. A.; Rovis, T. *Chem. Rev.* **2015,** *115,* 9307–9387. doi:10.1021/acs.chemrev.5b00060
27. Vora, H. U.; Rovis, T. *Aldrichimica Acta* **2011,** *44,* 3–11.
28. Nair, V.; Menon, R. S.; Biju, A. T.; Sinu, C. R.; Paul, R. R.; Jose, A.; Sreekumar, V. *Chem. Soc. Rev.* **2011,** *40,* 5336–5346. doi:10.1039/c1cs15139h
29. Bugaut, X.; Glorius, F. *Chem. Soc. Rev.* **2012,** *41,* 3511–3522. doi:10.1039/c2cs15333e
30. de Frémont, P.; Marion, N.; Nolan, S. P. *Coord. Chem. Rev.* **2009,** *253,* 862–892. doi:10.1016/j.ccr.2008.05.018
31. Duong, H. A.; Tekavec, T. N.; Arif, A. M.; Louie, J. *Chem. Commun.* **2004,** 112–113. doi:10.1039/B311350G
32. Tudose, A.; Demonceau, A.; Delaude, L. *J. Organomet. Chem.* **2006,** *691,* 5356–5365. doi:10.1016/j.jorganchem.2006.07.035
33. Van Ausdall, B. R.; Glass, J. L.; Wiggins, K. M.; Aarif, A. M.; Louie, J. *J. Org. Chem.* **2009,** *74,* 7935–7942. doi:10.1021/jo901791k
34. Sauvage, X.; Demonceau, A.; Delaude, L. *Adv. Synth. Catal.* **2009,** *351,* 2031–2038. doi:10.1002/adsc.200900422
35. Hans, M.; Delaude, L.; Rodriguez, J.; Coquerel, Y. *J. Org. Chem.* **2014,** *79,* 2758–2764. doi:10.1021/jo500108a
36. Nyce, G. W.; Csihony, S.; Waymouth, R. M.; Hedrick, J. L. *Chem. – Eur. J.* **2004,** *10,* 4073–4079. doi:10.1002/chem.200400196
37. Coulembier, O.; Lohmeijer, B. G. G.; Dove, A. P.; Pratt, R. C.; Mespouille, L.; Culkin, D. A.; Benight, S. J.; Dubois, P.; Waymouth, R. M.; Hedrick, J. L. *Macromolecules* **2006,** *39,* 5617–5628. doi:10.1021/ma0611366
38. Blum, A. P.; Ritter, T.; Grubbs, R. H. *Organometallics* **2007,** *26,* 2122–2124. doi:10.1021/om060949f

39. Garrison, J. C.; Youngs, W. J. *Chem. Rev.* **2005,** *105,* 3978–4008. doi:10.1021/cr050004s
40. Lin, I. J. B.; Vasam, C. S. *Coord. Chem. Rev.* **2007,** *251,* 642–670. doi:10.1016/j.ccr.2006.09.004
41. Benhamou, L.; Chardon, E.; Lavigne, G.; Bellemin-Laponnaz, S.; César, V. *Chem. Rev.* **2011,** *111,* 2705–2733. doi:10.1021/cr100328e
42. Arduengo, A. J., III. Preparation of 1,3-Disubstituted Imidazolium Salts. PCT Int. Appl. WO9114678, Oct 3, 1991.
43. Arduengo, A. J., III; Krafczyk, R.; Schmutzler, R.; Craig, H. A.; Goerlich, J. R.; Marshall, W. J.; Unverzagt, M. *Tetrahedron* **1999,** *55,* 14523–14534. doi:10.1016/S0040-4020(99)00927-8
44. Hintermann, L. *Beilstein J. Org. Chem.* **2007,** *3,* No. 22. doi:10.1186/1860-5397-3-22
45. Bantreil, X.; Nolan, S. P. *Nat. Protoc.* **2011,** *6,* 69–77. doi:10.1038/nprot.2010.177
46. Briggs, A. J. *Synth. Commun.* **2013,** *43,* 3258–3261. doi:10.1080/00397911.2013.768671
47. Herrmann, W. A.; Köcher, C.; Gooßen, L. J.; Artus, G. R. J. *Chem. – Eur. J.* **1996,** *2,* 1627–1636. doi:10.1002/chem.19960021222
48. Hans, M.; Wouters, J.; Demonceau, A.; Delaude, L. *Chem. – Eur. J.* **2015,** *21,* 10870–10877. doi:10.1002/chem.201501060
49. Archer, R. H.; Carpenter, J. R.; Hwang, S.-J.; Burton, A. W.; Chen, C.-Y.; Zones, S. I.; Davis, M. E. *Chem. Mater.* **2010,** *22,* 2563–2572. doi:10.1021/cm9035677
50. Starikova, O. V.; Dolgushin, G. V.; Larina, L. I.; Ushakov, P. E.; Komarova, T. N.; Lopyrev, V. A. *Russ. J. Org. Chem.* **2003,** *39,* 1467–1470. doi:10.1023/B:RUJO.0000010563.79902.47
51. Berding, J.; Kooijman, H.; Spek, A. L.; Bouwman, E. *J. Organomet. Chem.* **2009,** *694,* 2217–2221. doi:10.1016/j.jorganchem.2009.02.030
52. Leclercq, L.; Simard, M.; Schmitzer, A. R. *J. Mol. Struct.* **2009,** *918,* 101–107. doi:10.1016/j.molstruc.2008.07.023
53. Bouhrara, M.; Jeanneau, E.; Veyre, L.; Copéret, C.; Thieuleux, C. *Dalton Trans.* **2011,** *40,* 2995–2999. doi:10.1039/c0dt00932f
54. Arduengo, A. J., III; Rasika Dias, H. V.; Harlow, R. L.; Kline, M. *J. Am. Chem. Soc.* **1992,** *114,* 5530–5534. doi:10.1021/ja00040a007
55. Voges, M. H.; Rømming, C.; Tilset, M. *Organometallics* **1999,** *18,* 529–533. doi:10.1021/om980799b
56. Cole, M. L.; Junk, P. C. *CrystEngComm* **2004,** *6,* 173–176. doi:10.1039/b403451a
57. Huang, J.; Nolan, S. P. *J. Am. Chem. Soc.* **1999,** *121,* 9889–9890. doi:10.1021/ja991703n
58. Wei, S.; Wei, X.-G.; Su, X.; You, J.; Ren, Y. *Chem. – Eur. J.* **2011,** *17,* 5965–5971. doi:10.1002/chem.201002839
59. Li, S.; Kee, C. W.; Huang, K.-W.; Hor, T. S. A.; Zhao, J. *Organometallics* **2010,** *29,* 1924–1933. doi:10.1021/om900980a
60. Hans, M.; Wouters, J.; Demonceau, A.; Delaude, L. *Chem. – Eur. J.* **2013,** *19,* 9668–9676. doi:10.1002/chem.201204428
61. Arduengo, A. J., III; Goerlich, J. R.; Marshall, W. J. *J. Am. Chem. Soc.* **1995,** *117,* 11027–11028. doi:10.1021/ja00149a034
62. Delaude, L.; Szypa, M.; Demonceau, A.; Noels, A. F. *Adv. Synth. Catal.* **2002,** *344,* 749–756.
63. Ma, Y.; Song, C.; Jiang, W.; Wu, Q.; Wang, Y.; Liu, X.; Andrus, M. B. *Org. Lett.* **2003,** *5,* 3317–3319. doi:10.1021/ol035147k
64. Van Veldhuizen, J. J.; Gillingham, D. G.; Garber, S. B.; Kataoka, O.; Hoveyda, A. H. *J. Am. Chem. Soc.* **2003,** *125,* 12502–12508. doi:10.1021/ja0302228
65. Funk, T. W.; Berlin, J. M.; Grubbs, R. H. *J. Am. Chem. Soc.* **2006,** *128,* 1840–1846. doi:10.1021/ja055994d
66. Aidouni, A.; Demonceau, A.; Delaude, L. *Synlett* **2006,** 493–495. doi:10.1055/s-2006-932455
67. Aidouni, A.; Bendahou, S.; Demonceau, A.; Delaude, L. *J. Comb. Chem.* **2008,** *10,* 886–892. doi:10.1021/cc800101k
68. Hans, M.; Delaude, L. *Org. Synth.* **2010,** *87,* 77–87. doi:10.15227/orgsyn.087.0077
69. Higgins, E. M.; Sherwood, J. A.; Lindsay, A. G.; Armstrong, J.; Massey, R. S.; Alder, R. W.; O'Donoghue, A. C. *Chem. Commun.* **2011,** *47,* 1559–1561. doi:10.1039/C0CC03367G
70. Zhu, S.; Liang, R.; Jiang, H. *Tetrahedron* **2012,** *68,* 7949–7955. doi:10.1016/j.tet.2012.07.009
71. Berthon-Gelloz, G.; Siegler, M. A.; Spek, A. L.; Tinant, B.; Reek, J. N. H.; Markó, I. E. *Dalton Trans.* **2010,** *39,* 1444–1446. doi:10.1039/B921894G
72. Alexander, S. G.; Cole, M. L.; Morris, J. C. *New J. Chem.* **2009,** *33,* 720–724. doi:10.1039/b821368b

License and Terms

BEILSTEIN JOURNAL OF ORGANIC CHEMISTRY

Comparison of the catalytic activity for the Suzuki–Miyaura reaction of (η^5-Cp)Pd(IPr)Cl with (η^3-cinnamyl)Pd(IPr)(Cl) and (η^3-1-*t*-Bu-indenyl)Pd(IPr)(Cl)

Patrick R. Melvin, Nilay Hazari*, Hannah M. C. Lant, Ian L. Peczak and Hemali P. Shah

Full Research Paper

Open Access

Address:
The Department of Chemistry, Yale University, P. O. Box 208107, New Haven, Connecticut, 06520, USA

Email:
Nilay Hazari* - nilay.hazari@yale.edu.

* Corresponding author

Keywords:
cross-coupling; homogeneous catalysis; NHC ligands; palladium; Suzuki–Miyaura reaction

Beilstein J. Org. Chem. **2015,** *11,* 2476–2486.
doi:10.3762/bjoc.11.269

Received: 15 September 2015
Accepted: 27 November 2015
Published: 08 December 2015

This article is part of the Thematic Series "N-Heterocyclic carbenes".

Guest Editor: S. P. Nolan

Abstract

Complexes of the type (η^3-allyl)Pd(L)(Cl) and (η^3-indenyl)Pd(L)(Cl) are highly active precatalysts for the Suzuki–Miyaura reaction. Even though allyl and indenyl ligands are similar to cyclopentadienyl (Cp) ligands, there have been no detailed comparative studies exploring the activity of precatalysts of the type (η^5-Cp)Pd(L)(Cl) for Suzuki–Miyaura reactions. Here, we compare the catalytic activity of (η^5-Cp)Pd(IPr)(Cl) (IPr = 1,3-bis(2,6-diisopropylphenyl)-1,3-dihydro-2*H*-imidazol-2-ylidene, **Cp**) with two commercially available catalysts (η^3-cinnamyl)Pd(IPr)(Cl) (**Cin**) and (η^3-1-*t*-Bu-indenyl)Pd(IPr)(Cl) (**^{tBu}Ind**). We show that **Cp** gives slightly better catalytic activity than **Cin**, but significantly inferior activity than **^{tBu}Ind**. This order of activity is rationalized by comparing the rates at which the precatalysts are activated to the monoligated Pd(0) active species along with the tendency of the starting precatalysts to comproportionate with monoligated Pd(0) to form inactive Pd(I) dimers. As part of this work the Cp supported Pd(I) dimer (μ-Cp)(μ-Cl)Pd_2(IPr)$_2$ (**Cp^{Dim}**) was synthesized and crystallographically characterized. It does not readily disproportionate to form monoligated Pd(0) and consequently **Cp^{Dim}** is a poor catalyst for the Suzuki–Miyaura reaction.

Introduction

The Suzuki–Miyaura reaction is a powerful synthetic method for forming C–C bonds between aryl halides or pseudo halides and organoborane containing species [1-5]. The most active catalysts are generally based on Pd and feature strongly electron-donating and sterically bulky phosphine or N-heterocyclic carbene (NHC) ancillary ligands [6,7]. In particular, precatalysts of the type (η^3-allyl)Pd(NHC)(Cl) have shown excellent activity for the Suzuki–Miyaura reaction, with systems incorporating an η^3-cinnamyl moiety giving the best catalytic results (Figure 1) [8-12]. Recently, we showed that the excellent activity of the cinnamyl system is related to two factors: (i) the rate at which the Pd(II) precatalyst is reduced to the

active monoligated Pd(0) species; and (ii) the difficulty of comproportionation between L-Pd(0) and the starting precatalyst, which generates a Pd(I) μ-cinnamyl dimer of the form (μ-cinnamyl)(μ-Cl)$Pd_2(L)_2$, and removes L-Pd(0) from the reaction mixture [13,14]. Furthermore, we used this mechanistic information to design an improved precatalyst scaffold featuring an η^3-indenyl ligand [15]. In particular, precatalysts based on the (η^3-1-*t*-Bu-indenyl)Pd(L)(Cl) scaffold were highly active because Pd(I) dimer formation was effectively suppressed and the rate of reduction from Pd(II) to Pd(0) was increased [16].

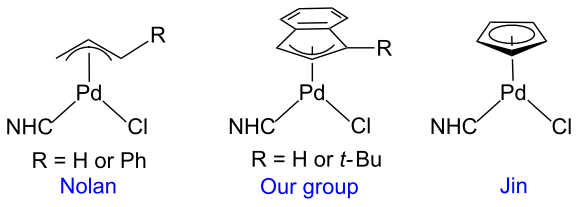

Figure 1: General depictions of allyl and related precatalysts that are highly active for the Suzuki–Miyaura reaction with NHC ligands.

In organometallic chemistry, allyl and indenyl ligands are considered to be closely related to cyclopentadienyl (Cp) ligands [17]. Nevertheless, to the best of our knowledge there are only two reports describing the catalytic activity of complexes of the type (η^5-Cp)Pd(NHC)(Cl) for the Suzuki–Miyaura coupling, as well as related cross-coupling reactions [18,19]. These preliminary reports indicate that (η^5-Cp)Pd(NHC)(Cl) precatalysts are highly active. For example, full conversion at room temperature was achieved using simple aryl chlorides as the substrate in Suzuki–Miyaura couplings at relatively low catalyst loadings (1 mol %) [18]. However, despite this impressive activity, a direct comparison of the performance of (η^5-Cp)Pd(NHC)(Cl) type precatalysts with the related commercially available (η^3-allyl)Pd(NHC)(Cl) and (η^3-indenyl)Pd(NHC)(Cl) systems under the same reaction conditions has never been performed. Here, we directly assess the activity of (η^5-Cp)Pd(IPr)(Cl) (IPr = 1,3-bis(2,6-diisopropylphenyl)-1,3-dihydro-2*H*-imidazol-2-ylidene, **Cp**) to the analogous (η^3-cinnamyl)Pd(IPr)(Cl) (**Cin**) and (η^3-1-*t*-Bu-indenyl)Pd(IPr)(Cl) (**^{tBu}Ind**) precatalysts [20]. We show that the performance of **Cp** fits into our model of precatalyst performance based on the speed at which a scaffold is reduced from Pd(II) to Pd(0) and its tendency to undergo comproportionation.

Results and Discussion

Catalytic comparison of (η^5-Cp)Pd(IPr)Cl, (η^3-cinnamyl)Pd(IPr)Cl and (η^3-1-*t*-Bu-indenyl)Pd(IPr)Cl

The IPr supported precatalyst for the Suzuki–Miyaura reaction **Cp** was synthesized using a literature method starting from the commercially available Pd(II) dimer (μ-Cl)$_2$Pd$_2$(η^3-allyl)$_2$ (Scheme 1) [18]. It is notable that in this synthesis dimeric {(IPr)Pd(Cl)}$_2$(μ-Cl)$_2$ is prepared as an intermediate, followed by treatment with two equivalents of NaCp to generate the monomer **Cp**. This synthesis makes rapid ligand screening using the Cp supported scaffold difficult as the Cp group is introduced after the ligand. In contrast, the syntheses of both **Cin** and **^{tBu}Ind** involve the initial preparation of dimers of the form {(η^3-cinnamyl)Pd}$_2$(μ-Cl)$_2$ or {(η^3-1-*t*-Bu-indenyl)Pd}$_2$(μ-Cl)$_2$, respectively [11,15], which can then be treated with a ligand to generate the ligated precatalyst. Despite repeated attempts we were unable to synthesize a related unligated Cp containing dimer, which could be used for ligand screening [21].

The catalytic activity of **Cp** for Suzuki–Miyaura reactions with different substrates under both strong (KO*t*-Bu) and weak (K_2CO_3) base conditions is compared to **Cin** and **^{tBu}Ind** in Figure 2 and Figure 3. In general, the performance of **Cp** is slightly better than **Cin**, but considerably worse than **^{tBu}Ind**. At

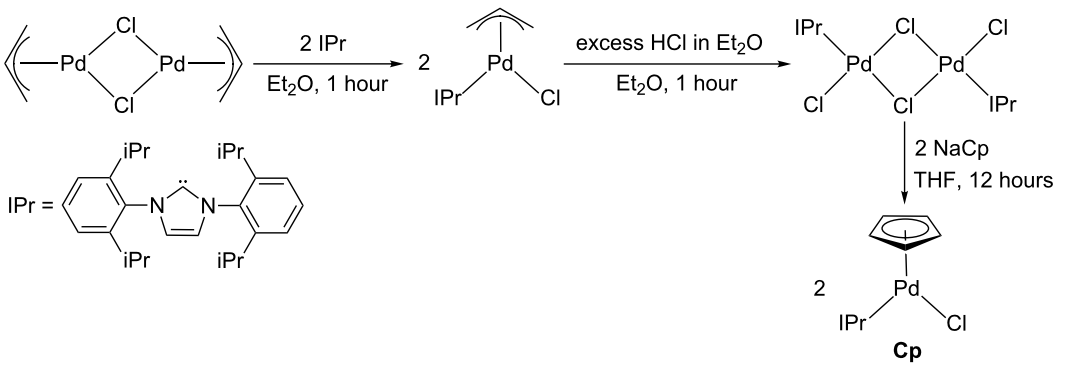

Scheme 1: Synthesis of **Cp**.

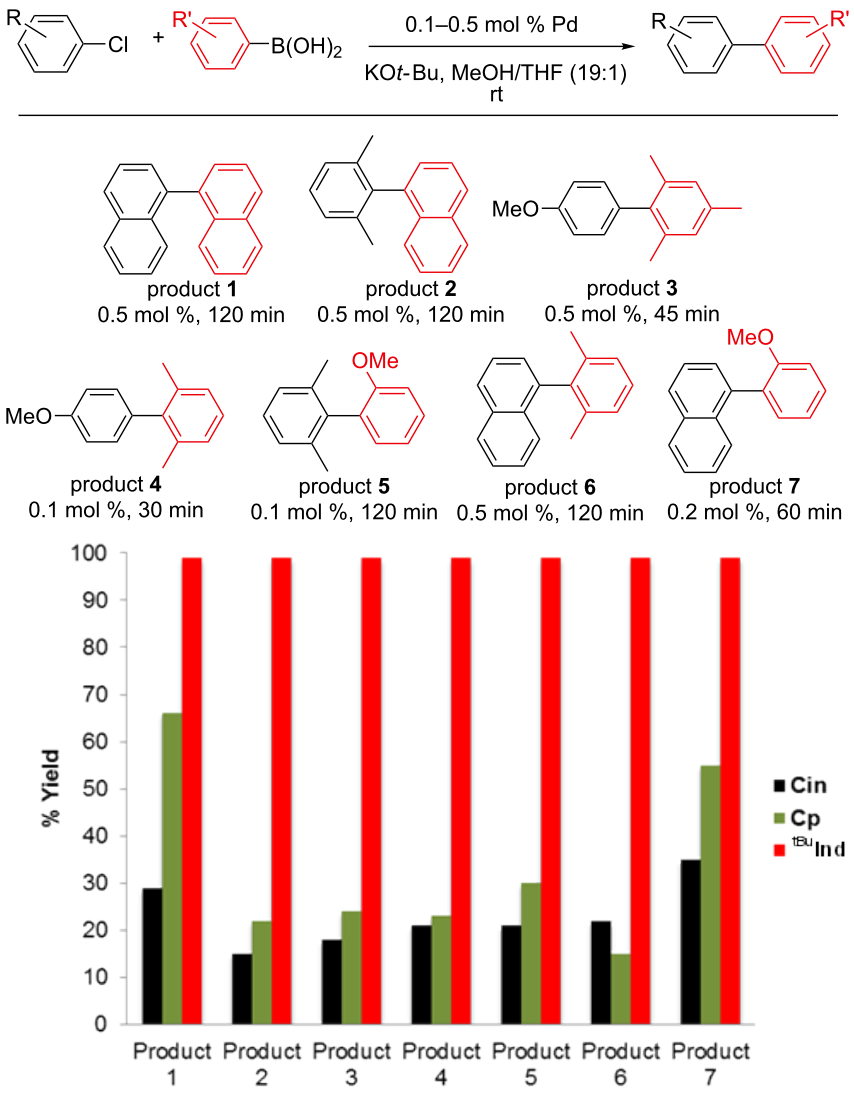

Figure 2: Comparison of catalytic performance of **Cin**, **Cp** and **^{tBu}Ind** for a series of Suzuki–Miyaura reactions using KO*t*-Bu as the base. Yields for **Cin** and **^{tBu}Ind** are from previous literature results [15]. All yields were determined using GC and are the average of two runs.

times when reactions using the **^{tBu}Ind** precatalyst are complete, between 10 and 60% conversion is achieved with **Cp**. If reactions catalyzed by **Cp** are left for longer periods of time complete conversion occurs, indicating that the difference in rates is not related to rapid catalyst decomposition in the case of **Cp**. These results confirm the previously reported high activity of Cp supported precatalysts [18]. Although the difference in performance between **Cin**, **Cp** and **^{tBu}Ind** varies depending on the specific substrate and catalyst loading, we are not able to discern any general trends in the data. For example, in some cases **Cp** gives better activity than **Cin** for the synthesis of di-*ortho*-substituted biaryls (products 1 and 7), whereas in another case **Cp** gives only slightly better activity (product 3). However, in general, the relative catalytic performance of the different precatalysts does not vary when the base is changed.

Understanding the relative activity of (η^5-Cp)Pd(IPr)Cl (Cp)

In order to understand the relative activity of **Cp** in comparison to **Cin** and **^{tBu}Ind**, we measured both the rate at which it is activated to monoligated Pd(0) and its tendency to undergo comproportionation to a Pd(I) dimer. The rate of activation was measured using the same procedure that we have previously used for **Cin** and **^{tBu}Ind** [16]. **Cp** was treated with base in the presence of ten equivalents of 1,3-divinyl-1,1,3,3-tetramethyldisiloxane (dvds) under a variety of conditions which are relevant to the Suzuki–Miyaura coupling and the reaction followed using ^{1}H NMR spectroscopy (Table 1). The metal containing product of this reaction is the Pd(0) complex (IPr)Pd(dvds) [22]. The rate of formation of (IPr)Pd(dvds) can be used as a model for the rate of Pd(0) formation in catalysis. In all cases **Cp** is

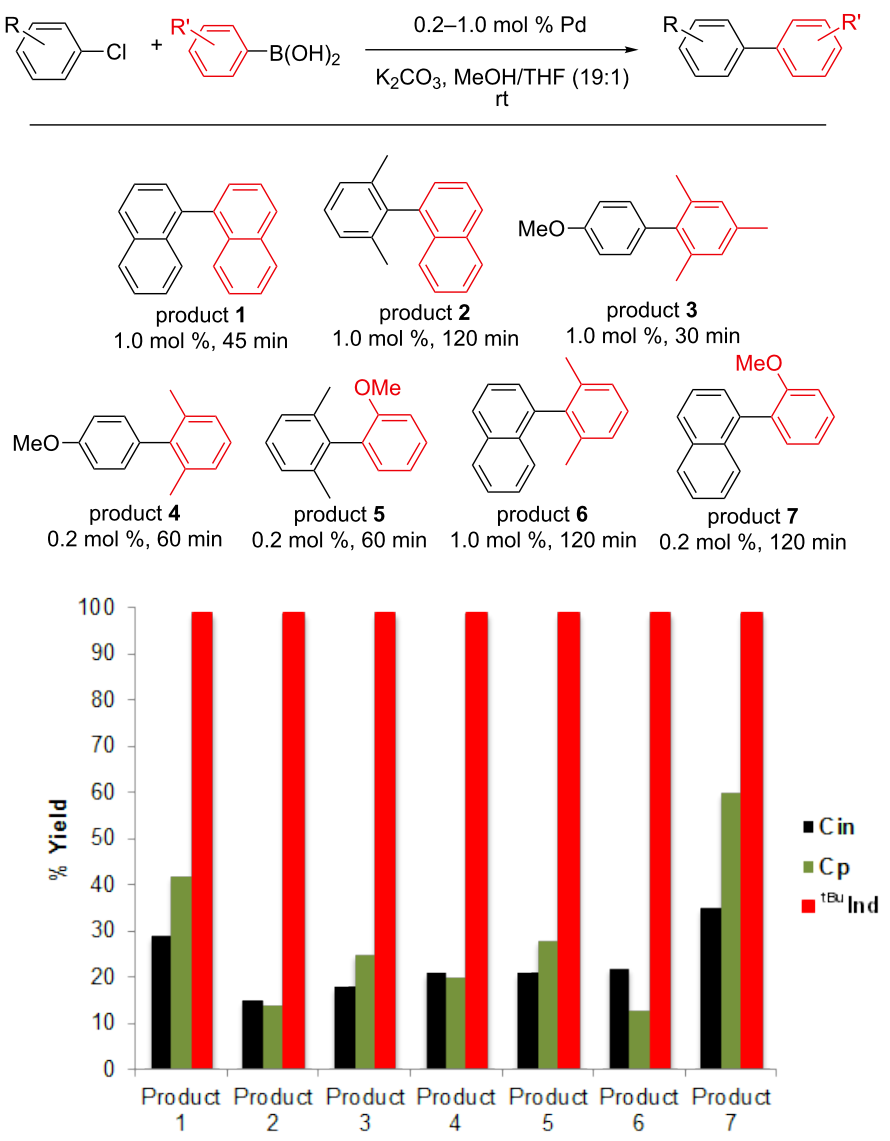

Figure 3: Comparison of catalytic performance of **Cin**, **Cp** and **^{tBu}Ind** for a series of Suzuki–Miyaura reactions using K_2CO_3 as the base. Yields for **Cin** and **^{tBu}Ind** are from previous literature results [15]. All yields were determined using GC and are the average of two runs.

activated slower than **^{tBu}Ind** [16], consistent with its inferior catalytic performance. For example, under the reaction conditions used in Table 1, entry 4, the rate of activation for **^{tBu}Ind** is $7.6 \pm 0.1 \times 10^{-4}$ s^{-1} compared to $3.4 \pm 0.1 \times 10^{-4}$ s^{-1} for **Cp** [16]. In contrast, **Cp** is generally activated faster than **Cin**. The rate of activation for **Cin** under the conditions used in Table 1, entry 3 is $4.2 \pm 0.1 \times 10^{-4}$, less than half the rate of that observed for **Cp**. The conditions used in Table 1, entry 4 are the most relevant to the catalysis described above, but although in this case it appears that **Cp** is activated faster than **Cin** ($3.4 \pm 0.1 \times 10^{-4}$ s^{-1} vs $1.4 \pm 0.2 \times 10^{-4}$ s^{-1}), the relatively large error associated with these numbers makes a firm conclusion difficult.

The mechanism of activation of **Cp** appears to be analogous to that previously described for **Cin** and **^{tBu}Ind** as the organic byproducts of **Cp** activation, cyclopentadiene and either acetone (in the case of reactions performed in iPrOH) or formaldehyde (in the case of reaction performed in MeOH), are consistent with the previously reported pathway (Scheme 2) [16]. In this mechanism initial substitution of a Cl^- ligand in **Cp** by the solvent gives rise to the alkoxide complex **A**. Subsequently, the η^5-Cp ring can undergo slippage to form complex **B**, with an η^1-Cp ligand. The η^1-Cp ligand is nucleophilic and can abstract a β-hydrogen from the alkoxide ligand to generate a Pd(0) species with a coordinated cyclopentadiene ligand (**C**). In this step the formaldehyde or acetone byproduct originating from

Table 1: Rates of activation of **Cp** under different conditions in the presence of dvds.[a]

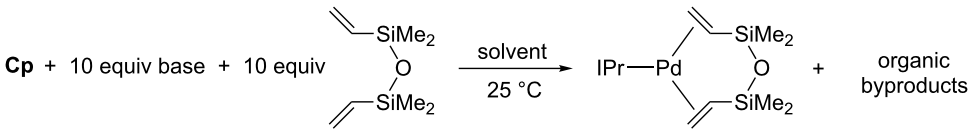

Entry	Base	Solvent	$PhB(OH)_2$ present	Rate of activation k_{obs} (s^{-1})[b]
1	KO*t*-Bu	iPrOH-d_8[c]	No	$2.8 \pm 0.1 \times 10^{-3}$
2	KO*t*-Bu	MeOH-d_4	No	$1.1 \pm 0.1 \times 10^{-3}$
3	K_2CO_3	MeOH-d_4[d]	No	$9.2 \pm 0.2 \times 10^{-4}$
4	K_2CO_3	MeOH-d_4[d]	Yes[e]	$3.4 \pm 0.1 \times 10^{-4}$

[a]Reaction conditions: 0.0087 mmol **Cp**, 0.087 mmol of base, 0.087 mmol of dvds in 500 µL of solvent. [b]All rates are the average of at least two runs and were measured using ^{1}H NMR spectroscopy. [c]100 µL of THF-d_8 was added along with only 400 µL of iPrOH. [d]Two equivalents of 18-crown-6 (relative to K_2CO_3) were added to solubilize the K_2CO_3. [e]0.0087 mmol precatalyst, 0.087 mmol phenylboronic acid, 0.096 mmol base, 0.087 mmol dvds in 500 µL MeOH-d_4.

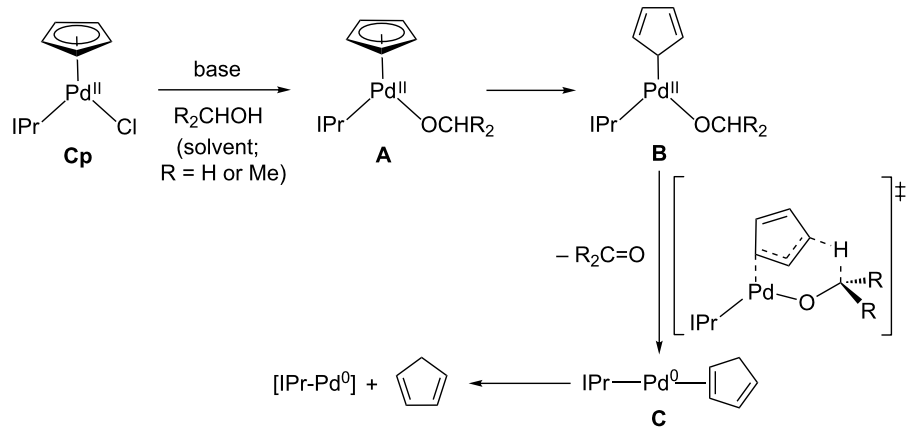

Scheme 2: Proposed mechanism for the activation of **Cp** to monoligated Pd(0).

the solvent is released. Finally, dissociation of the olefin ligand from **C** generates the active monoligated Pd(0) species, which in catalysis undergoes oxidative addition with the aryl halide, but in the case of our activation experiments is trapped by dvds.

The considerably faster rate of activation for **Cp** compared to **Cin**, suggests that **Cp** should be a much better precatalyst than **Cin**, which is inconsistent with our catalytic results (Figure 2 and Figure 3). In our model for precatalyst performance, catalytic activity is also related to the ease at which the starting precatalyst undergoes comproportionation with monoligated Pd(0) to form a Pd(I) dimer [13]. The reaction of **Cp** with a weak base, K_2CO_3, in an alcohol solvent (MeOH) provided the dimeric complex, (µ-Cp)(µ-Cl)$Pd_2(IPr)_2$ (**Cp^{Dim}**), in excellent yield (82%, Scheme 3). This is the same procedure we previously described for the preparation of Pd(I) dimers with a bridging chloride ligand and one bridging allyl or indenyl ligand [13].

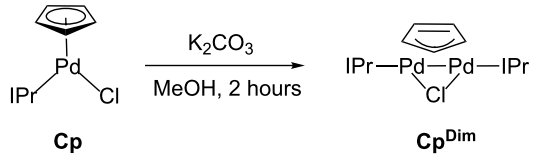

Scheme 3: Synthesis of **Cp^{Dim}**.

Cp^{Dim} was characterized by NMR spectroscopy and X-ray crystallography (see Figure 4). The binding of the bridging Cp ligand is similar to that observed in other Pd(I) dimers supported by a bridging Cp or indenyl ligand [23-39]. The two Pd centers are bound to three carbon atoms of the bridging Cp ligand. Two of the three carbon atoms are bound to only one Pd center, while the central carbon atom binds to both Pd centers. Pd–C bond distances of almost 3 Å clearly indicate that there is no interaction between the Pd centers and the other two carbon

atoms of the bridging Cp ligand. Consistent with this pseudo η^3-binding, the C–C bond distances relating to two long bonds, two bonds of intermediate length and one short bond in the bridging Cp ligand are similar to those observed in monomeric η^3-systems [40]. Strong evidence for a Pd–Pd single bond is provided by the Pd–Pd distance of 2.5669(4) Å [41]. Presumably for steric reasons the NHC ligands are bent away from the bridging Cp ligand and the C–Pd–Pd (C of IPr) bond angles are significantly less than 180° (Pd(1)–Pd(2)–C(7) 164.9(1) and Pd(2)–Pd(1)–C(6) 171.1(1)).

To determine if **Cp^{Dim}** is catalytically relevant modified conditions were used to allow for the reaction to be monitored by ^{1}H NMR spectroscopy (Scheme 4). In order to observe the Pd containing species, an increased catalyst loading was used, 4 mol % **Cp**, compared to the loadings described in Figure 2 and Figure 3. Peaks consistent with the formation of **Cp^{Dim}** are observed during catalysis, and approximately 40% of the Pd is in the form of **Cp^{Dim}** upon completion of the catalytic reaction. In contrast, for **Cin** under the same conditions, only a small amount of Pd was determined to be in the form of a Pd(I) dimer [13]. This suggests that **Cp** is more likely to undergo dimerization than **Cin**. **Cp^{Dim}** was confirmed to be a poor catalyst under the conditions employed in Figure 2 (Scheme 5). This result is indicative of **Cp^{Dim}** as an off-cycle deactivation product, which reduces the amount of the active Pd(0) species in solution.

Previously, we have demonstrated that the comproportionation of Pd(0) and Pd(II) species to IPr supported Pd(I) dimers with one bridging allyl and one bridging chloride ligand is reversible [13,14]. One method to measure the rate of disproportionation

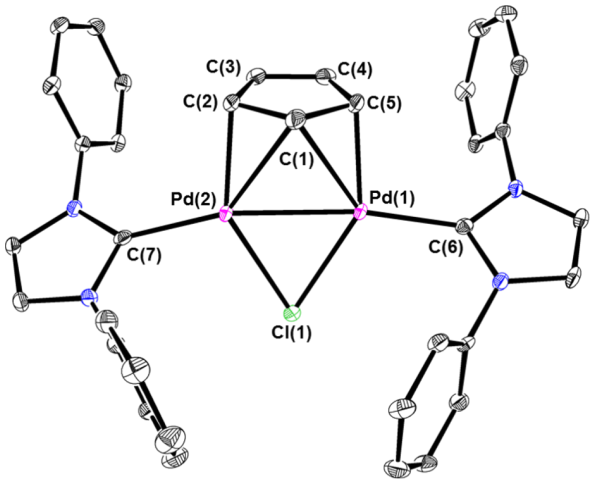

Figure 4: ORTEP of **Cp^{Dim}** at 30% probability. Hydrogen atoms and isopropyl groups of IPr are omitted for clarity. Selected bond lengths (Å) and angles (°) for: Pd(1)–Pd(2) 2.5669(4), Pd(1)–C(5) 2.102(4), Pd(1)–C(1) 2.480(4), Pd(2)–C(2) 2.119(4), Pd(2)–C(1) 2.449(4), Pd(1)–C(6) 2.022(4), Pd(2)–C(7) 2.031(4), Pd(1)–Cl(1) 2.402(2), Pd(2)–Cl(1) 2.398(1), C(1)–C(2) 1.433(6), C(2)–C(3) 1.463(8), C(3)–C(4) 1.347(6), C(4)–C(5) 1.465(7), C(1)–C(5) 1.438(7), Pd(1)–Cl(1)–Pd(2) 64.65(3), Pd(1)–C(1)–Pd(2) 62.8(2), Pd(1)–Pd(2)–C(7) 164.9(1), Pd(2)–Pd(1)–C(6) 171.1(1).

of Pd(I) dimers is to react these species with a trapping agent for Pd(0), such as dvds. This results in the formation of the Pd(0) species (IPr)Pd(dvds) and a Pd(II) species of the form (η^3-allyl)Pd(IPr)(Cl). We examined the tendency of **Cp^{Dim}** to undergo disproportionation in the presence of dvds. The disproportionation of **Cp^{Dim}** is extremely difficult and at 60 °C the

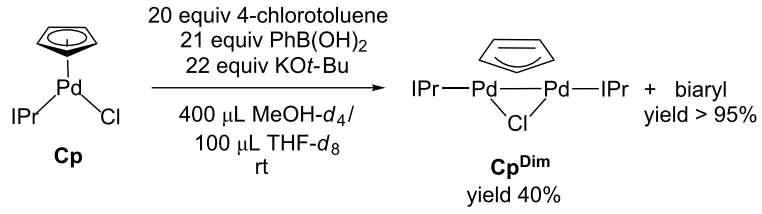

Scheme 4: Observation of **Cp^{Dim}** under modified catalytic conditions.

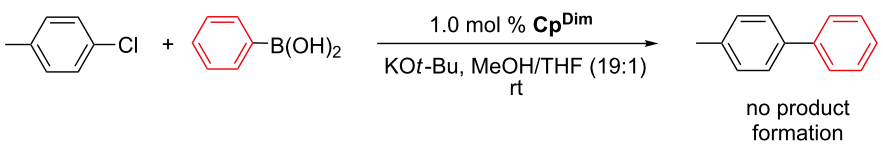

Scheme 5: **Cp^{Dim}** is not an active precatalyst for a Suzuki–Miyaura reaction at room temperature.

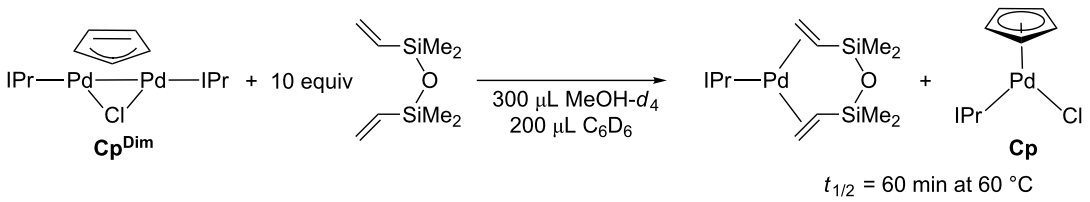

Scheme 6: Disproportionation of $\mathbf{Cp^{Dim}}$ with dvds.

half-life for the formation of **Cp** and (IPr)Pd(dvds) is 60 minutes (Scheme 6). In contrast, in the presence of dvds (μ-cinnamyl)(μ-Cl)$Pd_2(IPr)_2$ undergoes full disproportionation in approximately 40 minutes at 40 °C, while for (μ-allyl)(μ-Cl)$Pd_2(IPr)_2$ the reaction is complete in less than 10 minutes at room temperature [13]. Although these results show that disproportionation of $\mathbf{Cp^{Dim}}$ is more difficult than related allyl species, they provide no information on whether this is related to thermodynamic or kinetic effects.

To probe the relative thermodynamic favorability of dimer formation between allyl and Cp systems we performed a crossover experiment (Scheme 7a). In this experiment (μ-allyl)(μ-Cl)$Pd_2(IPr)_2$ was mixed with **Cp**. The products of crossover are $\mathbf{Cp^{Dim}}$ and (η^3-allyl)Pd(IPr)(Cl) and our experiments indicate that the equilibrium favors these species. The crossover reaction can be described as the combination of the disproportionation of the allyl dimer and the comproportionation of **Cp** with IPr-Pd(0) (Scheme 7b). From these results, we conclude that the comproportionation reaction to form $\mathbf{Cp^{Dim}}$ is more exergonic than in the allyl case ($|\Delta G°_{Cpdimerformation}| > |\Delta G°_{allyldimerformation}|$ in Scheme 7b). The results of this experiment indicate that in part disproportionation of $\mathbf{Cp^{Dim}}$ to form **Cp** and L-Pd(0) is more challenging than the corresponding allyl dimer for thermodynamic reasons.

Conclusion

We have performed the first detailed comparative investigation of the catalytic activity for the Suzuki–Miyaura reaction of (η^5-Cp)Pd(IPr)(Cl) (**Cp**), with the related commercially available catalysts (η^3-cinnamyl)Pd(IPr)(Cl) (**Cin**) and (η^3-1-*t*-Bu-indenyl)Pd(IPr)(Cl) ($\mathbf{^{tBu}Ind}$). We found that **Cp** is a slightly more efficient catalyst than **Cin**, but significantly less active than $\mathbf{^{tBu}Ind}$. The low activity of **Cp** in comparison to $\mathbf{^{tBu}Ind}$ is related both to its slower rate of activation to the monoligated Pd(0) active species and its tendency to form a significant amount of the inactive Pd(I) dimer (μ-Cp)(μ-Cl)$Pd_2(IPr)_2$ ($\mathbf{Cp^{Dim}}$) under catalytic conditions. The formation of this inactive dimer also explains why **Cp** is only a slightly more active precatalyst than **Cin**, which activates slower than **Cp**, but is less likely to form the corresponding inactive Pd(I) dimer. In principle, the addition of steric bulk to **Cp** could prevent the formation of a Pd(I) dimer and result in a more active precatalyst. However, an additional challenge that must be overcome if

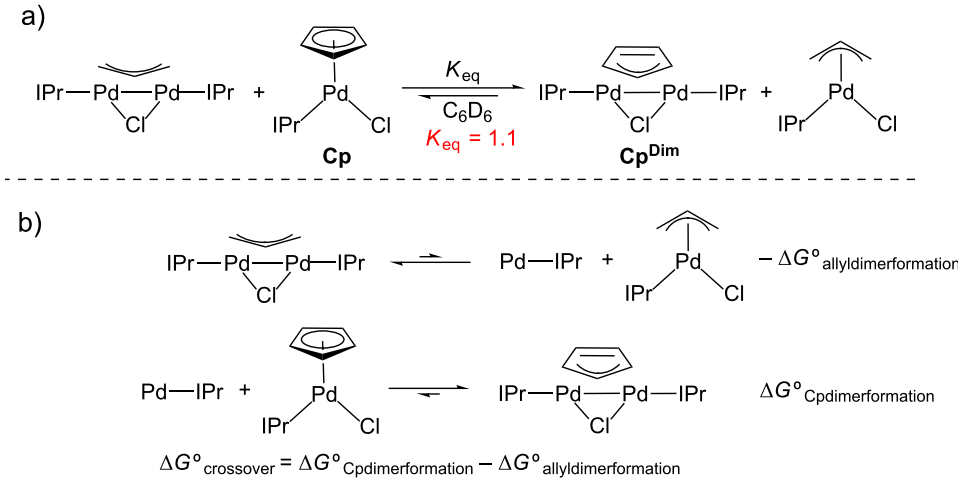

Scheme 7: a) Crossover experiment between **Cp** and (μ-allyl)(μ-Cl)$Pd_2(IPr)_2$. b) Crossover experiment expressed as the sum of disproportionation and comproportionation half reactions.

practical precatalyst scaffolds based on a Cp ligand are to be developed is that the synthetic routes to these species are currently not amenable to rapid ligand screening in an analogous fashion to **Cin** and **^{tBu}Ind**.

Experimental

General methods

As previously described in [13] and [15], experiments were performed under a dinitrogen atmosphere in an M-Braun dry box or using standard Schlenk techniques unless otherwise stated. Under standard glovebox conditions, purging was not performed between uses of pentane, benzene and toluene; thus when any of these solvents were used, traces of all these solvents were in the atmosphere and could be found intermixed in the solvent bottles. Stainless steel cannulas were used to transfer moisture- and air-sensitive liquids on a Schlenk line or in a dry box. THF, diethyl ether, and toluene were dried by passage through a column of activated alumina followed by storage under dinitrogen. All commercial chemicals were used as received; exceptions where noted. MeOH (J. T. Baker) and iPrOH (Macron Fine Chemicals) were not dried but were degassed by sparging with dinitrogen for one hour and stored under dinitrogen. Potassium *tert*-butoxide (99.99%, sublimed) was purchased from Aldrich. Potassium carbonate was purchased from Mallinckrodt and ground up with a mortar and pestle and stored in an oven at 130 °C prior to use. 1,3-Divinyltetramethyldisiloxane was purchased from TCI. Deuterated solvents were obtained from Cambridge Isotope Laboratories. MeOH-d_4 and THF-d_8 were not dried but were degassed prior to use through three freeze-pump-thaw cycles. Agilent-400, -500 and -600 spectrometers were used to record NMR spectra at ambient probe temperatures. Gas chromatography analyses (GC) were performed on a Shimadzu GC-2010 Plus apparatus equipped with a flame ionization detector and a Shimadzu SHRXI-5MS column (30 m, 250 μm inner diameter, film: 0.25 μm). The following conditions were utilized for GC analyses: flow rate 1.23 mL/min constant flow, column temperature 50 °C (held for 5 min), 20 °C/min increase to 300 °C (held for 5 min), total time 22.5 min. Literature procedures were used to prepare the following compounds: (η^3-cinnamyl)Pd(IPr)(Cl) (**Cin**) [11], (η^3-1-*t*-Bu-indenyl)Pd(IPr)(Cl) (**^{tBu}Ind**) [15], (η^5-Cp)Pd(IPr)(Cl) (**Cp**) [18] (μ-allyl)(μ-Cl)Pd_2(IPr)$_2$ [13].

X-ray crystallography

X-ray diffraction experiments were carried out on a Rigaku MicroMax-007HF diffractometer coupled to a Saturn994+ CCD detector with Cu Kα radiation (λ = 1.54178 Å) at −180 °C. The crystals were mounted on MiTeGen polyimide loops with immersion oil. The data frames were processed using Rigaku CrystalClear and corrected for Lorentz and polarization effects. Using Olex2 [42] the structure was solved with the XS [43] structure solution program by Patterson methods and refined with the XL [43] refinement package using least-squares minimization. The non-hydrogen atoms were refined anisotropically. Hydrogen atoms were refined using the riding model unless otherwise stated.

Synthetic procedures and characterizing data

(μ-Cp)(μ-Cl)Pd_2(IPr)$_2$ (**Cp^{Dim}**)

(η^5-Cp)Pd(IPr)(Cl) (**Cp**) (0.250 g, 0.42 mmol) and K_2CO_3 (0.116 g, 0.84 mmol) were added to a 100 mL Schlenk flask. Degassed MeOH (30 mL) was added to the flask via cannula. The reaction mixture was stirred at room temperature for 2 hours. The precipitate was filtered in air and washed with water to remove excess salts. The solid was washed with pentane and dried under vacuum to give **Cp^{Dim}** as a red solid. Yield: 0.188 g, 82%. X-ray quality crystals were grown from a saturated toluene solution layered with pentane (V(toluene):V(pentane) = 1:2) at −35 °C. ^{1}H NMR (C_6D_6, 400 MHz) 7.18 (t, *J* = 7.7 Hz, 4H), 7.11 (d, *J* = 7.7 Hz, 8H), 6.62 (s, 4H), 4.39 (s, 5H), 3.13 (sept, *J* = 6.8 Hz, 8H), 1.35 (d, *J* = 6.9 Hz, 24H), 1.11 (d, *J* = 6.9 Hz, 24H); ^{13}C{^{1}H} NMR (C_6D_6, 100 MHz) 186.5, 146.0, 137.3, 128.9, 123.4, 122.2, 84.3, 28.5, 25.3, 23.1.

Representative procedures for catalytic Suzuki–Miyaura reactions with **Cp**

KO*t*-Bu conditions

Reactions were performed under dinitrogen in a 1 dram vial containing a flea stir bar and sealed with a septum cap. To the vial was added 950 μL of a MeOH stock solution, containing 0.5263 M aryl chloride, 0.5525 M boronic acid, 0.5789 M KO*t*-Bu and 0.2632 M naphthalene. The vial was then heated using an aluminum block heater set to 25 °C. After thermal equilibration, the reaction was initiated via the addition of 50 μL of the appropriate precatalyst solution in THF (0.1 M [Pd]). Aliquots (≈50–100 μL) were removed at reaction times indicated. The aliquots were purified by filtration through pipet filters containing approximately 1 cm of silica and eluted with 1–1.2 mL of ethyl acetate directly into GC vials. Conversion was determined by comparison of the GC responses of product and the internal naphthalene standard. Biaryl products were initially synthesized using literature procedures [15], identified using NMR spectroscopy by comparison to the literature chemical shifts [11] and then these pure samples used to generate calibration plots for the GC.

K_2CO_3 conditions

Potassium carbonate (0.75 mmol) was transferred on the benchtop into a 1 dram vial containing a flea stir bar. The vial was sealed with a septum cap, and placed under dinitrogen (by

cycling three times between vacuum and dinitrogen) on a Schlenk line through a needle. To the vial was added 950 μL of a MeOH stock solution, containing 0.5263 M aryl chloride, 0.5525 M boronic acid and 0.2632 M naphthalene. The vial was then heated using an aluminum block heater set to 25 °C. After thermal equilibration, the reaction was initiated via the addition of 50 μL of the appropriate precatalyst solution in THF (0.1 M [Pd]). Aliquots (≈50–100 μL) were removed at reaction times indicated. The aliquots were purified by filtration through pipet filters containing approximately 1 cm of silica and eluted with 1–1.2 mL of ethyl acetate directly into GC vials. Conversion was determined by comparison of the GC responses of product and the internal naphthalene standard. Biaryl products were initially synthesized using literature procedures [15], identified using NMR spectroscopy by comparison to the literature chemical shifts [11] and then these pure samples used to generate calibration plots for the GC.

Experiments on activation of Pd(II) to Pd(0)

Experimental details for Table 1: Rates of activation of **Cp** under different conditions in the presence of dvds

iPrOH-d_8/KO*t*-Bu experiments: KO*t*-Bu (9.8 mg, 0.087 mmol) was dissolved in 300 μL of iPrOH-d_8 along with 100 μL of a 0.87 M solution of dvds in iPrOH-d_8. **Cp** (5.2 mg, 0.0087 mmol) was dissolved in 100 μL of THF-d_8. These solutions were combined in a J. Young NMR tube at −78 °C. The reaction mixture was degassed on a Schlenk line, after which dinitrogen was introduced into the NMR tube. An array of ^{1}H NMR spectra was taken at 25 °C over the course of 3 hours. During this time, the growth of the methyl protons of the (IPr)Pd(dvds) [22] product were monitored.

MeOH-d_4/KO*t*-Bu experiments: KO*t*-Bu (9.8 mg, 0.087 mmol) was dissolved in 300 μL of MeOH-d_4 along with 100 μL of a 0.87 M solution of dvds in MeOH-d_4. **Cp** (5.2 mg, 0.0087 mmol) was dissolved in 100 μL of MeOH-d_4. These solutions were combined in a J. Young NMR tube at −78 °C. The reaction mixture was degassed on a Schlenk line, after which dinitrogen was introduced into the NMR tube. An array of ^{1}H NMR spectra was taken at 25 °C over the course of 3 hours. During this time, the growth of the methyl protons of the (IPr)Pd(dvds) [22] product were monitored.

MeOH-d_4/K_2CO_3 experiments: K_2CO_3 (12.0 mg, 0.087 mmol) and 18-crown-6 ether (46.0 mg, 0.174 mmol) were dissolved in 300 μL of MeOH-d_4 along with 100 μL of a 0.87 M solution of dvds in MeOH-d_4. **Cp** (5.2 mg, 0.0087 mmol) was dissolved in 100 μL of MeOH-d_4. These solutions were combined in a J. Young NMR tube at −78 °C. The reaction mixture was degassed on a Schlenk line, after which dinitrogen was introduced into the NMR tube. An array of ^{1}H NMR spectra was taken at 25 °C over the course of 3 hours. The strong –CH_2 peak from the 18-crown-6 ether was suppressed by presaturating its signal during the experiment. During this time, the growth of the methyl protons of the (IPr)Pd(dvds) [22] product were monitored.

MeOH-d_4/K_2CO_3/PhB(OH)$_2$ experiments: KO*t*-Bu (10.8 mg, 0.096 mmol) and phenylboronic acid (10.6 mg, 0.087 mmol) were dissolved in 300 μL of MeOH-d_4 along with 100 μL of a 0.87 M solution of dvds in MeOH-d_4. **Cp** (5.2 mg, 0.0087 mmol) was dissolved in 100 μL of MeOH-d_4. These solutions were combined in a J. Young NMR tube at –78 °C. The reaction mixture was degassed on a Schlenk line, after which dinitrogen was introduced into the NMR tube. An array of ^{1}H NMR spectra was taken at 25 °C over the course of 3 hours. During this time, the growth of the methyl protons of the (IPr)Pd(dvds) [22] product were monitored.

Catalysis using Cp under NMR conditions: In a glovebox, phenylboronic acid (10.0 mg, 0.082 mmol), 4-chlorotoluene (9.2 μL, 0.0781 mmol), KO*t*-Bu (9.6 mg, 0.0859 mmol) and 2,6-dimethoxytoluene (6.0 mg, 0.039 mmol) were dissolved in 400 μL of MeOH-d_4. **Cp** (1.8 mg, 0.0031 mmol) was dissolved in 100 μL of THF-d_8. These solutions were combined in a J. Young NMR tube and the reaction was monitored by ^{1}H NMR spectroscopy for one hour at 25 °C. After this time, the solvent mixture was removed on a Schlenk line and benzene-d_6 was added. A final ^{1}H NMR spectrum was recorded to identify the Pd containing products of the reaction. **Cp^{Dim}** was observed as the main Pd containing product, with a yield of 40% compared to the internal standard 2,6-dimethoxytoluene.

Catalysis using Cp^{Dim} as precatalyst: 0.05 mmol of **Cp^{Dim}** was transferred into a 1 mL volumetric flask in a glovebox. The precatalyst was dissolved in THF, and the solution was diluted to 1 mL. The solution was transferred to a flask with a Kontes valve. Reactions were performed under dinitrogen in a 1 dram vial containing a flea stir bar and sealed with a septum cap. To the vial was added 950 μL of the MeOH stock solution described above. The vial was then heated using an aluminum block heater set to 25 °C. After thermal equilibration, the reaction was initiated via the addition of 50 μL of the THF solution containing **Cp^{Dim}** (0.1 M [Pd]). Aliquots (≈50–100 μL) were removed at 30 and 60 minutes. The aliquots were purified by filtration through pipet filters containing approximately 1 cm of silica and eluted with 1–1.2 mL of ethyl acetate directly into GC vials. Conversion was determined by comparison of the GC responses of product and the internal naphthalene standard. No conversion to the biphenyl product was observed at either time point.

Disproportionation of Cp^{Dim} using dvds: In a nitrogen filled glovebox, Cp^{Dim} (5.5 mg, 0.005 mmol), dvds (9.2 mg, 0.05 mmol) and 2,6-dimethocytoluene (0.8 mg, 0.005 mmol) were added to a vial. MeOH-d_4 (300 μL) and deuterated benzene (200 μL) were added and the homogeneous mixture was transferred to a J. Young tube and sealed. The contents were heated at 60 °C for one hour, at which time an NMR spectrum was recorded. The methyl protons of the product (IPr)Pd(dvds) [22] were compared to the internal standard. At one hour, the reaction had reached 50% conversion.

Crossover experiment using Cp and (μ-allyl)(μ-Cl)Pd_2(IPr)$_2$: In a nitrogen-filled glovebox, (μ-allyl)(μ-Cl)$Pd_2(IPr)_2$ (4.0 mg, 0.00375 mmol) and **Cp** (2.2 mg, 0.00375 mmol) were added to a vial. C_6D_6 (0.5 mL) was added and the solution was transferred to a J. Young tube and sealed. The mixture was heated to 60 °C and allowed to equilibrate over 36 hours. At this time, an NMR spectrum was recorded at room temperature. The equilibrium constant was calculated by using relative integrations of the Cp protons from **Cp** and Cp^{Dim} to yield a K of 1.1.

Supporting Information

Supporting Information File 1

^{1}H NMR spectrum for ^{tBu}**Ind**, **Cp** and ^{Cp}**Dim** and crystallographic information for ^{Cp}**Dim**.
[http://www.beilstein-journals.org/bjoc/content/supplementary/1860-5397-11-269-S1.pdf]

Supporting Information File 2

Crystallographic information file for ^{Cp}**Dim**.
[http://www.beilstein-journals.org/bjoc/content/supplementary/1860-5397-11-269-S2.cif]

Acknowledgements

PRM thanks the NSF for support as an NSF Graduate Research Fellow. NH is a fellow of the Alfred P. Sloan Foundation and a Camille and Henry-Dreyfus Foundation Teacher Scholar. We thank Dr. Brandon Mercado for assistance with X-ray crystallography.

References

1. Miyaura, N.; Suzuki, A. *Chem. Rev.* **1995,** *95,* 2457. doi:10.1021/cr00039a007
2. Kotha, S.; Lahiri, K.; Kashinath, D. *Tetrahedron* **2002,** *58,* 9633. doi:10.1016/S0040-4020(02)01188-2
3. Phan, N. T. S.; Van Der Sluys, M.; Jones, C. W. *Adv. Synth. Catal.* **2006,** *348,* 609. doi:10.1002/adsc.200505473
4. Martin, R.; Buchwald, S. L. *Acc. Chem. Res.* **2008,** *41,* 1461. doi:10.1021/ar800036s
5. Roughley, S. D.; Jordan, A. M. *J. Med. Chem.* **2011,** *54,* 3451. doi:10.1021/jm200187y
6. Johansson Seechurn, C. C. C.; Kitching, M. O.; Colacot, T. J.; Snieckus, V. *Angew. Chem., Int. Ed.* **2012,** *51,* 5062. doi:10.1002/anie.201107017
7. Li, H.; Johansson Seechurn, C. C. C.; Colacot, T. J. *ACS Catal.* **2012,** *2,* 1147. doi:10.1021/cs300082f
8. Viciu, M. S.; Germaneau, R. F.; Navarro-Fernandez, O.; Stevens, E. D.; Nolan, S. P. *Organometallics* **2002,** *21,* 5470. doi:10.1021/om020804i
9. Navarro, O.; Kaur, H.; Mahjoor, P.; Nolan, S. P. *J. Org. Chem.* **2004,** *69,* 3173. doi:10.1021/jo035834p
10. Navarro, O.; Oonishi, Y.; Kelly, R. A.; Stevens, E. D.; Briel, O.; Nolan, S. P. *J. Organomet. Chem.* **2004,** *689,* 3722. doi:10.1016/j.jorganchem.2004.04.001
11. Marion, N.; Navarro, O.; Mei, J.; Stevens, E. D.; Scott, N. M.; Nolan, S. P. *J. Am. Chem. Soc.* **2006,** *128,* 4101. doi:10.1021/ja057704z
12. Marion, N.; Nolan, S. P. *Acc. Chem. Res.* **2008,** *41,* 1440. doi:10.1021/ar800020y
13. Hruszkewycz, D. P.; Balcells, D.; Guard, L. M.; Hazari, N.; Tilset, M. *J. Am. Chem. Soc.* **2014,** *136,* 7300. doi:10.1021/ja412565c
14. Hruszkewycz, D. P.; Guard, L. M.; Balcells, D.; Feldman, N.; Hazari, N.; Tilset, M. *Organometallics* **2015,** *34,* 381. doi:10.1021/om501250y
15. Melvin, P. R.; Nova, A.; Balcells, D.; Dai, W.; Hazari, N.; Hruszkewycz, D. P.; Shah, H. P.; Tudge, M. T. *ACS Catal.* **2015,** *5,* 3680. doi:10.1021/acscatal.5b00878
16. Melvin, P. R.; Balcells, D.; Hazari, N.; Nova, A. *ACS Catal.* **2015,** *5,* 5596. doi:10.1021/acscatal.5b01291
17. Crabtree, R. H. *The Organometallic Chemistry of the Transition Metals,* 5th ed.; Wiley: New York, 2009.
18. Jin, Z.; Guo, S.-X.; Gu, X.-P.; Qiu, L.-L.; Song, H.-B.; Fang, J.-X. *Adv. Synth. Catal.* **2009,** *351,* 1575. doi:10.1002/adsc.200900098
19. Jin, Z.; Gu, X.-P.; Qiu, L.-L.; Wu, G.-P.; Song, H.-B.; Fang, J.-X. *J. Organomet. Chem.* **2011,** *696,* 859. doi:10.1016/j.jorganchem.2010.10.009
20. Even though the structure of **Cp** is drawn with an η^5-Cp ligand, the Pd–C bond distances in the crystal structure (see reference [18]) show 3 Pd–C bonds which are ≈0.1 Å shorter than the other 2 Pd–C bonds. Thus, the bonding is probably best described as intermediate between an η^5- and an η^3-Cp ligand and the analogy between **Cp**, and **All** and ^{tBu}**Ind**, where the allyl and 1-*t*-Bu-indenyl ligands are unambigiously η^3-coordinated, is even stronger upon detailed analysis of the **Cp** structure.
21. Most of our attempts to synthesize an unligated Cp dimer focused on using a similar synthetic method to that used to prepare {(η^3-cinnamyl)Pd}$_2$(m-Cl)$_2$ or {(η^3-1-*t*-Bu-indenyl)Pd}$_2$(μ-Cl)$_2$. See references [11] and [15] for more information.
22. Jackstell, R.; Harkal, S.; Jiao, H.; Spannenberg, A.; Borgmann, C.; Röttger, D.; Nierlich, F.; Elliot, M.; Niven, S.; Cavell, K.; Navarro, O.; Viciu, M. S.; Nolan, S. P.; Beller, M. *Chem. – Eur. J.* **2004,** *10,* 3891. doi:10.1002/chem.200400182
23. Werner, H.; Tune, D.; Parker, G.; Krüger, C.; Brauer, D. J. *Angew. Chem., Int. Ed. Engl.* **1975,** *14,* 185. doi:10.1002/anie.197501851
24. Ducruix, A.; Felkin, H.; Pascard, C.; Turner, G. K. *J. Chem. Soc., Chem. Commun.* **1975,** 615. doi:10.1039/c39750000615

25. Werner, H.; Kühn, A.; Tune, D. J.; Krueger, C.; Brauer, D. J.; Sekutowski, J. C.; Tsay, Y.-H. *Chem. Ber.* **1977,** *110,* 1763. doi:10.1002/cber.19771100522
26. Kühn, A.; Werner, H. *J. Organomet. Chem.* **1979,** *179,* 421. doi:10.1016/S0022-328X(00)91859-X
27. Werner, H.; Kraus, H.-J. *Angew. Chem., Int. Ed. Engl.* **1979,** *18,* 948. doi:10.1002/anie.197909481
28. Werner, H.; Kraus, H.-J. *J. Chem. Soc., Chem. Commun.* **1979,** 814. doi:10.1039/c39790000814
29. Yamamoto, T.; Saito, O.; Yamamoto, A. *J. Am. Chem. Soc.* **1981,** *103,* 5600. doi:10.1021/ja00408a068
30. Werner, H.; Kraus, H.-J.; Schubert, U.; Ackermann, K. *Chem. Ber.* **1982,** *115,* 2905. doi:10.1002/cber.19821150821
31. Kühn, A.; Burschka, C.; Werner, H. *Organometallics* **1982,** *1,* 496. doi:10.1021/om00063a016
32. Thometzek, P.; Zenkert, K.; Werner, H. *Angew. Chem., Int. Ed. Engl.* **1985,** *24,* 516. doi:10.1002/anie.198505161
33. Werner, H.; Thometzek, P.; Zenkert, K.; Goddard, R.; Kraus, H.-J. *Chem. Ber.* **1987,** *120,* 365. doi:10.1002/cber.19871200319
34. Tanase, T.; Nomura, T.; Yamamoto, Y.; Kobayashi, K. *J. Organomet. Chem.* **1991,** *410,* C25. doi:10.1016/0022-328X(91)80014-B
35. Tanase, T.; Nomura, T.; Fukushima, T.; Yamamoto, Y.; Kobayashi, K. *Inorg. Chem.* **1993,** *32,* 4578. doi:10.1021/ic00073a019
36. Sui-Seng, C.; Enright, G. D.; Zargarian, D. *J. Am. Chem. Soc.* **2006,** *128,* 6508. doi:10.1021/ja060747a
37. Norton, D. M.; Mitchell, E. A.; Botros, N. R.; Jessop, P. G.; Baird, M. C. *J. Org. Chem.* **2009,** *74,* 6674. doi:10.1021/jo901121e
38. Chalkley, M. J.; Guard, L. M.; Hazari, N.; Hofmann, P.; Hruszkewycz, D. P.; Schmeier, T. J.; Takase, M. K. *Organometallics* **2013,** *32,* 4223. doi:10.1021/om400415c
39. Dai, W.; Chalkley, M. J.; Brudvig, G. W.; Hazari, N.; Melvin, P. R.; Pokhrel, R.; Takase, M. K. *Organometallics* **2013,** *32,* 5114. doi:10.1021/om400687m
40. Bielinski, E. A.; Dai, W.; Guard, L. M.; Hazari, N.; Takase, M. K. *Organometallics* **2013,** *32,* 4025. doi:10.1021/om4002632
41. Hruszkewycz, D. P.; Wu, J.; Hazari, N.; Incarvito, C. D. *J. Am. Chem. Soc.* **2011,** *133,* 3280. doi:10.1021/ja110708k
42. Dolomanov, O. V.; Bourhis, L. J.; Gildea, R. J.; Howard, J. A. K.; Puschmann, H. *J. Appl. Crystallogr.* **2009,** *42,* 339. doi:10.1107/S0021889808042726
43. Sheldrick, G. *Acta Crystallogr., Sect. A: Found. Crystallogr.* **2008,** *64,* 112. doi:10.1107/S0108767307043930

License and Terms

BEILSTEIN JOURNAL OF ORGANIC CHEMISTRY

Rhodium, iridium and nickel complexes with a 1,3,5-triphenylbenzene tris-MIC ligand. Study of the electronic properties and catalytic activities

Carmen Mejuto[1], Beatriz Royo[2], Gregorio Guisado-Barrios[*1] and Eduardo Peris[*1]

Full Research Paper

Open Access

Address:
[1]Instituto de Materiales Avanzados (INAM), Universitat Jaume I, Avda. Vicente Sos Baynat, Castellón, 12071, Spain and [2]Instituto de Tecnologia Química e Biologica da Universidade Nova de Lisboa, Av. da República, EAN, Oeiras, 2780-157, Portugal

Email:
Gregorio Guisado-Barrios[*] - guisado@uji.es; Eduardo Peris[*] - eperis@uji.es

* Corresponding author

Keywords:
arylation of unsaturated ketones; mesoionic carbenes; nickel; iridium; rhodium

Beilstein J. Org. Chem. **2015,** *11,* 2584–2590.
doi:10.3762/bjoc.11.278

Received: 26 October 2015
Accepted: 03 December 2015
Published: 14 December 2015

This article is part of the Thematic Series "N-Heterocyclic carbenes".

Guest Editor: S. P. Nolan

Abstract

The coordination versatility of a 1,3,5-triphenylbenzene-tris-mesoionic carbene ligand is illustrated by the preparation of complexes with three different metals: rhodium, iridium and nickel. The rhodium and iridium complexes contained the [MCl(COD)] fragments, while the nickel compound contained [NiCpCl]. The preparation of the tris-MIC (MIC = mesoionic carbene) complex with three $[IrCl(CO)_2]$ fragments, allowed the estimation of the Tolman electronic parameter (TEP) for the ligand, which was compared with the TEP value for a related 1,3,5-triphenylbenzene-tris-NHC ligand. The electronic properties of the tris-MIC ligand were studied by cyclic voltammetry measurements. In all cases, the tris-MIC ligand showed a stronger electron-donating character than the corresponding NHC-based ligands. The catalytic activity of the tri-rhodium complex was tested in the addition reaction of arylboronic acids to α,β-unsaturated ketones.

Introduction

Highly symmetrical poly-NHCs are a very interesting type of ligands, because they allow the preparation of a variety of supramolecular assemblies that include molecular squares and triangles [1-6], cylinder-like structures [7-13], organometallic polymers [14-22] and even organometallic mesoporous materials [21,22]. Another interesting feature of this special type of poly-NHCs is its ability to form multimetallic catalysts whose catalytic performances can be compared with analogous monometallic NHC complexes [23-25]. On several occasions their activity has proven higher than the activities shown by their monometallic counterparts [23,26]. In the last few years we became interested in the design of several types of C_{3v}-

symmetric tris-NHCs, both for the preparation of self-assembly molecular cages [12,13,27] and for the design of discrete trimetallic molecules whose catalytic performances were explored [23,25,28,29]. Among these ligands, we found those featuring a nanoscale distance between the metals especially interesting [13,27] because for these systems a catalytic cooperation between the active metal sites should not be expected. As a consequence all catalytic improvements should be assigned to reasons dealing with supramolecular interactions [30] or with the higher nanolocal concentration of metal sites in the multimetallic catalyst [31]. In this context, we obtained the 1,3,5-triphenylbenzene-based C_3-symmetrical tris-NHC ligand **A** (Scheme 1), which was coordinated to rhodium and iridium [25]. The catalytic activity of the trirhodium complex was tested in the addition reaction of arylboronic acids to 2-cyclohexen-1-one, where it showed good activity. The same ligand was also used for the preparation of nanometer-sized cylinder-like structures of Cu, Ag and Au [13].

As mesoionic carbenes (MICs) are known to be stronger electron donors compared to NHCs [32-36], and because poly-MIC ligands are less explored [37-46], we very recently synthesized the tris-diarylated-(1,2,3-triazol-5-ylidene)-1,3,5-triphenylbenzene-based ligand (**B**). This ligand afforded trisilver and trigold cages with very interesting rearranging properties when mixed with the related 1,3,5-triphenylbenzene-based tris-NHC Ag cages [27]. Shortly afterwards, Sarkar and co-workers used a dialkylated (1,2,3-triazol-5-ylidene)-1,3,5-triphenylbenzene-based ligand for the preparation of the corresponding tris-Ir(III) and Pd(II) complexes and tested them for their catalytic activities [47].

Based on these previous findings, we herein report the synthesis of the tri-metallic complexes of Rh(I), Ir(I) and Ni(II) with the tris-MIC ligand **B**. The preparation of these complexes gives us an excellent opportunity to compare the electronic properties of the tris-MIC ligand **B** with those of its tris-NHC analogue, **A**. The catalytic activity of the tris-MIC-trirhodium complex was tested in the addition reaction of arylboronic acids to 2-cyclohexen-1-one and compared to the results obtained with the tris-NHC analogue.

Results and Discussion

Complex **2** was obtained by the in situ deprotonation of the tris-triazolium salt **1** with potassium bis(trimethyl)silyl amide (KHMDS) in the presence of $[RhCl(COD)]_2$ in THF at −78 °C (Scheme 2). It was isolated in 84% yield after purification by column chromatography. For the preparation of the related iridium(I) complex, we found it more convenient to use a preparative method inspired by a recent work by Plenio and co-workers [48]. In this way refluxing a mixture of **1** with $[IrCl(COD)]_2$ in the presence of K_2CO_3 in acetone for 24 h gave the triiridium(I) complex **3** in 60% yield after purification. The complexes **2** and **3** were characterized by NMR and mass spectrometry. Both, the ^{1}H and the ^{13}C NMR spectra of the complexes were consistent with the expected threefold symmetry of the molecules, as exemplified by the appearance of one only signal for the carbene carbons, at 173.4 ($^1J_{Rh–C}$ = 41.5 Hz) and 172.1 ppm, for **2** and **3**, respectively. The ^{1}H NMR spectra of complexes **2** and **3** exhibited relatively broad signals, which may indicate a fluxional behavior. This may be likely caused by the combined rotation around the C–C sigma bonds of the tris-MIC ligand and the $C_{carbene}$–M bond.

In order to widen the coordination scope of the tris-MIC ligand **B**, the corresponding Ni(II) complex was also synthesized. The reaction of **1** with $[NiCp_2]$ in the presence of NEt_4Cl in refluxing dioxane, afforded the tris-MIC complex of Ni(II) **4**, as

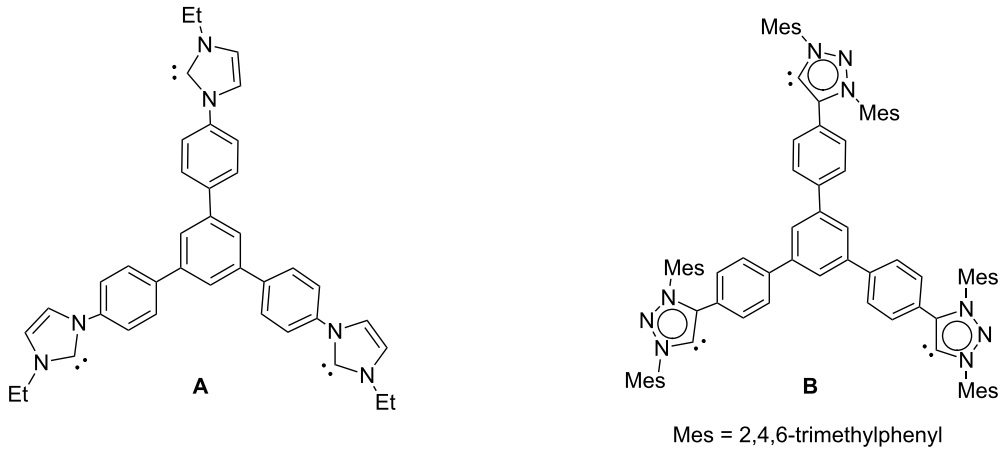

Scheme 1: Schematic representation of ligands **A** and **B**.

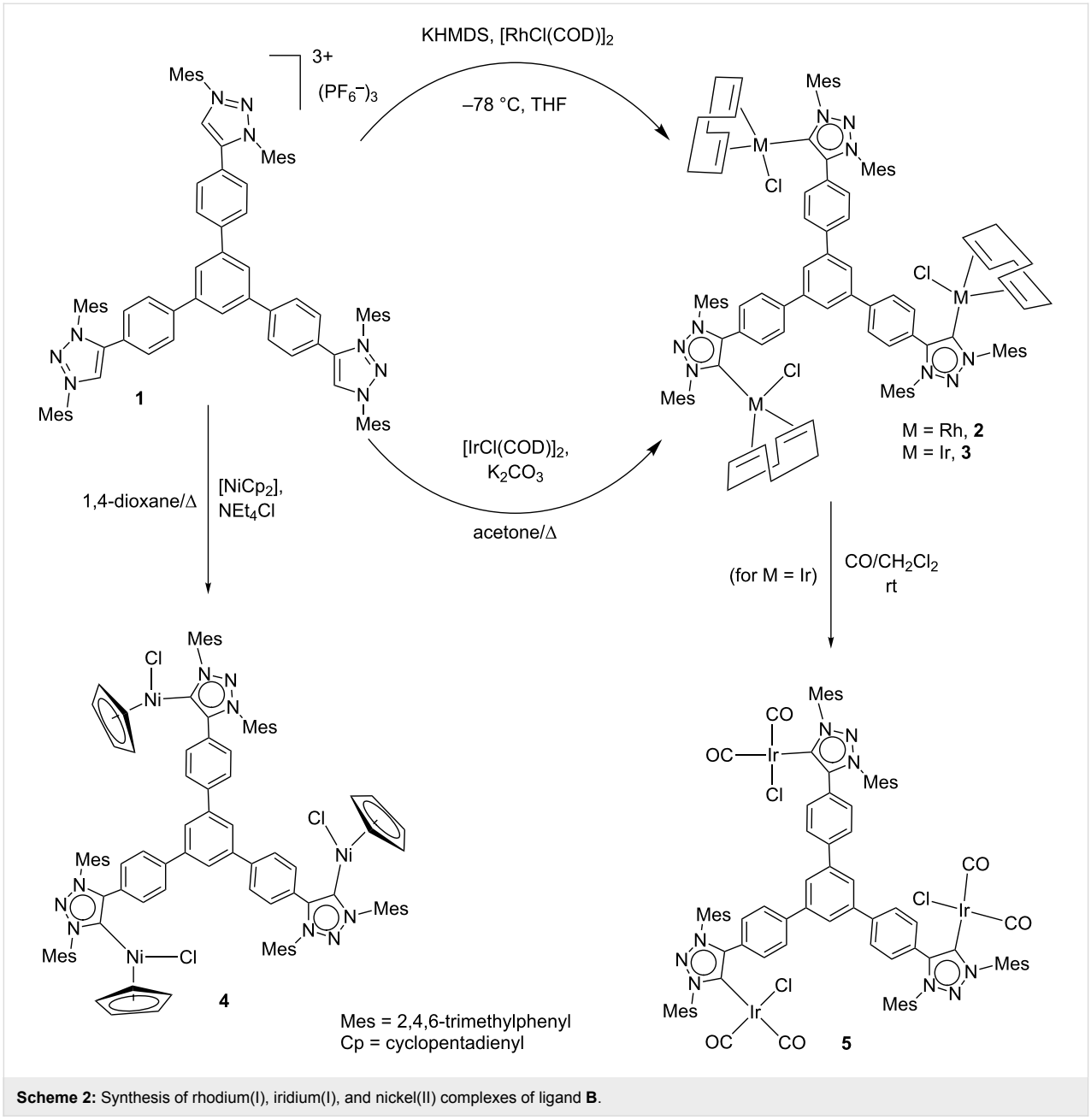

Scheme 2: Synthesis of rhodium(I), iridium(I), and nickel(II) complexes of ligand **B**.

a red solid in 40% yield after purification. The three-fold symmetry of this complex was also confirmed by its NMR spectra. In the 1H NMR a singlet assigned to the equivalent 15 protons of the three cyclopentadienyl rings was observed. As already indicated for complexes **2** and **3** the ^{1}H NMR spectrum of complex **4** showed broad signals as a consequence of the fluxionality due to the rotation about the C–C sigma bonds of the ligand, and the $C_{carbene}$–Ni bond. The ^{13}C NMR spectrum showed the distinctive signal due to the metalation of the carbene carbon at 151.4 ppm, which is in the same region of the previously reported [NiCpCl(MIC)] complex (148 ppm) [49]. The trimetallic nature of the complex was further confirmed by mass spectrometry, which revealed a peak at m/z 810.7, assigned to $[M - 2Cl]^{2+}$. Compound **4** is very interesting, because despite the fact that many [NiCpX(NHC)] complexes have already been reported [49-53], to our knowledge, this is the first tris-MIC-trinickel complex described so far.

To further evaluate the electron-donating character of the tris-MIC ligand **B**, the iridium hexacarbonyl complex **5** was obtained by bubbling carbon monoxide into a solution of **3** in CH_2Cl_2. The resulting yellow solid was obtained in 93% yield. The IR spectrum of a CH_2Cl_2 solution of **5** showed the characteristic CO stretching bands at 2057 and 1972 cm^{-1} from which

a Tolman electronic parameter (TEP) of 2042 cm^{-1} could be estimated by using the well-accepted correlations [54-56]. This obtained TEP value is slightly lower than the one shown by the tris-NHC analogue **A**, for which the reported TEP was 2045 cm^{-1}, therefore suggesting that the tris-MIC ligand **B** is a stronger electron donor than ligand **A**. However, this comparison must be taken with care, because the tris-carbene ligands **A** and **B**, not only differ in the nature of their carbenes (MIC vs NHC), but also in their substituents at the carbene rings, which may also affect the electronic nature of the ligands. It worth mentioning, that the monometallic complex $[IrCl(MIC)(CO)_2]$ (MIC = 1,3-bis(2,6-diisopropylphenyl)-4-phenyl-1,2,3-triazolylidene), which may be considered as the monometallic analogue of complex **5**, displays an average CO stretching frequency at 2018 cm^{-1} [32]. This frequency is 4 cm^{-1} higher than the average frequency observed for **5** (2014 cm^{-1}), indicating a stronger electron-donating character of the tris-MIC ligand. In a similar way, the Tolman electronic parameter of 1-ethyl-3-phenylimidazolyidene (which may be considered as the monocarbene analogue of **A**) is 2053 cm^{-1} [57], therefore 8 cm^{-1} higher than that reported for **A**. Scheme 3 displays the comparison of the TEP values of the triscarbene ligands **A** and **B**, and their related monocarbenes. The results clearly indicate that the tritopic nature of ligands **A** and **B** is significantly improving the electron-donating ability of the ligands which by no means should be regarded as the simple combination of the three monocarbenes that constitute the branches of these tris-carbenes.

To gain further insight into the electronic properties of the tris-MIC ligand **B**, cyclic voltammetry studies of **2** and **3** (Figure 1) and **4** (Figure 2) were performed. The rhodium complex **2** showed an irreversible wave at $E_{1/2}$ = 0.56 mV, while the iridium complex **3** displayed a pseudo-reversible wave at a half-wave potential of $E_{1/2}$ = 0.63 mV. Compared to the cyclic voltammetry data obtained for the analogous Rh and Ir complexes with the tris-NHC ligand **A** ($E_{1/2}$ = 0.67 mV, for both complexes) [25], the observed lower $E_{1/2}$ values for complexes **2** and **3** are consistent with a stronger electron-donating character of the tris-MIC ligand **B**. Further the observation of only one redox wave for both complexes **2** and **3** is consistent with the electronic disconnection of the three metals in both trimetallic complexes.

The cyclic voltammetry diagram of the tri-Ni(II) complex **4** is shown in Figure 2, together with the differential pulse voltammetry (DPV) plot. The complex shows a quasi-reversible wave at a half-wave potential of $E_{1/2}$ = 0.64 mV, which is significantly lower than the half-wave potential ($E_{1/2}$ = 0.72 mV) exhibited by the monometallic NHC-based complex [NiCpCl(IMes)] [50] (IMes = 1,3-mesitylimidazolylidene). This is in agreement with the stronger electron-donating character for the ligand in **4** compared to IMes. From the differential pulse voltammetry (DPV) analysis generated for **4** it can be seen that there is only one redox event taking place, thus evidencing that the trimetallic complex **4** contains three nickel fragments that are essentially decoupled.

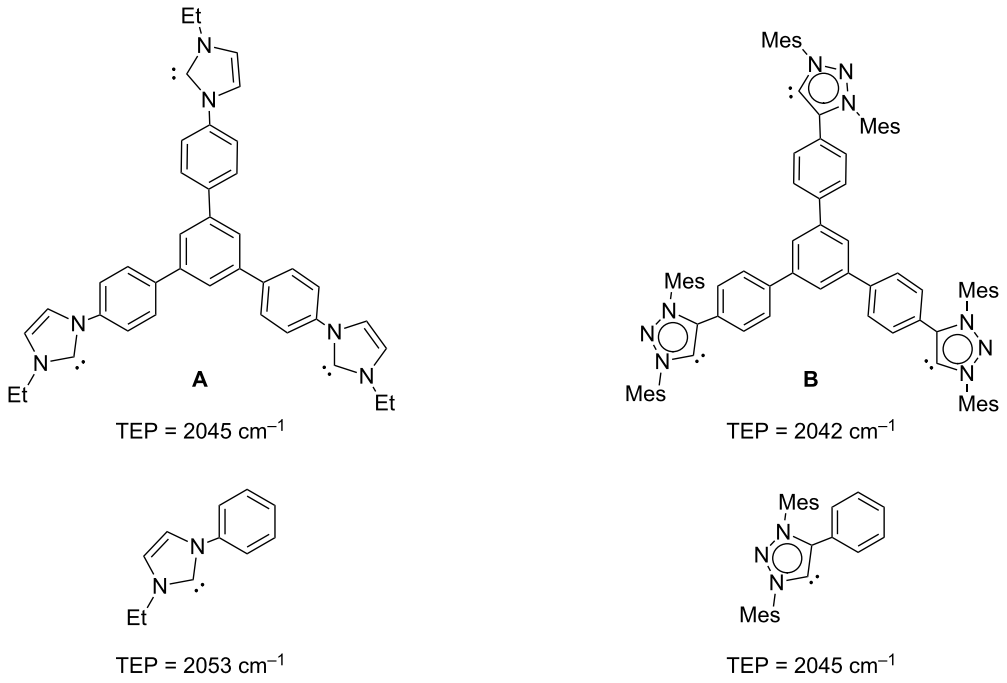

Scheme 3: Tolman electronic parameters (TEP) for **A**, **B** and their related monocarbenes.

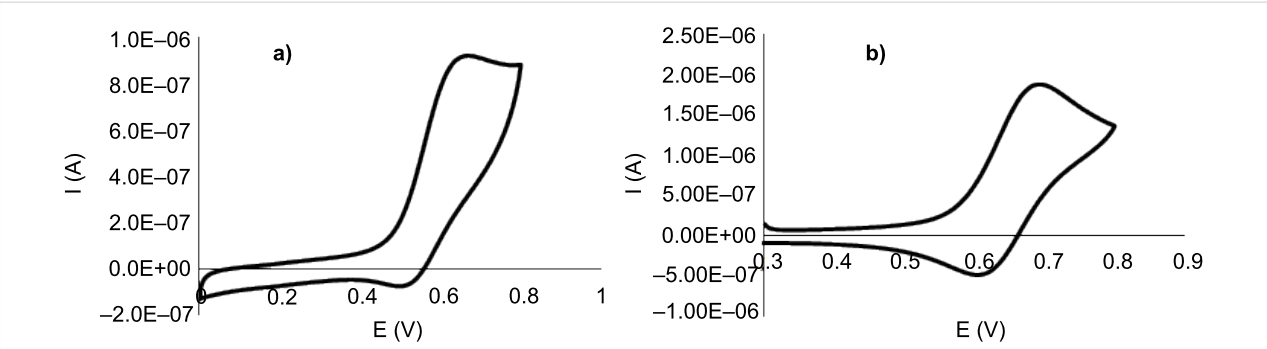

Figure 1: CV plots of complexes **2** (a), and **3** (b). Experiments were carried out using 1 mM solutions of the complexes in dry CH_2Cl_2 with 0.1 M $[NBu_4][PF_6]$ as the supporting electrolyte, 100 mVs^{-1} scan rate, Fc^+/Fc used as internal standard with $E_{1/2}$ (Fc/Fc^+) = 0.44 V vs SCE.

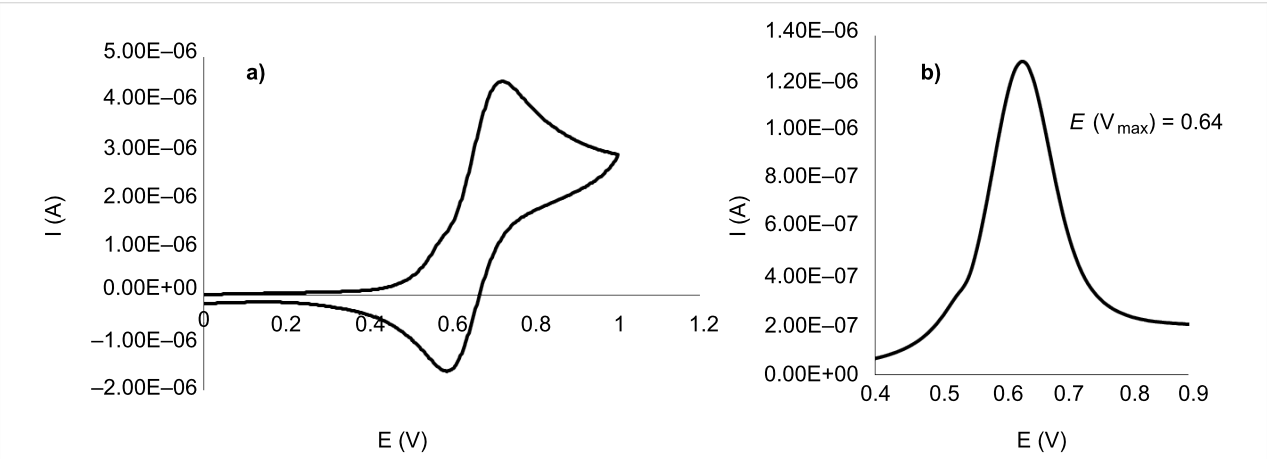

Figure 2: CV plot (a) and relevant DPV section (b) of complex **4**. Experiments were carried out using 1 mM solution of the complex in dry CH_2Cl_2 with 0.1 M $[NBu_4][PF_6]$ as the supporting electrolyte, 100 mVs^{-1} scan rate, Fc^+/ Fc used as internal standard with $E_{1/2}$ (Fc/Fc^+)= 0.44V vs SCE.

Since we previously evaluated the catalytic properties of the tris-NHC Rh(I) complex **6** (Scheme 4) in the rhodium-catalyzed addition of arylboronic acids to α,β-unsaturated ketones [25] we decided to study complex **2** in the same reaction. From these comparative data it was assumed to gaining more information about the effects of the nature of the carbene ligand while maintaining a similar structural environment on the catalyst. The catalytic addition of arylboronic acids to α,β-unsaturated ketones [58-62] is a process for which several Rh(I)-NHC complexes have afforded excellent activities and chemoselectivities [58,63,64].

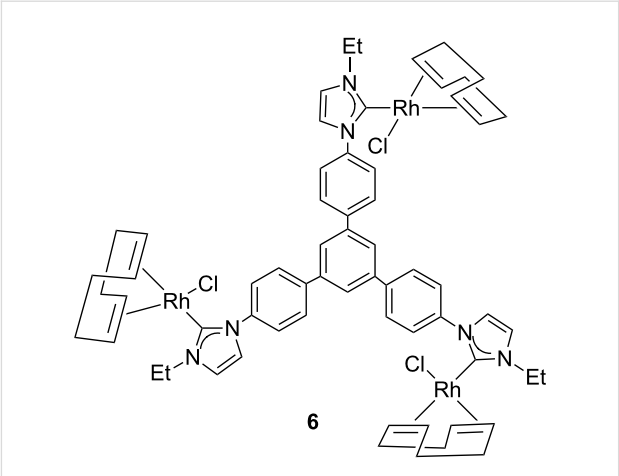

Scheme 4: Schematic representation of complex **6**.

For the catalytic experiments, the arylation of 2-cyclohexen-1-one with several arylboronic acids was studied. The results obtained with 0.066 mol % catalyst **2** were compared with those previously obtained with catalyst **6**. As can be seen from the data collected in Table 1, the activity of complex **2** is lower than that shown by complex **6**, both in terms of conversion and selectivity. For all reactions carried out in the presence of catalyst **2**, deborylation of the boronic acids took place. This side reaction explains the differences found between conversions and yields for all reactions performed. This observation is more relevant for the case of the use of 4-methoxyphenylboronic

Table 1: 1,4-Addition of arylboronic acids to 2-cyclohex-1-one.[a]

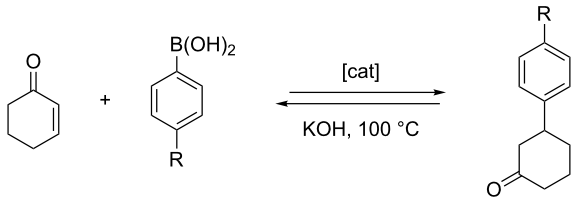

Entry	Catalyst	R	Conversion (yield, %)
1	**6**	H	100 (91)[b]
2	**2**	H	66 (43)[c]
3	**6**	Me	85 (69)[b]
4	**2**	Me	63 (34)[c]
5	**6**	OMe	48 (16)[c]
6	**2**	OMe	52 (15)[c]

[a]Reaction conditions: Catalyst (0.066 mol %), 2-cyclohexen-1-one (0.5 mmol), KOH (0.09 mmol), $ArB(OH)_2$ (0.6 mmol), dry toluene (3 mL). Conversions were determined by gas chromatography (GC), using [b]anisol or [c]2,4,6-trimethylphenol as internal standards. Yields are given in parentheses. The results given for the use of complex **6** were taken from reference [25].

acid, for which the formation of anisole is the dominant process (Table 1, entries 5 and 6).

Conclusion

In summary, this work illustrated the high coordination versatility of a nanosized tris-MIC ligand, by obtaining a series of Rh(I), Ir(I) and Ni(II) complexes. Interestingly, the tris-MIC complex of Ni is the first trimetallic Ni complex with a tris-carbene ligand. The electron-donating properties of the ligand were assessed by cyclic voltammetry and by IR spectroscopy of the corresponding carbonylated tris-Ir(I) complex. Both techniques indicate that the ligand is a stronger electron donor than its related tris-NHC analogue. It is even more important to mention that the tris-MIC ligand is a stronger electron donor than its more closely related mono-MIC ligand – a situation that is also true for the tris-NHC ligand **A**, compared to its related mono-NHC counterpart. This indicates that the triphenylbenzene core is significantly increasing the electron-donating character of the ligand, compared to the related monocarbenes, thus proving that the tris-carbene ligands should not be regarded as a simple combination of three independent monocarbenes.

Supporting Information

Supporting Information File 1

Experimental details and copies of spectra.
[http://www.beilstein-journals.org/bjoc/content/supplementary/1860-5397-11-278-S1.pdf]

Acknowledgements

We gratefully acknowledge financial support from MINECO of Spain (CTQ2014-51999-P), UJI (P11B2014-02), Generalitat Valenciana (GV/2015/097) and FCT-Fundação para a Ciência e a Tecnologia (UID/Multi/04551/2013 and PTDC/QEQ- QIN/0565/2012). C. M. is thankful to the FPI program for a fellowship, B. R. thanks FCT for IF/00346/2013 and G. G.-B. thanks the MINECO for a postdoctoral grant (FPDI-2013-16525). The authors are grateful to the Serveis Centrals d'Instrumentació Científica (SCIC) of the Universitat Jaume I for providing with spectroscopic and X-ray facilities, and to FCT (RECI/BBB-BQB/0230/2012).

References

1. Hahn, F. E.; Radloff, C.; Pape, T.; Hepp, A. *Organometallics* **2008,** *27,* 6408–6410. doi:10.1021/om801007u
2. Radloff, C.; Hahn, F. E.; Pape, T.; Fröhlich, R. *Dalton Trans.* **2009,** 7215–7222. doi:10.1039/b907896g
3. Radloff, C.; Weigand, J. J.; Hahn, F. E. *Dalton Trans.* **2009,** 9392–9394. doi:10.1039/b916651c
4. Conrady, F. M.; Fröhlich, R.; Schulte to Brinke, C.; Pape, T.; Hahn, F. E. *J. Am. Chem. Soc.* **2011,** *133,* 11496–11499. doi:10.1021/ja205021p
5. Schmidtendorf, M.; Pape, T.; Hahn, F. E. *Angew. Chem., Int. Ed.* **2012,** *51,* 2195–2198. doi:10.1002/anie.201107227
6. Viciano, M.; Sanaú, M.; Peris, E. *Organometallics* **2007,** *26,* 6050–6054. doi:10.1021/om7007919
7. Hahn, F. E.; Radloff, C.; Pape, T.; Hepp, A. *Chem. – Eur. J.* **2008,** *14,* 10900–10904. doi:10.1002/chem.200801877
8. Radloff, C.; Gong, H.-Y.; Schulte to Brinke, C.; Pape, T.; Lynch, V. M.; Sessler, J. L.; Hahn, F. E. *Chem. – Eur. J.* **2010,** *16,* 13077–13081. doi:10.1002/chem.201002276
9. Rit, A.; Pape, T.; Hahn, F. E. *J. Am. Chem. Soc.* **2010,** *132,* 4572–4573. doi:10.1021/ja101490d
10. Rit, A.; Pape, T.; Hepp, A.; Hahn, F. E. *Organometallics* **2011,** *30,* 334–347. doi:10.1021/om101102j
11. Wang, D.; Zhang, B.; He, C.; Wu, P.; Duan, C. *Chem. Commun.* **2010,** *46,* 4728–4730. doi:10.1039/c000793e
12. Segarra, C.; Guisado-Barrios, G.; Hahn, F. E.; Peris, E. *Organometallics* **2014,** *33,* 5077–5080. doi:10.1021/om500729b
13. Sinha, N.; Roelfes, F.; Hepp, A.; Mejuto, C.; Peris, E.; Hahn, F. E. *Organometallics* **2014,** *33,* 6898–6904. doi:10.1021/om500973b
14. Guerret, O.; Solé, S.; Gornitzka, H.; Teichert, M.; Trinquier, G.; Bertrand, G. *J. Am. Chem. Soc.* **1997,** *119,* 6668–6669. doi:10.1021/ja964191a
15. Karimi, B.; Akhavan, P. F. *Chem. Commun.* **2011,** *47,* 7686–7688. doi:10.1039/c1cc00017a
16. Karimi, B.; Akhavan, P. F. *Inorg. Chem.* **2011,** *50,* 6063–6072. doi:10.1021/ic2000766
17. Karimi, B.; Akhavan, P. F. *Chem. Commun.* **2009,** 3750–3752. doi:10.1039/b902096a
18. Boydston, A. J.; Bielawski, C. W. *Dalton Trans.* **2006,** 4073–4077. doi:10.1039/b607696n
19. Mercs, L.; Neels, A.; Albrecht, M. *Dalton Trans.* **2008,** 5570–5576. doi:10.1039/b809721f
20. Mercs, L.; Neels, A.; Stoeckli-Evans, H.; Albrecht, M. *Dalton Trans.* **2009,** 7168–7178. doi:10.1039/b907018d

21. Zhang, C.; Wang, J.-J.; Liu, Y.; Ma, H.; Yang, X.-L.; Xu, H.-B. *Chem. – Eur. J.* **2013,** *19,* 5004–5008. doi:10.1002/chem.201203975
22. Choi, J.; Yang, H. Y.; Kim, H. J.; Son, S. U. *Angew. Chem., Int. Ed.* **2010,** *49,* 7718–7722. doi:10.1002/anie.201003101
23. Gonell, S.; Poyatos, M.; Peris, E. *Angew. Chem., Int. Ed.* **2013,** *52,* 7009–7013. doi:10.1002/anie.201302686
24. Guisado-Barrios, G.; Hiller, J.; Peris, E. *Chem. – Eur. J.* **2013,** *19,* 10405–10411. doi:10.1002/chem.201300486
25. Mejuto, C.; Guisado-Barrios, G.; Peris, E. *Organometallics* **2014,** *33,* 3205–3211. doi:10.1021/om500547g
26. Mata, J. A.; Hahn, F. E.; Peris, E. *Chem. Sci.* **2014,** *5,* 1723–1732. doi:10.1039/c3sc53126k
27. Mejuto, C.; Guisado-Barrios, G.; Gusev, D.; Peris, E. *Chem. Commun.* **2015,** *51,* 13914–13917. doi:10.1039/C5CC05114B
28. Segarra, C.; Linke, J.; Mas-Marzá, E.; Kuck, D.; Peris, E. *Chem. Commun.* **2013,** *49,* 10572–10574. doi:10.1039/c3cc46155f
29. Gonell, S.; Alabau, R. G.; Poyatos, M.; Peris, E. *Chem. Commun.* **2013,** *49,* 7126–7128. doi:10.1039/c3cc44109a
30. Raynal, M.; Ballester, P.; Vidal-Ferran, A.; van Leeuwen, P. W. N. M. *Chem. Soc. Rev.* **2014,** *43,* 1660–1733. doi:10.1039/C3CS60027K
31. Helms, B.; Fréchet, J. M. J. *Adv. Synth. Catal.* **2006,** *348,* 1125–1148. doi:10.1002/adsc.200606095
32. Bouffard, J.; Keitz, B. K.; Tonner, R.; Guisado-Barrios, G.; Frenking, G.; Grubbs, R. H.; Bertrand, G. *Organometallics* **2011,** *30,* 2617–2627. doi:10.1021/om200272m
33. Guisado-Barrios, G.; Bouffard, J.; Donnadieu, B.; Bertrand, G. *Angew. Chem., Int. Ed.* **2010,** *49,* 4759–4762. doi:10.1002/anie.201001864
34. Keitz, B. K.; Bouffard, J.; Bertrand, G.; Grubbs, R. H. *J. Am. Chem. Soc.* **2011,** *133,* 8498–8501. doi:10.1021/ja203070r
35. Aldeco-Perez, E.; Rosenthal, A. J.; Donnadieu, B.; Parameswaran, P.; Frenking, G.; Bertrand, G. *Science* **2009,** *326,* 556–559. doi:10.1126/science.1178206
36. Mathew, P.; Neels, A.; Albrecht, M. *J. Am. Chem. Soc.* **2008,** *130,* 13534–13535. doi:10.1021/ja805781s
37. Zamora, M. T.; Ferguson, M. J.; Cowie, M. *Organometallics* **2012,** *31,* 5384–5395. doi:10.1021/om300423z
38. Maity, R.; van der Meer, M.; Sarkar, B. *Dalton Trans.* **2015,** *44,* 46–49. doi:10.1039/C4DT03239J
39. Hohloch, S.; Kaiser, S.; Duecker, F. L.; Bolje, A.; Maity, R.; Košmrlj, J.; Sarkar, B. *Dalton Trans.* **2015,** *44,* 686–693. doi:10.1039/C4DT02879A
40. Maity, R.; Hohloch, S.; Su, C.-Y.; van der Meer, M.; Sarkar, B. *Chem. – Eur. J.* **2014,** *20,* 9952–9961. doi:10.1002/chem.201402838
41. Keske, E. C.; Zenkina, O. V.; Wang, R.; Crudden, C. M. *Organometallics* **2012,** *31,* 456–461. doi:10.1021/om201104f
42. Keske, E. C.; Zenkina, O. V.; Wang, R.; Crudden, C. M. *Organometallics* **2012,** *31,* 6215–6221. doi:10.1021/om3005228
43. Cai, J.; Yang, X.; Arumugam, K.; Bielawski, C. W.; Sessler, J. L. *Organometallics* **2011,** *30,* 5033–5037. doi:10.1021/om200670f
44. Maity, R.; Van der Meer, M.; Hohloch, S.; Sarkar, A. *Organometallics* **2015,** *34,* 3090–3096. doi:10.1021/acs.organomet.5b00365
45. Bezuidenhout, D. I.; Kleinhans, G.; Guisado-Barrios, G.; Liles, D. C.; Ung, G.; Bertrand, G. *Chem. Commun.* **2014,** *50,* 2431–2433. doi:10.1039/c3cc49385g
46. Guisado-Barrios, G.; Bouffard, J.; Donnadieu, B.; Bertrand, G. *Organometallics* **2011,** *30,* 6017–6021. doi:10.1021/om200844b
47. Maity, R.; Mekic, A.; van der Meer, M.; Verma, A.; Sarkar, B. *Chem. Commun.* **2015,** *51,* 15106–15109. doi:10.1039/C5CC05506G
48. Savka, R.; Plenio, H. *Dalton Trans.* **2015,** *44,* 891–893. doi:10.1039/C4DT03449J
49. Wei, Y.; Petronilho, A.; Mueller-Bunz, H.; Albrecht, M. *Organometallics* **2014,** *33,* 5834–5844. doi:10.1021/om500593s
50. Luca, O. R.; Thompson, B. A.; Takase, M. K.; Crabtree, R. H. *J. Organomet. Chem.* **2013,** *730,* 79–83. doi:10.1016/j.jorganchem.2012.10.038
51. Abernethy, C. D.; Cowley, A. H.; Jones, R. A. *J. Organomet. Chem.* **2000,** *596,* 3–5. doi:10.1016/S0022-328X(99)00557-4
52. Kelly, R. A., III; Scott, N. M.; Diez-González, S.; Stevens, E. D.; Nolan, S. P. *Organometallics* **2005,** *24,* 3442–3447. doi:10.1021/om0501879
53. Valdés, H.; Poyatos, M.; Ujaque, G.; Peris, E. *Chem. – Eur. J.* **2015,** *21,* 1578–1588. doi:10.1002/chem.201404618
54. Chianese, A. R.; Li, X.; Janzen, M. C.; Faller, J. W.; Crabtree, R. H. *Organometallics* **2003,** *22,* 1663–1667. doi:10.1021/om021029+
55. Kelly, R. A., III; Clavier, H.; Giudice, S.; Scott, N. M.; Stevens, E. D.; Bordner, J.; Samardjiev, I.; Hoff, C. D.; Cavallo, L.; Nolan, S. P. *Organometallics* **2008,** *27,* 202–210. doi:10.1021/om701001g
56. Nelson, D. J.; Nolan, S. P. *Chem. Soc. Rev.* **2013,** *42,* 6723–6753. doi:10.1039/c3cs60146c
57. Gusev, D. G. *Organometallics* **2009,** *28,* 6458–6461. doi:10.1021/om900654g
58. Truscott, B. J.; Fortman, G. C.; Slawin, A. M. Z.; Nolan, S. P. *Org. Biomol. Chem.* **2011,** *9,* 7038–7041. doi:10.1039/c1ob06112g
59. Pucheault, M.; Darses, S.; Genet, J.-P. *Tetrahedron Lett.* **2002,** *43,* 6155–6157. doi:10.1016/S0040-4039(02)01288-1
60. Pucheault, M.; Darses, S.; Genet, J.-P. *Eur. J. Org. Chem.* **2002,** 3552–3557. doi:10.1002/1099-0690(200211)2002:21<3552::AID-EJOC3552>3.0.CO;2-4
61. Sakai, M.; Hayashi, H.; Miyaura, N. *Organometallics* **1997,** *16,* 4229–4231. doi:10.1021/om9705113
62. Hayashi, T.; Takahashi, M.; Takaya, Y.; Ogasawara, M. *J. Am. Chem. Soc.* **2002,** *124,* 5052–5058. doi:10.1021/ja012711i
63. Peñafiel, I.; Pastor, I. M.; Yus, M.; Esteruelas, M. A.; Oliván, M. *Organometallics* **2012,** *31,* 6154–6161. doi:10.1021/om300498e
64. Bratko, I.; Guisado-Barrios, G.; Favier, I.; Mallet-Ladeira, S.; Teuma, E.; Peris, E.; Gómez, M. *Eur. J. Org. Chem.* **2014,** 2160–2167. doi:10.1002/ejoc.201301220

License and Terms

BEILSTEIN JOURNAL OF ORGANIC CHEMISTRY

Direct estimate of the internal π-donation to the carbene centre within N-heterocyclic carbenes and related molecules

Diego M. Andrada[1], Nicole Holzmann[2], Thomas Hamadi[1] and Gernot Frenking[*1,§]

Full Research Paper

Open Access

Address:
[1]Fachbereich Chemie, Philipps-Universität Marburg, Hans-Meerwein-Strasse, D-35032 Marburg, Germany and
[2]Laboratoire International Associé Centre National de la Recherche Scientifique - UMR 7565, Université de Lorraine, 54506 Vandoeuvre-lès-Nancy, France

Email:
Gernot Frenking[*] - frenking@chemie.uni-marburg.de

* Corresponding author
§ Fax: +49-6421-2825566

Keywords:
bonding analysis; N-heterocyclic carbenes; π-donation

Beilstein J. Org. Chem. **2015,** *11,* 2727–2736.
doi:10.3762/bjoc.11.294

Received: 27 October 2015
Accepted: 11 December 2015
Published: 24 December 2015

This article is part of the Thematic Series "N-Heterocyclic carbenes" and is dedicated to Prof. F. Ekkehardt Hahn on the occasion of his 60th birthday.

Guest Editor: S. P. Nolan

Abstract

Fifteen cyclic and acylic carbenes have been calculated with density functional theory at the BP86/def2-TZVPP level. The strength of the internal X→p(π) π-donation of heteroatoms and carbon which are bonded to the C(II) atom is estimated with the help of NBO calculations and with an energy decomposition analysis. The investigated molecules include N-heterocyclic carbenes (NHCs), the cyclic alkyl(amino)carbene (cAAC), mesoionic carbenes and ylide-stabilized carbenes. The bonding analysis suggests that the carbene centre in cAAC and in diamidocarbene have the weakest X→p(π) π-donation while mesoionic carbenes possess the strongest π-donation.

Introduction

Since the isolation and unambiguous characterization of imidazol-2-ylidene by Arduengo in 1991 [1], the chemistry of stable singlet carbenes has become a major field of chemical research [2-4]. The outstanding stability and synthetic utility of N-heterocyclic carbenes (NHCs) is an ongoing subject to an ubiquitous number of experimental and computational studies exploring their structural and electronic properties [5-8]. In the last two decades, these versatile compounds have been widely employed in transition metal [9-13] and organocatalysis [14-16], organometallic [17-19] and main group synthesis [20-26], and activation of small molecules [27,28].

NHCs possess a divalent C(II) atom which is connected to one or two nitrogen atoms [2,29]. The adjacent heteroatoms stabilize the singlet form by both their σ-electron-withdrawing character and the π-electron-donation of their lone pairs into the formally empty 2p orbital of C(II), giving rise to a four π-electron three-centre system [1,2,30,31]. Thus, the lone pair placed in

the plane of the ring renders NHCs as nucleophilic compounds while the partially empty 2p orbital on C_{carb} provides some π-acceptor character. It has been initially claimed that the excellent ligand features of NHCs were due to their strong σ-donation abilities [32,33]. However, experimental and computational evidences have revealed non-negligible π-acceptor properties [34-38]. In recent years, several strategies have successfully been developed for tuning the π-acidity of NHCs by changing substitution and structural patterns, such as the size of the backbone ring [39-41], variation of the α-heteroatoms [7], anti-Bredt NHCs [42,43], mesoionic NHCs [44-47], ylide stabilized carbenes [48-51] and other [52-55]. A remarkable variation was introduced with the cyclic alkyl(amino)carbene (cAAC) by Bertrand in 2005 [20,56,57]. The replacement of one amino substituent by a saturated alkyl group makes the carbene more nucleophilic and electrophilic at the same time [20,56,57]. Since then, cAACs have been used as a superior ligand for the stabilization of unstable chemical species, radical and main group elements in different oxidation states [27,34,36,58-60], due to their stronger π-acceptor and σ-donor properties.

With such a wide range of NHCs, a thorough knowledge of the electronic nature is a prerequisite for a guided design of suitable applications. In this regard, a number of techniques have been developed to quantify the π-acceptor ability of carbenes [61,62]. Thus, NMR methods have been reported that allow the measurement of the π-acidity of NHCs [63]. Bertrand et al. and Ganter et al. have proposed the use of ^{31}P and ^{77}Se NMR chemical shift of the NHC-phenylphosphinidene and NHC-selenium adducts, respectively, to determine the π-acceptor strength of the parent NHCs [64,65]. In the same way, Nolan et al. have applied this technique to a wider range of NHCs and have established the connection between the π-accepting abilities and the NMR chemical shift [66]. Furthermore, different theoretical approaches can be found in the literature where natural bond orbital calculations (NBO) and energy decomposition analysis (EDA) have been applied to a broad variety of organometallic complexes [35,67-72]. Although all the procedures have proven to be a convenient way to evaluate the π-acceptor capacities of NHCs, they are limited by the fact that they inherently estimate properties of the parents systems after complexation. It would be helpful if the intrinsic π-donor strength of the substituents to the carbene centre would be directly estimated in the parent carbenes.

In the quest of a direct estimate of the NHC π-acceptor properties and its connection with the π-stabilization exerted by the adjacent α-heteroatoms to the carbene carbon atom, herein we report on the use of the EDA-NOCV (energy decomposition analysis with natural orbitals for chemical valence) method to evaluate the intrinsic electronic π-donation strength. In this context, we quantitatively estimate the differences in the electronic structure of 15 archetypical carbenes (Scheme 1). Here compounds **1**–**4**, **6**, and **7** are typical NHCs while **5** is an acylic diamidocarbene. Compounds **8**–**10** are so-called abnormal or mesoionic carbenes for which no resonance form without formal charges can be written [73]. Molecules **11** and **12** are NHCs with one nitrogen donor atom where the carbene centre is additionally stabilised by another hetero π-donor. Compounds **13** and **14** are ylide-stabilised carbenes while **15** is a diamidocarbene.

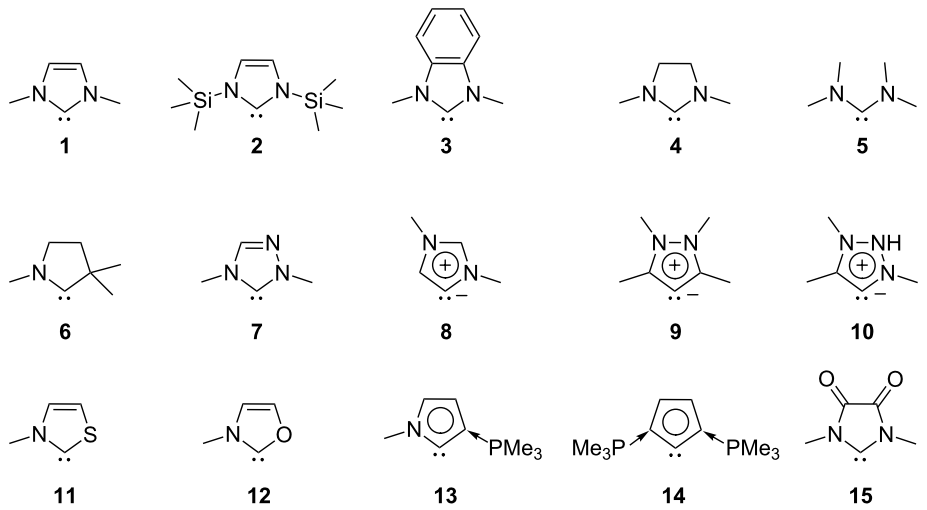

Scheme 1: Schematic view of the calculated carbenes **1–15**.

Computational Details

All geometries were optimized without symmetry constraint within the DFT framework using the BP86 functional [74,75] in combination with the Gaussian basis sets def2-TZVPP [76]. Stationary points were located with the Berny algorithm [77] using redundant coordinates. Analytical Hessians were computed to determinate the nature of the stationary points [78]. All geometry optimization computations were performed using the Gaussian 09 suite of programs [79]. Wiberg Bond Orders [80] and NPA [81,82] atomic partial charges have been calculated at the BP86/def2-TZVPP [74-76] level of theory with GAUSSIAN 09 [79] and GENNBO 5.9 programs [83].

All energy decomposition analyses were carried out using the BP86 functional in combination with uncontracted Slater-type orbitals (STOs) as basis function for the SCF calculations [84]. The basis sets for all elements were triple-ζ quality augmented by two sets of polarizations functions and one set of diffuse functions. Core electrons were treated by the frozen-core approximation. This level of theory is denoted as BP86/TZ2P+. We did not reoptimize the geometries but used the BP86/def2-TZVPP optimized structures, because we know from previous studies that the two basis sets give very similar geometries. An auxiliary set of s, p, d, f, and g STOs was used to fit the molecular densities and to represent the Coulomb and exchange potentials accurately in each SCF cycle [85]. Scalar relativistic effects have been incorporated by applying the zeroth-order regular approximation (ZORA) [86]. The nature of the stationary points on the potential energy surface was determined by calculating the vibrational frequencies at BP86/TZ2P+. These calculations were performed with the program package ADF.2013 [87].

The bonding situation of the donor–acceptor bonds was investigated by an energy decomposition analysis (EDA) which was developed by Morokuma [88] and by Ziegler and Rauk [89,90]. The bonding analysis focuses on the instantaneous interaction energy ΔE_{int} of a bond A–B between two fragments A and B in the particular electronic reference state and in the frozen geometry AB. This energy is divided into three main components (Equation 1).

$$\Delta E_{\text{int}} = \Delta E_{\text{elstat}} + \Delta E_{\text{Pauli}} + \Delta E_{\text{orb}} \qquad (1)$$

The term ΔE_{elstat} corresponds to the classical electrostatic interaction between the unperturbed charge distributions of the prepared atoms (or fragments) and it is usually attractive. The Pauli repulsion ΔE_{Pauli} is the energy change associated with the transformation from the superposition of the unperturbed wave functions of the isolated fragments to the wave function $\Psi^0 = N\hat{A}[\Psi_A\Psi_B]$, which properly obeys the Pauli principle through explicit antisymmetrization (Â operator) and renormalization (N = constant) of the product wave function. It comprises the destabilizing interactions between electrons of the same spin on either fragment. The orbital interaction ΔE_{orb} accounts for charge transfer and polarization effects [91]. The ΔE_{orb} term can be dissected into contributions from each irreducible representation of the point group of the interacting system. Further details on the EDA method and its applications to the analysis of the chemical bond [92-94] can be found in the literature.

The EDA with natural orbitals for chemical valence (EDA-NOCV) method [95] combines charge and energy decomposition schemes to split the deformation density which is associated with the bond formation, Δρ, into different components of the chemical bond. The EDA-NOCV calculations provide pairwise energy contributions for each pair of interaction orbitals to the total bond energy. NOCV is defined as the eigenvector of the valence operator, $\hat{V}$, given by Equation 2 [96-98].

$$\hat{V}\Psi_i = \upsilon_i\Psi_i \qquad (2)$$

In the EDA-NOCV scheme the orbital interaction term, ΔE_{orb}, is given by Equation 3.

$$\Delta E_{\text{orb}} = \sum_k \Delta E_k^{\text{orb}} = \sum_{k=1}^{N/2} \upsilon_k \left[-F_{-k,-k}^{TS} + F_{k,k}^{TS} \right] \qquad (3)$$

Where $F_{-k,-k}^{TS}$ and $F_{k,k}^{TS}$ are diagonal Kohn–Sham matrix elements corresponding to NOCVs with the eigenvalues $-\nu_k$ and ν_k, respectively. The ΔE_k^{orb} terms are assigned to a particular type of bond by visual inspection of the shape of the deformation density, $\Delta\rho_k$. The absolute values $|\nu_k|$ of the eigenvalues of Equation 3 give the charge flow which is associated with each pairwise orbital interaction. The EDA-NOCV scheme thus provides information about the charge deformation ($\Delta\rho_{\text{orb}}$) and the associated stabilization energy (ΔE_{orb}) of the orbital interactions in chemical bonds. For more details we refer to the literature [97,98].

Results and Discussion

The optimized geometries at the BP86/def2-TZVPP level of theory of the calculated carbenes and the most important bond lengths and angles are shown in Figure 1. Experimental values of substituted analogues are given in parentheses.

The theoretically predicted structures are in good agreement with experimental data [31,46,47,56,99-103]. In general the computed bond lengths are slightly longer than the experimental ones. The X–C_{carb}–X (X = N, C, O and S) angle in the

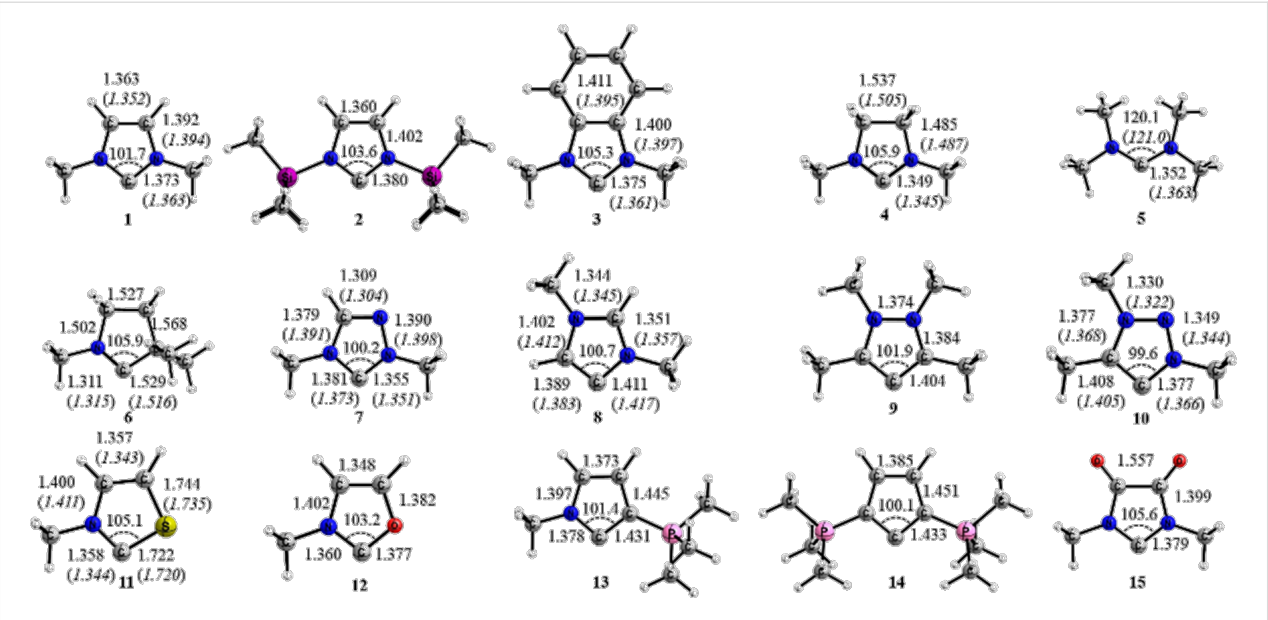

Figure 1: Optimized geometries of carbenes **1–15** at the BP86/def2-TZVPP level of theory. Bond lengths and angles are given in [Å] and [°]. Experimental values are given in parentheses: **1** (Ref. [31]); **3** (Ref. [99]); **4** (Ref. [100]); **5** (Ref. [101]); **6** (Ref. [56]); **7** (Ref. [102]); **8** (Ref. [46]); **10** (Ref. [47]); **11** (Ref. [103]).

five-membered rings slightly varies between 99.6° (**10**) and 105.6° (**15**) and is slightly larger (120.1°) in the acyclic carbene **5**. This angle is often associated with the σ-donor properties which are related to the sp^x hybridization of the carbene lone pair orbital [2]. A first hint of the strength of the π-donation is given by the C_{carb}–N bond lengths. The shortest C_{carb}–N bond of 1.311 Å is calculated for the cAAC species **6**, which is close to a standard C=N double bond (1.30 Å), while the longest value of 1.411 Å is calculated for the abnormal carbene **8**, which approaches a standard C–N single bond (1.46 Å) [104]. The C_{carb}–N bond lengths exhibit otherwise a remarkable small range between 1.35–1.38 Å. The C–N bond is slightly longer in the conjugated 6π-electron carbenes which possess some aromatic character than in the non-aromatic analogues which previously ascribed to stronger π-conjugation [105-107]. The introduction of the heteroatoms O and S in compounds **11** and **12** changes the C–N bond only slightly. The C_{carb}–C bond lengths in the conjugated carbenes are between 1.404 Å (**9**)–1.433 Å (**14**) while the cAAC system **6** has a much longer distance of 1.529 Å.

Figure 2 shows the shape and energy of the frontier molecular orbitals for compounds **1–15** which are relevant for the σ-donor and π-acceptor properties. The HOMO is in all cases a carbon σ-lone pair while the LUMO (LUMO + 1 for **1**, **7–10**) depicts a π-orbital which has the largest coefficient at the C_{carb} atom that makes it suitable for π-backdonation. The LUMOs of compounds **1**, and **7–10** which are not displayed in Figure 2 are also π-orbitals which have a node at the C_{carb} atom. The HOMO–LUMO energy difference varies considerably between 4.58 eV (**4**) and 1.55 eV (**15**). The small HOMO–LUMO gap of the diamidocarbene **15** comes from the very low lying LUMO which has been noted before [42]. There is clearly a correlation between the HOMO–LUMO energy difference and the calculated singlet–triplet gap of the compounds which are given at the bottom of Figure 2. The largest singlet–triplet (S/T) gap is predicted for compound **1** (91.6 kcal/mol) while compound **15** possesses the lowest S/T value (27.5 kcal/mol).

The focus of the present work lies on the π-donation from the neighboring atoms to the carbene center X(π)→C_{carb}. To estimate the size of the charge donation Δq(π) we calculated the occupation of p(π) AO of the carbene atom in molecules **1–15** which is available from the NBO analysis. Table 1 gives the computed values for the atomic charges, the orbital occupation of the σ-lone pair orbital and the occupation of p(π) AO of the C_{carb} atom. We also present the Wiberg Bond Orders for the C_{carb}–X bonds.

The NBO data indicate that the occupation of the p(π) AO of the C_{carb} atom is between 0.81 e (**8**, and **9**) and 0.49 e (**6**). The p(π) occupation at the C_{carb} atom is particularly large for the carbenes which have no heteroatoms bonded to it (**9**, and **14**) or only one heteroatom as in **8**. The special role of the cAAC species **6** which exhibits particular reactivity [52-55] that has recently been utilized for the stabilization of unusual compounds [108-117] comes to the fore by the smallest value of the p(π) occupation. Carbene **6** has also the largest bond order for

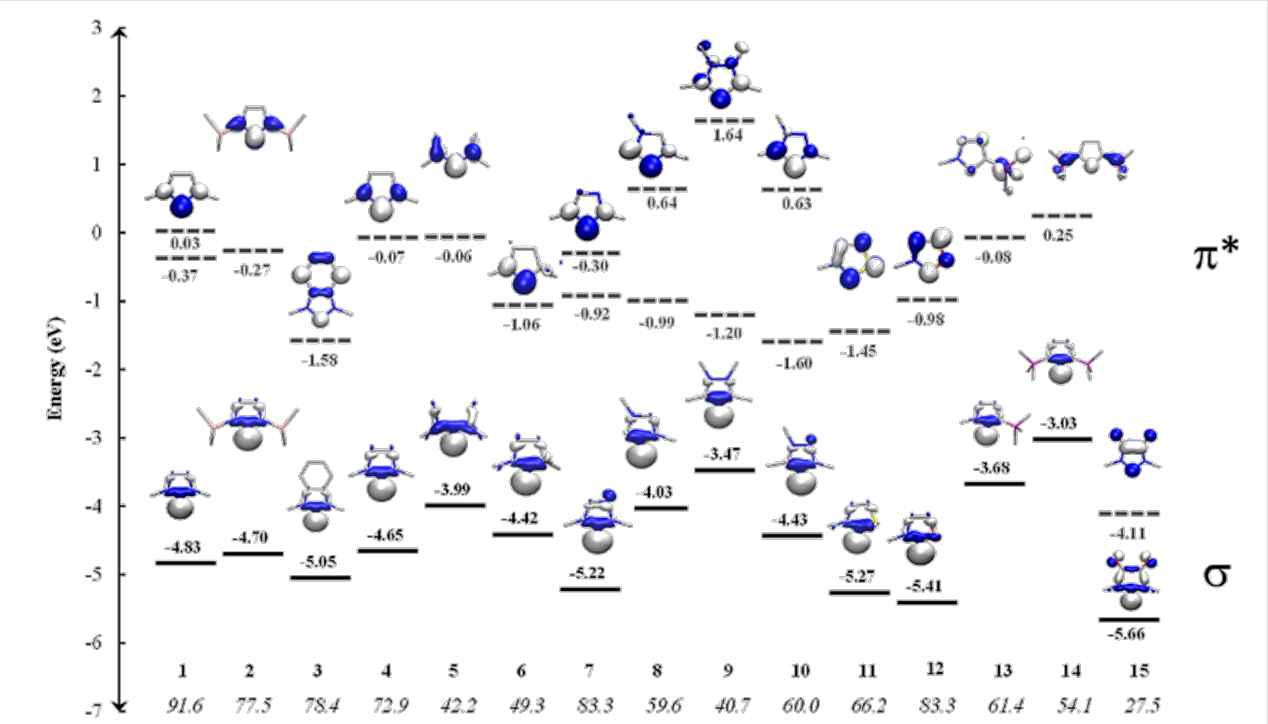

Figure 2: Frontier orbitals (BP86/def2-TZVPP) and eigenvalues (in eV) of the carbenes **1–15**. The isosurfaces were taken at the 0.06 isovalue. The hydrogen atoms are omitted for clarity.

Table 1: Calculated NBO partial charges q(C_{carb}) of the carbene carbon atom, occupation of the lone pair orbital C_{carb}(σ) and the p(π) AO at C_{carb}. Wiberg Bond Orders (WBO) for the C_{carb}–X (X = C, N, O and S) bonds at BP86/def2-TZVPP.

	q(C_{carb})	C_{carb}(σ)	p(π)	WBO
1	0.04	1.91	0.69	1.27
2	0.06	1.88	0.67	1.29
3	0.09	1.91	0.64	1.25
4	0.13	1.86	0.60	1.32
5	0.12	1.84	0.62	1.34
6	0.09	1.87	0.49	1.56/1.00[a]
7	0.05	1.90	0.67	1.22/1.35[a]
8	−0.19	1.88	0.81	1.14/1.60[a]
9	−0.39	1.83	0.81	1.46
10	−0.17	1.88	0.73	1.44/1.26[a]
11	−0.23	1.89	0.73	1.34/1.38[a]
12	0.19	1.91	0.63	1.33/1.13[a]
13	−0.16	1.88	0.74	1.25/1.37[a]
14	−0.37	1.85	0.80	1.36
15	0.19	1.93	0.51	1.20

[a]The first value is for the atom on the left side of C_{carb} as shown in Figure 1.

the C_{carb}–N bond and the smallest bond order for a C_{carb}–C bond. Note that the C_{carb} atom carries a negative partial charge when it is bonded to one or two carbon atoms (**8**–**11**, **13**, and **14**).

The energy contribution of the X(π)→C_{carb} donation can be calculated with the EDA-NOCV method which is described in the method section. We carried out EDA-NOCV calculations using a carbon atom in the ^{3}P ground state with the electronic configuration $2s^2 2p_\sigma^1 2p_{||}^1 2p_\perp^0$ and the remaining fragment as interacting moieties with unpaired electrons at X. Scheme 2 shows the directly interacting atoms C_{carb} and X where the electrons are placed in such a way that the unpaired electrons on both fragments are in the plane of the molecule yielding the σ-bonds while the lone pair electrons and the vacant p AO of

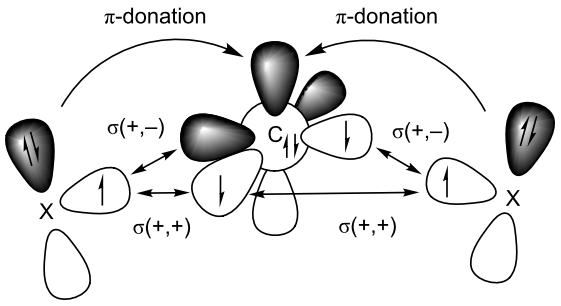

Scheme 2: Schematic view of the major orbital interactions between a carbon atom in the ^{3}P electronic ground state with the configuration $2s^2 2p_\sigma^1 2p_{||}^1 2p_\perp^0$ and atoms X which possess a p(π) lone pair orbital. There are σ(+,+) and σ(+,−) interactions which give the two C_{carb}–X σ-bonds and the π-donation X(π)→C_{carb}.

carbon have π-symmetry with respect to the molecular plane. This leads to three major orbital interactions for σ and π-bonding between C_{carb} and X. These are the σ(+,+) and σ(+,−) interactions that come from the in-phase and out-of-phase combinations of the lone-pairs, respectively, which give the two C_{carb}–X σ-bonds and the π-donation X(π)→C_{carb}.

Table 2 shows the numerical results of the EDA-NOCV calculations. The total interaction energy ΔE_{int} between the carbon atom and the remaining fragment in the frozen geometry [118] is composed from the stabilizing orbital (covalent) interactions ΔE_{orb} and the Coulombic term ΔE_{elstat} and the destabilizing Pauli repulsion ΔE_{Pauli}. The strongest attraction comes from the orbital term ΔE_{orb}. We want to point out that the trend of the intrinsic bond strength between C_{carb} and the remaining fragment does not correlate with the trend of covalent bonding. The largest ΔE_{int} values are calculated for compounds **8** and **9** but the ΔE_{orb} values of the two species are much smaller than those of most other carbenes. The strong net bonding in **8** and **9** is rather related to the comparatively weak Pauli repulsion ΔE_{Pauli} which is much weaker than in most other species (Table 2). The interplay of all three factors ΔE_{orb}, ΔE_{Pauli} and ΔE_{elstat} for determining the overall net strength of chemical bonding has been highlighted before [92-94,119,120].

The most important information of the EDA-NOCV calculations comes from contributions of the pairwise orbital interactions to ΔE_{orb}. Table 2 shows that there are indeed three major terms for each molecule which can easily be identified with the schematic description that is given in Scheme 2. The deformation densities associated with the three major orbital interactions ΔE_{σ} (+,−), ΔE_{σ} (+,+) and ΔE_{π} for compound **1** are shown in Figure 3. The color code of the charge deformation on bond formation is red→blue. The largest contributions comes from the formation of the C_{carb}–X σ-bonds while the π-donation X(π)→C_{carb} is much weaker which is reasonable. The ΔE_{σ}

Table 2: EDA-NOCV calculations at the BP86/TZ2P+ level of theory of compounds **1–15** using C(II) in the valence configuration $2s^2 2p_{\sigma}^1 2p_{||}^1 2p_{\perp}^0$ and the remaining fragment as interacting moieties[a]. Energy values are given in kcal/mol.

	1	**2**	**3**	**4**[b]	**5**[b]	**6**	**7**	**8**
ΔE_{int}	−322.7	−295.2	−309.6	−319.5	−314.5	−272.3	−302.1	−330.85
ΔE_{Pauli}	759.2	825.7	807.5	804.1	814.41	734.7	846.2	669.18
ΔE_{elstat}[a]	−397.8 (36.8%)	−415.2 (37.1%)	−413.4 (37.0%)	−416.5 (37.1%)	−414.6 (36.7%)	−387.1 (38.4%)	−426.5 (37.2%)	−371.9 (37.2%)
ΔE_{orb}[a]	−684.0 (63.2%)	−705.7 (62.9%)	−703.7 (63.0%)	−707.1 (62.9%)	−714.3 (63.3%)	−619.9 (61.6%)	−721.7 (62.9%)	−628.2 (62.8%)
$\Delta E_{\sigma\ (+,-)}$[c]	−319.3 (46.7%)	−331.1 (46.9%)	−322.1 (45.8%)	−335.9 (47.5%)	−353.4 (49.5%)	−331.7 (53.5%)	−338.7 (46.9%)	−327.6 (52.1%)
$\Delta E_{\sigma\ (+,+)}$[c]	−233.8 (34.2%)	−247.2 (35.0%)	−252.2 (35.8%)	−242.3 (34.3%)	−223.2 (31.2%)	−182.6 (29.5%)	−241.7 (33.5%)	−170.8 (27.2%)
$\Delta E_{\pi\text{-donation}}$[c]	**−93.4** (13.6%)	**−87.8** (12.4%)	**−89.3** (12.7%)	**−86.1** (12.2%)	**−90.2** (12.6%)	**−72.2** (11.6%)	**−92.6** (12.8%)	**−101.3** (16.1%)
ΔE_{rest}[c]	−37.5 (5.5%)	−39.6 (5.6%)	−40.1 (5.7%)	−42.8 (6.1%)	−47.5 (6.6%)	−33.4 (5.4%)	−48.7 (6.7%)	−28.5 (4.5%)
	9[b]	**10**	**11**	**12**	**13**	**14**	**15**	
ΔE_{int}	−336.5	−308.9	−263.9	−285.9	−312.1	−301.6	−280.6	
ΔE_{Pauli}	643.5	760.5	715.5	830.2	705.4	660.0	805.6	
ΔE_{elstat}[a]	−377.3 (38.5%)	−406.3 (38.0%)	−378.1 (38.6%)	−397.5 (35.6%)	−380.8 (37.4%)	−365.2 (38.0%)	−406.6 (37.4%)	
ΔE_{orb}[a]	−602.6 (61.5%)	−663.1 (62.0%)	−601.4 (61.4%)	−718.5 (65.4%)	−636.7 (62.6%)	−596.4 (62.0%)	−679.6 (62.6%)	
$\Delta E_{\sigma\ (+,-)}$[c]	−285.9 (47.4%)	−335.8 (50.6%)	−256.9 (42.7%)	−361.0 (50.2%)	−326.8 (51.3%)	−283.0 (47.5%)	−322.0 (47.4%)	
$\Delta E_{\sigma\ (+,+)}$[c]	−178.5 (29.6%)	−186.6 (28.1%)	−219.0 (36.4%)	−235.7 (32.8%)	−180.9 (28.4%)	−184.9 (31.0%)	−242.0 (35.6%)	
$\Delta E_{\pi\text{-donation}}$[c]	**−109.9** (18.2%)	**−100.6** (15.2%)	**−90.0** (15.0%)	**−82.4** (11.5%)	**−96.4** (15.1%)	**−100.8** (16.9%)	**−74.0** (10.9%)	
ΔE_{rest}[c]	−28.3 (4.6%)	−40.2 (6.1%)	−35.4 (5.9%)	−39.1 (5.4%)	−32.7 (5.1%)	−27.7 (4.6%)	−41.6 (6.1%)	

[a]The values in parentheses give the percentage contribution to the total attractive interactions $\Delta E_{elstat} + \Delta E_{orb}$. [b]The symmetry C_s was enforced. [c]The values in parentheses give the percentage contribution to the total orbital interactions ΔE_{orb}.

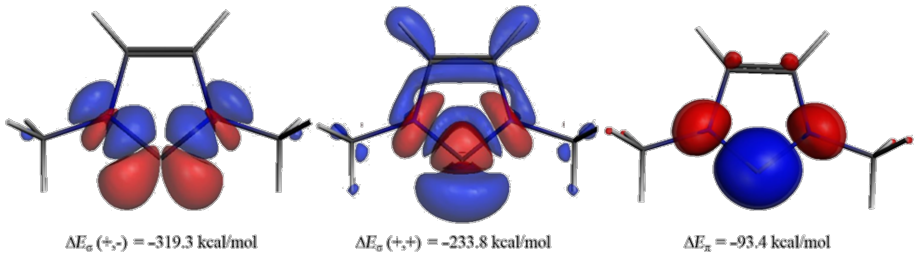

Figure 3: Plot of deformation densities Δρ of the pairwise orbital interactions between C(^{3}P) and N(Me)HC=CHN(Me), associated energies Δ*E* in kcal/mol. The color-code of the charge flow is red→blue.

(+,−) component of the C_{carb}–N σ-bond (−319.3 kcal/mol, Figure 3a) is bigger than the ΔE_σ (+,+) component (−233.8 kcal/mol, Figure 3b) which can be explained with the larger overlap of the former term (see Scheme 2). Note that the charge flows of the individual (+,+) and (+,−) interactions have different directions which cannot be easily associated to a physical meaning. It is the net charge flow which indicates the overall direction. The red and blue areas at the carbene carbon in Figure 3b indicates the polarization (change in hybridization) which takes place during the bond formation. The charge flow which is associated with the π-donation X(π)→C_{carb} shows the expected direction from nitrogen to carbon. The charge flow which is associated with the three dominant orbital interactions in compound **2**–**15** is shown in Figure S1 of Supporting Information File 1.

Inspection of the strength of ΔE_π should thus reveal information about the in internal π-donation to the C_{carb} atom in molecules **1**–**15**. Table 2 suggests that the strongest X(π)→C_{carb} donation is found in the 6π-conjugated carbenes **8**–**10**, **13**, and **14** where the C_{carb} atom is bonded to two (**9**, **14**) or one (**8**, **10**, **13**) carbon atoms. The weakest π-donor contributions are calculated for the cAAC species **6** and the diamidocarbene **15**. It appears as if the ΔE_π values which give the energy contribution of the X(π)→C_{carb} donation which come from the EDA-NOCV calculations and the p(π) occupation which is given by the NBO method correlate. Figure 4 shows a correlation diagram between ΔE_π and p(π). There is clearly a qualitative correlation between the two entries, but the correlation coefficient of $R^2 = 0.89$ indicates that charge donation and associated stabilization of the different systems do not completely agree. Both methods agree that the molecules of cAAC (**6**) and the diamidocarbene **15** possess extremely low π-stabilization of the carbene carbon atom.

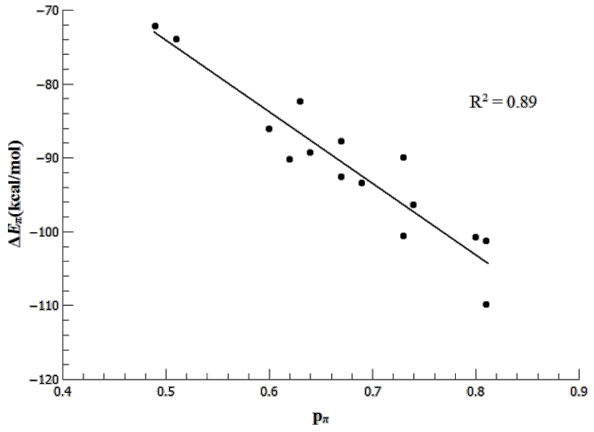

Figure 4: Plot of the ΔE_π values against NBO p_π occupation for the NHC family **1–15**.

Conclusion

The NBO and EDA-NOCV calculations of the fifteen carbenes show that the carbene centre in cAAC and in diamidocarbene have the weakest X→p(π) π-donation while mesoionic carbenes possess the strongest π-donation to the carbene centre. There is a reasonable correlation between the occupation of the p(π) AO at the C_{carb} atom and the energy which is associated with the X→p(π) π-donation.

Supporting Information

Supporting Information File 1

Additional information.
[http://www.beilstein-journals.org/bjoc/content/supplementary/1860-5397-11-294-S1.pdf]

Acknowledgements

This work was financially supported by the Deutsche Forschungsgemeinschaft. DMA acknowledges a postdoctoral fellowship from the DAAD (Deutscher Akademischer Austauschdienst).

References

1. Arduengo, A. J., III; Harlow, R. L.; Kline, M. *J. Am. Chem. Soc.* **1991,** *113,* 361. doi:10.1021/ja00001a054

2. Bourissou, D.; Guerret, O.; Gabbaï, F. P.; Bertrand, G. *Chem. Rev.* **2000,** *100,* 39. doi:10.1021/cr940472u
3. Schuster, O.; Yang, L.; Raubenheimer, H. G.; Albrecht, M. *Chem. Rev.* **2009,** *109,* 3445. doi:10.1021/cr8005087
4. Hopkinson, M. N.; Richter, C.; Schedler, M.; Glorius, F. *Nature* **2014,** *510,* 485. doi:10.1038/nature13384
5. Benhamou, L.; Chardon, E.; Lavigne, G.; Bellemin-Laponnaz, S.; César, V. *Chem. Rev.* **2011,** *111,* 2705. doi:10.1021/cr100328e
6. Martin, D.; Melaimi, M.; Soleilhavoup, M.; Bertrand, G. *Organometallics* **2011,** *30,* 5304. doi:10.1021/om200650x
7. Melaimi, M.; Soleilhavoup, M.; Bertrand, G. *Angew. Chem., Int. Ed.* **2010,** *49,* 8810. doi:10.1002/anie.201000165
8. Canac, Y.; Soleilhavoup, M.; Conejero, S.; Bertrand, G. *J. Organomet. Chem.* **2004,** *689,* 3857. doi:10.1016/j.jorganchem.2004.02.005
9. Díez-González, S.; Marion, N.; Nolan, S. P. *Chem. Rev.* **2009,** *109,* 3612. doi:10.1021/cr900074m
10. Levin, E.; Ivry, E.; Diesendruck, C. E.; Lemcoff, N. G. *Chem. Rev.* **2015,** *115,* 4607. doi:10.1021/cr400640e
11. Schaper, L.-A.; Hock, S. J.; Herrmann, W. A.; Kühn, F. E. *Angew. Chem., Int. Ed.* **2013,** *52,* 270. doi:10.1002/anie.201205119
12. Izquierdo, J.; Hutson, G. E.; Cohen, D. T.; Scheidt, K. A. *Angew. Chem., Int. Ed.* **2012,** *51,* 11686. doi:10.1002/anie.201203704
13. Radius, U.; Bickelhaupt, F. M. *Coord. Chem. Rev.* **2009,** *253,* 678. doi:10.1016/j.ccr.2008.05.020
14. Fèvre, M.; Pinaud, J.; Gnanou, Y.; Vignolle, J.; Taton, D. *Chem. Soc. Rev.* **2013,** *42,* 2142. doi:10.1039/c2cs35383k
15. Enders, D.; Niemeier, O.; Henseler, A. *Chem. Rev.* **2007,** *107,* 5606. doi:10.1021/cr068372z
16. Marion, N.; Díez-González, S.; Nolan, S. P. *Angew. Chem., Int. Ed.* **2007,** *46,* 2988. doi:10.1002/anie.200603380
17. Hahn, F. E.; Jahnke, M. C. *Angew. Chem., Int. Ed.* **2008,** *47,* 3122. doi:10.1002/anie.200703883
18. Zhang, D.; Zi, G. *Chem. Soc. Rev.* **2015,** *44,* 1898. doi:10.1039/C4CS00441H
19. Nelson, D. J. *Eur. J. Inorg. Chem.* **2015,** 2012. doi:10.1002/ejic.201500061
20. Soleilhavoup, M.; Bertrand, G. *Acc. Chem. Res.* **2015,** *48,* 256. doi:10.1021/ar5003494
21. Wang, Y.; Robinson, G. H. *Inorg. Chem.* **2014,** *53,* 11815. doi:10.1021/ic502231m
22. Wilson, D. J. D.; Dutton, J. L. *Chem. – Eur. J.* **2013,** *19,* 13626. doi:10.1002/chem.201302715
23. Wang, Y.; Robinson, G. H. *Dalton Trans.* **2012,** *41,* 337. doi:10.1039/C1DT11165E
24. Wang, Y.; Robinson, G. H. *Inorg. Chem.* **2011,** *50,* 12326. doi:10.1021/ic200675u
25. Rivard, E. *Dalton Trans.* **2014,** *43,* 8577. doi:10.1039/c4dt00481g
26. Martin, C. D.; Soleilhavoup, M.; Bertrand, G. *Chem. Sci.* **2013,** *4,* 3020. doi:10.1039/c3sc51174j
27. Martin, D.; Soleilhavoup, M.; Bertrand, G. *Chem. Sci.* **2011,** *2,* 389. doi:10.1039/C0SC00388C
28. Power, P. P. *Nature* **2010,** *463,* 171. doi:10.1038/nature08634
29. de Frémont, P.; Marion, N.; Nolan, S. P. *Coord. Chem. Rev.* **2009,** *253,* 862. doi:10.1016/j.ccr.2008.05.018
30. Regitz, M. *Angew. Chem., Int. Ed. Engl.* **1991,** *30,* 674. doi:10.1002/anie.199106741
31. Arduengo, A. J., III; Rasika Dias, H. V.; Harlow, R. L.; Kline, M. *J. Am. Chem. Soc.* **1992,** *114,* 5530. doi:10.1021/ja00040a007
32. Arduengo, A. J., III. *Acc. Chem. Res.* **1999,** *32,* 913. doi:10.1021/ar980126p
33. Herrmann, W. A. *Angew. Chem., Int. Ed.* **2002,** *41,* 1290. doi:10.1002/1521-3773(20020415)41:8<1290::AID-ANIE1290>3.0.CO;2-Y
34. Jacobsen, H.; Correa, A.; Poater, A.; Costabile, C.; Cavallo, L. *Coord. Chem. Rev.* **2009,** *253,* 687. doi:10.1016/j.ccr.2008.06.006
35. Jacobsen, H.; Correa, A.; Costabile, C.; Cavallo, L. *J. Organomet. Chem.* **2006,** *691,* 4350. doi:10.1016/j.jorganchem.2006.01.026
36. Nemcsok, D.; Wichmann, K.; Frenking, G. *Organometallics* **2004,** *23,* 3640. doi:10.1021/om049802j
37. Tonner, R.; Heydenrych, G.; Frenking, G. *Chem. – Asian J.* **2007,** *2,* 1555. doi:10.1002/asia.200700235
38. Hahn, F. E.; Zabula, A. V.; Pape, T.; Hepp, A.; Tonner, R.; Haunschild, R.; Frenking, G. *Chem. – Eur. J.* **2008,** *14,* 10716. doi:10.1002/chem.200801128
39. Scarborough, C. C.; Grady, M. J. W.; Guzei, I. A.; Gandhi, B. A.; Bunel, E. E.; Stahl, S. S. *Angew. Chem., Int. Ed.* **2005,** *44,* 5269. doi:10.1002/anie.200501522
40. Iglesias, M.; Beetstra, D. J.; Kariuki, B.; Cavell, K. J.; Dervisi, A.; Fallis, I. A. *Eur. J. Inorg. Chem.* **2009,** 1913. doi:10.1002/ejic.200801179
41. Lu, W. Y.; Cavell, K. J.; Wixey, J. S.; Kariuki, B. *Organometallics* **2011,** *30,* 5649. doi:10.1021/om200467x
42. Martin, D.; Lassauque, N.; Donnadieu, B.; Bertrand, G. *Angew. Chem., Int. Ed.* **2012,** *51,* 6172. doi:10.1002/anie.201202137
43. Martin, D.; Lassauque, N.; Steinmann, F.; Manuel, G.; Bertrand, G. *Chem. – Eur. J.* **2013,** *19,* 14895. doi:10.1002/chem.201302474
44. Lavallo, V.; Dyker, C. A.; Donnadieu, B.; Bertrand, G. *Angew. Chem., Int. Ed.* **2008,** *47,* 5411. doi:10.1002/anie.200801176
45. Fernández, I.; Dyker, C. A.; DeHope, A.; Donnadieu, B.; Frenking, G.; Bertrand, G. *J. Am. Chem. Soc.* **2009,** *131,* 11875. doi:10.1021/ja903396e
46. Aldeco-Perez, E.; Rosenthal, A. J.; Donnadieu, B.; Parameswaran, P.; Frenking, G.; Bertrand, G. *Science* **2009,** *326,* 556. doi:10.1126/science.1178206
47. Guisado-Barrios, G.; Bouffard, J.; Donnadieu, B.; Bertrand, G. *Angew. Chem., Int. Ed.* **2010,** *49,* 4759. doi:10.1002/anie.201001864
48. Borthakur, B.; Phukan, A. K. *Chem. – Eur. J.* **2015,** *21,* 11603–11609. doi:10.1002/chem.201500860
49. Nakafuji, S.-y.; Kobayashi, J.; Kawashima, T. *Angew. Chem., Int. Ed.* **2008,** *47,* 1141. doi:10.1002/anie.200704746
50. Asay, M.; Donnadieu, B.; Baceiredo, A.; Soleilhavoup, M.; Bertrand, G. *Inorg. Chem.* **2008,** *47,* 3949. doi:10.1021/ic800459p
51. Fürstner, A.; Alcarazo, M.; Radkowski, K.; Lehmann, C. W. *Angew. Chem., Int. Ed.* **2008,** *47,* 8302. doi:10.1002/anie.200803200
52. Hudnall, T. W.; Bielawski, C. W. *J. Am. Chem. Soc.* **2009,** *131,* 16039. doi:10.1021/ja907481w
53. Hudnall, T. W.; Tennyson, A. G.; Bielawski, C. W. *Organometallics* **2010,** *29,* 4569. doi:10.1021/om1007665
54. César, V.; Lugan, N.; Lavigne, G. *Chem. – Eur. J.* **2010,** *16,* 11432. doi:10.1002/chem.201000870
55. Braun, M.; Frank, W.; Reiss, G. J.; Ganter, C. *Organometallics* **2010,** *29,* 4418. doi:10.1021/om100728n
56. Lavallo, V.; Canac, Y.; Präsang, C.; Donnadieu, B.; Bertrand, G. *Angew. Chem., Int. Ed.* **2005,** *44,* 5705. doi:10.1002/anie.200501841
57. Jazzar, R.; Dewhurst, R. D.; Bourg, J.-B.; Donnadieu, B.; Canac, Y.; Bertrand, G. *Angew. Chem., Int. Ed.* **2007,** *46,* 2899. doi:10.1002/anie.200605083

58. Díez-González, S.; Nolan, S. P. *Coord. Chem. Rev.* **2007,** *251,* 874. doi:10.1016/j.ccr.2006.10.004
59. Curran, D. P.; Solovyev, A.; Makhlouf Brahmi, M.; Fensterbank, L.; Malacria, M.; Lacôte, E. *Angew. Chem., Int. Ed.* **2011,** *50,* 10294. doi:10.1002/anie.201102717
60. Frenking, G.; Tonner, R.; Klein, S.; Takagi, N.; Shimizu, T.; Krapp, A.; Pandey, K. K.; Parameswaran, P. *Chem. Soc. Rev.* **2014,** *43,* 5106. doi:10.1039/C4CS00073K
61. Dröge, T.; Glorius, F. *Angew. Chem., Int. Ed.* **2010,** *49,* 6940. doi:10.1002/anie.201001865
62. Nelson, D. J.; Nolan, S. P. *Chem. Soc. Rev.* **2013,** *42,* 6723. doi:10.1039/c3cs60146c
63. Fantasia, S.; Petersen, J. L.; Jacobsen, H.; Cavallo, L.; Nolan, S. P. *Organometallics* **2007,** *26,* 5880. doi:10.1021/om700857j
64. Back, O.; Henry-Ellinger, M.; Martin, C. D.; Martin, D.; Bertrand, G. *Angew. Chem., Int. Ed.* **2013,** *52,* 2939. doi:10.1002/anie.201209109
65. Liske, A.; Verlinden, K.; Buhl, H.; Schaper, K.; Ganter, C. *Organometallics* **2013,** *32,* 5269. doi:10.1021/om400858y
66. Vummaleti, S. V. C.; Nelson, D. J.; Poater, A.; Gómez-Suárez, A.; Cordes, D. B.; Slawin, A. M. Z.; Nolan, S. P.; Cavallo, L. *Chem. Sci.* **2015,** *6,* 1895. doi:10.1039/C4SC03264K
67. Alcarazo, M.; Stork, T.; Anoop, A.; Thiel, W.; Fürstner, A. *Angew. Chem., Int. Ed.* **2010,** *49,* 2542. doi:10.1002/anie.200907194
68. Tukov, A. A.; Normand, A. T.; Nechaev, M. S. *Dalton Trans.* **2009,** 7015. doi:10.1039/b906969k
69. Bernhammer, J. C.; Frison, G.; Huynh, H. V. *Chem. – Eur. J.* **2013,** *19,* 12892. doi:10.1002/chem.201301093
70. Huynh, H. V.; Frison, G. *J. Org. Chem.* **2013,** *78,* 328. doi:10.1021/jo302080c
71. Comas-Vives, A.; Harvey, J. N. *Eur. J. Inorg. Chem.* **2011,** 5025. doi:10.1002/ejic.201100721
72. Rezabal, E.; Frison, G. *J. Comput. Chem.* **2015,** *36,* 564. doi:10.1002/jcc.23852
73. Crabtree, R. H. *Coord. Chem. Rev.* **2013,** *257,* 755. doi:10.1016/j.ccr.2012.09.006
74. Becke, A. D. *Phys. Rev. A* **1988,** *38,* 3098. doi:10.1103/PhysRevA.38.3098
75. Perdew, J. P. *Phys. Rev. B* **1986,** *33,* 8822. doi:10.1103/PhysRevB.33.8822
76. Weigend, F.; Ahlrichs, R. *Phys. Chem. Chem. Phys.* **2005,** *7,* 3297. doi:10.1039/b508541a
77. Peng, C.; Ayala, P. Y.; Schlegel, H. B.; Frisch, M. J. *J. Comput. Chem.* **1996,** *17,* 49. doi:10.1002/(SICI)1096-987X(19960115)17:1<49::AID-JCC5>3.0.CO;2-0
78. McIver, J. W., Jr.; Komornicki, A. *J. Am. Chem. Soc.* **1972,** *94,* 2625. doi:10.1021/ja00763a011
79. *Gaussian 09,* Revision C.01; Gaussian, Inc.: Wallingford, CT, 2009.
80. Wiberg, K. B. *Tetrahedron* **1968,** *24,* 1083. doi:10.1016/0040-4020(68)88057-3
81. Reed, A. E.; Weinstock, R. B.; Weinhold, F. *J. Chem. Phys.* **1985,** *83,* 735. doi:10.1063/1.449486
82. Reed, A. E.; Curtiss, L. A.; Weinhold, F. *Chem. Rev.* **1988,** *88,* 899. doi:10.1021/cr00088a005
83. *GENNBO,* 5.9; Theoretical Chemistry Institute, University of Wisconsin: Madison, WI, 2009.
84. Van Lenthe, E.; Baerends, E. J. *J. Comput. Chem.* **2003,** *24,* 1142. doi:10.1002/jcc.10255
85. Krijn, J.; Baerends, E. J. *Fit Functions in the HFS-Method*; 1984.
86. Van Lenthe, E.; Baerends, E. J.; Snijders, J. G. *J. Chem. Phys.* **1993,** *99,* 4597. doi:10.1063/1.466059
87. te Velde, G.; Bickelhaupt, F. M.; Baerends, E. J.; Fonseca Guerra, C.; van Gisbergen, S. J. A.; Snijders, J. G.; Ziegler, T. *J. Comput. Chem.* **2001,** *22,* 931. doi:10.1002/jcc.1056
88. Morokuma, K. *J. Chem. Phys.* **1971,** *55,* 1236. doi:10.1063/1.1676210
89. Ziegler, T.; Rauk, A. *Inorg. Chem.* **1979,** *18,* 1755. doi:10.1021/ic50197a006
90. Ziegler, T.; Rauk, A. *Inorg. Chem.* **1979,** *18,* 1558. doi:10.1021/ic50196a034
91. Bickelhaupt, F. M.; Nibbering, N. M. M.; Van Wezenbeek, E. M.; Baerends, E. J. *J. Phys. Chem.* **1992,** *96,* 4864. doi:10.1021/j100191a027
92. Frenking, G.; Wichmann, K.; Fröhlich, N.; Loschen, C.; Lein, M.; Frunzke, J.; Rayón, V. M. *Coord. Chem. Rev.* **2003,** *238–239,* 55. doi:10.1016/S0010-8545(02)00285-0
93. Krapp, A.; Bickelhaupt, F. M.; Frenking, G. *Chem. – Eur. J.* **2006,** *12,* 9196. doi:10.1002/chem.200600564
94. Kovács, A.; Esterhuysen, C.; Frenking, G. *Chem. – Eur. J.* **2005,** *11,* 1813. doi:10.1002/chem.200400525
95. Mitoraj, M. P.; Michalak, A.; Ziegler, T. *J. Chem. Theory Comput.* **2009,** *5,* 962. doi:10.1021/ct800503d
96. Mitoraj, M.; Michalak, A. *Organometallics* **2007,** *26,* 6576. doi:10.1021/om700754n
97. Michalak, A.; Mitoraj, M.; Ziegler, T. *J. Phys. Chem. A* **2008,** *112,* 1933. doi:10.1021/jp075460u
98. Mitoraj, M.; Michalak, A. *J. Mol. Model.* **2008,** *14,* 681. doi:10.1007/s00894-008-0276-1
99. Hahn, F. E.; Wittenbecher, L.; Boese, R.; Bläser, D. *Chem. – Eur. J.* **1999,** *5,* 1931. doi:10.1002/(SICI)1521-3765(19990604)5:6<1931::AID-CHEM1931>3.0.CO;2-M
100. Arduengo, A. J., III; Goerlich, J. R.; Marshall, W. J. *J. Am. Chem. Soc.* **1995,** *117,* 11027. doi:10.1021/ja00149a034
101. Alder, R. W.; Allen, P. R.; Murray, M.; Orpen, A. G. *Angew. Chem., Int. Ed. Engl.* **1996,** *35,* 1121. doi:10.1002/anie.199611211
102. Korotkikh, N. I.; Rayenko, G. F.; Shvaika, O. P.; Pekhtereva, T. M.; Cowley, A. H.; Jones, J. N.; Macdonald, C. L. B. *J. Org. Chem.* **2003,** *68,* 5762. doi:10.1021/jo034234n
103. Arduengo, A. J., III; Goerlich, J. R.; Marshall, W. J. *Liebigs Ann./Recl.* **1997,** 365. doi:10.1002/jlac.199719970213
104. Pyykkö, P.; Atsumi, M. *Chem. – Eur. J.* **2009,** *15,* 186. doi:10.1002/chem.200800987
105. Heinemann, C.; Müller, T.; Apeloig, Y.; Schwarz, H. *J. Am. Chem. Soc.* **1996,** *118,* 2023. doi:10.1021/ja9523294
106. Tuononen, H. M.; Roesler, R.; Dutton, J. L.; Ragogna, P. J. *Inorg. Chem.* **2007,** *46,* 10693. doi:10.1021/ic701350e
107. Boehme, C.; Frenking, G. *J. Am. Chem. Soc.* **1996,** *118,* 2039. doi:10.1021/ja9527075
108. Mondal, K. C.; Roesky, H. W.; Schwarzer, M. C.; Frenking, G.; Niepötter, B.; Wolf, H.; Herbst-Irmer, R.; Stalke, D. *Angew. Chem., Int. Ed.* **2013,** *52,* 2963. doi:10.1002/anie.201208307
109. Mondal, K. C.; Roesky, H. W.; Schwarzer, M. C.; Frenking, G.; Tkach, I.; Wolf, H.; Kratzert, D.; Herbst-Irmer, R.; Niepötter, B.; Stalke, D. *Angew. Chem., Int. Ed.* **2013,** *52,* 1801. doi:10.1002/anie.201204487
110. Singh, A. P.; Samuel, P. P.; Roesky, H. W.; Schwarzer, M. C.; Frenking, G.; Sidhu, N. S.; Dittrich, B. *J. Am. Chem. Soc.* **2013,** *135,* 7324. doi:10.1021/ja402351x

111. Weinberger, D. S.; Melaimi, M.; Moore, C. E.; Rheingold, A. L.; Frenking, G.; Jerabek, P.; Bertrand, G. *Angew. Chem., Int. Ed.* **2013,** *52,* 8964. doi:10.1002/anie.201304820
112. Samuel, P. P.; Mondal, K. C.; Roesky, H. W.; Hermann, M.; Frenking, G.; Demeshko, S.; Meyer, F.; Stückl, A. C.; Christian, J. H.; Dalal, N. S.; Ungur, L.; Chibotaru, L. F.; Pröpper, K.; Meents, A.; Dittrich, B. *Angew. Chem., Int. Ed.* **2013,** *52,* 11817. doi:10.1002/anie.201304642
113. Mondal, K. C.; Samuel, P. P.; Roesky, H. W.; Carl, E.; Herbst-Irmer, R.; Stalke, D.; Schwederski, B.; Kaim, W.; Ungur, L.; Chibotaru, L. F.; Hermann, M.; Frenking, G. *J. Am. Chem. Soc.* **2014,** *136,* 1770. doi:10.1021/ja4123285
114. Weinberger, D. S.; Amin Sk, N.; Mondal, K. C.; Melaimi, M.; Bertrand, G.; Stückl, A. C.; Roesky, H. W.; Dittrich, B.; Demeshko, S.; Schwederski, B.; Kaim, W.; Jerabek, P.; Frenking, G. *J. Am. Chem. Soc.* **2014,** *136,* 6235. doi:10.1021/ja502521b
115. Mondal, K. C.; Samuel, P. P.; Roesky, H. W.; Aysin, R. R.; Leites, L. A.; Neudeck, S.; Lübben, J.; Dittrich, B.; Holzmann, N.; Hermann, M.; Frenking, G. *J. Am. Chem. Soc.* **2014,** *136,* 8919. doi:10.1021/ja504821u
116. Roy, S.; Mondal, K. C.; Meyer, J.; Niepötter, B.; Köhler, C.; Herbst-Irmer, R.; Stalke, D.; Dittrich, B.; Andrada, D. M.; Frenking, G.; Roesky, H. W. *Chem. – Eur. J.* **2015,** *21,* 9312. doi:10.1002/chem.201500758
117. Roy, S.; Stollberg, P.; Herbst-Irmer, R.; Stalke, D.; Andrada, D. M.; Frenking, G.; Roesky, H. W. *J. Am. Chem. Soc.* **2015,** *137,* 150. doi:10.1021/ja512089e
118. The molecules **4**, **5** and **9** were calculated for technical reasons with enforce C_s symmetry in order to align the single occupied orbitals in the right way. The energy differences to the fully optimized structures are negligible and thus, the results for the structures with C_s symmetry can be used for the bonding analysis of the equilibrium structures.
119. Esterhuysen, C.; Frenking, G. *Theor. Chem. Acc.* **2004,** *111,* 381. doi:10.1007/s00214-003-0535-2
120. Frenking, G.; Wichmann, K.; Fröhlich, N.; Grobe, J.; Golla, W.; Le Van, D.; Krebs, B.; Läge, M. *Organometallics* **2002,** *21,* 2921. doi:10.1021/om020311d

License and Terms

BEILSTEIN JOURNAL OF ORGANIC CHEMISTRY

New metathesis catalyst bearing chromanyl moieties at the N-heterocyclic carbene ligand

Agnieszka Hryniewicka*, Szymon Suchodolski, Agnieszka Wojtkielewicz, Jacek W. Morzycki and Stanisław Witkowski*

Full Research Paper

Open Access

Address:
University of Białystok, Institute of Chemistry, Ciołkowskiego Street 1K, 15-245 Białystok; Poland

Email:
Agnieszka Hryniewicka* - aga_h@uwb.edu.pl; Stanisław Witkowski* - wit@uwb.edu.pl

* Corresponding author

Keywords:
chromane derivatives; metathesis catalyst; nitrogen heterocycles; olefin metathesis; Ru-carbene

Beilstein J. Org. Chem. **2015,** *11,* 2795–2804.
doi:10.3762/bjoc.11.300

Received: 21 October 2015
Accepted: 09 December 2015
Published: 30 December 2015

This article is part of the Thematic Series "N-Heterocyclic carbenes".

Guest Editor: S. P. Nolan

Abstract

The synthesis of a new type of Hoveyda–Grubbs 2nd generation catalyst bearing a modified N-heterocyclic carbene ligands is reported. The new catalyst contains an NHC ligand symmetrically substituted with chromanyl moieties. The complex was tested in model CM and RCM reactions. It showed very high activity in CM reactions with electron-deficient α,β-unsaturated compounds even at 0 °C. It was also examined in more demanding systems such as conjugated dienes and polyenes. The catalyst is stable, storable and easy to purify.

Introduction

Olefin metathesis is still one of the most intensively studied transformations in synthetic organic chemistry. It has been frequently used as a key bond-forming reaction for total syntheses of many natural products [1]. The study on designing new metathesis catalysts and their synthesis has been a very fast developing area of organic chemistry since 1992, when Grubbs discovered the first well-defined ruthenium catalyst [2]. Nearly 400 ruthenium heterocyclic carbene-coordinated olefin metathesis catalysts were prepared until 2010 [3]. Since 2011, when Grubbs reported the synthesis of a *Z*-selective catalyst [4], several modified stereoselective catalysts were described [5-8]. Over the last few years, considerable attention has also been paid to immobilisation and tagging of catalysts and especially on making them more environmentally friendly [9-14].

Alkene cross-metathesis (CM) is a convenient route to the synthesis of functionalised olefins from simple precursors. Since the discovery of Grubbs 2nd generation catalyst (**1**, Figure 1) [15], Hoveyda–Grubbs 2nd generation catalyst (**2**, Figure 1) [16] and some successful modifications, e.g., nitro-Grela catalyst (**3**, Figure 1) [17] the utility of CM has been continuously expanded. The synthesis of complex structures bearing polar functional groups can be accomplished by CM [18]. Grubbs et al. recognised that CM can be selective when two partners

showing different reactivity are used, e.g., reactive terminal olefin (type I) and an electron-deficient olefin (e.g., acrylates or acrylonitriles, type II or III). In these cases, full conversion and high yields can be achieved [18]. Although the problem with the CM reactions of olefins with electron-withdrawing groups, such as α,β-unsaturated ketones and esters, is partly solved [19,20], the conditions of the reactions need some improvement (lower catalyst loading, lower temperature). To the best of our knowledge, there is no such type of reaction performed at 0 °C. A lower temperature of the reaction is important in the synthesis of unstable and thermally-sensitive natural products.

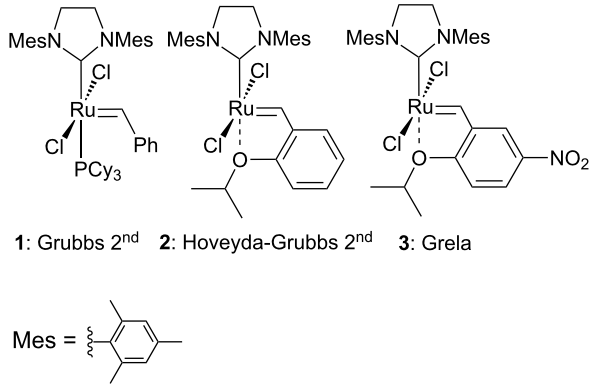

Figure 1: Examples of olefin metathesis ruthenium catalysts.

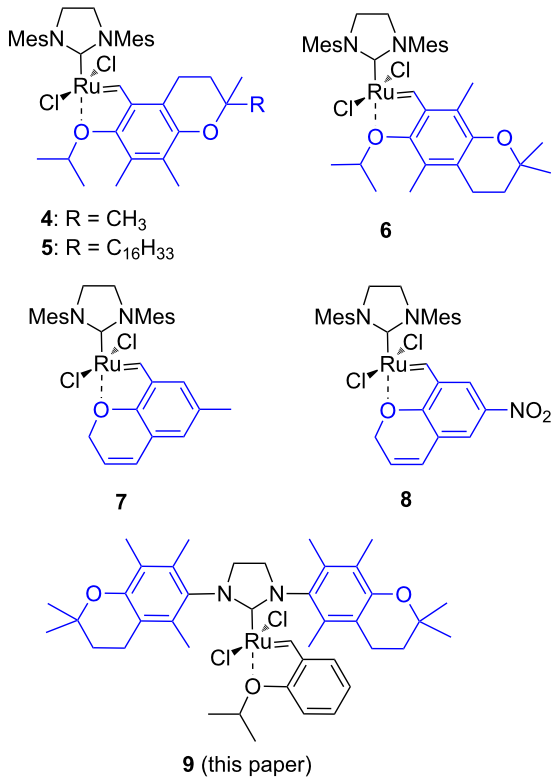

Figure 2: Selected ruthenium metathesis catalyst bearing chromanyl moieties.

We previously reported a few catalysts bearing the chromanyl moiety, derived from vitamin E [21-23]. In such a system as 2,2,5,7,8-pentamethyl-6-hydroxychromane (α-tocopherol model compound) specific stereoelectronic effects are observed [24,25], which might improve the activity of the catalyst bearing the above-mentioned moieties. The ruthenium complexes **4**–**6** (Figure 2) that we reported earlier appeared to be the so-called dormant catalysts. Their activity in RCM reactions was low at room temperature and higher at elevated temperature [21]. In catalyst **7** the chelating oxygen atom was provided by the rigid heterocyclic ring of the chromenylmethylidene moiety, whereas in the Hoveyda–Grubbs 2nd generation catalyst, the complexing oxygen atom comes from the freely rotating isopropoxy substituent. This complex proved to be quite efficient and showed activity comparable to that of commercially available catalysts **1** and **2** [23]. The introduction of a nitro group into the 6-position of the chromene moiety in catalyst **8** led to a decrease in the stability of the complex [22].

The aforementioned modifications concerned the benzylidene moiety of the catalysts and affected the initiation rate of the metathesis reaction. Changes in the NHC ligand are also very important because this part of the catalyst participates all along the metathetic process. As a result, the catalyst may gain new properties, increased activity or stereoselectivity. Following this idea, we decided to synthesise a new catalyst bearing two chromanyl moieties symmetrically N,N'-disubstituted in the imidazolinium ring (**9**, Figure 2). According to Smith et al. [26] α-tocopherol and its amino analogue (α-tocopheramine) have comparable properties, coming from the same stereoelectronic effects mentioned above [24,25]. We expected that these effects may confer new properties of the NHC ligand.

Results and Discussion

Synthesis of the carbene precursor

The synthesis of an imidazolinium salt as a carbene precursor was started from 2,2,5,7,8-pentamethylchromane (**10**), which was prepared by the reaction between 2,3,5-trimethylphenol and 3-methylbut-2-enol [27]. Chromane **10** was nitrated with fuming nitric acid to give 6-nitrochromane **11** in 58% yield according to Mahdavian [28] (Scheme 1). Nitration using the Smith procedure [29] led to the expected nitrochromane **11**, however, formation of an admixture of 5a,6-dinitrochromane was observed. Reduction of the nitro group in **11** was slightly troublesome, probably due to steric hindrance. The tellurium-rongalit system was found to be the most efficient [30], and 6-chromanylamine **12** was obtained in 50% yield. Imidazolinium salt **14** was prepared according to the classical

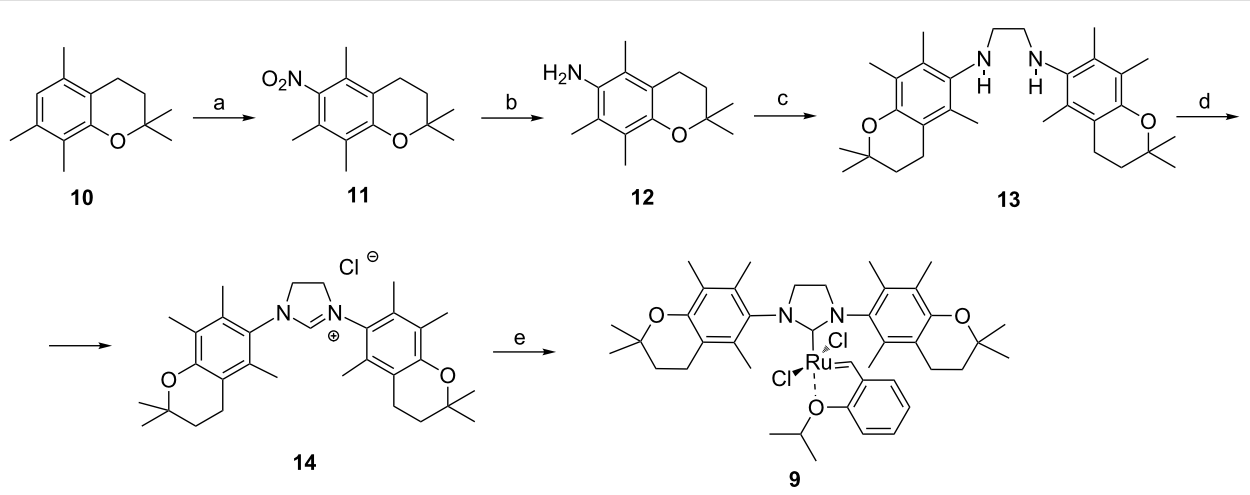

Scheme 1: Synthesis of the new NHC precursor. Reagents and conditions: a) HNO_3, CH_2Cl_2, 0 °C, 58%; b) $HOCH_2SOONa$, Te, NaOH, dioxane, 50 °C, 50%; c) 2,3-dihydroxy-1,4-dioxane, EtOH, HCOOH, rt, then $NaBH_3CN$, rt, 90%; d) NH_4Cl, $HC(OMe)_3$, reflux, 73%; e) I) *t*-AmOK, toluene, rt; II) Hoveyda–Grubbs 1st generation, toluene, 65 °C, 68%.

protocol. Chromanylamine **12** was subjected to reaction with 2,3-dihydroxy-1,4-dioxane (glyoxal equivalent) followed by reduction of the intermediate diimines by $NaBH_3CN$ to give ethylenediamine **13** in 90% yield. Usage of the more convenient sodium borohydride led to a prolonged reaction time (up to 20 h) and a lower reaction yield. Imidazolinium salt **14** was obtained by treatment of **13** with trimethyl orthoformate in 73% yield. It is worth noting that ethylenediamine **13** and imidazolinium salt **14** were sufficiently pure after precipitation, thus chromatographic purification was not necessary.

Some specific effects are observed in the NMR spectra of salt **14**. In the ^{1}H NMR spectrum, the signals from protons of the imidazolinium ring have atypical multiplicity. Two neighbouring triplets are also present besides the expected singlet from the ethylene bridge between the two nitrogen atoms symmetrically substituted by two identical chromenyl moieties. Similarly, the C-2 protons give two singlets instead of one. We suspected that there is a hindered rotation on the *N*–$C_{(chromenyl)}$ bond, so that two conformers are observed by NMR. However, the ^{1}H NMR spectrum recorded at elevated temperatures (30 and 50 °C) looked the same. In the ^{13}C NMR spectrum, signals from some of the carbon atoms are doubled. The HSQC correlation confirms that the doubled signals derive from one carbon atom. This fact also may suggest that two conformers are observed in the NMR spectra. This issue will be the subject of future detailed investigations.

Synthesis of the catalyst

The new catalyst, **9**, was obtained from imidazolinium salt **14** by deprotonation with potassium *tert*-amylate followed by the tricyclohexylphosphine ligand exchange in Hoveyda–Grubbs 1st generation catalyst to give the target catalyst **9**, which was purified on silica gel. The complex was stable in solid state at 0 °C for a few weeks (NMR test).

Attempts to obtain a monocrystal that would be suitable for X-ray analysis failed. The ^{1}H NMR spectrum confirmed the structure of the catalyst. In the ^{13}C NMR spectrum, some signals were broad and weak, e.g., signals of the quaternary aromatic carbon atoms and the primary carbon atoms of the methyl group attached to the aromatic ring of the chromanyl moieties. The HSQC correlation confirmed the structure of the catalyst and showed good correlation of the attached proton signals with the weak carbon peaks. When the ^{13}C NMR spectrum is recorded at 50 °C, the spectrum becomes simpler but still many signals are almost invisible (at the noise level). The mass spectrum (HRMS) of **9** clearly evidences the molecular weight and the elemental composition of the new catalyst. The most likely unusual NMR spectra of **9** can result from specific stereoelectronic effects observed in the chromanyl system [24,25]. The 2p-type lone pair of electrons of the heterocyclic ring oxygen atom adopts an orientation almost perpendicular to the plane of the aromatic ring allowing for an electronic interaction with the *para*-substituent of the chromanyl system (–OH in 6-hydroxychroman and $–NH_2$ in 6-aminochroman).

Testing of the new catalyst

The catalyst proved very active in model cross-metathesis reactions, especially with olefins containing electron-withdrawing groups. For example the reaction of allylbenzene and ethyl acrylate at room temperature was almost quantitative. These results prompted us to test this reaction at a lower temperature (0 °C). Commercially available catalysts **1** and **2** proved inac-

tive under these conditions, therefore we compared our catalyst with Grela catalyst **3** [17]. As is shown in Table 1 (entry 1), both catalysts, i.e., **3** and **9** proved very active. After reduction of the catalyst loading to 1 mol %, the yields of the ethyl acrylate reaction with allylbenzene catalysed by both complexes **3** and **9** were still very good (close to 80%, Table 1, entry 2). Encouraged by these results, we decided to test **9** in a CM reaction with other α,β-unsaturated compounds, e.g., methyl vinyl ketone (entry 3, Table 1) and acrylonitrile (entry 4, Table 1). The outcome of these reactions was also very promising for **9**. It should be added that in all cases a dimer of the electron-deficient olefin was not observed. The homodimerisation product of allylbenzene (entries 1 and 2, Table 1) was formed in less than 10% (in case of the reaction catalysed by **2** no dimeric products were observed), while the yield of the homodimer of hex-5-enyl acetate (entries 3 and 4, Table 1) was below 3%. Low conversion (especially that obtained with **1** and **2**) was related to substantial amounts of unreacted substrates.

The high activity of Grela catalyst **3** was a result of faster initiation of the catalytic cycle arising from the electron-withdrawing effect of the nitro group. Consequently, lowered electron density at the oxygen atom in the isopropoxybenzylidene fragment weakens the coordination to the ruthenium atom, and finally, facilitates the initiating process. In the new catalyst **9**, which is modified in the NHC ligand, different effects are responsible for its activity. According to Grubbs [31], catalyst **1** is able to react with α,β-unsaturated carbonyl compounds to form an enoic carbene [Ru]=CHCOX, which is kinetically favourable. As a result, a stronger electron-donating ligand should stabilise the electron-deficient enoic carbene [31]. One can speculate that specific stereoelectronic effects occurring in the chromanyl system, known from the vitamin E chemistry, contribute to high activity of **9**. The *N*-(2,2,5,7,8-pentamethyl-6-chromanyl) substituents, bearing electron releasing methyl groups as well as interplaying dihydropyranyl oxygen and nitrogen atoms in the imidazolidine cycle, can stabilise the enoic carbene (Scheme 2).

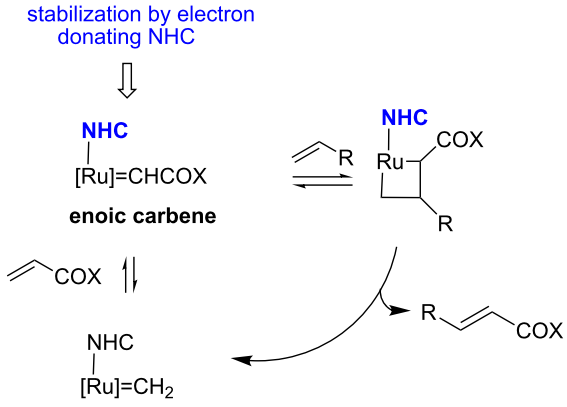

Scheme 2: CM with electron-deficient olefin.

The CM products of terminal olefins (entries 1–3, Table 2) were obtained in high and very high yields. Alkenes were converted almost quantitatively and the excess of (*Z*)-but-2-ene-1,4-diol diacetate was recovered. Some side products of self-metathesis (SM) of terminal alkenes were isolated. It should be added that two terminal olefins (entry 4, Table 2) gave also SM products besides the desired CM products. Furthermore, more dimeric products gave allyloxybenzene than hex-5-enyl acetate. It is worth noting that the CM reaction between styrene and (*Z*)-but-

Table 1: Comparative investigation of catalysts in CM reactions with electron-deficient olefins.

Entry	Alkene	Electron-deficient olefin	Product	Conditions[b]	Catalyst	Yield (*E*/*Z*)[c]
1	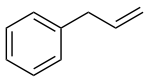	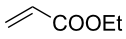	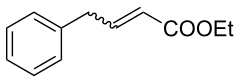	0 °C, 3 h, CH_2Cl_2 2.5 mol % [Ru]	**1** **2** **3** **9**	11% (*E*/*Z* 100:1) 13% (*E*/*Z* 32:1) 87% (*E*/*Z* 29:1) 91% (*E*/*Z* 23:1)
2	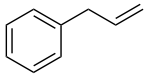	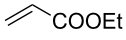	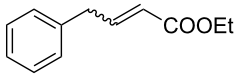	0 °C, 3 h, CH_2Cl_2 1 mol % [Ru]	**3** **9**	77% 76%
3	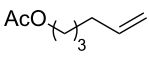		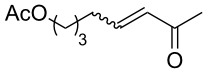	0 °C, 3 h, CH_2Cl_2 1 mol % [Ru]	**1** **2** **3** **9**	0% 38% (only *E*) 98% (only *E*) 99% (only *E*)
4	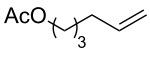		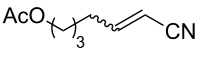	0 °C, 1 h, CH_2Cl_2 1 mol % [Ru]	**1** **2** **3** **9**	0% 59% (*E*/*Z* 2.5:1) 75% (*E*/*Z* 3:1) 97% (*E*/*Z* 2.5:1)

[a]Electron-deficient olefin was used in excess (2 equiv). [b]Concentration of alkene amounted 0.1 M. [c]Determined by ^{1}H NMR.

Table 2: Comparative investigation of the catalysts' performance in CM reactions.

Entry	Substrates	Product	Catalyst	Yield (*E*/*Z*)[a]
1[b]	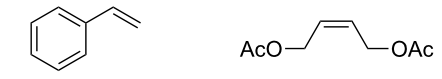	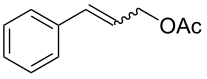	**1** **2** **9**	81% (*E*/*Z* 58:1) 80% (*E*/*Z* 43:1) 97% (*E*/*Z* 42:1)
2[b]	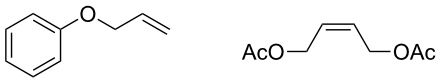	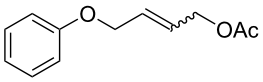	**1** **2** **9**	76% (*E*/*Z* 12:1) 75% (*E*/*Z* 12:1) 73% (*E*/*Z* 18:1)
3[b]		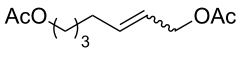	**1** **2** **9**	82% (*E*/*Z* 5:1) 86% (*E*/*Z* 5:1) 75% (*E*/*Z* 6:1)
4[c]		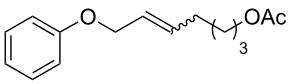	**1** **2** **9**	47% (*E*/*Z* 7:1) 53% (*E*/*Z* 5:1) 83% (*E*/*Z* 9:1)

[a]*E*/*Z* ratio determined by ^{1}H NMR, isolated yield. [b]Reaction conditions: 20 °C, 3 h, CH_2Cl_2, 0.1 M (terminal alkene), 2.5 mol % [Ru], *(Z)*-but-2-ene-1,4-diol diacetate (2 equiv). [c]Reaction conditions: 20 °C, 3 h, CH_2Cl_2, 0.1 M (both alkenes), 2.5 mol % [Ru].

2-ene-1,4-diol diacetate (entry 1, Table 2) was highly efficient (97% yield) using catalyst **9**. Moreover, in the CM of allyloxybenzene and hex-5-enyl acetate, the yield with **9** was almost twice higher than that obtained for **1** or **2** (entry 4, Table 2). In the model RCM, the activity of catalyst **9** was slightly lower than that of commercial complexes, supposedly due to steric reasons (Table 3).

The potency of the new catalyst **9** was tested not only in standard, model metathesis reactions but was also examined in more demanding systems, such as conjugated dienes and polyenes (Table 4). The CM reaction between alkene and diene (or polyene) often suffers from low regio- and stereoselectivity control. The CM reaction may be accompanied by various self-metathesis processes. Additionally, due to the competitive cleavage of both double bonds of the diene substrate, two different products may be formed in the CM reaction between alkene and diene (Scheme 3). A further complication is a *Z*/*E* isomer mixture formation.

The reactions of ethyl sorbate and its 3-methyl substituted analogue (ethyl (2*E*,4*Z*/*E*)-3-methylhexa-2,4-dienoate) with various alkenes were chosen to examine the activity and selectivity profile of catalyst **9** (Table 4). The results clearly indicate that carbene **9** can promote the CM reactions of dienes with different olefins as efficiently as commercial Grubbs 2nd generation and Hoveyda–Grubbs 2nd generation complexes **1** and **2**. Complex **9** catalysed the reactions of ethyl 3-methylhexa-2,4-dienoate in a completely selective manner taking into account product regio- and stereoselectivity. In all reactions the *E*-isomer of compound **A** was formed as a main product (Table 4, entries 1–3). Homodimerisation products of diene and alkene were obtained in very small amounts (<2% and <4% for entry 1 and 2, respectively, Table 4). The SM product of methyl

Table 3: Comparative investigation of catalysts in RCM.

Entry	Substrate	Product	Conditions	Catalyst	Conversion[a]
1	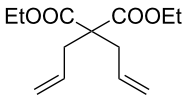	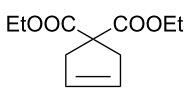	20 °C, CH_2Cl_2, 0.1 M, 1 h, 1 mol % [Ru]	**1** **2** **9**	95% 99% 70%
2	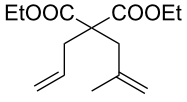	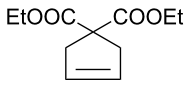	20 °C, CH_2Cl_2, 0.1 M, 1 h, 1 mol % [Ru]	**1** **2** **9**	83% 85% 65%
3	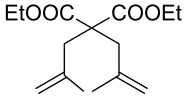	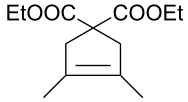	80 °C, toluene, 0.06 M, 16 h, 5 mol % [Ru]	**1** **2** **9**	38% 15% 22%

[a]Determined by ^{1}H NMR.

Table 4: CM reactions between dienes and alkenes in the presence of various 2nd-generation catalysts[a].

Entry	Diene	Alkene	Products	[Ru]	Yield[b] (*E*/*Z*) product **A**	Yield (*E*/*Z*) product **B**
1[c]	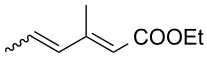	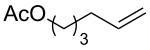	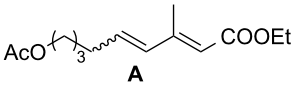 **A**	**1** **2** **9**	89% (only *E*) 72% (only *E*) 70% (only *E*)	– – –
2[d]	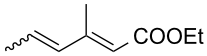	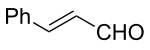	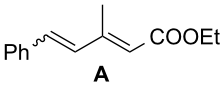 **A**	**1** **2** **9**	95% (only *E*) 92% (only *E*) 94% (only *E*)	– – –
3[d]	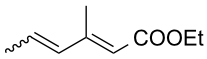		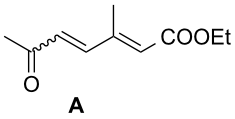 **A**	**1** **2** **9**	42% (only *E*) 40% (only *E*) 51% (only *E*)	– – –
4[c,e]	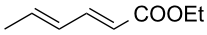	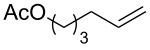	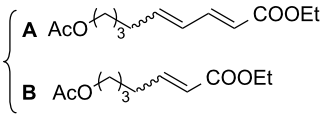 **A** **B**	**1** **2** **9**	40% (*E*/*Z* 12:1) 20% (*E*/*Z* 11:1) 17% (*E*/*Z* 8:1)	10% (only *E*) 22% (*E*/*Z* 8:1) 49% (*E*/*Z* 18:1)

[a]Reaction conditions: diene (3 equiv, 0.36 M), alkene (1 equiv, 0.12 M), and 10 mol % of catalyst in DCM or toluene at 45 °C for 16 h. [b]Isolated yield. Yields were calculated in relation to alkene. [c]*E*/*Z* ratio determined by GC/MS. [d]*E*/*Z* ratio determined by ^{1}H NMR. [e]Isolated as inseparable mixture of **A** and **B**. Yield calculated from ^{1}H NMR.

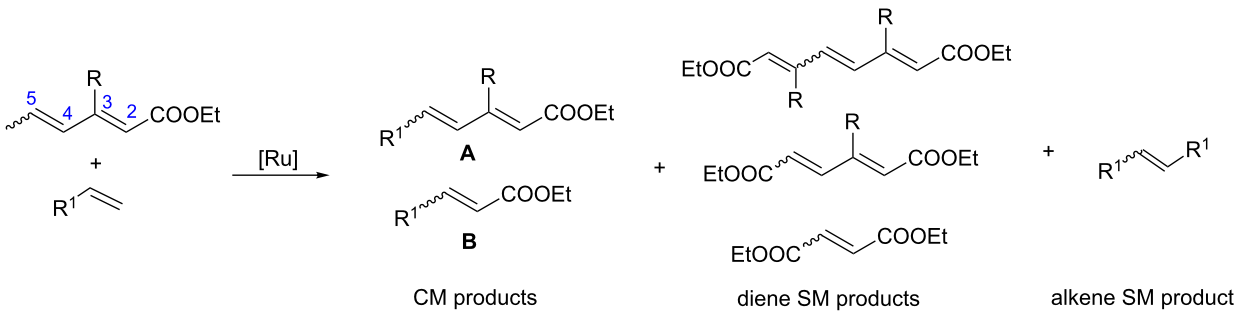

Scheme 3: Possible products of metathesis reaction between diene and alkene.

vinyl ketone was not observed (entry 3, Table 4). Additionally, isomerised diene (ethyl (2*E*,4*E*)-3-methylhexa-2,4-dienoate, used in excess) was isolated from the reaction mixture. When ethyl sorbate was used, the formation of two CM products, **A** and **B**, was observed due to unselective metathetic scission of the C2–C3 and C4–C5 double bonds (Table 4, entry 4) [32]. The low product yield was caused not only by the unselective attack of catalyst on diene substrate but also by competitive SM reactions of both substrates.

Interestingly, the new ruthenium complex showed a different regioselectivity compared to catalysts **1** and **2**. The metathetic scission of the less reactive C2–C3 double bond prevailed with complex **9** (Table 4, entry 4). This result could be explained by the higher affinity of the new catalyst toward electron-deficient olefins. It may also be assumed that the presence of the chromane system changes the electronic properties of the complex compared to other catalysts. It may favour chelation of the ruthenium centre of the catalyst by the carbonyl ester oxygen from the diene substrate. It seems that the oxygen–ruthenium bond is rather labile. The oxygen coordination does not decrease the activity of the catalyst but rather stabilises the π-complex and rutenacyclobutane intermediate (Figure 3), which promotes the metathesis reaction on the C2–C3 double bond. The formation of four- and five-membered chelates has been postulated previously [33,34].

The CM reactions of polyenes, β-carotene and retinyl acetate with ethyl 3-methylhexa-2,4-dienoate in the presence of catalyst **9** were also studied (Scheme 4). A previous investigation of

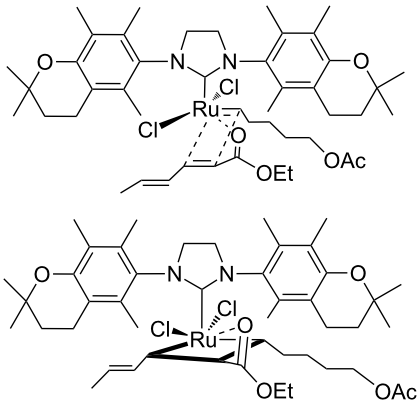

Figure 3: π-Complex and rutenacyclobutane intermediate with a five-membered ring chelate.

the CM reaction of β-carotene promoted by commercial Grubbs and Hoveyda–Grubbs 2nd generation catalysts (**1** and **2**) proved that the two double bonds, C11–C12 and C15–C15' of the β-carotene molecule were reactive in CM [35]. In the case of metathetic fragmentation of β-carotene, the use of **9** instead of **1** or **2** improved the regioselectivity. The product of the central C15–C15' double bond scission was formed preferably. The activity of **9** was comparable to that of **1**, albeit lower than **2** (Scheme 4). Regio- and stereoselectivity (>95% *E*-isomer) of retinyl acetate CM catalysed by **9** appeared to be the same as in analogous reactions that were carried out in the presence of catalysts **1** and **2** [36] (Scheme 4). However, the product was obtained in a slightly lower yield.

Conclusion

In summary, an efficient synthesis of new olefin metathesis catalyst **9** is reported. The catalyst contains a NHC ligand generated from the imidazolinium salt **14** bearing two symmetrically substituted 6-chromanyl moieties. The catalyst **9** was tested in model CM and RCM reactions and showed an activity comparable or superior to that of the commercial Grubbs and Hoveyda–Grubbs 2nd generation complexes. The new complex was also active in metathesis of more demanding systems such as conjugated dienes and polyenes. It proved reactive toward electron-deficient olefins even at lowered temperature (0 °C).

Experimental

General

All manipulations of organometallic compounds were performed using standard Schlenk techniques under an atmosphere of dry argon. CH_2Cl_2 was dried by distillation over CaH_2, toluene over Na. 1,4-Dioxane, ethanol (96%) and trimethyl orthoformate were used as received. Melting points were determined on a Kofler apparatus of the Boetius type and were uncorrected. ^1H and ^{13}C NMR spectra were recorded on a Bruker Avance II spectrometer (400 and 100 MHz, respectively). Spectra are referenced relative to the chemical shift (δ) of TMS. Mass spectra were obtained with Micromass LCT TOF and AutoSpec Premier (Waters) spectrometers. IR spectra were

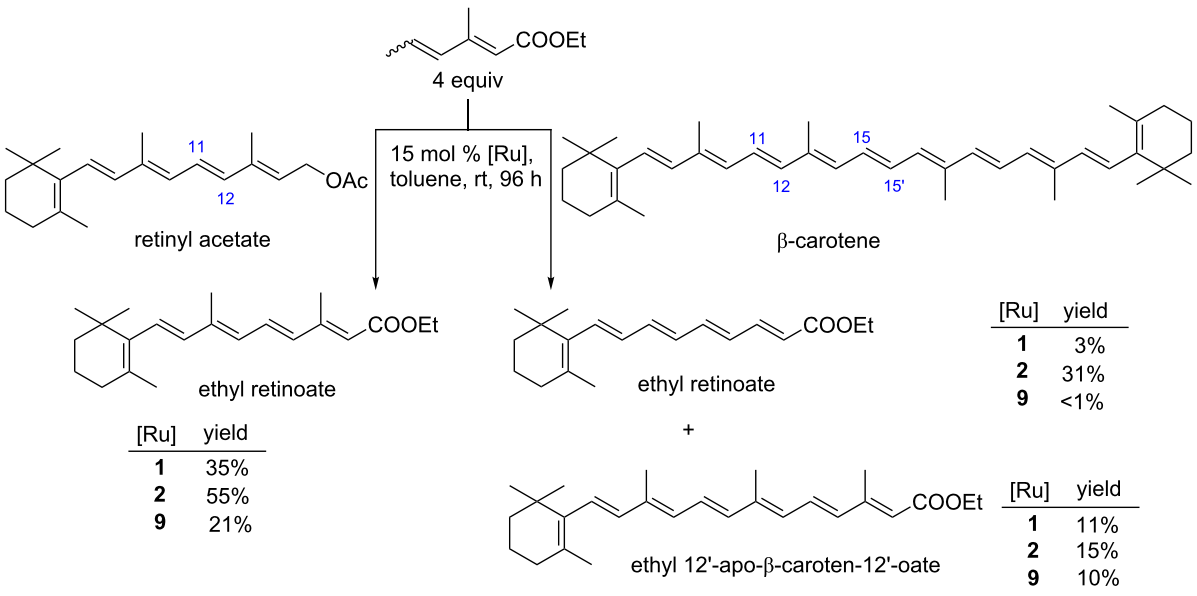

Scheme 4: CM reaction of β-carotene and retinyl acetate with ethyl (2*E*,4*Z*/*E*)-3-methylhexa-2,4-dienoate. Reaction conditions: diene (4 equiv, 0.325 M), alkene (1 eqiuv, 0.08 M). Yield was obtained by quantative HPLC analysis. Yields were calculated in relation to polyene (retinyl acetate or β-carotene). In case of the β-carotene reaction, yields were divided by two due to the symmetry of the β-carotene molecule.

recorded on a Nicolet series II Magna-IR 550 FTIR spectrometer. Flash chromatography (FC) was performed on silica gel 230–400 mesh. Catalysts: **1**, **2**, **3** and the Hoveyda–Grubbs 1st generation complex were purchased from Apeiron Synthesis. 2,2,5,7,8-Pentamethylchromane (**10**) was prepared from 2,3,5-trimethylphenol analogously to the procedure described for 2,2,5,8-tetramethyl-6-chromanol by Dean [27]. 2,3-Dihydroxy-1,4-dioxane was obtain according to Venuti [37]. Substrates for testing catalysts in RCM reactions were prepared by allylation of commercial diethyl malonate with allyl bromide and/or 3-chloro-2-methylpropene according to Hensle [38]. Their purity was estimated by ^{1}H NMR spectroscopy and found to be at least 95%. Other chemicals are commercially available and used as received. The numbering of carbon atoms in the chromanyl moiety was used as shown in Figure 4.

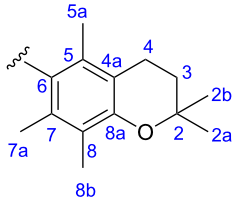

Figure 4: Numbering of carbon atoms in the chromanyl moiety.

6-Nitro-2,2,5,7,8-pentamethylchromane (**11**)

To the solution of 2,2,5,7,8-pentamethylchromane (**10**) (2.5 g, 0.012 mol) in dry CH_2Cl_2 (150 mL) cooled to 0 °C fuming nitric acid (1.5 mL, 3 equiv, 0.036 mol) was added in one portion. The reaction was carried out at 0 °C for 1.5 h. Next the reaction mixture was washed with saturated $NaHCO_3$, dried over Na_2SO_4 and evaporated. The crude product was purified by column chromatography (hexane/ethyl acetate 20:1) to give a yellow solid (1.75 g, 58%). Mp 120–123 °C; IR (KBr) ν: 2977, 2934, 1522, 1368, 1112 cm^{-1}; ^{1}H NMR (400 MHz, $CDCl_3$) δ 2.64 (t, J = 6.8 Hz, 2H, H-4), 2.15 and 2.12 (2s, 9H, H-5a, 7a, 8b), 1.83 (t, J = 6.8 Hz, 2H, H-3), 1.33 (s, 6H H-2a, 2b) ppm; ^{13}C NMR (100 MHz, $CDCl_3$) δ 152.6 (C-8a), 146.2 (C-6), 126.1 (C-8), 125.0 (C-5), 123.7 (C-7), 117.4 (C-4a), 74.0 (C-2), 32.4 (C-3), 26.7 (C-2a and 2b), 20.8 (C-4), 14.5, 13.7, 11.8 (C-5a, 7a and 8b) ppm. HRMS (ESI): $[M + Na]^+$ calcd for $C_{14}H_{19}NNaO_3$: 272.1257, found: 272.1252. Literature mp 125–126 °C; IR, ^{1}H NMR and ^{13}C NMR data are compatible with the data in [39].

2,2,5,7,8-Pentamethylchromanyl-6-amine (**12**)

To the solution of rongalite (sodium hydroxymethylsulfinate dihydrate) (4.62 g, 5 equiv, 30 mmol) in a solution of 1 M NaOH (150 mL) tellurium powder (154 mg, 0.2 equiv, 1.2 mmol) was added. Then the solution of 6-nitro-2,2,5,7,8-pentamethylchromane (**11**, 1.5 g, 6 mmol) in dioxane (20 mL) was added to the reaction mixture. The reaction was carried out at 50 °C for 8 h. The reaction mixture was filtered through a pad of Celite and the filtrate was extracted with methylene chloride (3 × 20 mL). The organic layers were combined and washed with brine and water, dried over Na_2SO_4 and evaporated. The crude product was purified by column chromatography (hexane/ethyl acetate 8:1) to give a white solid (660 mg, 50%). Mp 38–40 °C; IR (KBr) ν: 3455, 3364, 2975, 2921, 1625, 1447, 1420, 1269 cm^{-1}; ^{1}H NMR (400 MHz, $CDCl_3$) δ 3.31 (s, 2H NH_2), 2.67 (t, J = 6.9 Hz, 2H, H-4), 2.15, 2.12 and 2.08 (3s, 9H, H-5a, 7a, 8b), 1.80 (t, J = 6.9 Hz, 2H, H-3), 1.30 (s, 6H, H-2a, 2b) ppm; ^{13}C NMR (100 MHz, $CDCl_3$) δ 144.9 (C-8a), 134.9 (C-6), 122.2 (C-8), 120.4 (C-7), 117.6 (C-5), 116.9 (C-4a), 72.2 (C-2), 33.3 (C-3), 26.7 (C-2a and 2b), 21.4 (C-4), 13.5, 12.5, 11.9 (C-5a, 7a, 8b) ppm. HRMS (ESI): $[M + H]^+$ calcd for $C_{14}H_{22}NO$: 220.1696, found: 220.1691. Literature mp 51.5–53.5 °C; IR, ^{1}H NMR and ^{13}C NMR data are compatible with the data in [39].

N,*N*-Bis(2,2,5,7,8-pentamethylchroman-6-yl)ethane-1,2-diamine (**13**)

To a solution of 2,2,5,7,8-pentamethylchromanyl-6-amine (**12**, 500 mg, 2.3 mmol) in ethanol (96%, 20 mL), 2,3-dihydroxy-1,4-dioxane (138 mg, 1.15 mmol) and two drops of formic acid were added in a manner similar to a that described in [40]. The reaction mixture was stirred for 24 h. A yellow precipitate appeared. Then sodium cyanoborohydride (217 mg, 3 equiv, 3.45 mmol) was added and the reaction mixture was stirred for 1.5 h. The reaction mixture was quenched with water (20 mL) and extracted with dichloromethane (3 × 20 mL). The organic layers were washed with brine and water, dried over Na_2SO_4 and evaporated to dryness. After crystallization from ethanol a white solid was obtained (480 mg, 90%). Mp 182–183 °C; IR (KBr) ν: 3369, 2968, 2925, 2779, 1450, 1420, 1265 cm^{-1}; ^{1}H NMR (400 MHz, $CDCl_3$) δ 3.04 (s, 4H, -NCH_2CH_2N-), 2.64 (t, J = 6.8 Hz, 4H, H-4), 2.26, 2.22 and 2.13 (3s, 18H, H-5a, 7a, 8b), 1.81 (t, J = 6.8 Hz, 4H, H-3), 1.31 (s, 12H, H-2a, 2b) ppm; ^{13}C NMR (100 MHz, $CDCl_3$) δ 147.9 (C-8a), 137.6 (C-6), 129.1 (C-8), 127.1 (C-7), 122.6 (C-5), 117.2 (C-4a), 72.6 (C-2), 50.4 (-NH-*C*H_2-*C*H_2-NH-), 33.1 (C-3), 26.8 (C-2a and 2b), 21.4 (C-4), 14.4, 13.5, 12.1 (C-5a, 7a, 8b) ppm. HRMS (ESI): $[M + H]^+$ calcd for $C_{30}H_{45}N_2O_2$: 465.3476, found: 465.3465.

1,3-Bis(2,2,5,7,8-pentamethylchroman-6-yl)-4,5-dihydro-1*H*-imidazol-3-ium chloride (**14**)

To a solution of ethylenediamine **13** (200 mg, 0.43 mmol) in trimethyl orthoformate (5 mL), ammonium chloride (35 mg, 0.65 mmol) was added in a similar manner as described in [40]. The reaction mixture was refluxed for 2 h. Solids were filtered

off and the filtrate was evaporated to dryness. The resulting oil was stirred overnight with diethyl ether causing precipitation of a white solid (160 mg, 73% yield). Mp 246–247 °C; IR (KBr) ν: 3397, 2974, 2929, 1626, 1456, 1411, 1269 cm^{-1}; ^1H NMR (400 MHz, $CDCl_3$) δ 8.56 and 8.52 (2s, 1H, N-C<u>H</u>=N), 4.75–4.50 (m, 4H, -NCH_2CH_2N-), 2.64 (t, J = 6.8 Hz, 4H, H-4), 2.30, 2.28 and 2.12 (18H, 3s, H-5a, 7a, 8b), 1.82 (t, J = 6.8 Hz, 4H, H-3), 1.32 (s, 12H, H-2a, 2b) ppm; ^{13}C NMR (100 MHz, $CDCl_3$) δ 159.3, 159.2 (-N=CH-N-), 153.2 (C-8a), 131.8, 131.6 (C-6), 131.3, 131.0 (C-8), 124.4, 124.3 (C-7), 124.2 (C-5), 118.3, 118.2 (C-4a), 74.0 (C-2), 53.0 (-NH-CH_2-CH_2-NH-), 32.2 (C-3), 26.9, 26.8, 26.5, 26.47 (C-2a and 2b), 21.0 (C-4), 15.1, 15.0, 14.4, 14.3, 12.0 (C-5a, 7a, 8b) ppm; HRMS (ESI): $[M - Cl]^+$ calcd for $C_{31}H_{43}N_2O_2$: 475.3319, found: 475.3308. Some signals in ^{13}C NMR spectrum are doubled (see text "Synthesis of the carbene precursor").

1,3-Bis[(2,2,5,7,8-pentamethylchroman-6-yl)-2-imidazolidinylidene]dichloro(*o*-isopropoxyphenylmethylene)ruthenium (**9**)

In a Schlenk flask imidazolinium salt **14** (80 mg, 0.16 mmol) was dried under vacuum at 80 °C for 1 h. The flask was then cooled to rt and dry toluene (3 mL) was added under argon atmosphere. To the resulting suspension potassium *tert*-amylate (1.7 M in toluene, 94 µL, 0.16 mmol) was added and the reaction mixture was stirred for 20 min at rt. Then a solution of Hoveyda–Grubbs 1st generation catalyst (96 mg, 0.16 mmol) in toluene (3 mL) was added and the reaction was carried out at 65 °C for 2 h. The reaction mixture was purified by column chromatography (hexane/ethyl acetate 10:1) to give a green solid (86 mg, 68% yield) Mp 162–164 °C; IR (KBr) ν: 2973, 2925, 2854, 1475, 1457, 1274 cm^{-1}; ^1H NMR (400 MHz, $CDCl_3$) δ 16.74 (s, 1H, Ru=CH-), 7.47, 6.94, 6.84 and 6.78 (4m, 4H, -C<u>H</u>$_{Ar}$), 4.89 (sept., J = 6.1 Hz, 1H, -CH_{iPr}), 4.16 (s, 4H, -N-CH_2CH_2-N-), 2.69 (m, 4H, H-4), 2.42, 2.29 and 2.20 (3s (2 br s and 1s), 18H, 3s H-5a, 7a, 8b), 1.88 (*t, J* = 6.5 Hz, 4H, H-3), 1.44 (s, 12H, H-2a, 2b), 1.28 (d, J = 6.0 Hz, 6H, $CH_{3\ iPr}$) ppm; ^{13}C NMR (100 MHz, $CDCl_3$) δ 297.5 (CH=Ru), 211.7 (C_{NHC}), 152.1 ($^{IV}C_{Ar}$), 145.4 ($^{IV}C_{Ar}$), 135.0 ($^{IV}C_{Ar\ weak}$), 133.5 ($^{IV}C_{Ar\ weak}$), 132.2 ($^{IV}C_{Ar\ weak}$), 129.1 ($^{III}CH_{Ar}$), 129.0 ($^{IV}C_{weak}$), 123.3 ($^{IV}C_{Ar\ weak}$), 122.9 ($^{III}CH_{Ar}$), 122.4 ($^{III}CH_{Ar}$), 117.1 ($^{IV}C_{Ar\ weak}$), 112.8 ($^{III}CH_{Ar}$), 74.7 (CH_{IPr}), 73.3 ($C_{chroman}$-2), 53.1 and 51.8 (N-(CH_2)$_2$-N), 33.1 ($C_{chroman}$-3), 27.9 ($C_{chroman}$-2a and 2b), 25.7 ($CH_{3\ IPr}$), 21.2 ($C_{chroman}$-4), 18.3 ($CH_{3\ chroman\ weak}$), 15.2 ($CH_{3\ chroman\ weak}$), 12.0 ($CH_{3\ chroman}$) ppm; EIMS *m*/*z*: 796 (10), 794 (10), 610 (14), 572 (7), 473 (41), 472 (100), 416 (31), 243 (7), 181 (8), 108 (12), 69 (14), 44 (14%); HRMS (EI): $[M]^+$ calcd for $C_{41}H_{54}Cl_2N_2O_3{}^{102}Ru$: 794.2549, found: 794.2571. Some signals in ^{13}C NMR spectrum are weak (see text "Synthesis of the catalyst").

Supporting Information

Supporting Information File 1

Experimental procedures of the testing of the new catalyst and copies of ^1H and ^{13}C NMR spectra of new compounds.
[http://www.beilstein-journals.org/bjoc/content/supplementary/1860-5397-11-300-S1.pdf]

Acknowledgements

The authors acknowledge financial support from the Polish National Science Centre (UMO-2011/02/A/ST5/00459). All syntheses were performed in the Centre of Synthesis and Analysis BioNanoTechno of University of Bialystok. The equipment of the Centre was funded by the EU, as a part of the Operational Program Development of Eastern Poland 2007-2013, project: POPW.01.03.00-20-034/09-00.

References

1. Fürstner, A. *Chem. Commun.* **2011,** *47,* 6505–6511. doi:10.1039/c1cc10464k
2. Nguyen, S. T.; Johnson, L. K.; Grubbs, R. H.; Ziller, J. W. *J. Am. Chem. Soc.* **1992,** *114,* 3974–3975. doi:10.1021/ja00036a053
3. Vougioukalakis, G. C.; Grubbs, R. H. *Chem. Rev.* **2010,** *110,* 1746–1787. doi:10.1021/cr9002424
4. Endo, K.; Grubbs, R. H. *J. Am. Chem. Soc.* **2011,** *133,* 8525–8527. doi:10.1021/ja202818v
5. Keitz, B. K.; Endo, K.; Patel, P. R.; Herbert, M. B.; Grubbs, R. H. *J. Am. Chem. Soc.* **2012,** *134,* 693–699. doi:10.1021/ja210225e
6. Rosebrugh, L. E.; Herbert, M. B.; Marx, V. M.; Keitz, B. K.; Grubbs, R. H. *J. Am. Chem. Soc.* **2013,** *135,* 1276–1279. doi:10.1021/ja311916m
7. Occhipinti, G.; Hansen, F. R.; Törnroos, K. W.; Jensen, V. R. *J. Am. Chem. Soc.* **2013,** *135,* 3331–3334. doi:10.1021/ja311505v
8. Khan, R. K. M.; O'Brien, R. V.; Torker, S.; Li, B.; Hoveyda, A. H. *J. Am. Chem. Soc.* **2012,** *134,* 12774–12779. doi:10.1021/ja304827a
9. Buchmeiser, M. R. *Chem. Rev.* **2009,** *109,* 303–321. doi:10.1021/cr800207n
10. Klučiar, M.; Grela, K.; Mauduit, M. *Dalton Trans.* **2013,** *42,* 7354–7358. doi:10.1039/c2dt32856a
11. Kośnik, W.; Grela, K. *Dalton Trans.* **2013,** *42,* 7463–7467. doi:10.1039/c3dt33010a
12. Śledź, P.; Mauduit, M.; Grela, K. *Chem. Soc. Rev.* **2008,** *37,* 2433–2442. doi:10.1039/b711482f
13. Szczepaniak, G.; Kosiński, K.; Grela, K. *Green Chem.* **2014,** *16,* 4474–4492. doi:10.1039/C4GC00705K
14. Pastva, J.; Skowerski, K.; Czarnocki, S. J.; Žilková, N.; Čejka, J.; Bastl, Z.; Balcar, H. *ACS Catal.* **2014,** *4,* 3227–3236. doi:10.1021/cs500796u
15. Scholl, M.; Ding, S.; Lee, C. W.; Grubbs, R. H. *Org. Lett.* **1999,** *1,* 953–956. doi:10.1021/ol990909q
16. Garber, S. B.; Kingsbury, J. S.; Gray, B. L.; Hoveyda, A. H. *J. Am. Chem. Soc.* **2000,** *122,* 8168–8179. doi:10.1021/ja001179g

17. Grela, K.; Harutyunyan, S.; Michrowska, A. *Angew. Chem., Int. Ed.* **2002,** *41,* 4038–4040. doi:10.1002/1521-3773(20021104)41:21<4038::AID-ANIE4038>3.0.CO;2-0
18. Chatterjee, A. K.; Choi, T.-L.; Sanders, D. P.; Grubbs, R. H. *J. Am. Chem. Soc.* **2003,** *125,* 11360–11370. doi:10.1021/ja0214882
19. Abbas, M.; Leitgeb, A.; Slugovc, C. *Synlett* **2013,** *24,* 1193–1196. doi:10.1055/s-0033-1338425
20. Abbas, M.; Slugovc, C. *Tetrahedron Lett.* **2011,** *52,* 2560–2562. doi:10.1016/j.tetlet.2011.03.038
21. Hryniewicka, A.; Morzycki, J. W.; Siergiejczyk, L.; Witkowski, S.; Wójcik, J.; Gryff-Keller, A. *Aust. J. Chem.* **2009,** *62,* 1363–1370. doi:10.1071/CH08443
22. Hryniewicka, A.; Kozłowska, A.; Witkowski, S. *J. Organomet. Chem.* **2012,** *701,* 87–92. doi:10.1016/j.jorganchem.2011.12.024
23. Hryniewicka, A.; Morzycki, J. W.; Witkowski, S. *J. Organomet. Chem.* **2010,** *695,* 1265–1270. doi:10.1016/j.jorganchem.2010.02.025
24. Burton, G. W.; Doba, T.; Gabe, E. J.; Hughes, L.; Lee, F. L.; Prasad, L.; Ingold, K. U. *J. Am. Chem. Soc.* **1985,** *107,* 7053–7065. doi:10.1021/ja00310a049
25. Burton, G. W.; Ingold, K. U. *Acc. Chem. Res.* **1986,** *19,* 194–201. doi:10.1021/ar00127a001
26. Smith, L. I.; Renfrow, W. B., Jr.; Opie, J. W. *J. Am. Chem. Soc.* **1942,** *64,* 1082–1084. doi:10.1021/ja01257a020
27. Dean, F. M.; Matkin, D. A.; Orabi, M. O. A. *J. Chem. Soc., Perkin Trans. 1* **1981,** 1437–1442. doi:10.1039/p19810001437
28. Mahdavian, E.; Sangsura, S.; Landry, G.; Eytina, J.; Salvatore, B. A. *Tetrahedron Lett.* **2009,** *50,* 19–21. doi:10.1016/j.tetlet.2008.10.056
29. Smith, L. I.; Hoehn, H. H.; Ungnade, H. E. *J. Org. Chem.* **1939,** *4,* 351–357. doi:10.1021/jo01215a019
30. Suzuki, H.; Manabe, H.; Inouye, M. *Chem. Lett.* **1985,** *14,* 1671–1674. doi:10.1246/cl.1985.1671
31. Choi, T.-L.; Lee, C. W.; Chatterjee, A. K.; Grubbs, R. H. *J. Am. Chem. Soc.* **2001,** *123,* 10417–10418. doi:10.1021/ja016386a
32. Funk, T. W.; Efskind, J.; Grubbs, R. H. *Org. Lett.* **2005,** *7,* 187–190. doi:10.1021/ol047929z
33. Choi, T.-L.; Chatterjee, A. K.; Grubbs, R. H. *Angew. Chem., Int. Ed.* **2001,** *40,* 1277–1279. doi:10.1002/1521-3773(20010401)40:7<1277::AID-ANIE1277>3.0.CO;2-E
34. Engelhardt, F. C.; Schmitt, M. J.; Taylor, R. E. *Org. Lett.* **2001,** *3,* 2209–2212. doi:10.1021/ol016061z
35. Wojtkielewicz, A.; Maj, J.; Morzycki, J. W. *Tetrahedron Lett.* **2009,** *50,* 4734–4737. doi:10.1016/j.tetlet.2009.06.032
36. Wojtkielewicz, A.; Maj, J.; Dzieszkowska, A.; Morzycki, J. W. *Tetrahedron* **2011,** *67,* 6868–6875. doi:10.1016/j.tet.2011.06.086
37. Venuti, M. C. *Synthesis* **1982,** 61–63. doi:10.1055/s-1982-29701
38. Hensle, E. M.; Tobis, J.; Tiller, J. C.; Bannwarth, W. *J. Fluorine Chem.* **2008,** *129,* 968–973. doi:10.1016/j.jfluchem.2008.05.024
39. Stępień, D. K.; Cyrański, M. K.; Dobrzycki, Ł.; Wałejko, P.; Baj, A.; Witkowski, S.; Paradowska, K.; Wawer, I. *J. Mol. Struct.* **2014,** *1076,* 512–517. doi:10.1016/j.molstruc.2014.08.003
40. Hryniewicka, A.; Misztalewska, I.; Czajkowska-Szczykowska, D.; Urbańczyk-Lipkowska, Z.; Morzycki, J. W.; Witkowski, S. *Tetrahedron* **2014,** *70,* 6810–6816. doi:10.1016/j.tet.2014.07.056

License and Terms

BEILSTEIN JOURNAL OF ORGANIC CHEMISTRY

Effective immobilisation of a metathesis catalyst bearing an ammonium-tagged NHC ligand on various solid supports

Krzysztof Skowerski*[1], Jacek Białecki[1], Stefan J. Czarnocki[1], Karolina Żukowska[2] and Karol Grela*[3]

Full Research Paper

Open Access

Address:
[1]Apeiron Synthesis, Duńska 9, 54-427 Wrocław, Poland, [2]Institute of Organic Chemistry, Polish Academy of Sciences, Kasprzaka 44/52, 01-224 Warsaw, Poland and [3]Biological and Chemical Research Centre, Faculty of Chemistry, University of Warsaw, Żwirki i Wigury 101, 02-089 Warsaw, Poland

Email:
Krzysztof Skowerski* - krzysztof.skowerski@apeiron-synthesis.com;
Karol Grela* - karol.grela@gmail.com

* Corresponding author

Keywords:
catalysis; immobilisation; N-heterocyclic carbenes; olefin metathesis; ruthenium

Beilstein J. Org. Chem. **2016,** *12,* 5–15.
doi:10.3762/bjoc.12.2

Received: 03 November 2015
Accepted: 17 December 2015
Published: 05 January 2016

This article is part of the Thematic Series "N-Heterocyclic carbenes".

Guest Editor: S. P. Nolan

Abstract

An ammonium-tagged ruthenium complex, **8**, was deposited on several widely available commercial solid materials such as silica gel, alumina, cotton, filter paper, iron powder or palladium on carbon. The resulting catalysts were tested in toluene or ethyl acetate, and found to afford metathesis products in high yield and with extremely low ruthenium contamination. Depending on the support used, immobilised catalyst **8** shows also additional traits, such as the possibility of being magnetically separated or the use for metathesis and subsequent reduction of the obtained double bond in one pot.

Introduction

Over the past decade olefin metathesis has undergone a grand development. The design of stable and active ruthenium-based metathesis catalysts has been the cardinal factor to distribute olefin metathesis in the synthesis of many important compounds [1-4]. Commercially available homogeneous complexes, including phosphine-containing **Gru-II**, **Ind-II** or phosphine-free **Hov-II** and **Gre-II** are usually employed in such cases (Figure 1) [5]. However, heterogenisation of these complexes was also extensively tested, as their applications in a solid form can be beneficial [6]. The efficient removal of ruthenium from metathesis products, possibility of catalyst recovery and reuse as well as their potential use in continuous processes are the main benefits of heterogeneous systems [7]. Unfortunately, their application is associated with some drawbacks. These catalysts usually exhibit lower activity than their homogeneous counterparts as reflected by a noticeably lower

turnover frequency (TOF). Moreover, their synthesis, due to the need for sophisticated linkers and tags, is significantly more complicated.

Several protocols were developed for heterogenisation of ruthenium catalysts and this topic has been thoroughly reviewed [8-18]. The implementation of such concepts requires the presence of remotely functionalised ligands within the metal coordination sphere. A very efficient covalent immobilisation through anionic ligands was reported by Buchmeiser et al., who synthesised a series of monolith-supported catalysts (such as **1**) which gave metathesis products with extremely low residual ruthenium [19-24]. In other contributions originating from the same group, heterogeneous catalysts covalently connected to a monolithic support via NHC ligands were presented [25,26]. These initiators were suitable for continuous metathesis processes and provided products with low residual ruthenium; however, they were less active than complex **1**. A very similar idea was explored by Grubbs et al. who obtained catalysts **2** and **3** covalently bonded to silica gel through the NHC ligand [27-29]. This work revealed that, for complexes supported on silica gel, the heterogenization via the NHC backbone is a much better approach than the previously used ones (e.g., via phosphine or benzylidene ligands).

An early example of a non-covalent attachment is complex **4**, an activated catalyst deposited on glass polymer Raschig rings, which was tested in various metathesis reactions carried out in batch and circulating flow reactor, as well as in an industrial setup [30,31]. The concept was explored further, and a pyridinium-tagged complex deposited on modified silica gel was recently obtained by Kirschning, Mauduit et al., exhibiting much better activity and efficiency than **4** [32]. Specially functionalised Hoveyda-type catalysts bearing polar ammonium groups were non-covalently immobilised on silica-gel [33-36]. However, it is worth highlighting that alkylidene and pyridine

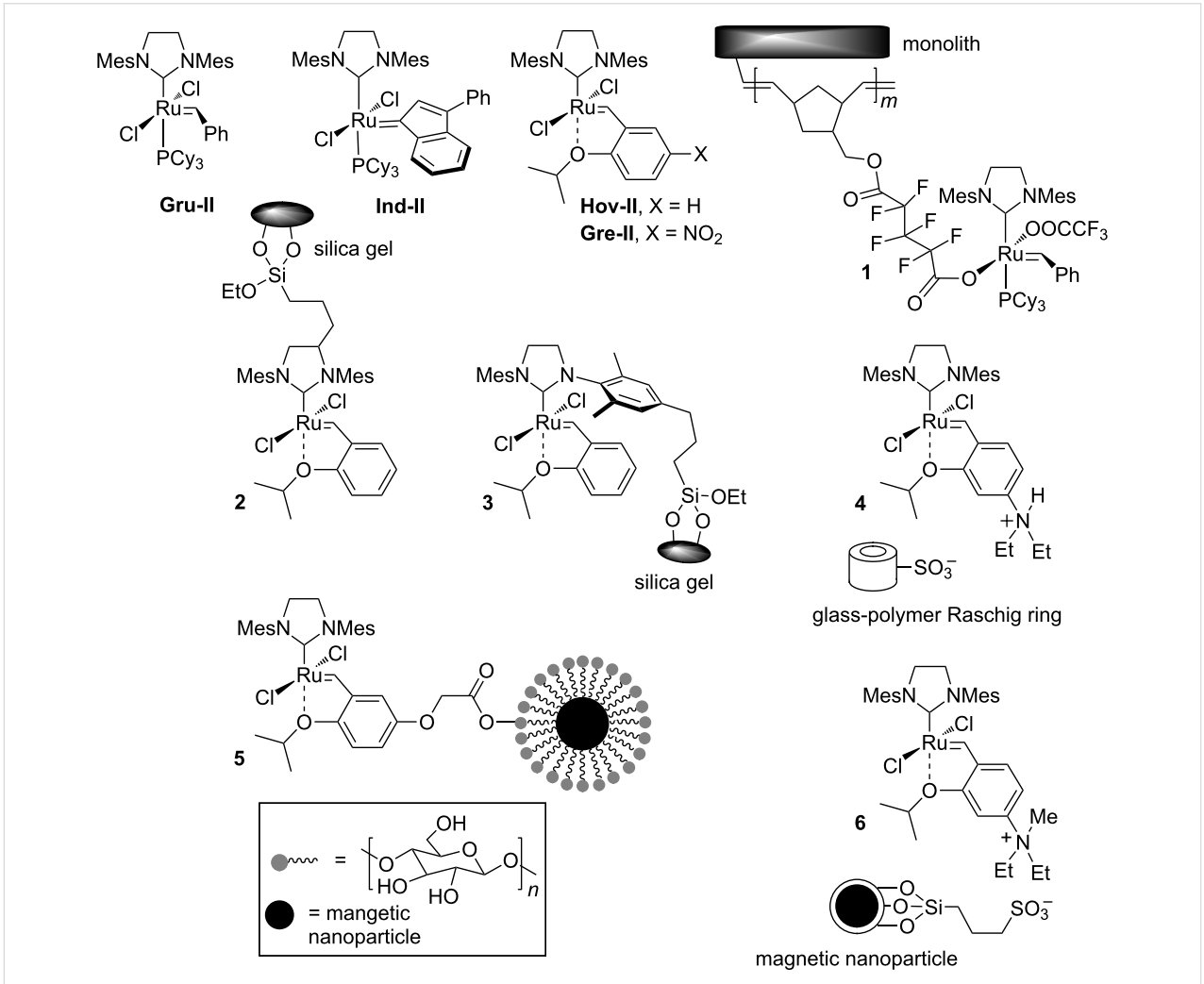

Figure 1: Selected classical and heterogeneous ruthenium complexes.

ligands dissociate during the catalytic cycle and as a result the active species containing heavy metal are leaching to the solution.

A different valuable concept is the covalent or electrostatic immobilisation of ruthenium initiators on magnetically active nanoparticles. Complexes **5** [37] and **6** [38] presented in Figure 1 can serve as an examples, but others were also prepared [39]. These compounds are carefully designed to facilitate straightforward removal of the metal-containing species after the reaction is completed. Although this idea is simple, the preparation of such sophisticated nanoparticle-supported catalysts is often a complicated multistep procedure.

Definitely, the simplest and quickest immobilisation strategy is to support an unmodified, commercially available homogeneous catalyst on silica gel. This plan was tested by Jacobs et al. [40] and more recently Limbach and co-workers [41], who proved that even the classical **Hov-II** catalyst can be successfully immobilised on silica gel via physisorption. Recently, two other commercial Hoveyda-type homogeneous catalysts have been immobilised on silica using the same physisorption approach [42]. This strategy, although easy and economical, has a drawback of being limited in terms of the solvents in which the system stays heterogeneous. Since these commercial Hoveyda complexes have good solubility in methylene chloride (CH_2Cl_2) and toluene, olefin metathesis reactions with these systems have to be conducted in pentane or hexane.

Recently we have reported on the synthesis and catalytic activity of a series of olefin metathesis catalysts bearing a quaternary ammonium group attached to the NHC ligand (Figure 2) [43-47]. These, now commercially available [48], complexes were synthesised by on-site quarternisation of catalysts containing a tertiary amine functional group with the use of either methyl chloride or methyl iodide. This simple yet powerful procedure gives access to a modified complex with multitude of possible applications [43-47]. We have found that the introduction of an ammonium chloride tag into the NHC ligand results in catalysts with interesting properties such as solubility in neat water as well as extremely high affinity to silica gel. The latter property was of particular interest to us. Having in hand a complex with such properties we became interested in its ability to bind non-covalently to various easily available supports.

What is more important, the resulting material should inherit the key characteristic of the support, thus allowing for easy and efficient removal of residual ruthenium from metathesis products, or being utilised in different ways. This heterogenisation strategy seemed to us a much more straightforward and universal approach than methods requiring a sophisticated design of the catalyst, linker or support. However, the reported physicosorbed systems [40-42] consisting of supported commercial catalysts can only be used in non-polar solvents [33-36,43-47]. Taking into account that many advanced polyfunctionalised substrates can be insoluble in pentane, this could be considered as a drawback. Therefore, we decided to further explore the potential of NHC-ammonium tagged catalysts, aiming to develop a more versatile process.

In this present report, we disclose a new heterogeneous catalytic system, compatible with more polar solvents and substrates. It is important to note that in this study we focused on establishing the scope of this heterogenisation method, i.e., by testing a wide number of potential supports, such as silica, alumina, charcoal, iron powder, as well as biocompatible wool and paper, and by examining different catalyst removal strategies, rather than tackling recyclability issues. The latter was studied in a separate project conducted in our laboratories and recently published [49]. In that parallel study the NHC ammonium-tagged catalyst was heterogenised and subjected to various re-

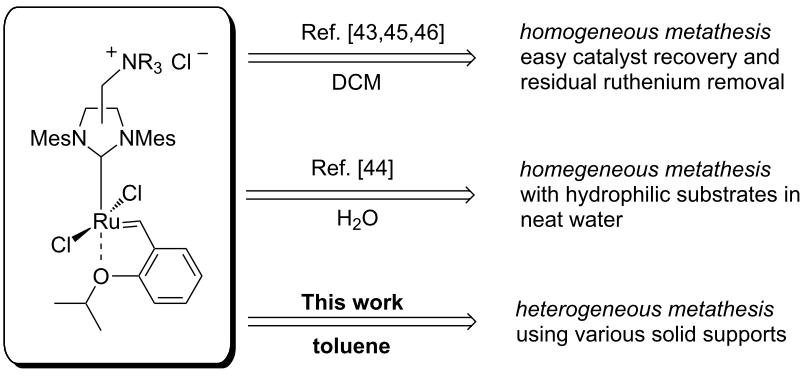

Figure 2: Applications of NHC ammonium-tagged catalysts.

cyclability tests, proving high potential (up to 23 recycles) and really high total turnover numbers (up to 35,000).

Results and Discussion

Synthesis of tagged catalyst 8

Complex **7** was synthesised according to the previously reported procedure [43]. The obtained material was subsequently subjected to the on-site quaternisation reaction with methyl chloride (Scheme 1). Catalyst **8** was isolated in excellent yield after simple filtration through a short pad of neutral aluminium oxide, using a mixture of EtOAc/MeOH 92:8 v/v as eluent. We realised that one of the important properties of this complex is its insolubility in toluene, a solvent of known industrial potential [50].

Preparation of high-surface 8 by precipitation and by immobilisation on charcoal, silica, alumina, cotton and paper and the application of such materials in catalysis

Microcrystalline **8** showed only marginal activity in olefin metathesis when applied as a suspension in toluene. This was ascribed to the low surface area of this material. Therefore, we decided to deposit **8** on a solid support characterised by a high surface. The initially chosen support for the catalyst deposition was activated carbon (charcoal, C*), which is known to have a high surface area [51]. Addition of C* to a CH_2Cl_2 solution of **8** and subsequent removal of the solvent in vacuo resulted in a complete deposition. Other solvents for the deposition process were tested as well, with the AcOEt/MeOH 95:5 v/v system being a greener alternative to CH_2Cl_2. The thus obtained material was dried and used directly in metathesis reactions. In both of these solvent systems, complete (100%) deposition was achieved, according to gravimetric analysis of the obtained loose powder. In addition, visual inspection showed no remains of unsupported complex **8** deposited on the flask walls, etc.

Having in hand the catalyst supported on activated carbon (**8**-C*) we were eager to test its catalytic properties. A model ring-closing metathesis (RCM) reaction leading to product **10** (Scheme 2) was used to check the influence of temperature and concentration on the activity of **8** on the solid support.

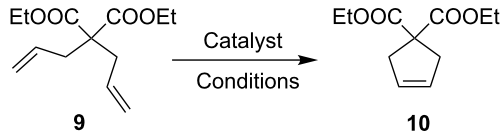

Scheme 2: Model RCM reaction.

We observed that the use of higher temperature and concentration results in faster substrate consumption what is quite intuitive (Figure 3). We were pleased to see almost full conversion of **9** after only 20 minutes of reaction carried out at 80 °C at

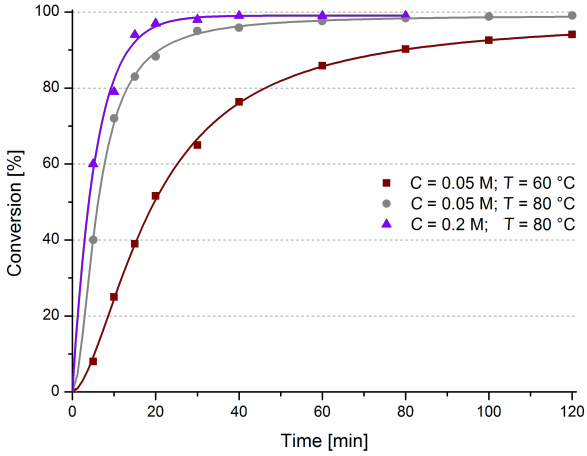

Figure 3: Influence of temperature and concentration on RCM of **9**. Conditions: 1 mol % of **8**-C* (5 wt % on C*), in toluene.

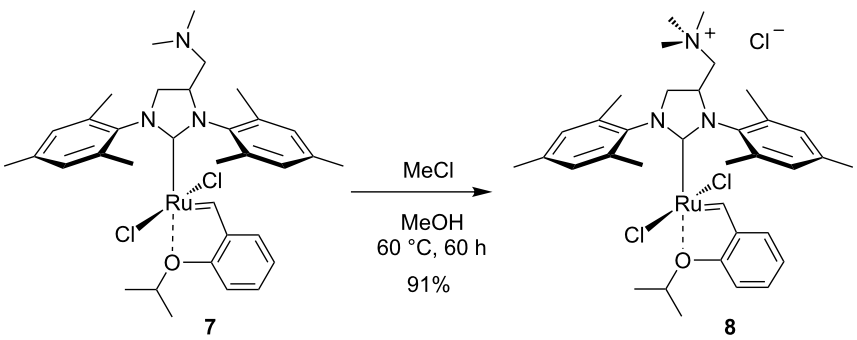

Scheme 1: Synthesis of ammonium-tagged complex **8**.

0.2 M concentration. It is worth noting that such a fast reaction is rather unusual in the case of heterogeneous olefin metathesis [19-24,52].

Encouraged by this initial success, we deposited **8** on several other widely available solid supports, commonly utilised in everyday laboratory and industrial practice. Those included silica gel (flash chromatography grade), neutral aluminium oxide, cotton-viscose wool (cosmetic) and even filter paper. In each case 5 wt % of catalyst was deposited on the selected support (see Supporting Information File 1 for details). During this part of the study we also discovered that the protocol involving fast precipitation of **8** from diluted CH_2Cl_2 solution with *c*-hexane, can provide solid catalyst **8** as a fine powder exhibiting activity in RCM comparable with that observed for immobilised **8**-C*. The morphology of the obtained materials is presented in Figure 4.

Figure 4: Presentation of various Ru-based catalysts. From the left: 20 mg of **Gre-II** powder, 20 mg of **8** as fine powder, 20 mg of **8** supported on 380 mg of silica gel, 20 mg of **8** supported on 380 mg of activated carbon, 20 mg of **8** supported on 380 mg of cotton-viscose wool, 20 mg of **8** supported on 380 mg of filter paper (6 × 8 cm).

Next, we aimed to test the activity of the obtained heterogenised **8** in the model RCM of **9**. The results are presented in Figure 5. The efficiency of **8** supported on cotton-viscose wool and on filter paper (**8**-cotton and **8**-paper) was only slightly lower than that one of unsupported catalyst **8**-powder. These non-expensive supports, however, are very attractive due to the exceptional ease of handling and product purification. Lower efficiency was observed in the case of catalyst supported on neutral aluminium oxide (**8**-Al_2O_3) which provided product **10** in diminished yield. On the other hand, the catalyst supported on unmodified silica gel (**8**-SiO_2) showed the fastest initiation rate among all tested materials, giving over 99% of conversion of **9** after only 10 minutes.

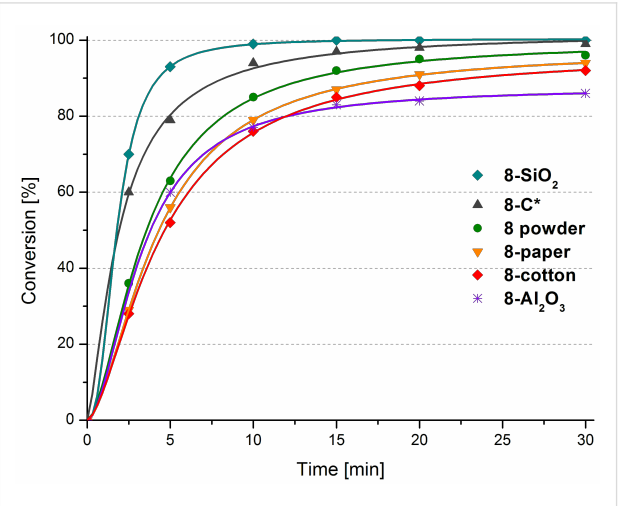

Figure 5: Influence of the support type on the metathesis outcome. Conditions: 1 mol % **8**, toluene 80 °C; [9] = 0.2 M.

We observed that simple decantation of the crude reaction mixture or – in case of unsupported catalyst **8**-powder, Figure 6 – its filtration through a piece of cotton provides colourless mixtures. This suggests that under these conditions there are no active ruthenium species dissolved in toluene.

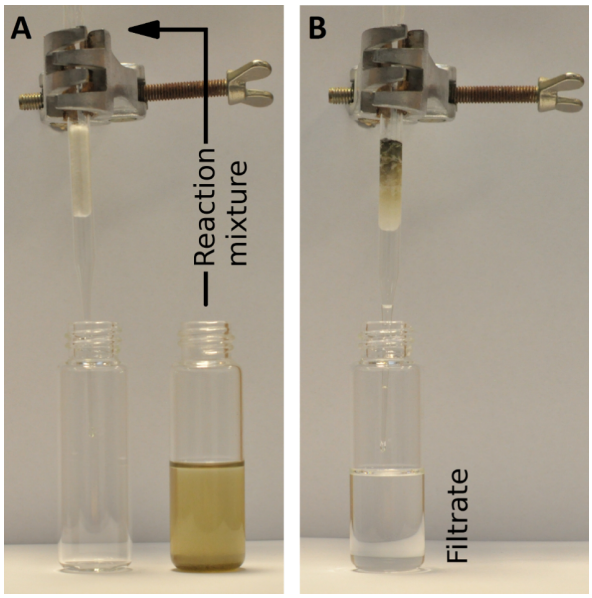

Figure 6: Filtration of the reaction mixture after RCM of **9** catalysed by 1 mol % of **8**-powder.

To check this hypothesis, split tests were carried out during the RCM of **9** catalysed by 1 mol % of **8**-powder, **8**-C*, and **8**-SiO_2. The split test procedure is commonly used to prove the heterogeneity of a process in question [53]. After 3 minutes of each investigated transformation, a part of the reaction mixture was filtered via a very small piece of cotton to a new preheated flask (the cotton plug was washed with hot toluene). The filtered mixtures were immediately analysed to calculate the conversion at the split time. After the following 30 minutes the conversion was determined in both filtered and non-filtered reaction mixtures, again. The appropriate data is presented in Figure 7.

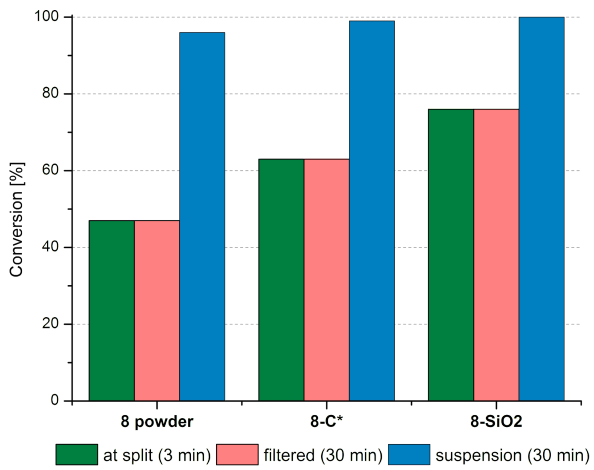

Figure 7: Split test during RCM of **9** (1 mol % cat, toluene 80 °C, [9] = 0.2 M). The reaction mixtures were filtered through a piece of cotton under argon to a flask placed in an oil bath pre-heated to 80 °C.

In all the examined cases there was no increase of conversion in the filtered reaction mixtures. At the same time, the reactions proceeded further in the fractions that were not filtered. This proves that the active species are not present in solution, thus suggesting that these reactions are truly heterogeneous.

We suspect that immobilisation of polar **8** is strengthened by physicochemical interactions of the polar ammonium tag with the surface of the support. To shed more light on this, we compared the behaviour of **8**-powder and **8**-C* in the RCM reaction of diene **9** conducted in ethyl acetate at 50 °C. Complex **8** is partially soluble in this solvent. The split tests, made during RCM reactions, revealed a great difference between the immobilised and unsupported **8** (Table 1). In the case of **8**-powder, the reaction was (at least in a part) homogeneous, and the Ru content present in solution was noticeable (257 ppm, Table 1). On the other hand, the immobilised catalyst (**8**-C*) worked in the same solvent in truly heterogeneous fashion, with only minimal leaching (3.2 ppm). This seems to suggest that the interactions between tagged catalyst **8** and activated carbon are strong enough to allow heterogeneous catalysis even in the solvent in which **8** is partially soluble and therefore cannot be used unsupported. It should be noted that untagged catalysts, like **Hov-II** immobilised on solid supports were reported to work only in non-polar solvents such as hexane or pentane, in which the catalyst is completely insoluble [40-42]. According to this observation, **Hov-II** immobilised on charcoal (using the procedure described above) and applied for RCM of **9** in AcOEt lead to a non-heterogenous reaction and severe leaching (Table 1).

To establish the scope and limitations of the studied heterogeneous system, we selected the most active supported complex (**8**-SiO_2) and a set of olefin metathesis reactions in toluene (Scheme 3). The outcome of this study along with the ruthenium content in crude metathesis products is summarised in Table 2.

The products of RCM and ene–yne metathesis were obtained with good to excellent yields with the use of 0.1–0.5 mol % of catalyst. Functionalised olefins **19** and **21** were isolated with excellent yield after cross metathesis (CM) reactions run with only 1 mol % of catalyst. Importantly, the residual ruthenium content in the crude products was very low (determined by ICP-MS method). Reaction work-up was performed solely by filtration of the reaction mixture through a piece of cotton and evaporation of the volatiles, to yield the crude products. The simplicity and effectiveness of this approach can be utilised in many applications, e.g., in pharmaceutical R&D and production [31,36]. The isolation of highly polar **21** in very good yield and with low residual ruthenium should be especially highlighted in this context [54].

Encouraged by the above results, in the final part of this work we decided to utilise the observed great affinity of **8** to various supports to briefly test some more unconventional heterogenisation strategies. It should be noted that two experiments described below shall be treated only as a preliminary endeavour aimed at getting a broader perspective.

Table 1: Results of olefin metathesis conducted in AcOEt.[a]

RCM of **9** in AcOEt	Promoted by **8**-powder		Promoted by **8**-C*		Promoted by **Hov-II-C***	
	Conv. [%]	Residual Ru [ppm]	Conv. [%]	Residual Ru [ppm]	Conv. [%]	Residual Ru [ppm]
At split	70	n.d.	57	n.d.	80	n.d.
Filtered (30 min)	91	n.d.	57	n.d.	>99	n.d.
Suspension (30 min)	>99	257	88	3.2	>99	1760

[a]n.d.: not determined.

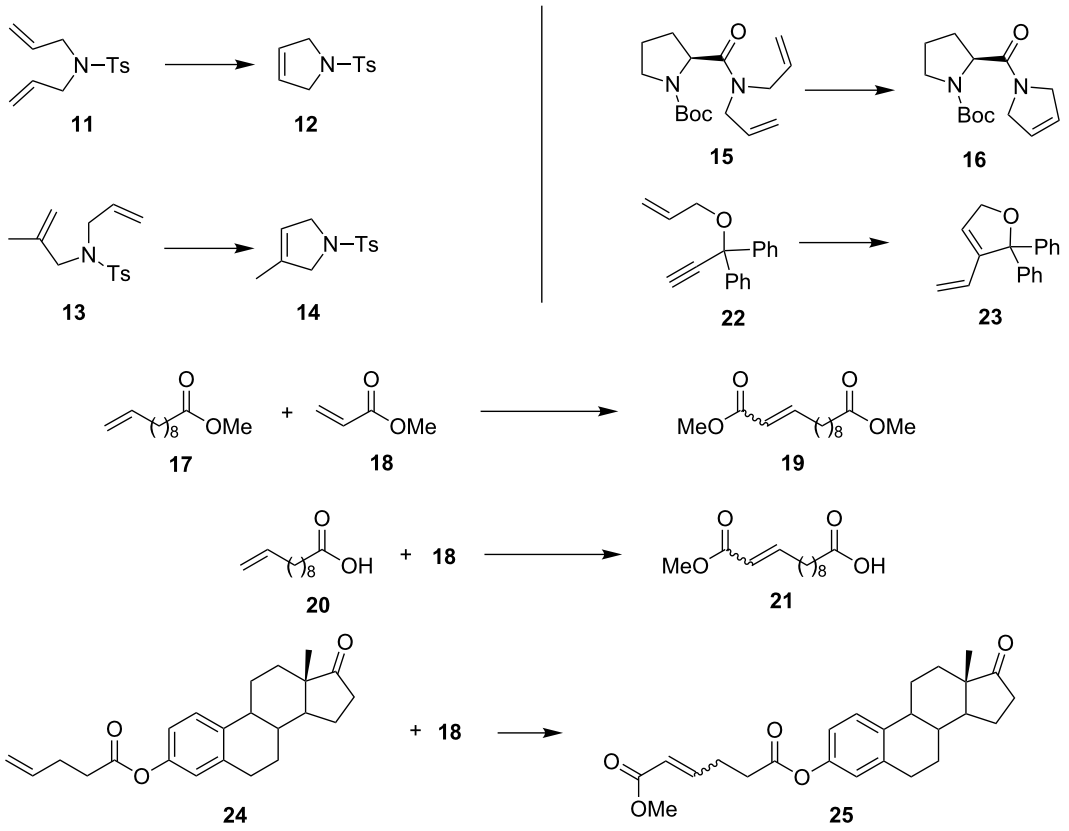

Scheme 3: Model metathesis reactions used in tests.

Table 2: Results of olefin metathesis conducted in toluene, 80 °C.

Entry	Product	Catalyst [mol %]	Time [min]	Conv. (yield) [%][a]	Ru content [ppm][b]
1	**10**	**8**-powder (1)	60	98 (94)	2.0
2	**10**	**8**-C* (1)	15	98 (98)	1.2
3	**10**	**8**-SiO_2 (1)	10	99 (93)	1.4
4	**10**	**8**-SiO_2 (0.5)	20	99 (93)	2.4
5	**12**	**8**-SiO_2 (0.1)	30	85 (83)	0.30
6	**14**	**8**-SiO_2 (0.2)	30	98 (95)	b.d.l.[c]
7	**16**	**8**-SiO_2 (0.5)	30	99 (92)	19
8	**19**[d]	**8**-SiO_2 (1)	10	95 (92)[e]	0.61
9	**21**[d]	**8**-SiO_2 (1)	20	98 (96)[e,f]	0.38
10	**25**[d]	**8**-SiO_2 (1)	10	>95 (75)[g]	0.44
11	**23**	**8**-SiO_2 (0.5)	30	89 (85)	115

[a]Yields of isolated pure products; [b]measured for products purified by filtration of reaction mixture through a piece of cotton; [c]b.d.l. – below detection level; [d]4 equiv of **18** were used; [e]*E*/*Z* = 19:1; [f]determined by GC after esterification of the crude product; [g]yield of pure *E*-isomer.

Immobilisation of **8** on iron powder

First, we attempted to prepare a model for a magnetically separable catalyst [55]. This idea has been explored previously by attaching tagged Ru complexes to specially designed magnetically active nanoparticles. We wondered whether supporting **8** on commercially available iron powder (spherical, <10 μm), would result in a magnetically removable system. In fact, complex **8** can indeed be non-covalently immobilised on iron powder, to form **8**-Fe, although in this case the catalyst/support mass ratio had to be lowered to 0.01 in order to provide fully Fe-supported complex **8**. This method for the preparation of a magnetically removable catalyst is obviously less complicated

than the reported syntheses of catalysts on magnetic nanoparticles [37-39]. The main difference is that the latter materials are much more technologically advanced and work rather as quasi-homogeneous catalysts [56]. The resulting **8**-Fe was tested in the RCM of **9** and its overall efficiency was found to be almost identical with that observed for the unsupported powdered catalyst (Figure 8).

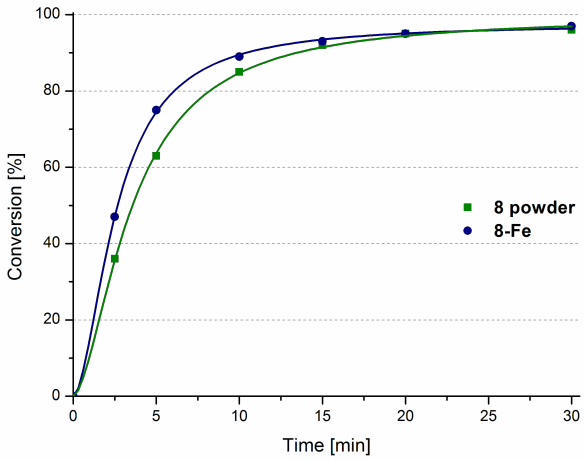

Figure 8: RCM of **9** catalysed by **8** and **8**-Fe. Conditions: 1 mol % catalyst, toluene 80 °C, [9] = 0.2 M.

Reactions with **8**-Fe were performed in a standard reaction vial containing a magnetic stirring bar. During the reaction course the catalyst remained fully suspended in the solution due to the centrifugal force (Figure 9A), whereas once the solution was no longer stirred after reaction completion, all Fe-supported material clung to the mixing element (Figure 9B). It was then mechanically removed, providing the colourless product in very good yield (93%) and with low residual ruthenium content (25 ppm, Figure 9C). This level of contamination is higher than in the case of **8**-SiO2 or **8**-C*, however, we think that immobilisation of a metathesis catalyst on iron is still of interest. It brings some additional possibilities to be explored, such as on-demand catalyst removal and insertion controlled by a magnetic field.

If it is required, complex **8** can then easily be recovered from the support by simply washing the heterogeneous material **8**-Fe with a polar solvent, such as water, alcohol or CH_2Cl_2 (Figure 9D and Figure 9E) and possibly deposited on other supports or used as a homogeneous catalyst. As it was noted earlier, we are not considering high recyclability of immobilised complex **8**. However, the possibility of removing the deactivated catalyst from the support and reloading the latter with a fresh portion of the complex (or to replace a catalyst by another one on a given support) is a potentially viable option, worthy of being explored, especially in industrial setups [30].

Immobilisation of **8** on carbon containing 10% Pd

It is described in the literature that ruthenium residues, present in the reaction mixture after olefin metathesis, can serve as an in situ homogeneous catalyst for high pressure hydrogenation of the newly formed C–C double bonds [57-61]. On this basis, we assumed that the ruthenium complex impregnated on carbon **8**-C* might serve as in situ heterogeneous catalyst for a tandem olefin metathesis-hydrogenation transformation.

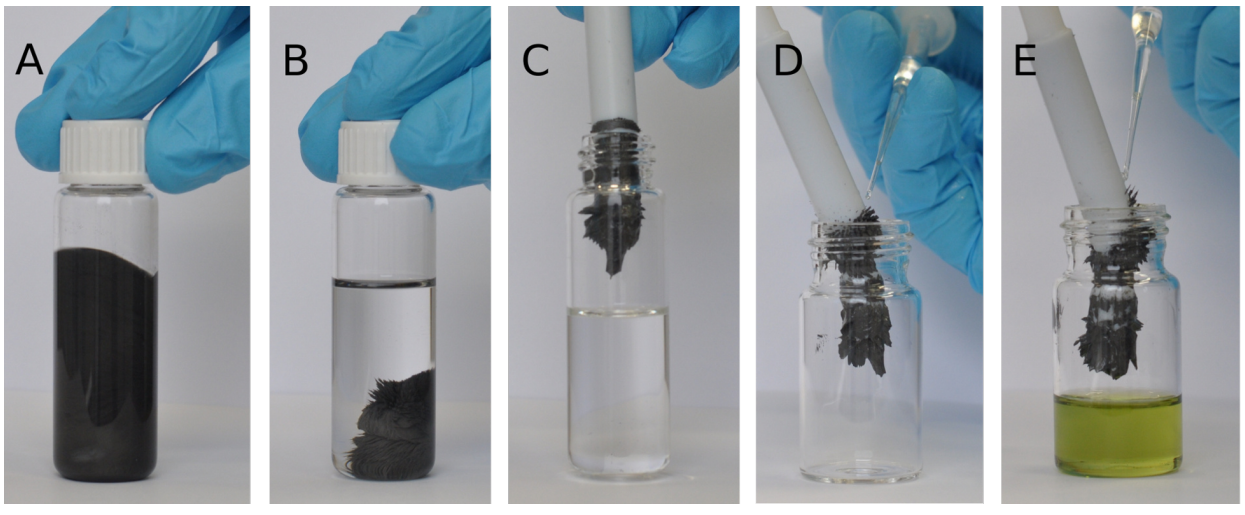

Figure 9: Removal of **8**-Fe and subsequent recovery of **8**. A: stirred reaction mixture containing **8-Fe**, B: the same reaction mixture after stirring ceased, C: catalysts **8**-Fe attached to the magnetic rod and removed, D: catalyst **8**-Fe being washed with CH_2Cl_2, E: CH_2Cl_2 solution of catalyst **8** removed from Fe powder.

To test this possibility we ran CM of **17** and **18** and when the metathesis reaction was complete the resulting product was subjected to reduction by applying hydrogen gas at atmospheric pressure. Unfortunately, only traces of the desired compound **26** were observed after 2 h at 80 °C (Scheme 4). This failure did not discourage us from further attempts. Being interested in development of a catalytic system that would lead to products of tandem metathesis–hydrogenation under mild conditions, we deposited **8** on commercially available palladium on carbon (10 wt % Pd/C) [62]. The resulting bimetallic Ru–Pd heterogeneous catalyst **8**-Pd/C exhibited the same activity in metathesis as catalyst deposited on activated carbon. Interestingly, the *E*/*Z* selectivity in reaction carried out with **8**-C* was significantly different from that observed in reaction promoted by **8**-SiO_2 (11.5:1 and 19:1, respectively).

Advantageously, clean and fast conversion of **19** into **26** was observed when a balloon containing hydrogen gas was applied at 80 °C. After optimisation of the conditions, the saturated diester **26** was obtained in 91% isolated yield and was found to contain only 5.7 ppm of residual ruthenium after simple filtration (Scheme 4). It should be emphasised that this result was obtained without application of high pressure of hydrogen gas, and did not require any specific equipment.

Conclusion

In summary, we have reported on an olefin metathesis catalyst, bearing a quaternary ammonium-tagged NHC ligand. This catalyst can be non-covalently immobilised on various organic and inorganic solid supports in a straightforward and universal manner. Depending on the nature of the support chosen, the properties of the resulting catalyst are different, allowing for various applications such as separation in magnetic field, or a one-pot metathesis–hydrogenation sequence. Practical advantages of the immobilised NHC-tagged catalyst, such as possibility of being applied in more polar solvents (toluene, ethyl acetate), wide substrate scope, good yields and very low residual ruthenium content obtained make it potentially interesting in target-oriented synthesis, applications in pharmaceutical industry and similar areas.

In this work we focused on studying the immobilisation techniques and determining the application profile of the resulted system. In parallel work, the recyclability of an immobilised Ru-catalyst bearing quaternary ammonium-tagged NHC ligand was described.

Supporting Information

Supporting Information File 1

Experimental procedures and analytical data of obtained compounds.
[http://www.beilstein-journals.org/bjoc/content/supplementary/1860-5397-12-2-S1.pdf]

Acknowledgements

K.G. acknowledges the “TEAM” project operated within the Foundation for Polish Science Team program co-financed by the EU European Regional Development Fund, Operational

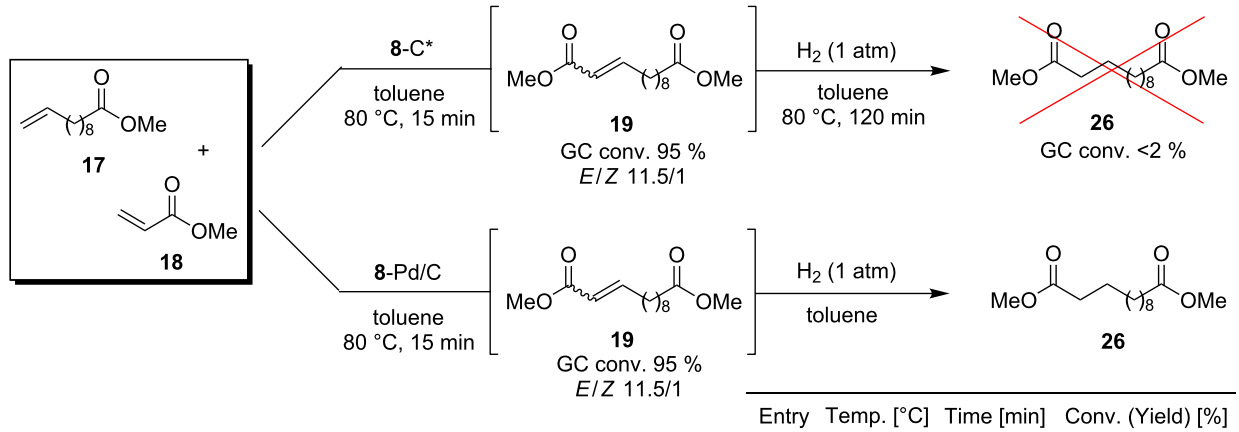

Entry	Temp. [°C]	Time [min]	Conv. (Yield) [%]
1	80	20	>99 (85)
2	40	20	40
3	40	40	>99 (91)[a]

[a] [Ru] = 5.7 ppm

Scheme 4: Supported catalyst **8** in sequential cross metathesis and reduction.

Program Innovative Economy 2007-2013. K.Ż. thanks for the „Diamond Grant" research project financed from the governmental funds for science for 2012–2015.

References

1. Grubbs, R. H.; Wenzel, A. G.; O'Leary, D. J.; Khosravi, E., Eds. *Handbook of Metathesis,* 2nd ed.; Wiley- VCH: Weinheim, 2015. doi:10.1002/9783527674107
2. Grela, K., Ed. *Olefin Metathesis: Theory and Practice,* 1st ed.; Wiley & Sons, Inc.: Hoboken, 2014. doi:10.1002/9781118711613
3. Fürstner, A. *Angew. Chem., Int. Ed.* **2000,** *39,* 3012–3043. doi:10.1002/1521-3773(20000901)39:17<3012::AID-ANIE3012>3.0.CO;2-G
4. Vidavsky, Y.; Anaby, A.; Lemcoff, N. G. *Dalton Trans.* **2012,** *41,* 32–43. doi:10.1039/C1DT11404B
5. Busacca, C. A.; Fandrick, D. R.; Song, J. J.; Senanayake, C. H. *Adv. Synth. Catal.* **2011,** *353,* 1825–1864. doi:10.1002/adsc.201100488
6. Bru, M.; Dehn, R.; Teles, J. H.; Deuerlein, S.; Danz, M.; Müller, I. B.; Limbach, M. *Chem. – Eur. J.* **2013,** *19,* 11661–11671. doi:10.1002/chem.201203893
7. Clavier, H.; Grela, K.; Kirschning, A.; Mauduit, M.; Nolan, S. P. *Angew. Chem., Int. Ed.* **2007,** *46,* 6786–6801. doi:10.1002/anie.200605099
8. Szczepaniak, G.; Kosiński, K.; Grela, K. *Green Chem.* **2014,** *16,* 4474–4492. doi:10.1039/C4GC00705K
9. Buchmeiser, M. R. *New J. Chem.* **2004,** *28,* 549–557. doi:10.1039/b315236g
10. Dragutan, I.; Dragutan, V.; Delaude, L.; Demonceau, A. *ARKIVOC* **2005,** 206–253.
11. Sommer, W. J.; Weck, M. *Coord. Chem. Rev.* **2007,** *251,* 860–873. doi:10.1016/j.ccr.2006.07.004
12. Copéret, C.; Basset, J.-M. *Adv. Synth. Catal.* **2007,** *349,* 78–92. doi:10.1002/adsc.200600443
13. Copéret, C. *Dalton Trans.* **2007,** 5498–5504. doi:10.1039/b713314f
14. Šebesta, R.; Kmentová, I.; Toma, Š. *Green Chem.* **2008,** *10,* 484–496. doi:10.1039/b801456f
15. Śledź, P.; Mauduit, M.; Grela, K. *Chem. Soc. Rev.* **2008,** *37,* 2433–2442. doi:10.1039/b711482f
16. Buchmeiser, M. R. *Chem. Rev.* **2009,** *109,* 303–321. doi:10.1021/cr800207n
17. Bergbreiter, D. E.; Tian, J.; Hongfa, C. *Chem. Rev.* **2009,** *109,* 530–582. doi:10.1021/cr8004235
18. Copéret, C. *Beilstein J. Org. Chem.* **2011,** *76,* 13–21. doi:10.3762/bjoc.7.3
19. Krause, J. O.; Lubbad, S. H.; Nuyken, O.; Buchmeiser, M. R. *Macromol. Rapid Commun.* **2003,** *24,* 875–878. doi:10.1002/marc.200300024
20. Yang, L.; Mayr, M.; Wurst, K.; Buchmeiser, M. R. *Chem. – Eur. J.* **2004,** *10,* 5761–5770. doi:10.1002/chem.200400278
21. Krause, J. O.; Nuyken, O.; Wurst, K.; Buchmeiser, M. R. *Chem. – Eur. J.* **2004,** *10,* 777–784. doi:10.1002/chem.200305031
22. Halbach, T. S.; Mix, S.; Fischer, D.; Maechling, S.; Krause, J. O.; Sievers, C.; Blechert, S.; Nuyken, O.; Buchmeiser, M. R. *J. Org. Chem.* **2005,** *70,* 4687–4694. doi:10.1021/jo0477594
23. Nieczypor, P.; Buchowicz, W.; Meester, W. J. N.; Rutjes, F. P. J. T.; Mol, J. C. *Tetrahedron Lett.* **2001,** *42,* 7103–7105. doi:10.1016/S0040-4039(01)01460-5
24. Vehlow, K.; Maechling, S.; Köhler, K.; Blechert, S. *J. Organomet. Chem.* **2006,** *691,* 5267–5277. doi:10.1016/j.jorganchem.2006.08.019
25. Mayr, M.; Mayr, B.; Buchmeiser, M. R. *Angew. Chem., Int. Ed.* **2001,** *40,* 3839–3842. doi:10.1002/1521-3773(20011015)40:20<3839::AID-ANIE3839>3.0.CO;2-O
26. Mayr, M.; Wang, D.; Kröll, R.; Schuler, N.; Prühs, S.; Fürstner, A.; Buchmeiser, M. R. *Adv. Synth. Catal.* **2005,** *347,* 484–492. doi:10.1002/adsc.200404197
27. Allen, D. P.; van Wingerden, M. M.; Grubbs, R. H. *Org. Lett.* **2009,** *11,* 1261–1264. doi:10.1021/ol9000153
28. Prühs, S.; Lehmann, C. W.; Fürstner, A. *Organometallics* **2004,** *23,* 280–287. doi:10.1021/om0342006
29. Mayr, M.; Buchmeiser, M. R.; Wurst, K. *Adv. Synth. Catal.* **2002,** *344,* 712–719.
30. Michrowska, A.; Mennecke, K.; Kunz, U.; Kirsching, A.; Grela, K. *J. Am. Chem. Soc.* **2006,** *128,* 13261–13267. doi:10.1021/ja063561k
31. Kirschning, A.; Harmrolfs, K.; Mennecke, K.; Messinger, J.; Schön, U.; Grela, K. *Tetrahedron Lett.* **2008,** *49,* 3019–3022. doi:10.1016/j.tetlet.2008.02.134
32. Borré, E.; Rouen, M.; Laurent, I.; Magrez, M.; Caijo, F.; Crévisy, C.; Solodenko, W.; Toupet, L.; Frankfurter, R.; Vogt, C.; Kirschning, A.; Mauduit, M. *Chem. – Eur. J.* **2012,** *18,* 16369–16382. doi:10.1002/chem.201201589
33. Michrowska, A.; Gułajski, Ł.; Kaczmarska, Z.; Mennecke, K.; Kirschning, A.; Grela, K. *Green Chem.* **2006,** *8,* 685–688. doi:10.1039/b605138c
34. Gułajski, Ł.; Michrowska, A.; Narożnik, J.; Kaczmarska, Z.; Rupnicki, L.; Grela, K. *ChemSusChem* **2008,** *1,* 103–109. doi:10.1002/cssc.200700111
35. Kirschning, A.; Gułajski, Ł.; Mennecke, K.; Meyer, A.; Busch, T.; Grela, K. *Synlett* **2008,** 2692–2696. doi:10.1055/s-0028-1083512
36. Cabrera, J.; Padilla, R.; Dehn, R.; Deuerlein, S.; Gułajski, Ł.; Chomiszczak, E.; Teles, J. H.; Limbach, M.; Grela, K. *Adv. Synth. Catal.* **2012,** *354,* 1043–1051. doi:10.1002/adsc.201100863
37. Yinghuai, Z.; Kuijin, L.; Huimin, N.; Chuanzhao, L.; Stubbs, L. P.; Siong, C. F.; Muihua, T.; Peng, S. C. *Adv. Synth. Catal.* **2009,** *351,* 2650–2656. doi:10.1002/adsc.200900370
38. Byrnes, M. J.; Hilton, A. M.; Woodward, C. P.; Jackson, W. R.; Robinson, A. J. *Green Chem.* **2012,** *14,* 81–84. doi:10.1039/C1GC16084B
39. Che, C.; Li, W.; Lin, S.; Chen, J.; Zheng, J.; Wu, J.-c.; Zheng, Q.; Zhang, G.; Yang, Z.; Jiang, B. *Chem. Commun.* **2009,** 5990–5992. doi:10.1039/b911999j
40. van Berlo, B.; Houthoofd, K.; Sels, B. F.; Jacobs, P. A. *Adv. Synth. Catal.* **2008,** *350,* 1949–1953. doi:10.1002/adsc.200800211
41. Cabrera, J.; Padilla, R.; Bru, M.; Lindner, R.; Kageyama, T.; Wilckens, K.; Balof, S. L.; Schanz, H.-J.; Dehn, R.; Teles, J. H.; Deuerlein, W.; Müller, K.; Rominger, F.; Limbach, M. *Chem. – Eur. J.* **2012,** *18,* 14717–14724. doi:10.1002/chem.201202248
42. Solodenko, W.; Doppiu, A.; Frankfurter, R.; Vogt, C.; Kirschning, A. *Aust. J. Chem.* **2013,** *66,* 183–191. doi:10.1071/CH12434
43. Skowerski, K.; Wierzbicka, C.; Szczepaniak, G.; Gułajski, Ł.; Bieniek, M.; Grela, K. *Green Chem.* **2012,** *14,* 3264–3268. doi:10.1039/c2gc36015b

44. Skowerski, K.; Szczepaniak, G.; Wierzbicka, C.; Gułajski, Ł.; Bieniek, M.; Grela, K. *Catal. Sci. Technol.* **2012,** *2,* 2424–2427. doi:10.1039/c2cy20320k
45. Kośnik, W.; Grela, K. *Dalton Trans.* **2013,** *42,* 7463–7467. doi:10.1039/c3dt33010a
46. Klučiar, M.; Grela, K.; Mauduit, M. *Dalton Trans.* **2013,** *42,* 7354–7358. doi:10.1039/c2dt32856a
47. Jordan, J. P.; Grubbs, R. H. *Angew. Chem., Int. Ed.* **2007,** *46,* 5152–5155. doi:10.1002/anie.200701258
48. http://apeiron-synthesis.com/index.php?option=com_content&view=category&layout=blog&id=18&Itemid=123&lang=en#catalyst.
49. Skowerski, K.; Pastva, J.; Czarnocki, S. J.; Janoscova, J. *Org. Process Res. Dev.* **2015,** *19,* 872–877. doi:10.1021/acs.oprd.5b00132
50. Nicola, T.; Brenner, M.; Donsbach, K.; Kreye, P. *Org. Process Res. Dev.* **2005,** *9,* 513–515. doi:10.1021/op0580015 See for application of toluene as a solvent in a large-scale RCM in pharmaceutical production.
51. Chen, J.; Zhu, D.; Sun, C. *Environ. Sci. Technol.* **2007,** *41,* 2536–2541. doi:10.1021/es062113+ See for charcoal that interacts with cations, including ammonium cations.
52. Bek, D.; Gawin, R.; Grela, K.; Balcar, H. *Catal. Commun.* **2012,** *21,* 42–45. doi:10.1016/j.catcom.2012.01.020 See for a hybrid catalyst exhibiting a similar reaction rate.
53. Sheldon, R. A.; Wallau, M.; Arends, I. W. C. E.; Schuchardt, U. *Acc. Chem. Res.* **1998,** *31,* 485–493. doi:10.1021/ar9700163
54. Goldup, S. M.; Pilkington, C. J.; White, A. J. P.; Burton, A.; Barrett, A. G. M. *J. Org. Chem.* **2006,** *71,* 6185–6191. doi:10.1021/jo060931e See for polar substrates which are known to cause purification issues.
55. Shylesh, S.; Schünemann, V.; Thiel, W. R. *Angew. Chem., Int. Ed.* **2010,** *49,* 3428–3459. doi:10.1002/anie.200905684
56. Baig, R. B. N.; Varma, R. S. *Chem. Commun.* **2013,** *49,* 752–770. doi:10.1039/C2CC35663E
57. Louie, J.; Bielawski, C. W.; Grubbs, R. H. *J. Am. Chem. Soc.* **2001,** *123,* 11312–11313. doi:10.1021/ja016431e
58. Malacea, R.; Fischmeister, C.; Bruneau, C.; Dubois, J.-L.; Couturier, J.-L.; Dixneuf, P. H. *Green Chem.* **2009,** *11,* 152–155. doi:10.1039/B816917A
59. Miao, X.; Fischmeister, C.; Bruneau, C.; Dixneuf, P. H.; Dubois, J.-L.; Couturier, J.-L. *ChemSusChem* **2012,** *5,* 1410–1414. doi:10.1002/cssc.201200086
60. Fogg, D. E.; Amoroso, D.; Drouin, S. D.; Snelgrove, I.; Conrad, J.; Zamanian, F. *J. Mol. Catal. A* **2002,** *190,* 177–184. doi:10.1016/S1381-1169(02)00242-X
61. Dragutan, V.; Dragutan, I. *J. Organomet. Chem.* **2006,** *691,* 5129–5147. doi:10.1016/j.jorganchem.2006.08.012
62. Boulard, L.; BouzBouz, S.; Cossy, J.; Franck, X.; Figadère, B. *Tetrahedron Lett.* **2004,** *45,* 6603–6605. doi:10.1016/j.tetlet.2004.07.025 See for examples of H_2 and Pd/C application for in situ reduction of C–C double bond after the metathesis event.

License and Terms

BEILSTEIN JOURNAL OF ORGANIC CHEMISTRY

N-Methylphthalimide-substituted benzimidazolium salts and PEPPSI Pd–NHC complexes: synthesis, characterization and catalytic activity in carbon–carbon bond-forming reactions

Senem Akkoç[*1,2,§], Yetkin Gök[3], İlhan Özer İlhan[2] and Veysel Kayser[*1,¶]

Full Research Paper

Open Access

Address:
[1]Faculty of Pharmacy, The University of Sydney, 2006 Sydney, Australia, [2]Department of Chemistry, Faculty of Sciences, Erciyes University, Talas Street, 38039 Kayseri, Turkey and [3]Department of Chemistry, Faculty of Arts and Sciences, Inönü University, 44280 Malatya, Turkey

Email:
Senem Akkoç[*] - senem.akkoc@sydney.edu.au; Veysel Kayser[*] - veysel.kayser@sydney.edu.au

* Corresponding author
§ Tel: +61 2 9351 2330; Tel: +90 352 437 52 62; Fax: +90 352 437 49 33
¶ Tel: +61 2 9351 3391; Fax: +61 2 9351 4391

Keywords:
arylation; benzimidazolium salts; catalysis; N-heterocyclic carbene; PEPPSI complex; Suzuki–Miyaura cross-coupling reaction

Beilstein J. Org. Chem. **2016,** *12,* 81–88.
doi:10.3762/bjoc.12.9

Received: 07 November 2015
Accepted: 05 January 2016
Published: 15 January 2016

This article is part of the Thematic Series "N-Heterocyclic carbenes".

Guest Editor: S. P. Nolan

Abstract

A series of novel benzimidazolium salts (**1–4**) and their pyridine enhanced precatalyst preparation stabilization and initiation (PEPPSI) themed palladium *N*-heterocyclic carbene complexes [$PdCl_2$(NHC)(Py)] (**5–8**), where NHC = 1-(*N*-methylphthalimide)-3-alkylbenzimidazolin-2-ylidene and Py = 3-chloropyridine, were synthesized and characterized by means of ^{1}H and ^{13}C{^{1}H} NMR, UV–vis (for **5–8**), ESI-FTICR-MS (for **2**, **4**, **6–8**) and FTIR spectroscopic methods and elemental analysis. The synthesized compounds were tested in Suzuki–Miyaura cross-coupling (for **1–8**) and arylation (for **5–8**) reactions. As catalysts, they demonstrated a highly efficient route for the formation of asymmetric biaryl compounds even though they were used in very low loading. For example, all compounds displayed good catalytic activity for the C–C bond formation of 4-*tert*-butylphenylboronic acid with 4-chlorotoluene.

Introduction

The use of N-heterocyclic carbenes (NHCs) as ligands was started by Wanzlick [1] and Öfele [2] almost fifty years ago. There have been major advances in the design and synthesis of metal complexes containing N-heterocyclic carbene ligands in the last two decades, and they had a wide range of applications in different fields, particularly in homogeneous/heterogeneous catalysis [3-8] and bioorganometallic chemistry [9-11]. This is because NHC complexes are easily obtained by deprotonating

imidazolium or benzimidazolium salts and most are relatively stable in air and moisture. They are weak π-acceptors and strong σ-donors and can form strong M–C bonds with transition metal ions compared to trivalent phosphine ligands [12,13].

As catalysts, palladium N-heterocyclic carbene (Pd–NHC) complexes display remarkable activities in coupling reactions [5,14-17]. Among various Pd–NHC complexes such as [Pd(NHC)(dmba)Cl] (dmba = *N*,*N*-dimethylbenzylamine) and [Pd(NHC)(Im)Cl_2] (Im = imidazole) [18,19], [PEPPSI Pd–NHC] complexes are prevalent due to the combination of efficiency and versatility [20,21]. The synthesis conditions for these complexes are generally mild and do not require an inert atmosphere. The steric and electronic parameters are also easily modified by attaching substituents. PEPPSI Pd–NHC complexes have been used in different coupling reactions such as Mizoroki–Heck cross-coupling [22,23], Suzuki–Miyaura cross-coupling [24,25], Sonogashira [26] and arylation reactions [27].

There are suitable precatalyst scaffolds, which were developed by Nolan [28], Organ [21] and Buchwald [29]. To find more effective catalysts containing an Organ type scaffold among these precatalyst scaffolds, we synthesized four new pure *N*-methylphthalimide substituted benzimidazolium salts (**1–4**) and their PEPPSI Pd–NHC complexes (**5–8**) in this study. The structures of all compounds were confirmed by various spectroscopic methods (^{1}H and ^{13}C{^{1}H} NMR, UV–vis, ESI-FTICR-MS, FTIR) and elemental analysis. The PEPPSI Pd–NHC complexes were tested for catalytic activities both in direct arylation and Suzuki–Miyaura cross-coupling reactions. The catalytic activities of benzimidazolium salts were only tested in a Suzuki–Miyaura cross-coupling reaction. The compounds were found to be very efficient in the symmetric and asymmetric C–C bond-forming reactions.

Results and Discussion

Synthesis of *N*-methylphthalimide substituted benzimidazolium salts

New benzimidazolium salts **1–4**, which are carbene precursors, were synthesized by *N*-alkylbenzimidazole and various alkyl halides in DMF (Scheme 1). These salts, especially containing benzyl and 3-methylbenzyl groups, were obtained in very high yields (81–97%) as white or cream solids. The salt containing the 2-morpholinoethyl group was obtained in a much lower yield of 62%.

The benzimidazolium salts include an acidic NC*H*N proton, which can be deprotonated easily to form an NHC, at the C2 position of the benzimidazole ring. The sharp salt peak indicating the synthesis of a benzimidazolium salt came quite downfield at δ 10.13, 11.10, 9.65 and 10.83 ppm in the ^{1}H NMR spectra for **1–4**, respectively. The N*C*HN peaks of the carbene precursors were observed at δ 144.56, 144.69, 143.55 and 145.26 ppm in the ^{13}C{^{1}H} NMR spectra for **1–4**, respectively. The formation of the benzimidazolium salts was also evident through their IR spectra, which showed peaks at 1562.2, 1558.4, 1562.2 and 1554.5 cm^{-1} for the $\nu_{(CN)}$ bond of **1–4**, respectively. Compounds **2** and **4** among these salts were further characterized by using high-resolution mass spectrometry (HRMS). The mass spectra demonstrated *m*/*z* peaks at 382.16 and 391.18 for the cationic moieties against the calculated value of *m*/*z* 382.43 and 391.44 for **2** and **4**, respectively.

Synthesis of PEPPSI Pd–NHC complexes

Our aim was to synthesize novel Pd–NHC complexes containing a PEPPSI skeleton. The target PEPPSI Pd–NHC complexes **5–8** were successfully synthesized by using carbene precursors **1–4**, $PdCl_2$ and K_2CO_3 as a base in 3-chloropyridine (Scheme 1). The colors of the obtained solid complexes were either yellow or cream. These complexes, which are stable both in solution and in solid states against air, light and moisture,

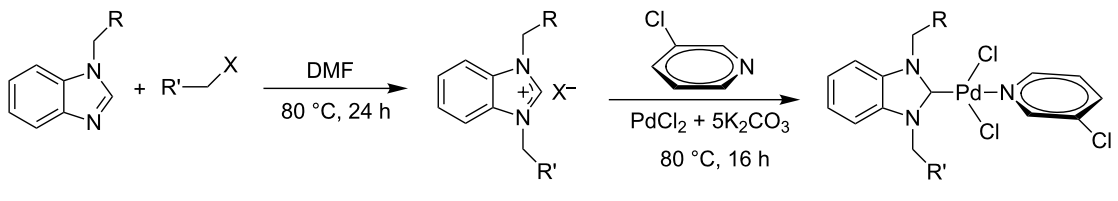

R = $N(C{=}O)_2C_6H_4$
R' = C_6H_5 (**1**)
$C_6H_4(CH_3)$-3 (**2**)
$N(C{=}O)_2C_6H_4$ (**3**)
$CH_2N(CH_2CH_2)_2O$ (**4**)

R' = C_6H_5 (**5**)
$C_6H_4(CH_3)$-3 (**6**)
$N(C{=}O)_2C_6H_4$ (**7**)
$CH_2N(CH_2CH_2)_2O$ (**8**)

Scheme 1: Synthesis of benzimidazolium salts and their PEPPSI Pd–NHC complexes.

were obtained in low yields of 25–60%. All complexes with a benzimidazolium moiety display characteristic signals for the 3-chloropyridine ligand in the ^{1}H and $^{13}C\{^{1}H\}$ NMR spectra. For the ^{1}H NMR spectra of the metal complexes, sharp peaks in the lower field belonging to the benzimidazolium salts (NC*H*N) were not observed between δ 10 and 12 ppm. The FTIR data clearly indicated the presence of $\nu_{(CN)}$ at 1508.2, 1446.5, 1394.4 and 1444.6 cm^{-1} for the PEPPSI Pd–NHC complexes **5–8**, respectively. The formation of a C–N module in the benzimidazole ring correlated with a shift of IR (CN) band. The complexes **6–8** were further characterized by means of HRMS which showed *m*/*z* peaks at 637.02, 691.99 and 574.99 for the cationic moieties against the calculated values of *m*/*z* 636.84, 691.84 and 574.95, respectively. Unfortunately, we were unable to yield a proper single crystal from these compounds for X-ray diffraction. Unlike the salts, the metal complexes showed absorbance in UV–vis experiments.

Absorption spectroscopy studies

The absorption spectra of the complexes were recorded in DMSO and are shown in Figure 1A.

Only metal complexes show an absorbance above 330 nm and have the highest absorption, whereas salts did not display any absorbance except for an intense peak below 330 nm. Therefore, we only discuss the metal complexes here. For the metal complexes, the spectra are characterized by a broad band between 350 and 430 nm and display a strong absorption below 350 nm. Complex **5** exhibits the overall highest absorption, whereas the overall absorption of complex **7** seems to be the lowest of the six investigated complexes. Very broad absorption spectra are indicative of a charge transfer, and to deconvolute the shoulder or ripple of the absorption spectra, we applied the second derivative analysis (Figure 1B). The second derivative spectra were noisy, as can clearly be seen after smoothing three positive peaks (at 315, 345 and 430 nm) and two negative peaks (at 380 and 405 nm). In the second derivative analysis, a negative band has a minimum at the same wavelength as the maximum on the main absorption spectrum. With this in mind, there are at least two absorbance bands buried between 350–430 nm.

Catalytic activity of PEPPSI Pd–NHC complexes as catalysts in arylation reaction

First, we performed the arylation reaction between the 4-bromoacetophenone, which is electron-deficient, with 2-*n*-butylthiophene without the catalyst at 110 °C for 1 h in DMAc as solvent and the reaction resulted in only a 1% yield. When we attempted the same reaction using **8** as a catalyst at 130 °C, the efficiency of the reaction was 27% (Table 1, entry 3). For catalyst **5**, the yield dropped to 9%, the temperature was decreased to 110 °C and the procedure time was increased from 1 h to 1.5 h (Table 1, entry 2).

When 4-bromoacetophenone was used as a substrate with catalyst **6**, sp^2–sp^2 C–C bond formation with 2-*n*-butylfuran was achieved with a yield of 49% in just 1 h (Table 1, entry 5). The product was obtained in a much lower yield when the same reaction was carried out with **5** as a catalyst. Compounds **7** and **8** as catalysts were displaying better results than complexes **5** and **6** for the same reaction (Table 1, entries 6 and 7). When we employed electron-neutral bromobenzene as a substrate instead

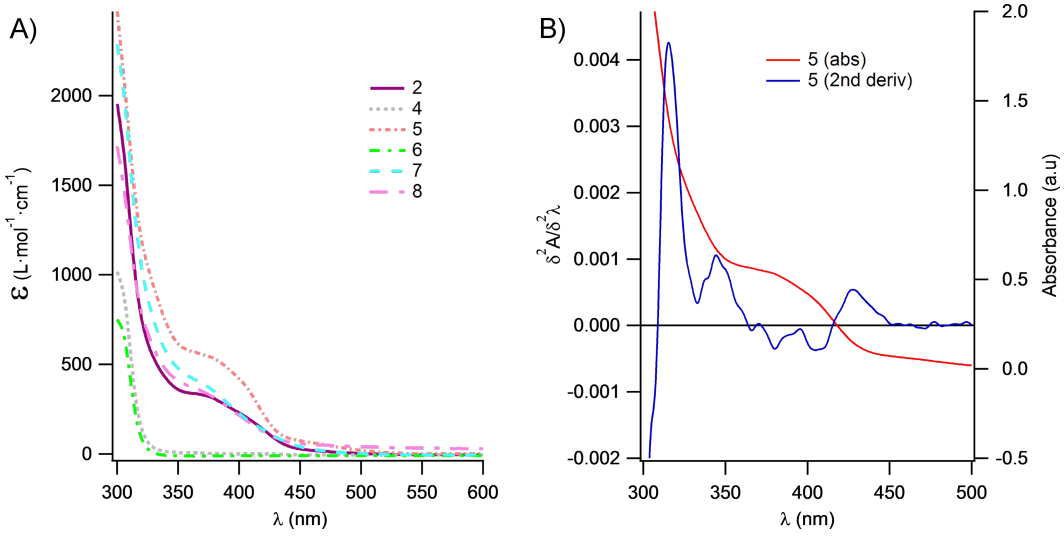

Figure 1: (A) UV–vis absorbance spectra were taken in DMSO. (B) The second derivative of the compound **5** calculated from A. Other metal complexes have similar second derivative bands but are omitted for simplicity.

Table 1: PEPPSI Pd–NHC catalyzed direct intermolecular arylation of heteroaryl derivatives with various aryl bromides[a,b].

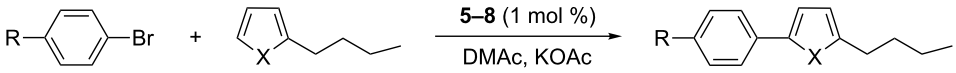

Entry	R	X	Time (h)	Temp. (°C)	Comp.	Yield (%)
1	$CH_3(C=O)$-	S	1	110	–	1
2			1.5	110	**5**	9
3			1	130	**8**	27
4		O	1	110	**5**	14
5			1	110	**6**	49
6			1	110	**7**	83
7			1	110	**8**	89
8	H-	S	1	110	**8**	97
9		O	21	80	**7**	71
10			21	90	**7**	84
11			21	110	**7**	98
12	CH_3O-	S	1	130	**5**	79

[a]Reaction conditions: 2-*n*-butylthiophene or 2-*n*-butylfuran (2 mmol), 4-bromoacetophenone, bromobenzene or 4-bromoanisole (1 mmol), PEPPSI Pd–NHC **5–8** (1 mol %), KOAc (1 mmol), DMAc (2 mL), 80–130 °C, 1 or 21 h. Product purity was checked by GC and NMR. [b]Yields were calculated according to aryl bromides.

of 4-bromoacetophenone, C–C bond formation (2-butyl-5-phenylthiophene) was achieved in 97% yield using catalyst **8** at 110 °C with a reaction time of 1 h (Table 1, entry 8). When bromobenzene was used with catalyst **7** at 80 °C for 21 h, the product 2-butyl-5-phenylfuran was obtained in 71% yield. By increasing the reaction temperature by 10 degree centigrade, as shown in entry 10, the result showed a reaction yield that was 13% higher than that of entry 9. However, when we further increased the temperature by more than 30 degrees to 110 °C, a maximum yield of 98% was obtained (Table 1, entry 11). In the reaction catalyzed by **5**, 2-butyl-5-(4-methoxyphenyl)thiophene was obtained in 79% yield (Table 1, entry 12).

Catalytic activity of synthesized compounds in Suzuki–Miyaura cross-coupling reaction

The Suzuki–Miyaura cross-coupling reaction, which has mostly been performed in organic solvents until recently, can now be performed using green solvents under mild conditions [29-34]. We used H_2O with DMF as solvents in different proportions in this work. We preferred to use a 1:1 ratio in the Suzuki–Miyaura reaction as there was not much difference between the obtained results when the ratios used were 3:1 or 1:1. To optimize the reaction conditions, a series of experiments with different bases such as KOH, NaOH and K_2CO_3 were conducted at different temperatures to provide the coupling of the C–C bond of different substrates with phenylboronic acid. The best results were obtained with the base KOH. We also employed different time periods ranging from 1 to 3 h. When the reaction time was extended, the yield increased in a linear manner.

The Suzuki–Miyaura reaction was carried out using electron-rich (4-chloroanisole, 4-chlorotoluene), electron-poor (4-chloroacetophenone, 4-chloronitrobenzene) and electron-neutral (chlorobenzene) substrates. We studied the catalytic activity of compound **1** regarding C–C bond coupling of 4-iodoacetophenone as a substrate with phenylboronic acid (Table 2, entry 2). This catalytic system showed a better performance for aryl iodide than for aryl chlorides except chlorobenzene (Table 2, entries 1–17). 4-Acetylbiphenyl was obtained in 99% yield and 100% conversion at 80 °C and 1 h (Table 2, entry 2). The best results were obtained when chlorobenzene was used as a substrate (Table 2, entries 18–21) whereas least favorable results were obtained when the electron-poor substrates were used. Among the employed carbene precursors, compound **4** gave the best result to acquire the 4-nitrobiphenyl product (Table 2, entries 8 and 9). Compounds **2** and **4** gave very good results to get the 4-methoxybiphenyl product from among the used carbene precursors (Table 2, entries 11 and 13).

Melvin et al. found the coupling of phenylboronic acid with 4-chlorotoluene with a yield of approximately 45% within 90 minutes at room temperature and reaction conditions of 1.0 mol % PEPPSI-IPr, K_2CO_3, MeOH/THF (19:1). They obtained the same coupling product with a yield of around 50% when they changed the amount of PEPPSI-IPr to 0.5 mol %, the base to KO*t*-Bu and extended the reaction time to 2 h [35]. However, we obtained the same product in much higher yields such as 90 and 93% under reaction conditions of 1 mol % of $Pd(OAc)_2$, 1 mol % of **1** and **2**, KOH, DMF/H_2O within a short period of time (1 h) at 80 °C.

Table 2: Suzuki–Miyaura cross-coupling reaction of phenylboronic acid with aryl chlorides[a,b].

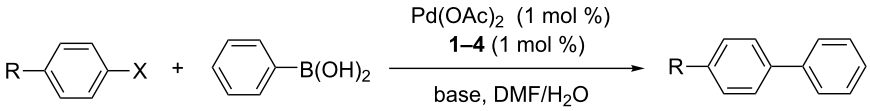

Entry	R-C_6H_4-X	LHX	Base	Time (h)	Temp (°C)	DMF (mL)	H_2O (mL)	Yield (%)	Conv. (%)
1	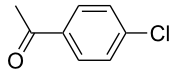	**1**	KOH	1	80	3	1	41	53
2	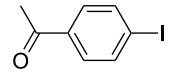	**1**	KOH	1	80	3	1	99	100
3		**1**	KOH	1	80	3	1	27	42
4		**2**	KOH	2	80	2	2	34	40
5		**2**	KOH	3	80	2	2	74	77
6	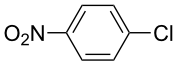	**3**	KOH	2	80	2	2	25	62
7		**3**	KOH	3	80	2	2	30	77
8		**4**	KOH	2	80	2	2	75	76
9		**4**	KOH	3	80	2	2	75	97
10		**1**	KOH	1	80	3	1	52	68
11	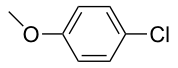	**2**	KOH	2	80	3	1	94	99
12		**3**	KOH	2	80	3	1	23	55
13		**4**	KOH	2	80	3	1	95	98
14		**1**	KOH	1	80	3	1	90	92
15	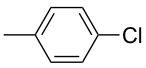	**2**	KOH	1	80	2	2	93	99
16		**3**	KOH	1	80	2	2	44	92
17		**4**	KOH	1	80	2	2	12	99
18		**1**	KOH	2	70	2	2	99.9	99.9
19	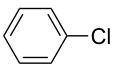	**1**	NaOH	2	70	2	2	99.8	99.8
20		**1**	K_2CO_3	2	70	2	2	96	98
21		**1**	KOH	1	80	3	1	99.9	100

[a]Reaction conditions: *p*-R-C_6H_4Cl (1.0 mmol), $Pd(OAc)_2$ (1.0 mol %), phenylboronic acid (1.5 mmol), base (2.0 mmol), **1–4** (1 mol %), DMF/H_2O, 70–80 °C, 1–3 h. [b]Yields were calculated according to aryl chlorides by using GC or GC–MS.

The synthesized carbene precursors consist of an electron-neutral group (benzyl), electron-donating group (3-methylbenzyl) and electron-withdrawing group (*N*-methylphthalimide) on the benzimidazolium salts. These groups are important for the catalytic performance and to understand the electronic effect of the ligands. In the presence of the catalysts formed in the in situ medium, the coupling of 4-methoxy-1-chlorobenzene with 2,5-dimethoxyphenylboronic acid was performed with overall low yields (Table 3, entries 1–4). While carbene precursor **2** showed the lowest catalytic activity, **3** gave the highest catalytic activity (Table 3, entries 2 and 3). We acquired excellent catalytic activity results using 4-*tert*-butylphenylboronic acid which is a derivative of phenylboronic acid (Table 3, entries 5–8). All compounds were found to be very effective for this coupling reaction and the product yield was between 94–100%.

The C–C bond formation of thianaphthene-2-boronic acid with 4-chloronitrobenzene using an in situ formed Pd–NHC complex as catalyst resulted in low yields and conversions (Table 3, entries 9–12). The usage of the morpholinoethyl substituted benzimidazolium compound **4** with $Pd(OAc)_2$ resulted in higher yields of 2-(4-nitrophenyl)benzo[*b*]thiophene compared to the usage of compounds **1–3**.

Generally, the PEPPSI Pd–NHC complexes showed similar catalytic activity with in situ formed Pd–NHC complexes under the same experiment conditions (Table 3 and Table 4). The 2-morpholinoethyl substituted Pd–NHC complex **8**, on the other hand, displayed very low activity compared to the other three complexes for the coupling of 2,5-dimethoxyphenylboronic acid with 4-methoxy-1-chlorobenzene (Table 4, entry 4). High

Table 3: Suzuki–Miyaura cross-coupling reaction of boronic acid derivatives with aryl halides[a,b].

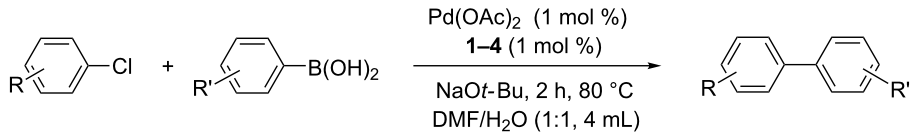

Entry	Aryl halide	Derivatives of boronic acid	LHX	Product	Yield (%)	Conv. (%)
1	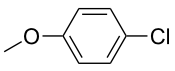	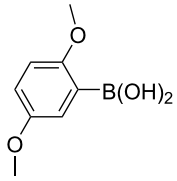	**1**	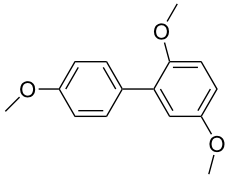	35	68
2			**2**		15	26
3			**3**		77	80
4			**4**		24	33
5	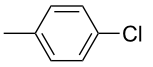	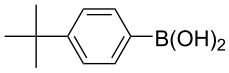	**1**	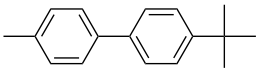	94	96
6			**2**		99	99.7
7			**3**		98	99
8			**4**		99.9	100
9	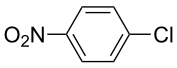	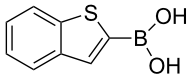	**1**	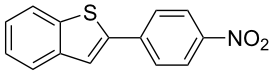	10	38
10			**2**		8	15
11			**3**		6	7
12			**4**		45	48

[a]Reaction conditions: 4-methoxy-1-chlorobenzene, 4-chlorotoluene, 4-chloronitrobenzene (1.0 mmol), $Pd(OAc)_2$ (1.0 mol %), 2,5-dimethoxyphenylboronic acid, 4-*tert*-butylphenylboronic acid, thianaphthene-2-boronic acid (1.5 mmol), NaO*t*-Bu (2.0 mmol), **1–4** (1 mol %), DMF/H_2O (1:1, 4 mL), 80 °C, 2 h. [b]Yields were calculated according to aryl chlorides by using GC or GC–MS.

Table 4: Suzuki–Miyaura cross-coupling reaction of boronic acid derivatives with aryl chlorides[a,b].

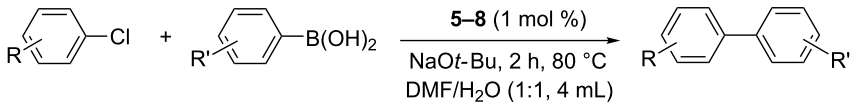

Entry	Aryl chloride	Derivatives of boronic acid	PEPPSI Pd–NHC	Product	Yield (%)	Conv. (%)
1	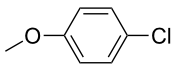	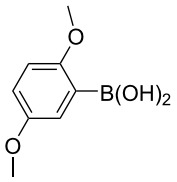	**5**	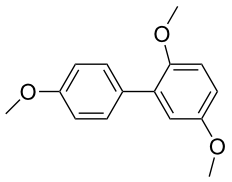	56	67
2			**6**		51	55
3			**7**		59	77
4			**8**		9	25
5	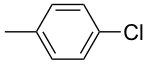	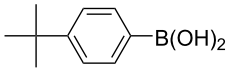	**5**	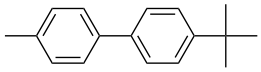	92	99
6			**6**		95	99
7			**7**		93	98
8			**8**		99.9	100
9	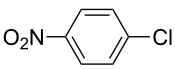	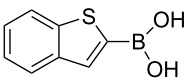	**5**	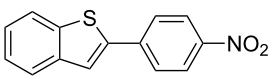	3	5
10			**6**		1	9
11			**7**		35	55
12			**8**		14	30

[a]Reaction conditions: 4-methoxy-1-chlorobenzene, 4-chlorotoluene, 4-chloronitrobenzene (1.0 mmol), 2,5-dimethoxyphenylboronic acid, 4-*tert*-butylphenylboronic acid, thianaphthene-2-boronic acid (1.5 mmol), NaO*t*-Bu (2.0 mmol), **5–8** (1 mol %), DMF/H_2O (1:1, 4 mL), 80 °C, 2 h. [b]Yields were calculated according to aryl chlorides by using GC or GC–MS.

yields were obtained in the presence of low amounts of catalysts **5–8** (1 mol %) in the coupling reaction of 4-*tert*-butylphenylboronic acid with 4-chlorotoluene (Table 4, entries 5–8). All synthesized compounds demonstrated low activity in the coupling of thianaphthene-2-boronic acid with 4-chloronitrobenzene (Table 3, entries 9–12; Table 4, entries 9–12). In C–C bond-forming reactions of different substrates with 2,5-dimethoxyphenylboronic acid and thianaphthene-2-boronic acid, complex **7** was found to be a good catalyst for the synthesis of biaryl systems in comparison to the other complexes. We observed that compounds **4** and **7** were more effective than the other compounds as catalyst (Table 3, entry 12; Table 4 entry 11).

Conclusion

In the present study, a series of benzimidazolium salts (**1–4**) and PEPPSI Pd–NHC complexes (**5–8**) were successfully synthesized and their structures were confirmed via ^{1}H and ^{13}C{^{1}H} NMR, ESI-FTICR-MS (for **2**, **4**, **6–8**), UV–vis, FTIR and elemental analysis. All the compounds exhibited good solubility in organic solvents and were tested in both arylation (for **5–8**) and Suzuki–Miyaura cross-coupling (for **1–8**) reactions. Pd-catalyzed direct intermolecular arylation was investigated using electron-poor, electron-rich or electron-neutral substrates. In general, an electron-neutral group was found to be more effective in the formation of biaryl product. Both in situ generated Pd–NHC and PEPPSI Pd–NHC complexes as catalysts were studied in Suzuki–Miyaura cross-coupling reactions without an inert atmosphere. Both complex types were quite effective in the coupling of 4-chlorotoluene with 4-*tert*-butylphenylboronic acid.

Supporting Information

Supporting Information File 1

Experimental section.
[http://www.beilstein-journals.org/bjoc/content/supplementary/1860-5397-12-9-S1.pdf]

Acknowledgments

This work was financially supported by TUBITAK (1059B141400496) and Erciyes University Research Fund. We thank Dr Nial Wheate and Zehra Elgundi (University of Sydney) for useful comments and critical reading of the paper.

References

1. Wanzlick, H.-W.; Schönherr, H.-J. *Angew. Chem., Int. Ed. Engl.* **1968,** *7,* 141–142. doi:10.1002/anie.196801412
2. Öfele, K. *J. Organomet. Chem.* **1968,** *12,* P42–P43. doi:10.1016/S0022-328X(00)88691-X
3. Mangalum, A.; McMillen, C. D.; Tennyson, A. G. *Inorg. Chim. Acta* **2015,** *426,* 29–38. doi:10.1016/j.ica.2014.11.003
4. Akkoç, S.; Gök, Y.; Akkurt, M.; Tahir, M. N. *Inorg. Chim. Acta* **2014,** *413,* 221–230. doi:10.1016/j.ica.2014.01.015
5. Akkoç, S.; Gök, Y. *Appl. Organomet. Chem.* **2014,** *28,* 854–860. doi:10.1002/aoc.3220
6. Serrano, J. L.; Pérez, J.; García, L.; Sánchez, G.; García, J.; Lozano, P.; Zende, V.; Kapdi, A. *Organometallics* **2015,** *34,* 522–533. doi:10.1021/om501160n
7. Lee, J.-Y.; Ghosh, D.; Lee, J.-Y.; Wu, S.-S.; Hu, C.-H.; Liu, S.-D.; Lee, H. M. *Organometallics* **2014,** *33,* 6481–6492. doi:10.1021/om500834y
8. Hashmi, A. S. K.; Lothschütz, C.; Böhling, C.; Hengst, T.; Hubbert, C.; Rominger, F. *Adv. Synth. Catal.* **2010,** *352,* 3001–3012. doi:10.1002/adsc.201000472
9. Li, Y.; Tan, C.-P.; Zhang, W.; He, L.; Ji, L.-N.; Mao, Z.-W. *Biomaterials* **2015,** *39,* 95–104. doi:10.1016/j.biomaterials.2014.10.070
10. Haque, R. A.; Choo, S. Y.; Budagumpi, S.; Iqbal, M. A.; Al-Ashraf, A. A. *Eur. J. Med. Chem.* **2015,** *90,* 82–92. doi:10.1016/j.ejmech.2014.11.005
11. Gök, Y.; Akkoç, S.; Albayrak, S.; Akkurt, M.; Tahir, M. N. *Appl. Organomet. Chem.* **2014,** *28,* 244–251. doi:10.1002/aoc.3116
12. Boehme, C.; Frenking, G. *J. Am. Chem. Soc.* **1996,** *118,* 2039–2046. doi:10.1021/ja9527075
13. Viciu, M. S.; Navarro, O.; Germaneau, R. F.; Kelly, R. A.; Sommer, W.; Marion, N.; Stevens, E. D.; Cavallo, L.; Nolan, S. P. *Organometallics* **2004,** *23,* 1629–1635. doi:10.1021/om034319e
14. Zhang, T.; Shi, M.; Zhao, M. *Tetrahedron* **2008,** *64,* 2412–2418. doi:10.1016/j.tet.2008.01.017
15. Polshettiwar, V.; Varma, R. S. *Tetrahedron* **2008,** *64,* 4637–4643. doi:10.1016/j.tet.2008.02.098
16. Górna, M.; Szulmanowicz, M. S.; Gniewek, A.; Tylus, W.; Trzeciak, A. M. *J. Organomet. Chem.* **2015,** *785,* 92–99. doi:10.1016/j.jorganchem.2015.03.009
17. Demir, S.; Özdemir, İ.; Çetinkaya, B.; Arslan, H.; VanDerveer, D. *Polyhedron* **2011,** *30,* 195–200. doi:10.1016/j.poly.2010.10.015
18. Kantchev, E. A. B.; Ying, J. Y. *Organometallics* **2009,** *28,* 289. doi:10.1021/om8008475
19. Zhou, X.-X.; Shao, L.-X. *Synthesis* **2011,** 3138–3142. doi:10.1055/s-0030-1260169
20. Lin, Y.-C.; Hsueh, H.-H.; Kanne, S.; Chang, L.-K.; Liu, F.-C.; Lin, I. J. B.; Lee, G.-H.; Peng, S.-M. *Organometallics* **2013,** *32,* 3859–3869. doi:10.1021/om4003297
21. O'Brien, C. J.; Kantchev, E. A. B.; Valente, C.; Hadei, N.; Chass, G. A.; Lough, A.; Hopkinson, A. C.; Organ, M. G. *Chem. – Eur. J.* **2006,** *12,* 4743–4748. doi:10.1002/chem.200600251
22. Yang, L.; Zhao, J.; Li, Y.; Ge, K.; Zhuang, Y.; Cao, C.; Shi, Y. *Inorg. Chem. Commun.* **2012,** *22,* 33–36. doi:10.1016/j.inoche.2012.05.017
23. Zhao, J.; Yang, L.; Ge, K.; Chen, Q.; Zhuang, Y.; Cao, C.; Shi, Y. *Inorg. Chem. Commun.* **2012,** *20,* 326–329. doi:10.1016/j.inoche.2012.03.041
24. Yaşar, S.; Şahin, Ç.; Arslan, M.; Özdemir, İ. *J. Organomet. Chem.* **2015,** *776,* 107–112. doi:10.1016/j.jorganchem.2014.10.047
25. Rajabi, F.; Thiel, W. R. *Adv. Synth. Catal.* **2014,** *356,* 1873–1877. doi:10.1002/adsc.201300841
26. John, A.; Modak, S.; Madasu, M.; Katari, M.; Ghosh, P. *Polyhedron* **2013,** *64,* 20–29. doi:10.1016/j.poly.2013.01.062
27. Akkoç, S.; Gök, Y. *Inorg. Chim. Acta* **2015,** *429,* 34–38. doi:10.1016/j.ica.2015.01.019

28. Viciu, M. S.; Germaneau, R. F.; Nolan, S. P. *Org. Lett.* **2002,** *4,* 4053–4056. doi:10.1021/ol026745m
29. Kinzel, T.; Zhang, Y.; Buchwald, S. L. *J. Am. Chem. Soc.* **2010,** *132,* 14073–14075. doi:10.1021/ja1073799
30. Akkoc, S.; Gok, Y. *J. Coord. Chem.* **2013,** *66,* 1396–1404. doi:10.1080/00958972.2013.786053
31. Sun, J.; Fu, Y.; He, G.; Sun, X.; Wang, X. *Appl. Catal., B* **2015,** *165,* 661–667. doi:10.1016/j.apcatb.2014.10.072
32. Liu, D.-X.; Gong, W.-J.; Li, H.-X.; Gao, J.; Li, F.-L.; Lang, J.-P. *Tetrahedron* **2014,** *70,* 3385–3389. doi:10.1016/j.tet.2014.03.098
33. Ratniyom, J.; Chaiprasert, T.; Pramjit, S.; Yotphan, S.; Sangtrirutnugul, P.; Srisuratsiri, P.; Kongsaeree, P.; Kiatisevi, S. *J. Organomet. Chem.* **2014,** *752,* 161–170. doi:10.1016/j.jorganchem.2013.12.015
34. Zhong, L.; Chokkalingam, A.; Cha, W. S.; Lakhi, K. S.; Su, X.; Lawrence, G.; Vinu, A. *Catal. Today* **2015,** *243,* 195–198. doi:10.1016/j.cattod.2014.08.038
35. Melvin, P. R.; Nova, A.; Balcells, D.; Dai, W.; Hazari, N.; Hruszkewycz, D. P.; Shah, H. P.; Tudge, M. T. *ACS Catal.* **2015,** *5,* 3680–3688. doi:10.1021/acscatal.5b00878

License and Terms

BEILSTEIN JOURNAL OF ORGANIC CHEMISTRY

Versatile deprotonated NHC: C,N-bridged dinuclear iridium and rhodium complexes

Albert Poater

Full Research Paper

Open Access

Address:
Institut de Química Computacional i Catàlisi, Departament de Química, Universitat de Girona, Campus de Montilivi, E-17071 Girona, Spain

Email:
Albert Poater - albert.poater@udg.edu

Keywords:
DFT; head-to-head; head-to-tail; iridium; isomerization; N-heterocyclic carbene; rhodium

Beilstein J. Org. Chem. **2016,** *12,* 117–124.
doi:10.3762/bjoc.12.13

Received: 29 November 2015
Accepted: 08 January 2016
Published: 22 January 2016

This article is part of the Thematic Series "N-Heterocyclic carbenes".

Guest Editor: S. P. Nolan

Abstract

Bearing the versatility of N-heterocyclic carbene (NHC) ligands, here density functional theory (DFT) calculations unravel the capacity of coordination of a deprotonated NHC ligand (pNHC) to generate a doubly C2,N3-bridged dinuclear complex. Here, in particular the discussion is based on the combination of the deprotonated 1-arylimidazol (aryl = mesityl (Mes)) with [M(cod)(μ-Cl)] (M = Ir, Rh) generated two geometrical isomers of complex [M(cod){μ-$C_3H_2N_2$(Mes)-κC2,κN3}$]_2$). The latter two isomers display conformations head-to-head (H-H) and head-to-tail (H-T) of C_S and C_2 symmetry, respectively. The isomerization from the H-H to the H-T conformation is feasible, whereas next substitutions of the cod ligand by CO first, and PMe_3 later confirm the H-T coordination as the thermodynamically preferred. It is envisaged the exchange of the metal, from iridium to rhodium, confirming here the innocence of the nature of the metal for such arrangements of the bridging ligands.

Introduction

In the framework of organometallic chemistry, N-heterocyclic carbenes (NHC) centre a well stablished class of relatively new ligands since in 1991 Arduengo and collaborators isolated the first stable NHC of the imidazole type with bulky N-substituents [1]. However the existence of stable NHCs was before postulated by Wanzlick et al. during the 1960s [2-4] and supported later by Öfele [5,6]. NHCs have become useful ligands in many transition metal-catalyzed reactions, stimulating the study of the unique features of the M–NHC bond [7,8], which favored the synthesis of new NHCs and to their use as ligands in transition metal complexes. The latter complexes were usually obtained by an easy replacement of a phosphine by the new NHC ligand, displaying a very high stability under many catalytic conditions. Furthermore, NHCs exhibit better activity, despite bearing its carbene functionality. Of course, these good results in basic research supposed and explosion of industrial efforts to design the right metal NHC-based catalyst for any kind of reaction. Anyway, neither a unique nor a few list of

catalysts turned out to be effective for any catalytic reaction, but some successful applications were achieved in the field of Ru-catalyzed metathesis of olefins [9-12], Ir-catalyzed hydrogenation [13,14], Pd-catalyzed C=C coupling reactions [15,16], Ir-catalyzed CO_2 fixation [17,18], and/or functionalization of alkenes and alkynes by Au-catalyzed reactions [19-21].

It is not feasible to exclude the asymmetry thanks to the modification of any of the two groups on the imidazolin-2-ylidene ring for two reasons. First, H atoms on the backbone of the either saturated or unsaturated imidazolin-2-ylidene ring suppose a key structural feature for the introduction of asymmetry in the NHC ring. Second, these H atoms might transform the corresponding NHCs in potentially efficient chiral NHCs in asymmetric synthesis [22]. Following with the latter recipe, protic NHCs (pNHCs) consist of the presence of a N-bound H atom. Although most of the studies on NHCs together with metal moieties are based on the interaction of the carbene carbon of the NHC with the metal [23-26], the high instability due the NH group of the pNHCs can induce secondary interactions leading to bifunctional catalysis [27,28], substrate recognition [29] and/or biological systems [30,31]. Among the synthetic methodologies to access to pNHC metal complexes [32-40], recently *N*-arylimine functionalized pNHC iridium complexes were obtained using excess of $[Ir(cod)(\mu\text{-}Cl)]_2$ [41], and next deprotonation of the pNHC leads to an equilibrium between a mononuclear complex containing a C-bound anionic imidazolide [42-44] and its dimer [45-58], where the NHC moiety binds in a μ-C,N bridging mode (see Scheme 1) [44].

Even though during the last two decades thousands of papers have presented and described the NHC based catalysis, bearing a carbene–metal coordination [7], catalytically few efforts have been dedicated to other types of coordination of the NHC with the metal. Braunstein and collaborators have smartly faced the challenge to mix the reactivity of both coordinative atoms of pNHCs [59], either the carbene carbon or the non-substituted nitrogen, i.e., the N from the former N–H group, bearing 1-arylimidazolide ligands. Scheme 2 contains the general scheme that leads to a particular case of the "equilibrium" be-

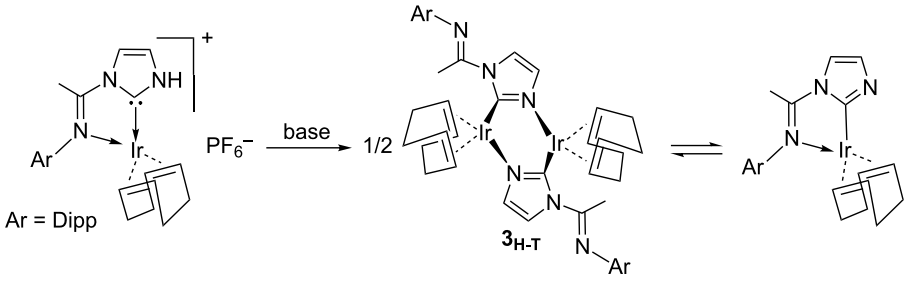

Scheme 1: Equilibrium between the monoiridum complex bearing a C-bound anionic imidazolide and its corresponding dimer, once deprotonated a pNHC.

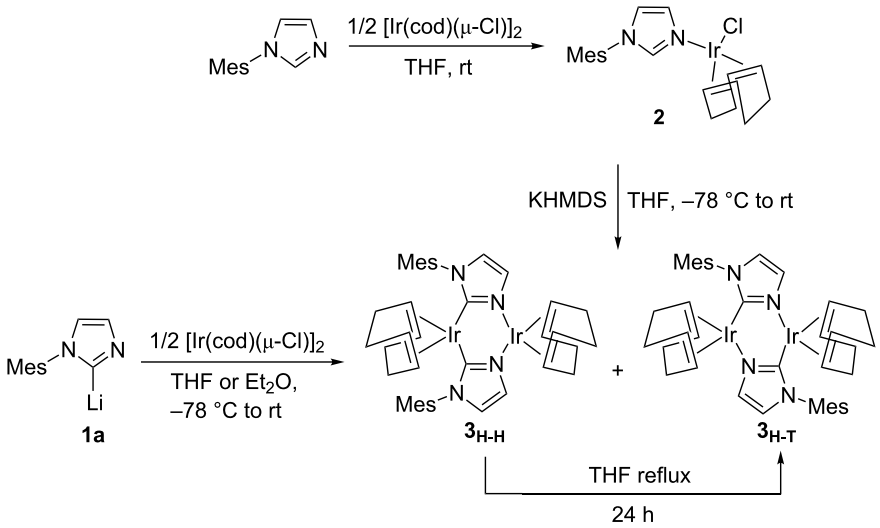

Scheme 2: Experimental routes to the "equilibrium" between $\mathbf{3_{H\text{-}H}}$ and $\mathbf{3_{H\text{-}T}}$.

tween two dinuclear complexes, labelled $\mathbf{3_{H\text{-}H}}$ and $\mathbf{3_{H\text{-}T}}$ (where H-H = head-to-head and H-T = head-to-tail). By DFT calculations here we contribute in the understanding of the thermodynamics of the subsequent C,N-bridged dinuclear iridium and rhodium complexes [59], and the facility for the interconversion between these latter dimeric species.

Results

To shed light about both isomers of the dinuclear complex **3**, $\mathbf{3_{H\text{-}H}}$ and $\mathbf{3_{H\text{-}T}}$, we envisaged DFT calculations (see Figure 1). The optimized geometry of $\mathbf{3_{H\text{-}H}}$ is in perfect agreement with the X-ray structure [60] (rmsd = 0.065 Å and 1.1° for the selected main distances and angles) [61,62]. In agreement with experiments that indicated $\mathbf{3_{H\text{-}T}}$ is 5.2 kcal/mol more stable than $\mathbf{3_{H\text{-}H}}$, which means that with free tautomerism only the thermodynamic isomer $\mathbf{3_{H\text{-}T}}$ would not coexist with $\mathbf{3_{H\text{-}H}}$, but as the unique isomer [59].

Furthermore, the strength of the two H-H and H-T arrangements of the bridging pNHC ligand with the iridium was examined with the Mayer bond order (MBO) [63], which is valuable for evaluating bonding in main group compounds, but has been also used as a tool for the characterization of transition metal systems [64,65]. For $\mathbf{3_{H\text{-}H}}$ the NHC coordination to the metal through the carbene carbon, the MBO is 0.874, whereas through the N atom is only 0.438. The type of coordination of pNHCs around the iridium atoms, either H-H or H-T, does not modify significantly the strength of the Ir–C and Ir–N bonds. For $\mathbf{3_{H\text{-}T}}$ the MBO values are 0.841 and 0.410. Further, the structure of the dinuclear complexes may be determined by steric effects of both monomeric moieties. To evaluate only the sterics, topographic steric maps were used, which are calculated through the SambVca package developed by Cavallo et al. [66]. This analysis allows the rationalization of the first coordination sphere around metal centres where catalytic processes take place. Basically the method calculates the buried volume of a given ligand [67] based on the quantification of the proportion of the first coordination sphere of the metal occupied by this ligand. The encumbered zones (color-coded in brown) belong to the part of the ligand that protrudes in the direction of the reacting groups, thus restricting the space they can fill, whereas empty zones (color coded in blue) correspond to the part where the ligand retracts from the reacting groups [68,69].

For $\mathbf{3_{H\text{-}H}}$ the percentage of buried volume (%VBur) is 26.2 bearing a metal–carbene coordination, whereas it decreases to only 19.1 when the NHC bonds to the metal through the deprotonated nitrogen atom. However, the steric maps in Figure 2 confirm completely that the system prefers the latter N-bound coordination. Splitting the map into four quadrants the carbene coordination reveals a quadrant highly sterically hindered (37.2) due to the rotation of the aromatic ring on the NHC which facilitates the allocation of such a NHC ligand in the dinuclear complexes. The other quadrant where this aromatic ring participates displays a value of 29.2, whereas the other two are innocuous for the metal sphere with low values of 19.3 and 19.1. On the other hand, the coordination of the NHC through the nitrogen is sterically innocent towards the metal sphere because the four quadrants show low sterical occupations (19.1, 18.7, 19.4 and 19.1). Thus, the N-bound coordination of the NHC can be regarded as the perfect coordination to facilitate a free "first coordination sphere", with enough space for allowing the for-

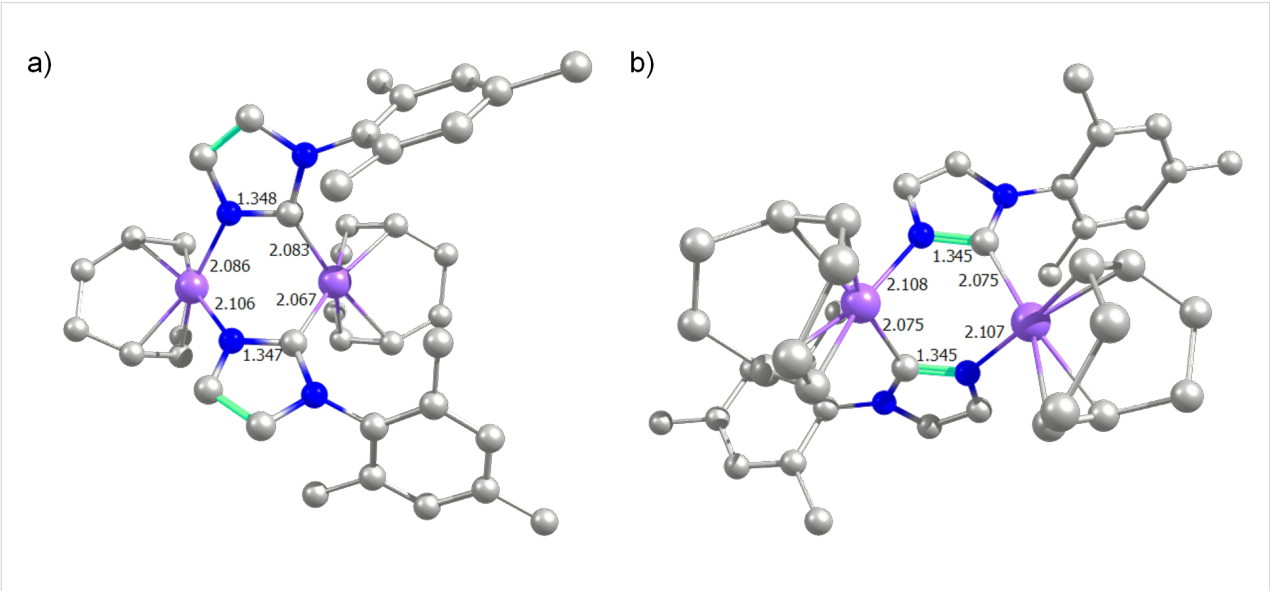

Figure 1: View of the molecular structure of a) $\mathbf{3_{H\text{-}H}}$ and b) $\mathbf{3_{H\text{-}T}}$. Hydrogen atoms have been omitted for the sake of clarity (main distances in Å).

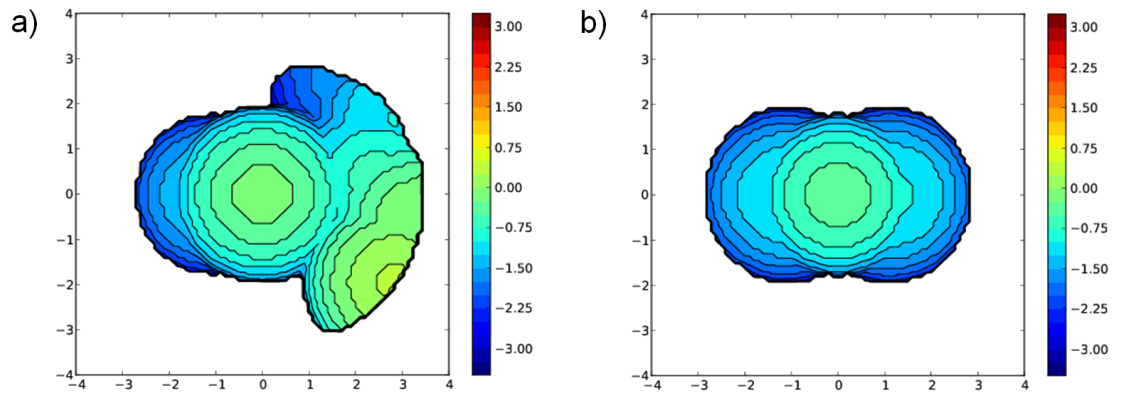

Figure 2: Steric maps for the NHC ligand of $\mathbf{3_{H\text{-}H}}$, coordinated to iridium by a) carbene or b) nitrogen. The isocontour curves are given in Å. The systems are oriented along the *z*-axis defined by the metal and the coordinating atom bonded to the metal. The two maps are computed with a radius of the sphere equal to 3.5 Å.

mation of a dinuclear complex. For $\mathbf{3_{H\text{-}T}}$ the %VBur is nearly identical, displaying values of 26.4 and 19.0, for carbene and nitrogen coordination to the iridium centre, respectively.

Natural bond order (NBO) analysis on the iridium reveal that the two equivalent iridium centres in $\mathbf{3_{H\text{-}T}}$ display a charge on the metal of 0.009*e*, whereas −0.143 and 0.189*e* for $\mathbf{3_{H\text{-}H}}$ for the iridium bonded to two carbene carbons and two nitrogen atoms of the NHC, respectively. This confirms that the metal–carbene coordination allocates more electron density on the metal than through the nitrogen.

Despite the dimeric nature of complex **3**, hypothetically they might be discussed as aggregates of two monomeric moieties. However the coupling between the two metal centres seems demonstrated by removing an electron of the system, thus the expected mixed valent Ir(I)/Ir(II) species turns out to display two identical metal centres that distribute equally the cost of the electrolysis of **3**. Geometrically no asymmetry is observed, and together with the positive charge increase of 0.306*e* on each former Ir(I) centre, shows that the effect on system **3** of the released electron is mainly paid by the metal centres, but also partially spread over the ligands [59].

To follow up the experimental results the tautomerism/metallotropism between pNHC and imidazole ligands in these iridium complexes bearing a doubly C,N-bridged dinuclear core was also computationally studied after the displacement of cod

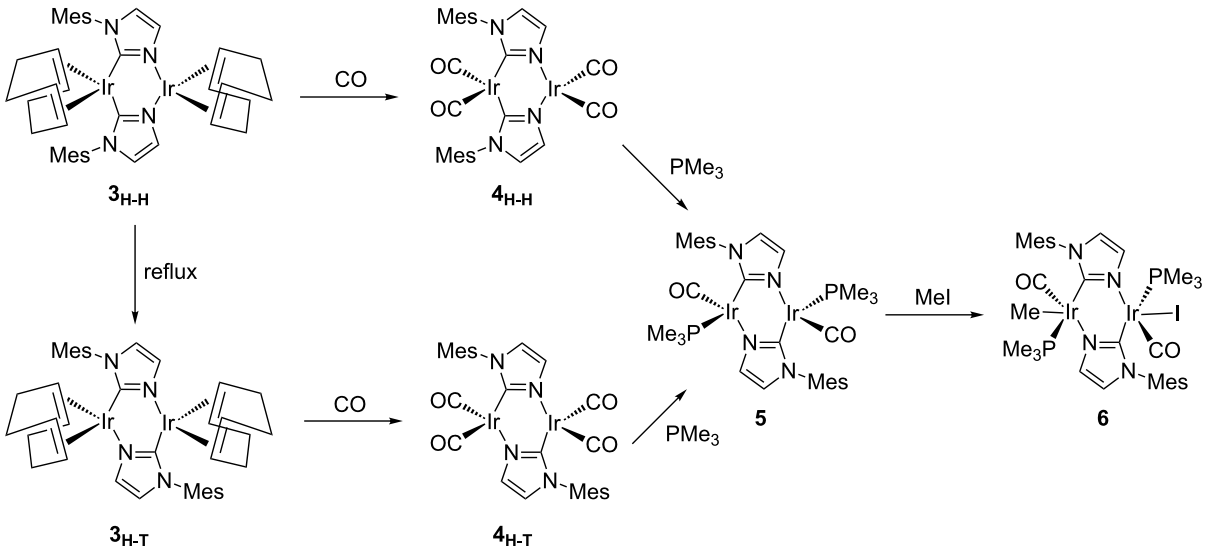

Scheme 3: Equilibrium between complexes **3**–**6**, in the presence of CO, PMe_3, and MeI.

ligands of $\mathbf{3_{H\text{-}H}}$ and $\mathbf{3_{H\text{-}T}}$ by CO in Scheme 3 [59], affording the tetracarbonyl complexes $[M(CO)_2\{\mu\text{-}C_3H_2N_2(Mes)\text{-}\kappa C2,\kappa N3\}]_2$, $\mathbf{4_{H\text{-}H}}$ and $\mathbf{4_{H\text{-}T}}$, respectively. Next we evaluated the substitution of CO ligands by PMe_3 affording complex $[M(CO)(PMe_3)\{\mu\text{-}C_3H_2N_2(Mes)\text{-}\kappa C2,\kappa N3\}]_2$ (**5**) and finally, oxidative addition of MeI to the latter complex **5** afforded the dinuclear complex $[M(CO)_2(PMe_3)_2(Me)I\{\mu\text{-}C_3H_2N_2(Mes)\text{-}\kappa C2,\kappa N3\}]_2$.

In agreement with experiments [59], without reflux conditions, the substitution of cod ligands by CO is extremely favored, being isomer $\mathbf{4_{H\text{-}T}}$ 48.5 kcal/mol more stable than $\mathbf{3_{H\text{-}T}}$, and again the equilibrium between $\mathbf{4_{H\text{-}H}}$ and $\mathbf{4_{H\text{-}T}}$ is displaced towards the latter species, by a difference of 3.0 kcal/mol. Furthermore, the third CO ligand coordination on each iridium atom in **4** was faced but discarded due to a destabilization of 6.7 and 14.8 kcal/mol with respect to $\mathbf{4_{H\text{-}H}}$ and $\mathbf{4_{H\text{-}T}}$, respectively. Basically this lower stability is not only due to the sterical hindrance, but to the preferred quasi perfect square planar type of coordination on each iridium centre (see Figure 3). Going into electronic details, this **3**→**4** transformation also follows the principle of maximum hardness [70,71], i.e., the chemical hardness evolves from 39.6 to 46.7 kcal/mol bearing a H-T type of coordination. This increase of chemical hardness is a consequence of the increased stability of the HOMO, which results in a larger HOMO–LUMO gap [61,65]. To point out that the two types of coordination, H-H and H-T, do not suppose a significant change of chemical hardness, just an increase for H-T of only 0.6 kcal/mol for species **4**, whereas a decrease of 0.1 for species **3**. Thus the electronics do not affect the equilibrium between both arrangements of the bridging ligands, but sterics as stated above. Further, the NBO charges show a decrease of the charge on both metals of 0.777*e* in the **3**→**4** transformation. Despite the π-backdonation of CO the donation to the iridium centres is larger than the corresponding electron density transferred by the cod ligands in species **3**.

$\mathbf{4_{H\text{-}H}}$ and $\mathbf{4_{H\text{-}T}}$ evolves to complex **5**, exchanging one CO by a PMe_3 ligand on each iridium centre, releasing 5.0 and 2.0 kcal/mol, respectively. Bearing an energy difference of 11.7 kcal/mol the H-T isomer is favored with respect to the H-H, in agreement with experiments [59], because the H-H coordination was not locate for **5**, and further thermodynamics do not support the H-H coordination for **5**, with an energy endergonicity of 6.7 kcal/mol with respect the previous corresponding complex **4**. Oxidative addition of MeI to **5** affords complex **6**, in an exergonic release of 16.5 kcal/mol, pointing out that there are several other isomers of complex **6** that differ from the Me and I coordination to each corresponding iridium centre. However all these alternative isomers of complex **6** are placed higher in energy by at least 12.9 kcal/mol (see Supporting Information File 1). The Ir–Ir distance in **6** is only 2.857 Å (see Figure 4), which is a clear proof of concept of a formally metal–metal bonded d^7–d^7 complex, to be compared with complex **5**, where this Ir–Ir distance elongates till 3.497 Å. Furthermore, the MBO for the metal–metal bond reveals a significant value of 0.626 for complex **6** [72], being null for **5** and the previous complexes. Electronically, the charge on metals for complex **6** is 0.334 less charged, which is explained by, among other reasons, the weaker back-bonding from the metal to the CO ligands compared to **5**, which affords the metal–metal interaction in **6**.

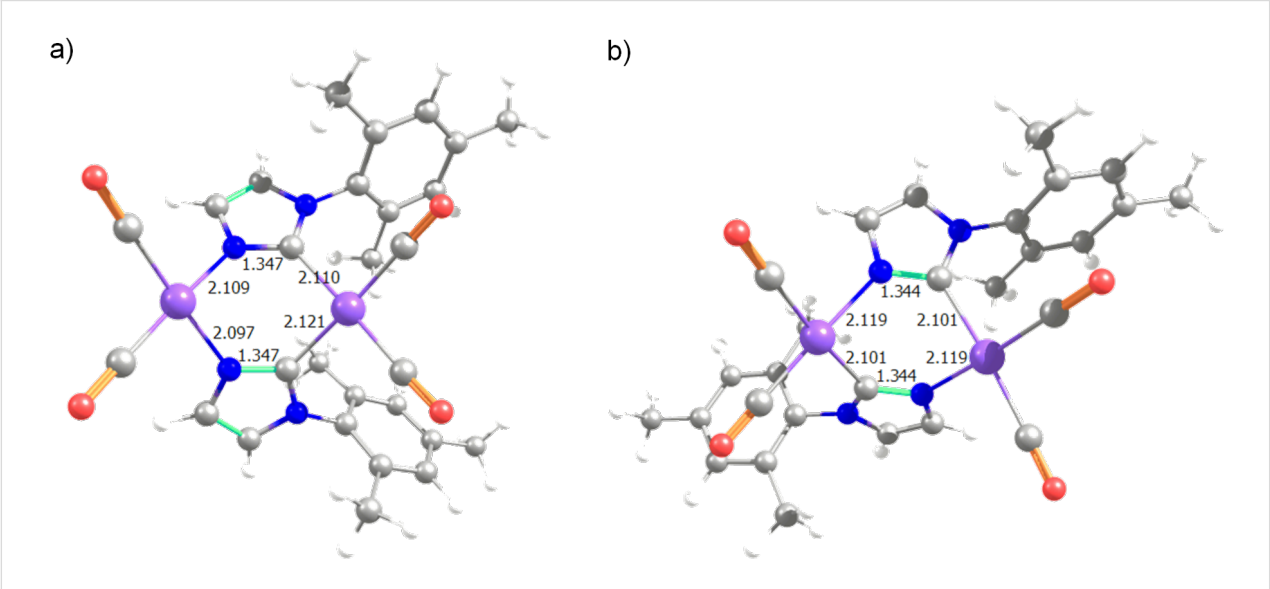

Figure 3: View of the molecular structure of a) $\mathbf{4_{H\text{-}H}}$ and b) $\mathbf{4_{H\text{-}T}}$ (main distances in Å).

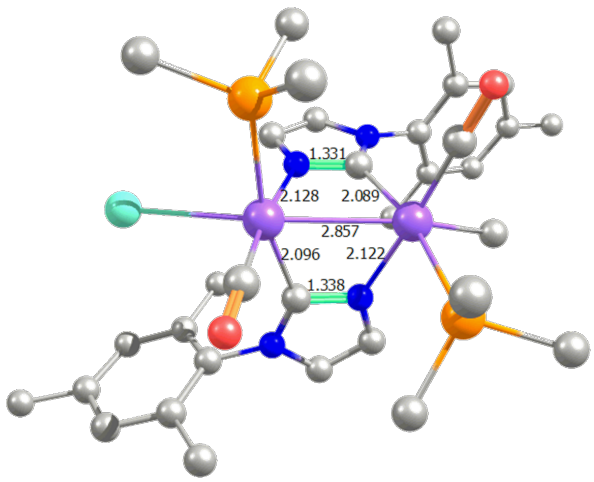

Figure 4: View of the molecular structure of **6**. Hydrogen atoms have been omitted for the sake of clarity (main distances in Å).

To extent the scope of the reactivity of the NHC here, the cod ligands were first exchanged by ethylene, revealing a preferred H-T type of coordination of the NHC (5.1 kcal/mol). On the other hand, the iridium was replaced by rhodium to verify the innocent nature of the electronic properties of the metal, maintaining nearly completely the geometry features for complexes **3**–**6**. Bearing rhodium complex $\mathbf{3}_{\mathbf{H\text{-}T}}$ is again more stable than $\mathbf{3}_{\mathbf{H\text{-}H}}$, even 0.2 kcal/mol more stable. To sum up, no change of behaviour between iridium and homologous rhodium complexes was observed. On the other hand, the evolution from H-T to H-H arrangement was evaluated and mechanistically this process is predicted to be dissociative since neither intramolecular transition state was located nor the linear transits suggested energy barriers affordable at the experimental conditions.

Conclusion

The two possible H-T and H-H arrangements of a bridging NHC here have been studied in detail by DFT calculations. This is a contribution in the understanding of the thermodynamics of the subsequent C,N-bridged dinuclear iridium and rhodium complexes defined by Braunstein et al. [59] and the facility for the interconversion between these latter dimeric species. Steric maps confirm that the H-T is preferred since the metal centres are less sterically hindered, thus revealing the relatively unstable kinetic H-H isomers with respect to the H-T ones. However, screening the evolution from complex **3** to **6**, going through complexes **4** and **5**, the relative thermodynamics show a constant and sharp decay of energy, not due to steric factors, but mainly electronics.

Computational Details

The density functional calculations were performed on all the systems with the Gaussian 09 set of programs [73], Revision D.01, at the BP86 GGA level [74-76], adding the Grimme D3 dispersion term [77]. For iridium and rhodium we used the small-core, quasi-relativistic Stuttgart/Dresden (SDD) effective core potential with an associated valence contracted basis set (standard SDD keywords in Gaussian 09) [78-80]. The electronic configuration of the molecular systems was described with the triple-ζ valence plus polarization (TZVP keyword in Gaussian) basis set on all main group atoms during geometry optimizations [81]. The reported energies have been obtained via single point calculations on the BP86 geometries with triple-ζ valence plus polarization using the M06 functional [82]. Solvent effects, using either tetrahydrofuran, dichloromethane or toluene, were calculated with the polarizable continuous solvation model polarizable continuum model (PCM) model [83,84], and non-electrostatic terms were also included. The cavity is created via a series of overlapping spheres. However, the numbers reported throughout the text here are based on THF because this is the solvent employed in the experiments bearing the H-H to H-T rearrangement [59]. The geometry optimizations were performed without symmetry constraints, and the nature of the extrema was checked by analytical frequency calculations. Furthermore, all the extrema were confirmed by calculation of the intrinsic reaction paths.

The reported free energies in this work include energies obtained at the M06/TZVP level of theory in solvent corrected with zero-point energies at 298.15 K, together with the model of Martin et al. [85] which consists of thermal corrections and entropy effects evaluated at 1354 atm [86-89], with the BP86-d3/TZVP method in the gas phase [90,91].

%VBur calculations: The buried volume calculations were performed with the SambVca package developed by Cavallo et al. [90]. The radius of the sphere around the metal centre was set to 3.5 Å, while for the atoms we adopted the Bondi radii scaled by 1.17, and a mesh of 0.1 Å was used to scan the sphere for buried voxels. The steric maps were evaluated with a development version of the SambVca package.

Supporting Information

Supporting Information File 1

Energies, cartesian coordinates, and 3D view for all DFT optimized species.
[http://www.beilstein-journals.org/bjoc/content/supplementary/1860-5397-12-13-S1.pdf]

Acknowledgements

A.P. thanks the Spanish MINECO for a project CTQ2014-59832-JIN.

References

1. Arduengo III, A. J.; Harlow, R. L.; Kline, M. *J. Am. Chem. Soc.* **1991,** *113,* 361–363. doi:10.1021/ja00001a054
2. Wanzlick, H.-W.; Kleiner, H.-J. *Angew. Chem.* **1961,** *73,* 493. doi:10.1002/ange.19610731408
3. Wanzlick, H.-W. *Angew. Chem., Int. Ed. Engl.* **1962,** *1,* 75–80. doi:10.1002/anie.196200751
4. Wanzlick, H.-W.; Schönherr, H.-J. *Angew. Chem., Int. Ed. Engl.* **1968,** *7,* 141–142. doi:10.1002/anie.196801412
5. Öfele, K. *J. Organomet. Chem.* **1968,** *12,* P42–P43. doi:10.1016/S0022-328X(00)88691-X
6. Öfele, K.; Herberhold, M. *Angew. Chem., Int. Ed. Engl.* **1970,** *9,* 739–740. doi:10.1002/anie.197007391
7. Jacobsen, H.; Correa, A.; Poater, A.; Costabile, C.; Cavallo, L. *Coord. Chem. Rev.* **2009,** *253,* 687–703. doi:10.1016/j.ccr.2008.06.006
8. Jacobsen, H.; Correa, A.; Poater, A.; Costabile, C.; Cavallo, L. *Coord. Chem. Rev.* **2009,** *253,* 2784. doi:10.1016/j.ccr.2009.04.007
9. Vougioukalakis, G.; Grubbs, R. H. *Chem. Rev.* **2010,** *110,* 1746–1787. doi:10.1021/cr9002424
10. Poater, A.; Cavallo, L. *Beilstein J. Org. Chem.* **2015,** *11,* 1767–1780. doi:10.3762/bjoc.11.192
11. Yuan, W.; Wei, Y.; Shi, M. *ChemistryOpen* **2013,** *2,* 63–68. doi:10.1002/open.201300002
12. Credendino, R.; Poater, A.; Ragone, F.; Cavallo, L. *Catal. Sci. Technol.* **2011,** *1,* 1287–1297. doi:10.1039/c1cy00052g
13. Vázquez-Serrano, L. D.; Owens, B. T.; Buriak, J. M. *Chem. Commun.* **2002,** 2518–2519. doi:10.1039/b208403a
14. Lee, H. M.; Jiang, T.; Stevens, E. D.; Nolan, S. P. *Organometallics* **2001,** *20,* 1255–1258. doi:10.1021/om000990x
15. Grasa, G. A.; Viciu, M. S.; Huang, J.; Nolan, S. P. *J. Org. Chem.* **2001,** *66,* 7729–7737. doi:10.1021/jo010613+
16. Marion, N.; Navarro, O.; Mei, J.; Stevens, E. D.; Scott, N. M.; Nolan, S. P. *J. Am. Chem. Soc.* **2006,** *128,* 4101–4111. doi:10.1021/ja057704z
17. Vummaleti, S. V. C.; Talarico, G.; Nolan, S. P.; Cavallo, L.; Poater, A. *Eur. J. Inorg. Chem.* **2015,** 4653–4657. doi:10.1002/ejic.201500905
18. Vummaleti, S. V. C.; Talarico, G.; Nolan, S. P.; Cavallo, L.; Poater, A. *Org. Chem. Front.* **2016,** *3,* 19–23. doi:10.1039/C5QO00281H
19. Dorel, R.; Echavarren, A. M. *Chem. Rev.* **2015,** *115,* 9028–9072. doi:10.1021/cr500691k
20. Nun, P.; Gaillard, S.; Poater, A.; Cavallo, L.; Nolan, S. P. *Org. Biomol. Chem.* **2011,** *9,* 101–104. doi:10.1039/C0OB00758G
21. Nun, P.; Dupuy, S.; Gaillard, S.; Poater, A.; Cavallo, L.; Nolan, S. P. *Catal. Sci. Technol.* **2011,** *1,* 58–61. doi:10.1039/c0cy00055h
22. Hoveyda, A. H.; Schrock, R. R. *Chem. – Eur. J.* **2001,** *7,* 945–950. doi:10.1002/1521-3765(20010302)7:5<945::AID-CHEM945>3.0.CO;2-3
23. Melaimi, M.; Soleilhavoup, M.; Bertrand, G. *Angew. Chem., Int. Ed.* **2010,** *49,* 8810–8849. doi:10.1002/anie.201000165
24. Bourissou, D.; Guerret, O.; Gabbaï, F. P.; Bertrand, G. *Chem. Rev.* **2000,** *100,* 39–92. doi:10.1021/cr940472u
25. de Frémont, P.; Marion, N.; Nolan, S. P. *Coord. Chem. Rev.* **2009,** *253,* 862–892. doi:10.1016/j.ccr.2008.05.018
26. Hahn, F. E.; Jahnke, M. C. *Angew. Chem., Int. Ed.* **2008,** *47,* 3122–3172. doi:10.1002/anie.200703883
27. Kuwata, S.; Ikariya, T. *Chem. – Eur. J.* **2011,** *17,* 3542–3556. doi:10.1002/chem.201003296
28. Kuwata, S.; Ikariya, T. *Chem. Commun.* **2014,** *50,* 14290–14300. doi:10.1039/C4CC04457F
29. Hahn, F. E. *ChemCatChem* **2013,** *5,* 419–430. doi:10.1002/cctc.201200567
30. Hsieh, C.-H.; Pulukkody, R.; Darensbourg, M. Y. *Chem. Commun.* **2013,** *49,* 9326–9328. doi:10.1039/c3cc45091k
31. Brackemeyer, D.; Hervé, A.; Schulte to Brinke, C.; Jahnke, M. C.; Hahn, F. E. *J. Am. Chem. Soc.* **2014,** *136,* 7841–7844. doi:10.1021/ja5030904
32. Hahn, F. E.; Langenhahn, V.; Lügger, T.; Pape, T.; Le Van, D. *Angew. Chem., Int. Ed.* **2005,** *44,* 3759–3763. doi:10.1002/anie.200462690
33. Kösterke, T.; Pape, T.; Hahn, F. E. *J. Am. Chem. Soc.* **2011,** *133,* 2112–2115. doi:10.1021/ja110634h
34. Dobereiner, G. E.; Chamberlin, C. A.; Schley, N. D.; Crabtree, R. H. *Organometallics* **2010,** *29,* 5728–5731. doi:10.1021/om100452g
35. Kösterke, T.; Kösters, J.; Würthwein, E.-U.; Mück-Lichtenfeld, C.; Schulte to Brinke, C.; Lahoz, F.; Hahn, F. E. *Chem. – Eur. J.* **2012,** *18,* 14594–14598. doi:10.1002/chem.201202973
36. Kunz, P. C.; Wetzel, C.; Kögel, S.; Kassack, M. U.; Spingler, B. *Dalton Trans.* **2011,** *40,* 35–37. doi:10.1039/C0DT01089H
37. Das, R.; Hepp, A.; Daniliuc, C. G.; Hahn, F. E. *Organometallics* **2014,** *33,* 6975–6987. doi:10.1021/om501120u
38. Das, R.; Daniliuc, C. G.; Hahn, F. E. *Angew. Chem., Int. Ed.* **2014,** *53,* 1163–1166. doi:10.1002/anie.201308269
39. Hahn, F. E.; Langenhahn, V.; Pape, T. *Chem. Commun.* **2005,** 5390–5392. doi:10.1039/b510996e
40. Ruiz, J.; García, G.; Mosquera, M. E. G.; Perandones, B. F.; Gonzalo, M. P.; Vivanco, M. *J. Am. Chem. Soc.* **2005,** *127,* 8584–8585. doi:10.1021/ja042879e
41. He, F.; Braunstein, P.; Wesolek, M.; Danopoulos, A. A. *Chem. Commun.* **2015,** *51,* 2814–2817. doi:10.1039/C4CC10109J
42. Hill, C.; Bosold, F.; Harms, K.; Lohrenz, J. C. W.; Marsch, M.; Schmieczek, M.; Boche, G. *Chem. Ber./Recl.* **1997,** *130,* 1201–1212. doi:10.1002/cber.19971300907
43. Hilf, C.; Bosold, F.; Harms, K.; Marsch, M.; Boche, G. *Chem. Ber./Recl.* **1997,** *130,* 1213–1221. doi:10.1002/cber.19971300908
44. Marchenko, A. P.; Koidan, H. N.; Pervak, I. I.; Huryeva, A. N.; Zarudnitskii, E. V.; Tolmachev, A. A.; Kostyuk, A. N. *Tetrahedron Lett.* **2012,** *53,* 494–496. doi:10.1016/j.tetlet.2011.11.054
45. Beveridge, K. A.; Bushnell, G. W.; Stobart, S. R.; Atwood, J. L.; Zaworotko, M. J. *Organometallics* **1983,** *2,* 1447–1451. doi:10.1021/om50004a035
46. Bushnell, G. W.; Fjeldsted, D. O. K.; Stobart, S. R.; Zaworotko, M. J.; Knox, S. A. R.; MacPherson, K. A. *Organometallics* **1985,** *4,* 1107–1114. doi:10.1021/om00125a029
47. Brost, R. D.; Stobart, S. R. *Inorg. Chem.* **1989,** *28,* 4307–4308. doi:10.1021/ic00323a001
48. Brost, R. D.; Fjeldsted, D. O. K.; Stobart, S. R. *J. Chem. Soc., Chem. Commun.* **1989,** 488–490. doi:10.1039/c39890000488
49. Lichtenberger, D. L.; Copenhaver, A. S.; Gray, H. B.; Marshall, J. L.; Hopkins, M. D. *Inorg. Chem.* **1988,** *27,* 4488–4493. doi:10.1021/ic00297a030
50. Bonati, F.; Oro, L. A.; Pinillos, M. T.; Tejel, C.; Bovio, B. *J. Organomet. Chem.* **1994,** *465,* 267–274. doi:10.1016/0022-328X(94)87065-9
51. Yuan, Y.; Jiménez, M. V.; Sola, E.; Lahoz, F. J.; Oro, L. A. *J. Am. Chem. Soc.* **2002,** *124,* 752–753. doi:10.1021/ja016753i
52. Bushnell, G. W.; Fjeldsted, D. O. K.; Stobart, S. R.; Zaworotko, M. J. *J. Chem. Soc., Chem. Commun.* **1983,** 580–581. doi:10.1039/c39830000580

53. Atwood, J. L.; Beveridge, K. A.; Bushnell, G. W.; Dixon, K. R.; Eadie, D. T.; Stobart, S. R.; Zaworotko, M. J. *Inorg. Chem.* **1984,** *23,* 4050–4057. doi:10.1021/ic00192a042
54. Bushnell, G. W.; Fjeldsted, D. O. K.; Stobart, S. R.; Wang, J. *Organometallics* **1996,** *15,* 3785–3787. doi:10.1021/om9601864
55. Coleman, A. W.; Eadie, D. T.; Stobart, S. R.; Zaworotko, M. J.; Atwood, J. L. *J. Am. Chem. Soc.* **1982,** *104,* 922–923. doi:10.1021/ja00367a076
56. Bushnell, G. W.; Decker, M. J.; Eadie, D. T.; Stobart, S. R.; Vefghi, R.; Atwood, J. L.; Zaworotko, M. J. *Organometallics* **1985,** *4,* 2106–2111. doi:10.1021/om00131a007
57. Fjeldsted, D. O. K.; Stobart, S. R.; Zaworotko, M. J. *J. Am. Chem. Soc.* **1985,** *107,* 8258–8259. doi:10.1021/ja00312a074
58. Arthurs, M. A.; Bickerton, J.; Stobart, S. R.; Wang, J. *Organometallics* **1998,** *17,* 2743–2750. doi:10.1021/om970554j
59. He, F.; Ruhlmann, L.; Gisselbrecht, J.-P.; Choua, S.; Orio, M.; Wesolek, M.; Danopoulos, A. A.; Braunstein, P. *Dalton Trans.* **2015,** *44,* 17030–17044. doi:10.1039/C5DT02403J
60. Root-mean-square deviation (rmsd) is calculated for distances and angles: $s_{n-1} = [\sum_{i=1\rightarrow N} (CV - EV)^2/(N - 1)]^{1/2}$, where CV means calculated value, EV means experimental value (X-ray data), and N is the number of distances or angles taken into account.
61. Costas, M.; Ribas, X.; Poater, A.; López Balvuena, J. M.; Xifra, R.; Company, A.; Duran, M.; Solà, M.; Llobet, A.; Corbella, M.; Usón, M. A.; Mahía, J.; Solans, X.; Shan, X.; Benet-Buchholz, J. *Inorg. Chem.* **2006,** *45,* 3569–3581. doi:10.1021/ic051800j
62. Mola, J.; Rodríguez, M.; Romero, I.; Llobet, A.; Parella, T.; Poater, A.; Duran, M.; Solà, M.; Benet-Buchholz, J. *Inorg. Chem.* **2006,** *45,* 10520–10529. doi:10.1021/ic061126l
63. Mayer, I. *Int. J. Quantum Chem.* **1984,** *26,* 151–154. doi:10.1002/qua.560260111
64. Poater, A.; Ragone, F.; Correa, A.; Cavallo, L. *J. Am. Chem. Soc.* **2009,** *131,* 9000–9006. doi:10.1021/ja902552m
65. Poater, A. *J. Phys. Chem. A* **2009,** *31,* 9030–9040. doi:10.1021/jp9040716
66. Poater, A.; Cosenza, B.; Correa, A.; Giudice, S.; Ragone, F.; Scarano, V.; Cavallo, L. *Eur. J. Inorg. Chem.* **2009,** 1759–1766. doi:10.1002/ejic.200801160
67. Bosson, J.; Poater, A.; Cavallo, L.; Nolan, S. P. *J. Am. Chem. Soc.* **2010,** *132,* 13146–13149. doi:10.1021/ja104961s
68. Poater, A.; Ragone, F.; Mariz, R.; Dorta, R.; Cavallo, L. *Chem. – Eur. J.* **2010,** *16,* 14348–14353. doi:10.1002/chem.201001938
69. Giovanni, C.; Poater, A.; Benet-Buchholz, J.; Cavallo, L.; Solà, M.; Llobet, A. *Chem. – Eur. J.* **2014,** *20,* 3898–3902. doi:10.1002/chem.201304699
70. Parr, R. G.; Donnelly, R. A.; Levy, M.; Palke, W. E. *J. Chem. Phys.* **1978,** *68,* 3801–3807. doi:10.1063/1.436185
71. Parr, R. G.; Pearson, R. G. *J. Am. Chem. Soc.* **1983,** *105,* 7512–7516. doi:10.1021/ja00364a005
72. Poater, A.; Moradell, S.; Pinilla, E.; Poater, J.; Solà, M.; Martínez, M. A.; Llobet, A. *Dalton Trans.* **2006,** 1188–1196. doi:10.1039/B511625M
73. *Gaussian 09,* Revision D.01; Gaussian, Inc.: Wallingford, CT, 2009.
74. Becke, A. D. *Phys. Rev. A* **1988,** *38,* 3098–3100. doi:10.1103/PhysRevA.38.3098
75. Perdew, J. P. *Phys. Rev. B* **1986,** *33,* 8822–8824. doi:10.1103/PhysRevB.33.8822
76. Perdew, J. P. *Phys. Rev. B* **1986,** *34,* 7406. doi:10.1103/PhysRevB.34.7406
77. Grimme, S.; Antony, J.; Ehrlich, S.; Krieg, H. *J. Chem. Phys.* **2010,** *132,* 154104. doi:10.1063/1.3382344
78. Häussermann, U.; Dolg, M.; Stoll, H.; Preuss, H.; Schwerdtfeger, P.; Pitzer, R. M. *Mol. Phys.* **1993,** *78,* 1211–1224. doi:10.1080/00268979300100801
79. Küchle, W.; Dolg, M.; Stoll, H.; Preuss, H. *J. Chem. Phys.* **1994,** *100,* 7535–7542. doi:10.1063/1.466847
80. Leininger, T.; Nicklass, A.; Stoll, H.; Dolg, M.; Schwerdtfeger, P. *J. Chem. Phys.* **1996,** *105,* 1052–1059. doi:10.1063/1.471950
81. Schäfer, A.; Horn, H.; Ahlrichs, R. *J. Chem. Phys.* **1992,** *97,* 2571–2577. doi:10.1063/1.463096
82. Zhao, Y.; Truhlar, D. G. *Theor. Chem. Acc.* **2008,** *120,* 215–241. doi:10.1007/s00214-007-0310-x
83. Barone, V.; Cossi, M. *J. Phys. Chem. A* **1998,** *102,* 1995–2001. doi:10.1021/jp9716997
84. Tomasi, J.; Persico, M. *Chem. Rev.* **1994,** *94,* 2027–2094. doi:10.1021/cr00031a013
85. Martin, R. L.; Hay, P. J.; Pratt, L. R. *J. Phys. Chem. A* **1998,** *102,* 3565–3573. doi:10.1021/jp980229p
86. Poater, A.; Pump, E.; Vummaleti, S. V. C.; Cavallo, L. *J. Chem. Theory Comput.* **2014,** *10,* 4442–4448. doi:10.1021/ct5003863
87. Pump, E.; Slugovc, C.; Cavallo, L.; Poater, A. *Organometallics* **2015,** *34,* 3107–3111. doi:10.1021/om501246q
88. Urbina-Blanco, C. A.; Poater, A.; Lebl, T.; Manzini, S.; Slawin, A. M. Z.; Cavallo, L.; Nolan, S. P. *J. Am. Chem. Soc.* **2013,** *135,* 7073–7079. doi:10.1021/ja402700p
89. Manzini, S.; Poater, A.; Nelson, D. J.; Cavallo, L.; Slawin, A. M. Z.; Nolan, S. P. *Angew. Chem., Int. Ed.* **2014,** *53,* 8995–8999. doi:10.1002/anie.201403770
90. Manzini, S.; Poater, A.; Nelson, D. J.; Cavallo, L.; Nolan, S. P. *Chem. Sci.* **2014,** *5,* 180–188. doi:10.1039/C3SC52612G
91. García-Melchor, M.; Pacheco, M. C.; Nájera, C.; Lledós, A.; Ujaque, G. *ACS Catal.* **2012,** *2,* 135–144. doi:10.1021/cs200526x

License and Terms

BEILSTEIN JOURNAL OF ORGANIC CHEMISTRY

Simple activation by acid of latent Ru-NHC-based metathesis initiators bearing 8-quinolinolate co-ligands

Julia Wappel[1], Roland C. Fischer[2], Luigi Cavallo[3], Christian Slugovc[1] and Albert Poater[*3,4]

Full Research Paper

Open Access

Address:
[1]Institute for Chemistry and Technology of Materials, Graz University of Technology, NAWI Graz, Stremayrgasse 9, 8010 Graz, Austria, [2]Institute of Inorganic Chemistry, Graz University of Technology, Stremayrgasse 9, 8010 Graz, Austria, [3]KAUST Catalysis Center, Physical Sciences and Engineering Division, King Abdullah University of Science and Technology, Thuwal 23955-6900, Saudi Arabia and [4]Institut de Química Computacional i Catàlisi, Departament de Química, Universitat de Girona, Campus de Montilivi, E-17071 Girona, Spain

Email:
Albert Poater[*] - albert.poater@udg.edu

* Corresponding author

Keywords:
acid; activation by acid; metathesis; polymer; quinolin; ruthenium; triggerable

Beilstein J. Org. Chem. **2016,** *12,* 154–165.
doi:10.3762/bjoc.12.17

Received: 27 November 2015
Accepted: 14 January 2016
Published: 28 January 2016

This article is part of the Thematic Series "N-Heterocyclic carbenes".

Guest Editor: S. P. Nolan

Abstract

A straightforward synthesis utilizing the ring-opening metathesis polymerization (ROMP) reaction is described for acid-triggered N,O-chelating ruthenium-based pre-catalysts bearing one or two 8-quinolinolate ligands. The innovative pre-catalysts were tested regarding their behavior in ROMP and especially for their use in the synthesis of poly(dicyclopentadiene) (pDCPD). Bearing either the common phosphine leaving ligand in the first and second Grubbs olefin metathesis catalysts, or the Ru–O bond cleavage for the next Hoveyda-type catalysts, this work is a step forward towards the control of polymer functionalization and living or switchable polymerizations.

Introduction

The modulation of the activity of enzymes by chemical triggers, e.g., by allosteric binding is ubiquitous in nature [1,2], but exploiting similar strategies for synthetic catalysts is still in its infancy [3-5]. Prominent examples in catalytic polymerization [6,7] comprise the regulation of molecular weight by allosteric effects [8,9] or influencing the polymers' microstructure upon changing the monomer pressure [10]. Such kind of regulation of the catalysts activity does not only comprise a switching on of a particular feature but also the switching off of this feature upon another (different) stimulus. A simpler but related concept is to turn a latent catalyst [11] or initiator (i.e., ideally a completely inactive pre-catalyst/initiator) into an active form by an external trigger [12]. This principle is well and long known and frequently exploited in polymer chemistry where thermally or

photochemically switchable initiators are the key for many applications of, e.g., radically or cationically prepared polymers [13-15].

Focusing on the origin of organic synthesis, basically based on reactions that drive to the formation of carbon–carbon bonds [16], olefin metathesis turns out to be one potential route to get unsaturated molecules bearing C–C double bonds [17-21], thus by extension polymers, as well. Olefin metathesis polymerizations are transition metal-mediated processes which emerged as powerful alternatives to these conventional polymerization methods [22,23]. Thus, it is not surprising that a series of latent but triggerable initiators have been disclosed in the last years [24-26]. The latent initiators are ideal if they have the capacity of storage in combination with the monomer for a long period [27]. Then the reaction only initiates once an appropriate exogenous stimulus is exerted [28,29]. Amongst this important property, the latent initiator should be as insensitive as possible to any other potentially present chemical, most importantly oxygen and water [30]. Particularly for the latter reason ruthenium based latent initiators play the most important role in literature [24,31-33].

Last but not least, bearing in mind changes in activity or levels of transforming growth factor-beta (TGF-beta) are associated with a broad variety of diseases and that TGF-beta is biologically inert when takes part of the complex that bears its corresponding peptide [34]. From this latter latent complex, most available immunoassays require controlled activation by acid to release the TGF-beta. On the other hand, myostatin belongs to the transforming growth factor 13 superfamily, known because it decreases the skeletal muscle mass. Bearing the fact that experiments have shown that myostatin activity is detected only after activation by acid [35], myostatin demonstrates to be a latent complex, and can be transported more easily. Once described the latter successful practical application of the acid triggered activation of an enzyme, here, at a chemical molecular level, we unravel the performance of the acid triggered N,O-chelating ruthenium based pre-catalysts [36] bearing one or two 8-quinolinolate ligands.

Results and Discussion

Synthesis and characterization

Herein we investigate 8-hydroxyquinoline derivatives as the chelating, "pacifying" ligands. 8-Hydroxyquinoline and its derivatives are known to be excellent ligands for many transition metals [37]. They can be readily electronically modified and many derivatives are commercially available. Furthermore, 8-hydroxyquinoline ligands are generally very cheap. Surprisingly this class of ligands is not frequently used in transition metal chemistry [38-40].

The synthesis involved the reaction of N-heterocyclic carbene bearing precursor complexes **M31**, **HovII** or **M32** with excess of 5,7-dichloro-8-hydroxyquinoline or 5,7-dibromo-8-hydroxyquinoline in the presence of excess Cs_2CO_3 as the base (see Scheme 1). The silver-free method [41] resulted in any case in the formation of at least two new products (as evidenced by thin-layer chromatography) which were separated by means of column chromatography. All obtained complexes are very stable in the solid state and can be stored for several days in solution in the presence of oxygen without any sign of decomposition. Most striking, all complexes possess an outstanding solubility in nonpolar solvents such as *n*-pentane as well as in nonpolar substrates such as dicylopentadiene (DCPD). Both properties are desired properties for employing the compounds as initiators in solvent free polymerizations.

In case of the reaction of **M31** with 5,7-dichloro-8-hydroxyquinoline two products could be isolated and characterized. The major product **1a** resulted from the exchange of one chloride ligand from **M31** for the oxygen of the quinolinolate and exchange of pyridine for the nitrogen of the incoming ligand. Thus the chelating quinolinolate is assumed to bind as it is expected from a series of published N,O-chelating ligands [42]. The minor isolated product **1b** featured two 5,7-dichloro-8-quinolinolate ligands and was identified as the OC-6-32 isomer (see Scheme 1). Complexes **1a** and **1b** account for 90% of the theoretical yield. In case of **HovII** as the starting complex again two products, **2a** and **2b**, were isolated. In this case both complexes featured, according to NMR analysis, two 5,7-dichloro-8-quinolinolate ligands. The overall yield amounted to 83% in this case. Single crystal X-ray structure analyses elucidated the solid state structure of **2a** and **2b** (see Figure 1). The minor isomer **2a** (28% yield) was identified as the OC-6-14 diastereomer featuring the two oxygen atoms in *trans* disposition (and the nitrogen atom *trans* to the benzylidene ligand). The major isomer **2b** (57% yield) is the OC-6-32 diastereomer bearing the two oxygen ligands in *cis* disposition (and one oxygen atom is coordinated *trans* to the benzylidene ligand).

Elemental analysis confirmed the proposed stoichiometry of the complexes. Characteristic ^{1}H NMR signals comprise the protons in position 2 of the quinolinolate moieties. These protons resonate in the low-field (between 9.00 ppm in **2b** and 7.90 ppm in **3**) when the N-heterocyclic carbene ligand is situated *trans* to the N-atom of the quinolinolate. The corresponding proton of the second quinolinolate ligand (with the N-atom situated *cis* to the NHC) is high-field shifted and resonates at 5.48 (in **1b**), 5.32 (in **2b**) and 5.9 (in **4**). The OC-6-14 derivative **2a** is characterized by a pronounced low-field shift of the latter signal to about 6.1 ppm (signal superimposed by other resonances). Based on these observations an OC-6-32 stereo-

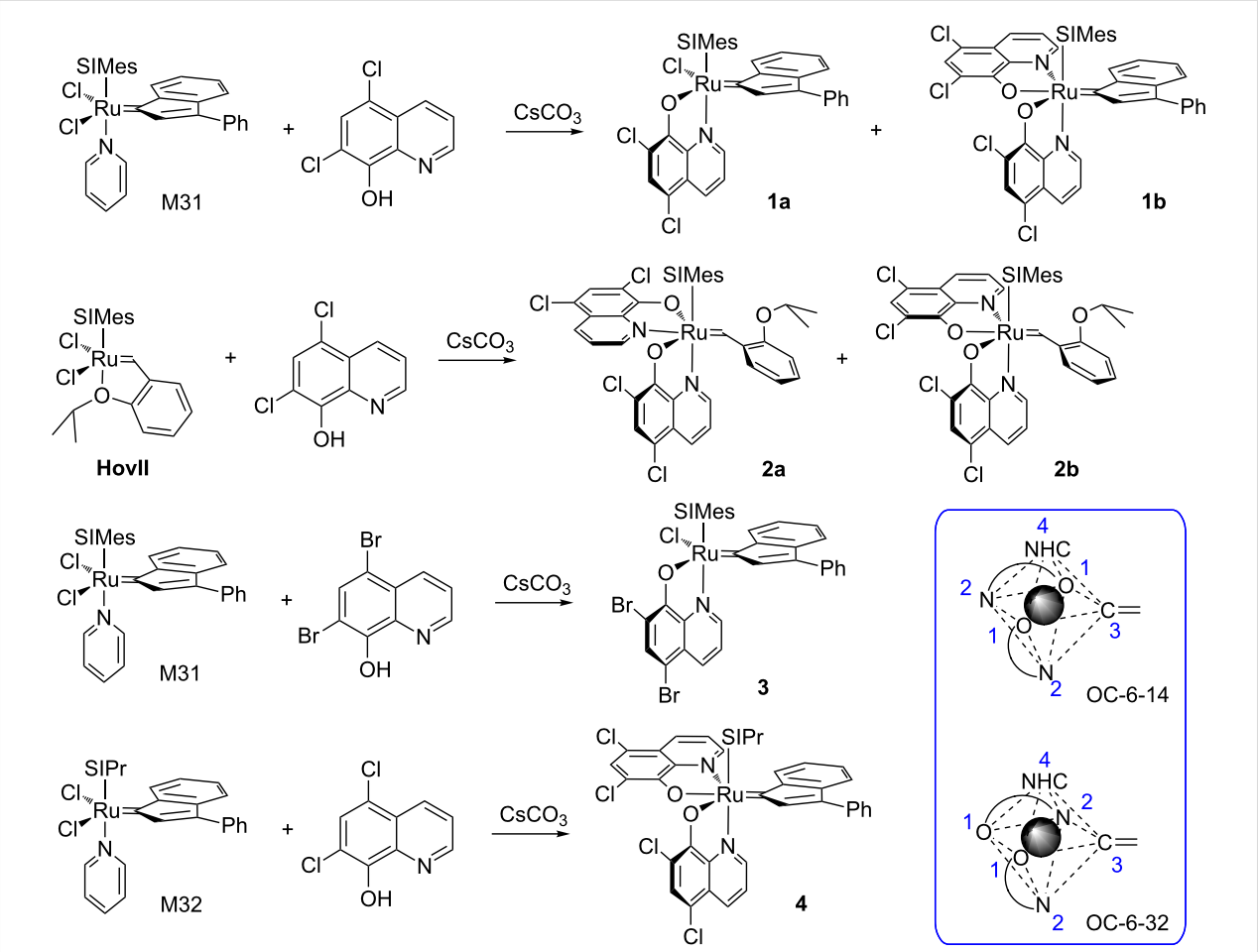

Scheme 1: Synthesis of **1**-**4**; only the isolated and characterized complexes are shown.

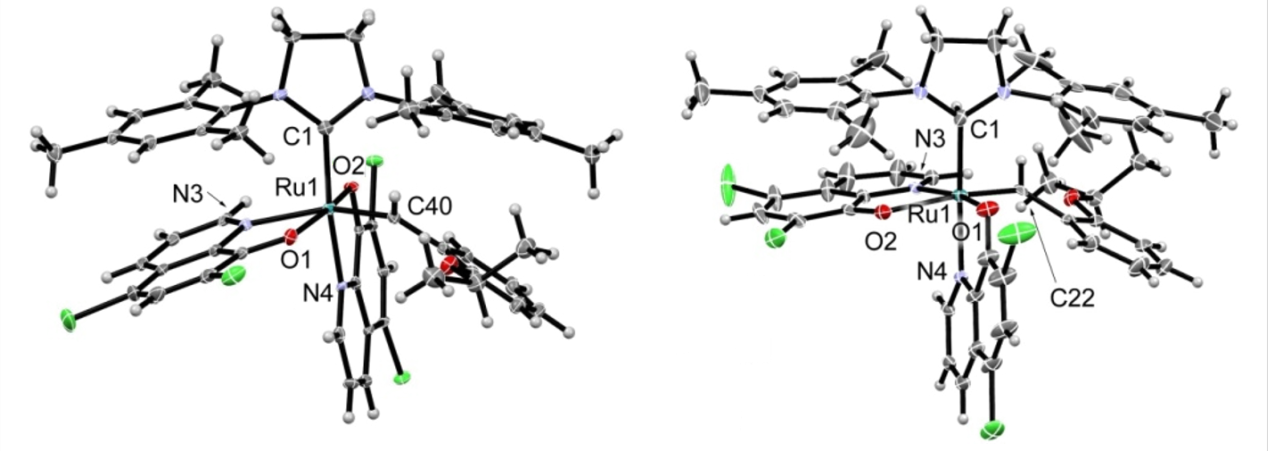

Figure 1: Solid state structure of complexes **2a** and **2b** as retrieved from single crystal X-ray diffraction.

chemistry is tentatively assigned to complex **1b**. Decoordination of the isopropoxy group during formation of **2a** and **2b** is readily evident from the benzylidene proton chemical shifts of 19.10 and 18.24 ppm, which are distinctly low-field shifted in comparison to the same signal in **HovII** (16.56 ppm). From single crystal X-ray structure analyses of **2a** and **2b** it became

evident that, in general, bond lengths and angles are very similar to each other. For example, the Ru–NHC bond is in both complexes 2.05 ± 0.01 Å and the Ru–benzylidene bonds measure 1.89 ± 0.01 Å. Of interest are the different bond lengths of the two quinolinolate ligands. While the first quinolinolate in the OC-6-14 derivative **2a** (N *trans* to the NHC and O trans to O of the second quinolinolate moiety) exhibits a Ru–N bond length of 2.11 Å and a Ru–O bond lengths of 2.04 Å, the second quinolinolate ligand (with N *trans* to the benzylidene) show distinctly longer Ru–O (2.09 Å) and Ru–N (2.20 Å) bonds. In the OC-6-32 derivative **2b**, bond lengths of the first quinolinolate are similar as in **2a** (Ru–N 2.12 Å and Ru–O 2.04 Å). The coordination of the second quinolinolate in characterized by a Ru–N bond of 2.08 Å and a Ru–O bond length of 2.17 Å. In contrast to related complexes described by Grubbs et al. no isomerization of **2a** into **2b** or the other way round was observed upon heating at 80 °C for 48 h [43].

Catalytic activity

The polymerization activity of the complexes was initially tested using dimethyl bicyclo[2.2.1]hept-5-ene-2,3-dicarboxylate (**5**) as the benchmark monomer. Monomer **5** was used because its polymers are not prone to backbiting. Therefore the average number molecular weight (M_n) can be used to characterize the ratio of initiation rate to propagation rate (k_i/k_p) of a given initiator to monomer combination [28,44-46]. Under the applied conditions (prolonged reaction time, reaction temperature up to 100 °C, UV-irradiation) none of the initiators was able to convert the monomer to a polymer. Therefore, efforts to activate the initiators via acid have been made. Upon addition of HCl aq complexes **1** to **4** became active and initiated the ROMP reaction of **5**. The activation process is accompanied by a colour change from deep red, to brownish to dark green in complexes **1**–**3** and from brownish to red to yellow in **4**. The reaction progress of the polymerization reaction was monitored using thin-layer chromatography. After complete consumption of the monomer, the reaction was stopped with an excess of ethyl vinyl ether, precipitated in vigorously stirred methanol and dried. Noteworthy, hydrochloric acid is the only acid which activates the preinitiators under investigation. Addition of other acids (or acid liberating reagents) such as acetyl chloride or trifluoroacetic acid, were not able to promote the polymerization. Also the addition of chloride containing salts, e.g., triethanolamine hydrochloride failed in promoting the metathesis reaction. Therefore, initiators **1**–**4** were benchmarked in the polymerizations of **5** using 50 equiv HCl. The reactions were carried with a [initiator]:[**5**] ratio of 1:300, at room temperature in CH_2Cl_2.

Table 1 summarizes the results of the polymerization data, bearing substrate **5** (see Supporting Information File 1 for further details). Generally it can be concluded, that except of **4**, the ini-

Table 1: Polymerization of **5** by preinitiators **1**–**4** (eth = ethereal; aq = aqueous; molecular weights (M_n) and the corresponding polydispersity indices (PDI) were determined using gel permeation chromatography (GPC) against polystyrene standards).

Complex	Temperature [°C]	Activation	Time [h]	Conversion [%]	Isol. yield [%]	M_n [kg/mol]	PDI
1–**4**	20	–	24	–	–	–	–
1–**4**	80	–	24	–	–	–	–
1–**4**	20	UV light	24	–	–	–	–
1a	20	HCl eth	6.25	100	75	413	2.0
1b	20	HCl eth	2	100	78	181	1.9
2a	20	HCl eth	23	65	42	254	2.2
2b	20	HCl eth	4	100	85	148	2.4
3	20	HCl eth	24	76	23	278	2.1
4	20	HCl eth	2.15	100	45	48	1.3
1a	20	HCl aq	3	95	80	392	2.0
1b	20	HCl aq	1.25	100	84	196	1.7
2a	20	HCl aq	23	44	20	296	1.8
2b	20	HCl aq	4.5	100	78	266	1.8
3	20	HCl aq	23	66	20	275	1.8
4	20	HCl aq	2	100	58	52	1.4
1a	80	HCl aq	2.25	100	84	411	2.1
1b	80	HCl aq	1	100	88	159	1.9
2a	80	HCl aq	24	77	46	132	2.3
2b	80	HCl aq	1	100	83	418	2.2
3	80	HCl aq	1.25	100	81	142	1.7
4	80	HCl aq	0.75	100	75	52	1.6

tiators show a relatively slow initiation compared to their propagation. The high molecular weights indicate a slow activation process or incomplete activation. In contrast preinitiator **4** yields polymers with low M_n and PDI values indicating an almost full activation of the preinitiator by the acid. The PDI's are slightly increased compared to the values of known living initiators such as **M31** [47].

A striking observation is that **2a** and **3**, even if according to the demonstrated activation mechanism should form the same active species as **1a**, **1b** and **2b** they show different polymerization behaviour. Bearing the fact that **3** has only one quinolinate ligand when compared to **1a**, and differentiated by the size of the substituents in the α-position to the oxygen group, hypothetically, more energy for the dissociation of the quinolinolate ligands is required maybe caused by the different geometric arrangement of the ligands around the ruthenium centre. This speculation is supported by the reactions performed at 80 °C where **3** (which possess just one quinolinolate ligand) reaches full conversion after the approximately same time as the other initiators.

Additionally time/conversion plots were acquired via arrayed ^{1}H NMR measurements of the polymerization of **5** initiated by **1**–**4** and HCl (see Figure 2 and Supporting Information File 1 for further details) in the presence of air. The fastest polymerizations show the indenylidene derivatives bearing dichloroquinolinolate ligand(s) (**1a**, **1b** and **4**). Preinitiator **2b** is slower in converting **5** but still satisfying conversion is obtained after about 4.5 hours. In contrast, preinitiators **2a** and **3** provided distinctly worse conversions. It is noteworthy that **2a** as well as **3** perform better in the Schlenk experiments (which were performed under nitrogen atmosphere) presented above.

To elucidate the activation mechanism of complexes **1**–**4** upon HCl addition, the actual active species of the initiators was investigated. For that purpose, **4** was mixed with 5 equiv of monomer **5** in $CDCl_3$ and activated it with 5 equiv of etherical HCl in a NMR tube. After few minutes, the characteristic carbene peak for propagating alkylidenes at 18.1 ppm appeared (see Figure 3). To identify this carbene peak, the same experiment was repeated reacting **M32** with **5**, leading to the same characteristic carbene peak. We assume that, as proposed by Grubbs and co-workers [43], the hydrochloric acid protonates both ligands which are subsequently exchanged by chlorides forming the same active 14-electron species as the original starting complex **M32** does. Trapping the active species of the SIMes analogues failed.

To shed light about the different behavior of complexes **2a** and **2b** we envisaged DFT calculations. The optimized geometry of **2b** is in perfect agreement with the X-ray structure [48] (rmsd = 0.032 Å and 0.9° for the selected main distances and angles) [49,50]. In agreement with experiments that indicated **2b** as the most stable isomer, calculations estimate that **2b** is 2.0 kcal/mol more stable than **2a**. To rationalize the different reactivity of **2a** and **2b** we compared the basicity of the four O atoms by calculating the energy of the acid–base equilibrium (see Scheme 2), where [Ru] is **2a** or **2b**, $[Ru]H^+$ is **2a** or **2b** with a protonated O atom. The energy of [Ru] and $[Ru]H^+$ is calculated in CH_2Cl_2 using the protocol described in the computational details sections, while for the aqueous solvation free

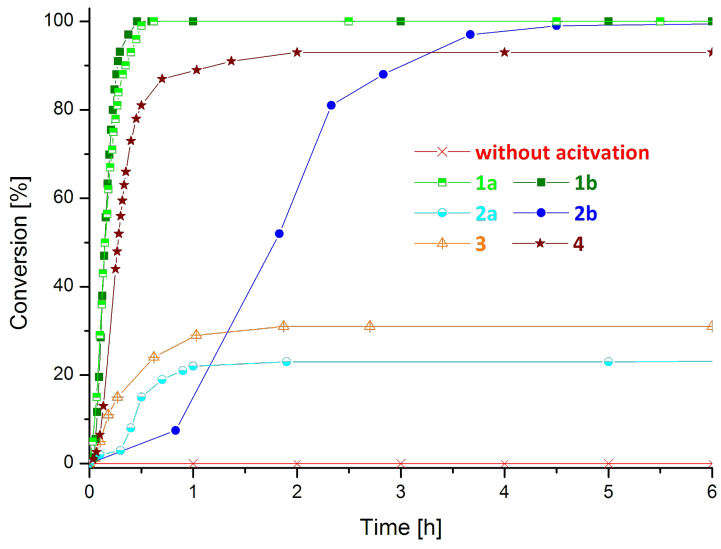

Figure 2: Time/conversion plot for the polymerization of **5** by preinitiators **1**–**4** in the presence of HCl ([**5**]:[HCl]:[I] = 50:25:1; [**5**] = 0.1 mol/L; solvent:$CDCl_3$).

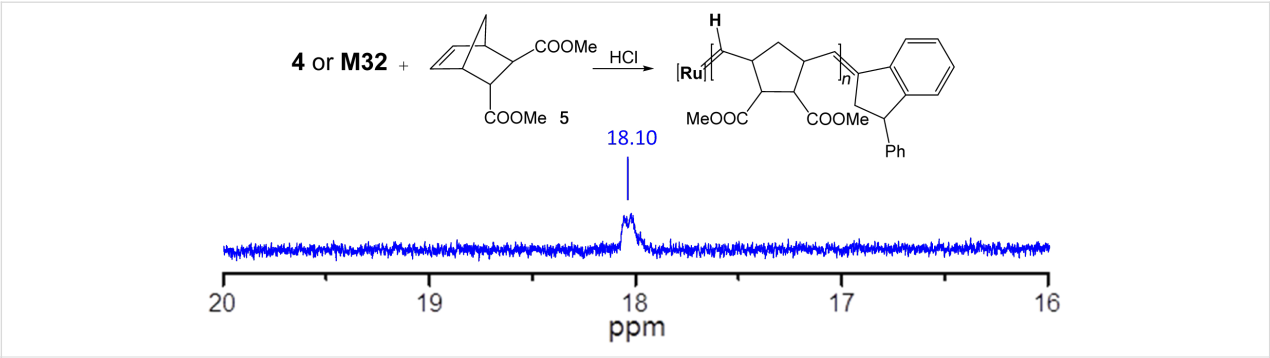

Figure 3: ^{1}H NMR spectrum in the low-field region of the active species for complexes **4** and **M32**.

energy of the proton we assumed the value of −262.2 kcal/mol from the literature [51,52]. It is assumed that the protonated Ru species remains in the organic phase. The energetics for the four oxygen protonated species of **2a** and **2b** is reported in Scheme 2.

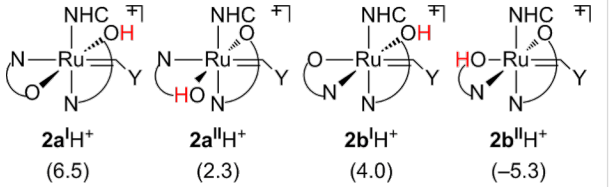

Scheme 2: Energetics of **2a** and **2b** protonation in kcal/mol.

According to the number reported, protonation of one O atom of **2a**, leading to species **2a^{I}H^{+}** and **2a^{II}H^{+}**, is unfavored, as well as protonation of the O atom of **2b** *cis* to the NHC ligand, leading to **2b^{I}H^{+}**. The only O atom presenting favorable protonation energy is the *trans* one to the Ru–alkylidene bond of **2b**, leading to **2b^{II}H^{+}**. The accuracy of the absolute protonation energies are difficult to estimate, since they can vary with the computational protocol (i.e., functional, basis set and solvation model) and they also depend on experimental considerations, bearing the assumption that all the Ru species are in the organic phase, while HCl is dissociated in the aqueous phase. For this reason the absolute value of the protonation energies is not stressed further. However, the relative trend in the protonation energies is in agreement with the general idea that protonation of the O atom *trans* to the Ru–alkylidene bond should be favored, since this leads to a much softer –OH ligand *trans* to the Ru–alkylidene bond. Consistently, the protonated Ru–O distance increases by roughly 0.11 Å in **2a^{I}H^{+}**, **2^{II}H^{+}**, and **2b^{I}H^{+}**, whereas it increases by 0.18 Å in **2b^{II}H^{+}**.

Having established a possible entry point to the activation of **2b** by HCl the whole reaction pathway leading to the conversion of **2b** to a classical Hoveyda type complex was investigated (see Figure 4). After protonation of the O atom *trans* to the alkylidene ligand, a chloride anion could dissociate the Ru–OH bond through transition state **2b^{II}H^{+}** → **2b^{II}**, with displacement of the –OH group and coordination of the chloride *trans* to the alkylidene group. The next step corresponds to a rotation of the chloride ligand from the coordination position *trans* to alkylidene ligand to a coordination position *cis* to both the alkylidene and the SIMes ligands. This rearrangement requires dissociation of the quinolinolate N atom and the complete release of a neutral quinolinolate type ligand, leading to **2b^{III}**, which is 13.5 kcal/mol below in energy compared to **2b**.

Protonation of the second O atom is disfavored by 7 kcal/mol. For this reason, the search for a transition state in which the protonation of **2b^{III}** occurs by a HCl molecule through a concerted transition state in which the proton of HCl protonates the oxygen of the quinolinolate while the chloride coordinates *trans* to the ylidene group was emphasized. This concerted transition state costs only 1.5 kcal/mol and thus is favored over protonation followed by Cl^- coordination. The final product is **2b^{IV}**, 17.0 kcal/mol below **2b**, with the attacking Cl atom *trans* to the Ru–alkylidene bond. A direct HCl attack to **2b** via a concerted transition state is not possible, since the Ru center of **2b** has no vacant coordination position. Back to the second protonation step, **2b^{IV}** evolves to **2b^{V}** through a shift of the second Cl atom from the coordination position *trans* to the Ru–alkylidene bond to reach a geometry with a *trans* disposition of the two Ru–Cl bonds. Species **2b^{V}** corresponds to a 14 e^- species that can be formed by dissociation of the isopropoxy group from the classical Hoveyda catalyst **II**, which can be obtained by **2b^{V}** through coordination of the isopropoxy group. The overall energy balance for the transformation of **2b** to **II** is 33.1 kcal/mol down in energy. Similar energy profiles, corresponding to the transformation of **2a^{I}H^{+}**, **2a^{II}H^{+}**, and **2b^{I}H^{+}** into **II** are reported in Supporting Information File 1, where also the protonation of the N atom of the quinolinolate ligand are explored.

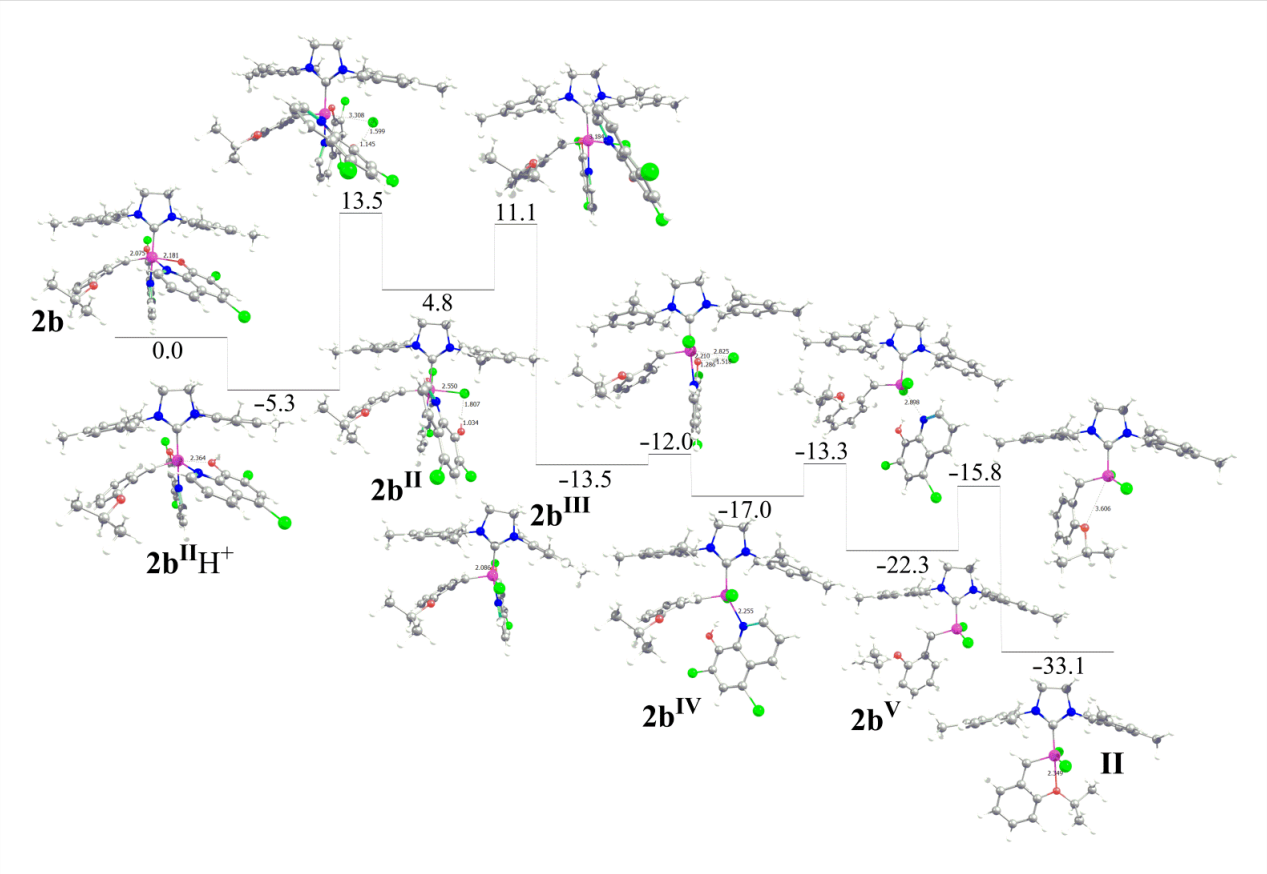

Figure 4: Reaction pathway of the transformation of **2b** to **HovII** (energies in kcal/mol; main distances in Å).

Due to the latent character of the pre-initiators, they may be suitable candidates for the polymerization of very active strained monomers such as DCPD. Another benefit for their use in the polymerization of DCPD is their outstanding solubility in the neat monomer. The main challenge of the polymerization of DCPD is to guarantee an adequate mixing of monomer and catalyst to obtain a homogenous reaction mixture and moreover a steady polymerization product. DCPD is also prone to undergo a retro-Diels–Alder reaction at higher temperatures, causing a mass loss during polymerization if higher temperatures are applied for the reaction.

To test the pre-catalysts regarding their performance in the polymerization of DCPD, two different test-reactions were carried out: a) STA measurements to gain an insight into the course of polymerization and b) tensile strength tests to characterize the obtained polymers.

In the STA plot (see Supporting Information File 1 for further details), representative examples for a successful, a partly successful and an unsuccessful DCPD polymerization are shown. **2a** and **3** totally fail the polymerization of DCPD. The monomer decomposes completely before any curing occurs. On the other hand, **1b** and **2b** polymerize DCPD which can be seen by the exothermic peaks on the left hand side of Figure 5. **2b** requires more time to start the polymerization which causes a higher mass loss of the monomer. **1a** shows some curing, but the main part of the monomer decomposes before it can be polymerized. The exothermic peak of the polymerization merges into the endothermic peak of the monomer decomposition.

Additionally, pDCPD shoulder test bars were made and trialled in a Tensile Strength Test. Tensile strength values (R_m) and the Young's modulus (ε) were determined and used for comparison with literature data. The most reactive complexes **2b** and **4** exhibit the highest R_m and Young's Modulus values (see Table 2), which exceed data taken from literature. This indicates a higher cross linking density of the test specimens.

Conclusion

In conclusion we were able to synthesize a new family of N,O-chelating initiators bearing 5,7-dihalide-hydroxyquinoline co-ligands. We showed that it is possible to synthesize these initiators using starting complexes bearing different carbene- and different NHC ligands. At the example of initiators **2a** and **2b** it

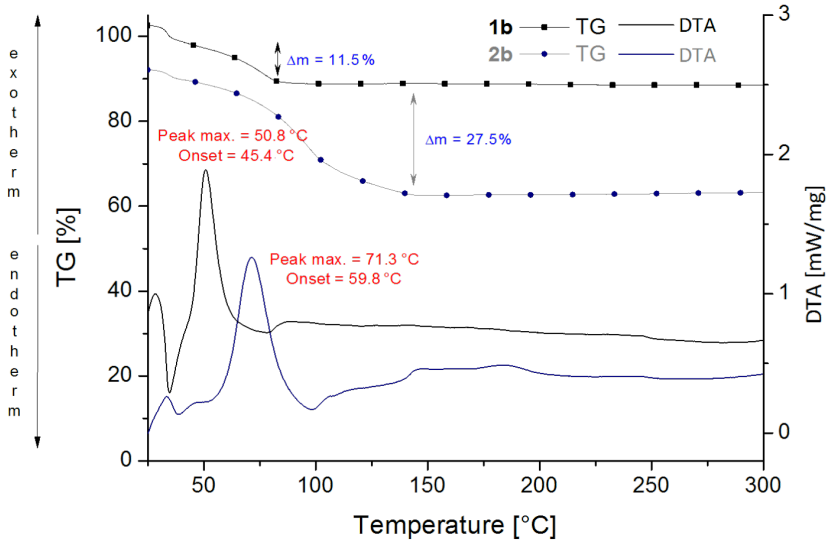

Figure 5: DTA-TGA measurements for polymerizations of DCPD with catalysts **1b** and **2b**; Reaction conditions: [catalyst]:[DCPD]:[HCl]: 1:10.000:25; Temperature program: 3 °C/min.

Table 2: Tensile test values for shoulder test bars initiated with complexes **1**–**4**.

Initiator	*E* [MPa]	R_m [MPa]
1a	2137	25.2
1b[a]	–	–
2a	–	
2b	2635	43.8
3	1277	20.7
4	2664	52.3
comparative example [53]	1870–1980	43.0–46.8

[a]Unexpectedly all attempts to produce shoulder test bars failed.

was shown that the arrangement of the ligands around the ruthenium centre can drastically influence the activity of metathesis initiators. Just by changing the positioning of one of the two quinolinolate ligands the catalytic activity is decreased manifoldly.

Even though since the 1980s thousands of papers have presented and described the olefin metathesis catalysis [54], neither the location of a right catalyst for any metathesis reaction [55,56], nor the recipe to rationalize the behaviour of a given catalyst have been fulfilled [57-59]. Thus this study opens a door to find out new families of olefin metathesis catalysts [60], overcoming the issue of bearing a phosphine or to break a Ru–O bond in the precatalysts [55,61].

The initiators exhibit an excellent stability in the solid state as well as in solution and an outstanding latency towards cyclic olefins. The new pre-catalysts can be triggered using HCl. Due to their extremely good solubility in apolar solvents and substrates they are useful candidates for solvent-free polymerizations. Their latency also makes them very suitable for the polymerization of strained monomers such as DCPD.

Experimental

Unless otherwise noted, all reactions were carried out under nitrogen atmosphere in pre-dried glass ware using Schlenk technique. Materials were purchased from commercially available sources such as Aldrich, Fluka or Alfa Aesar and used without further purification. Complexes **M31** and **M32** were obtained from Umicore. Complex **HovII** was prepared according to literature [46]. Monomer **5** (dimethyl bicyclo[2.2.1]hept-5-ene-2,3-dicarboxylate) was synthesized according to literature [62]. CH_2Cl_2 was degassed with nitrogen. Column chromatography was performed on Merck silica gel 60, 230–400 mesh. TLC was performed on aluminum sheets, Merck 60F 254. NMR (^{1}H, ^{13}C) spectra were recorded on a Bruker Avance 300 MHz or an INOVA 500 MHz spectrometer, in $CDCl_3$ as the solvent. The solvent peak of residual $CHCl_3$ was used for referencing the NMR spectra to 7.26 (^{1}H) and 77.16 ppm (^{13}C), respectively. Gel permeation chromatography was used to determine molecular weights and the polydispersity index (PDI). The measurements were run in THF against a polystyrene standard using following arrangement: a Merck Hitachi L6000 pump, separation columns of Polymer Standards Service (5 µm grade size) and a refractive-index detector from Wyatt Technology. X-ray measurements were performed on a Bruker AXS Kappa APEX II diffractometer. The structure was solved by direct methods using SHELXS and refined with SHELXL. The absorption correction was performed using the program SADABS.

DTA/TG measurements were done using a NETZSCH STA 449 C with a temperature program of 3 °C/min. The TGA is operated with a helium flow rate of 50 mL/min used in combination with a protective flow of 8 mL/min. Tensile stress tests were performed using a Shimadzu tensile stress test machine. The strain rate for the analysis was set with 1 mm/min. The tested shoulder test bars had a diameter of 37.4 mm and a length of 80 mm.

General procedure for the preparation of Ru complexes

In a Schlenk flask the corresponding starting material (1 equiv) was dissolved in degassed CH_2Cl_2. 5,7-Dihalide-8-hydroxyquinoline (20 equiv) and Cs_2CO_3 (20 equiv) were added. The reaction mixture was stirred under an atmosphere of argon for 12 h at 25 °C. Insoluble components were removed by filtration over celite. Column chromatography (silica gel) using cyclohexane/ethylacetate = 10/1 (v/v) yielded the corresponding complexes. The synthesis of the following Ru-based complexes belongs to a patent application [63].

Chloro-(κ^2-(*N*,*O*)-5,7-dichloro-8-quinolinolate)-(3-phenyl-1-indenylidene)-(1,3-bis(2,4,6-trimethylphenyl)-4,5-dihydroimidazol-2-ylidene)ruthenium (**1a**). Complex **1a** was prepared according to the general procedure given above, using **M31** (142 mg, 0.189 mmol), 5,7-dichloro-8-hydroxyquinoline (810 mg, 3.785 mmol) and Cs_2CO_3 (1.24 g, 3.815 mmol) as the starting materials. CH_2Cl_2 (18 mL) was used as the solvent. Chromatographic work-up gave **1a** in pure form. Yield: 117 mg (70%). Anal. calcd for $C_{45}H_{40}Cl_3N_3ORu$: C, 63.87; H, 4.76; N, 4.97; found: C, 64.01; H, 4.89; N, 5.01; ^{1}H NMR (δ, 20 °C, $CDCl_3$, 300 MHz) 8.0 (d, *J* = 8.1 Hz, 1H), 7.97 (d, *J* = 4.8 Hz, 1H), 7.74 (d, *J* = 8.1 Hz), 7.30 (dd, 2H), 7.23 (d, 2H), 7.12 (d, *J* = 7.14 Hz, 1H), 7.05 (s, 2H), 7.03 (m, 1H), 6.44 (s, 3H), 6.23 (s, 2H), 6.20 (d, 1H), 3.87 (s, 4H), 2,32, 2.08, 1.92 (s, 18H); ^{13}C NMR (δ, 20 °C, $CDCl_3$, 75 MHz) Ru=C and Ru-C not observed, 167.2, 164.6, 146.7, 143.8, 143.2, 142.8, 141.8, 138.0, 136.9, 136.8, 136.5, 133.2, 132.7, 129.1, 129.1, 128.7, 128.0, 127.9, 127.6, 126.0, 125.9, 125.7, 121.8, 121.0, 118.9, 118.5, 117.6, 111.7, 109.3, 51.6, 20.9, 18.1.

(OC-6-32)-Bis(κ^2-(N,O)-5,7-dichloro-8-quinolinolate)-(3-phenyl-1-indenylidene)-(1,3-bis(2,4,6-trimethylphenyl)-4,5-dihydroimidazol-2-ylidene)ruthenium (**1b**). Complex **1b** was isolated from the same experiment than **1a** using column chromatography. Yield 8.4 mg (20%). Anal. calcd for $C_{54}H_{44}Cl_4N_4O_2Ru$: C, 63.35; H, 4.33; N, 5.47; found: C, 63.45; H, 4.56; N, 5.76; ^{1}H NMR (δ, 20 °C, $CDCl_3$, 300 MHz) 8.15 (d, *J* = 4.8 Hz, 1H), 7.99 (dd, *J* = 8.4 Hz, 1H), 7.9 (3H), 7.60 (1H), 7.52 (1H), 7.47 (1H), 7.31 (s, 1H), 7.24 (s, 1H), 7.2 (m, 2H), 6.81 (m, 1H), 6.65 (t, 1H), 6.53 (s, 2H), 6.50 (dd, 1H), 6.35 (s, 2H), 6.28 (d, *J* = 7.2 Hz), 5.48 (dd, *J* = 4.8 Hz, 1H), 3.89 (s, 4H), 2.36, 2.28, 2.08 (s, 18H); ^{13}C NMR (δ, 20 °C, $CDCl_3$, 75 MHz) Ru=C not observed, 204.3 (1C, Ru-NHC), 166.3, 161.2, 150.0, 145.8, 145.1, 143.1, 142.0, 141.7, 140.4, 137.9, 137.5, 137.3, 136.8, 136.4, 136.3, 136.4, 136.3, 136.2, 133.3, 133.2, 130.0, 129.7, 129.6, 129.4, 129.3, 129.1, 128.5, 128.2, 128.1, 126.6, 126.0, 125.9, 125.8, 125.4, 120.9, 120.7, 120.1, 118.5, 118.2, 112.2, 108.2, 53.3, 20.9, 20.3, 19.5.

(OC-6-14)-Bis(κ^2-(N,O)-5,7-dichloro-8-quinolinolate)-(2-isopropylbenzylidene)-(1,3-bis(2,6-diisopropylphenyl)-4,5-dihydroimidazol-2-ylidene)ruthenium (**2a**). Complex **2a** was prepared according to the general procedure given above, using **HovII** (106 mg, 0.169 mmol), 5,7-dichloro-8-hydroxyquinoline (707 mg, 3.303 mmol) and Cs_2CO_3 (881 mg, 2.704 mmol) as the starting materials. CH_2Cl_2 (18 mL) was used as the solvent. Chromatographic work-up gave **2a** in pure form. Yield: 46.5 mg (28%). ^{1}H NMR (δ, 20 °C, $CDCl_3$, 300 MHz) 19.10 (s, 1H), 8.09 (d, *J* = 4.04 Hz, 1H), 7.95 (d, *J* = 8.56 Hz, *J* = 1.43 Hz, 1H), 7.68 (d, *J* = 8.43 Hz, *J* = 1.30 Hz, 1H), 7.49 (s, 1H), 7.17 (s, 1H), 7.05 (m, 2H), 6.56 (d, *J* = 8.04 Hz, 1H), 6.48 (s, 2H), 6.43 6,39 (m, 2H), 6.14 (s, 2H), 6.06 (m, 2H), 3.97 (m, 5H), 2.45 (s, 6H), 2.27 (s, 6H), 1.90 (s, 6H), 1.43 (d, 3H), 1.05 (d, 3H); ^{13}C NMR (δ, 20 °C, $CDCl_3$, 75 MHz) 315.5 (1C, Ru=CH), Ru-NHC not observed, 162.6, 161.3, 149.7, 149.4, 149.0, 144.2, 143.2, 142.4, 142.3, 138.1, 136.9, 136.6 135.8, 132.3, 131.7, 129.3, 129.2, 128.7, 127.7, 126.2, 125.8, 125.7, 122.2, 121.6, 121.0, 119.5, 118.9, 112.0, 109.2, 76.2, 51.6, 23.1, 21.5, 20.8, 18.8, 18.5.

(OC-6-32)-Bis(κ^2-(N,O)-5,7-dichloro-8-quinolinolate)-(2-isopropylbenzylidene)-(1,3-bis(2,6-diisopropylphenyl)-4,5-dihydroimidazol-2-ylidene)ruthenium (**2b**). Complex **2b** was isolated from the same experiment than **2a** using column chromatography. Yield 91 mg (57%). Anal. calcd for $C_{54}H_{44}Cl_4N_4O_2Ru$: C, 63.51; H, 4.25; N, 5.48; found: C, 60.19; H, 4.86; N, 5.88; ^{1}H NMR (δ, 20 °C, $CDCl_3$, 300 MHz) 18.24 (bs, 1H), 9.00 (d, *J* = 4.67 Hz, 1H), 8.09 (d, *J* = 8.56 Hz, 1H), 7.83 (d, *J* = 8.30 Hz, 1H) 7.57 (s, 1H), 7.12 (s, 1H), 7.06 (m, 1H), 6.94 (m, 1H), 6.59 (s, 2H), 6.39 (d, 1H), 6.26 (s, 2H), (d, 1H), (m, 1H), 5.98 (m, 1H), 5.32 (d, *J* = 4.54 Hz), 4.54 (m, 1H), 3.92 (q, 4H), 2.57 (s, 6H), 2.04 (s, 6H), 1.91 (s, 6H), 1.53 (d, 3H), 1.31 (d, 3H); ^{13}C NMR (δ, 20 °C, $CDCl_3$, 75 MHz) Ru=C not observed, 209.5 (1C, Ru-NHC), 166.4, 160.9, 147.7, 146.7, 147.1, 146.7, 164.5, 146.5, 144.9, 141.2, 137.1, 137.0, 136.7, 136.5, 119.3, 125.8, 132.7, 132.2, 129.2, 129.1, 129.0, 128.6, 127.9, 126.4, 120.7, 120.1, 119.7, 118.0, 111.3, 110.5, 106.4, 68.7, 51.7, 22.7, 22.3, 20.9, 18.9, 18.1.

Chloro-(κ^2-(N,O)-5,7-dibromo-8-quinolinolate)-(3-phenyl-1-indenylidene)-(1,3-bis(2,4,6-trimethylphenyl)-4,5-dihydro-

imidazol-2-ylidene)ruthenium (**3**). Complex **3** was prepared according to the general procedure given above, using **M31** (160 mg, 0.214 mmol), 5,7-dibromo-8-hydroxyquinoline (960 mg, 3.169 mmol) and Cs_2CO_3 (1.00 g, 3.077 mmol) as the starting materials. Diethyl ether (20 mL) was used as the solvent. Chromatographic work-up gave **3** in pure form. Yield: 50 mg (25%). Anal. calcd for $C_{45}H_{40}Br_2ClN_3ORu$: C, 57.80; H, 4.31; N, 4.49; found: C, 57.89; H, 4.32; N, 4.72; ^{1}H NMR (δ, 20 °C, $CDCl_3$, 300 MHz) 7.97 (d, *J* = 8.52, 1H), 7.90 (d, *J* = 4.26 Hz, 1H), 7.81 (s, 1H), 7.71 (d, *J* = 8.33 Hz, 1H), 7.57 (s, 1H), 7.53 (bs, 3H), 7.34 (bs, 3H, CH), 7.11 (d, *J* = 7.00 Hz, 1H), 7.03 (q, 1H, CH), 6.49 (bs, 1H), 6.42 (s, 3H), 6.27 (s, 2H), 6.18 (1H, bs), 3.89 (s, 4H), 2.30 (s, 6H), 2.15 (bs, 6H), 1.93 (s, 6H); ^{13}C NMR (δ, 20 °C, $CDCl_3$, 75 MHz) Ru=C not observed, 241.9 (Ru-NHC), 168.8, 144.5, 144.1, 143.7, 143.0, 137.8, 137.0, 136.9, 136.6, 135.6, 135.2, 134.2, 133.4, 129.2, 129.1, 128.2, 127.8, 127.6, 127.5, 125.9, 122.6, 121.6, 117.4, 108.7, 108.3, 98.2, 51.5 (2C), 21.0, 19.2 (6C).

(OC-6-32)-Bis(κ^2-(N,O)-5,7-dichloro-8-quinolinolate)-(3-phenyl-1-indenylidene)-(1,3-bis(2,6-diisopropylphenyl)-4,5-dihydroimidazol-2-ylidene)ruthenium (**4**). Complex **4** was prepared according to the general procedure given above, using **M32** (58 mg, 0.070 mmol), 5,7-dichloro-8-hydroxyquinoline (136 mg, 0.636 mmol) and Cs_2CO_3 (300 mg, 0.923 mmol) as the starting materials. CH_2Cl_2 (6 mL) was used as the solvent. Chromatographic work-up gave **4** in pure form. Yield: 40.3 mg (52%). Anal. calcd for $C_{60}H_{56}Cl_4N_4O_2Ru$: C, 65.04; H, 5.09; N, 5.06; found: C, 64.95; H, 4.87; N, 5.04; ^{1}H NMR (δ, 20 °C, $CDCl_3$, 300 MHz) 8.03 (m, 3H), 7.91 (m, 2H), 7.67 (m, 1H), 7.53 (m, 2H), 7.41 (m, 3H), 7.30 (m, 2H), 7.21 (s, 1H), 7.16 (m, 2H), 6.79 (m, 2H), 6.65 (m, 2H), 6.47 (m, 1H), 6.26 (m, 2H), 5.9 (d, *J* = 4.51 Hz, 1H), 4.66, 4.17, 3.9, 3.76, 3.48 (8H), 1.65, 1.34, 1.27, 1.17, 0.91, 0.61, 0.45 (24H); ^{13}C NMR (δ, 20 °C, $CDCl_3$, 75 MHz) 286.2 (Ru=C), 206.6 (1C, Ru-NHC), 165.4, 162.0, 151.0, 147.4, 146.4, 145.8, 145.6, 145.3, 145.2, 145.1, 144.7, 144.0, 141.2, 141.1, 139.3, 138.4, 137.0, 133.8, 132.6, 130.0, 129.8, 129.7, 128.9, 127.8, 127.7, 127.6, 126.0, 125.8, 125.3, 125.2, 124.8, 124.4, 124.3, 123.1, 121.5, 120.4, 120.0, 117.9, 117.7, 112.6, 108.4, 58.7, 55.9, 29.7, 28.6, 28.5, 27.3, 26.9, 26.1, 25.6, 24.8, 24.6, 22.0, 21.9, 21.2.

General polymerization procedure

Defined solutions of pre-initators **1**–**4** and **5** (300 equiv, 0.01 mmol/mL) were prepared. The reactions were performed in CH_2Cl_2 at room temperature and in toluene for 80 °C polymerizations. Ethereal HCl (50 equiv; HCl relative to ruthenium) was added to activate the reaction. The reaction was followed by TLC (cyclohexane/ethyl acetate = 3:1) and after complete conversion stopped with an excess of ethyl vinyl ether. The Polymer was precipitated in vigorously stirred methanol (approx. 25 mL for 100 mg polymer), and the white to yellowish precipitate was sampled and dried in vacuum.

Computational details

All calculations were performed with the Gaussian 09 package [64], Revision A.1, at the BP86 GGA level [65-67] using the SDD ECP on Ru [68-70] and the split-valence plus one polarization function SVP basis set on all main group atoms during geometry optimizations [71]. Furthermore diffuse basis sets have been incorporated for O and Cl [72]. The reported energies have been optimized via single point calculations on the BP86 geometries with triple-ζ valence plus polarization (TZVP keyword in Gaussian) using the M06 functional [73]. Solvent effects, dichloromethane, were calculated with the PCM model [74,75], and non-electrostatic terms were also included. The geometry optimizations were performed without symmetry constraints, and the nature of the extrema was checked by analytical frequency calculations.

Supporting Information

Crystallographic data for complexes **2a** and **2b** have also been deposited with the CCDC, nos. 1439204 and 1439205, and can be obtained free of charge from http://www.ccdc.cam.ac.uk.

Supporting Information File 1

Experimental data, energies, Cartesian coordinates, and 3D view for all DFT optimized species discussed in this work.
[http://www.beilstein-journals.org/bjoc/content/supplementary/1860-5397-12-17-S1.pdf]

Acknowledgements

A.P. thanks the Spanish MINECO for a project CTQ2014-59832-JIN, and European Commission for a Career Integration Grant (CIG09-GA-2011-293900). L.C. thanks King Abdullah University of Science and Technology (CCF project) for support.

References

1. Traut, T. *Allosteric Regulatory Enzymes;* Springer: New York, NY, U.S.A., 2008.
2. Oyen, D.; Fenwick, R. B.; Stanfield, R. L.; Dyson, H. J.; Wright, P. E. *J. Am. Chem. Soc.* **2015,** *137,* 9459–9468. doi:10.1021/jacs.5b05707
3. Wang, J.; Feringa, B. L. *Science* **2011,** *331,* 1429–1432. doi:10.1126/science.1199844
4. Blanco, V.; Carlone, A.; Hänni, K. D.; Leigh, D. A.; Lewandowski, B. *Angew. Chem., Int. Ed.* **2012,** *51,* 5166–5169. doi:10.1002/anie.201201364
5. Blanco, V.; Leigh, D. A.; Marcos, V. *Chem. Soc. Rev.* **2015,** *44,* 5341–5370. doi:10.1039/c5cs00096c

6. Yinghuai Zhu, Y.; Hosmane, N. S. *ChemistryOpen* **2015,** *4,* 408–417. doi:10.1002/open.201402172
7. Schjoeth-Eskesen, C.; Hansen, P. H.; Kjaer, A.; Gillings, N. *ChemistryOpen* **2015,** *4,* 65–71. doi:10.1002/open.201402081
8. Yoon, H. J.; Kuwabara, J.; Kim, J.-H.; Mirkin, C. A. *Science* **2010,** *330,* 66–69. doi:10.1126/science.1193928
9. Henkelis, J. J.; Blackburn, A. K.; Dale, E. J.; Vermeulen, N. A.; Nassar, M. S.; Stoddart, J. F. *J. Am. Chem. Soc.* **2015,** *137,* 13252–13255. doi:10.1021/jacs.5b08656
10. Guan, Z.; Cotts, P. M.; McCord, E. F.; McLain, S. J. *Science* **1999,** *283,* 2059–2062. doi:10.1126/science.283.5410.2059
11. Ginzburg, Y.; Anaby, A.; Vidavsky, Y.; Diesendruck, C. E.; Ben-Asuly, A.; Goldberg, I.; Lemcoff, N. G. *Organometallics* **2011,** *30,* 3430–3437. doi:10.1021/om200323c
12. Casitas, A.; Poater, A.; Solà, M.; Stahl, S. S.; Costas, M.; Ribas, X. *Dalton Trans.* **2010,** *39,* 10458–10463. doi:10.1039/c0dt00284d
13. Naumann, S.; Buchmeiser, M. R. *Macromol. Rapid Commun.* **2014,** *35,* 682–701. doi:10.1002/marc.201300898
14. Osorio-Planes, L.; Rodriguez-Escrich, C.; Pericàs, M. A. *Org. Lett.* **2014,** *16,* 1704–1707. doi:10.1021/ol500381c
15. Wang, J.; Hou, L.; Browne, W. R.; Feringa, B. L. *J. Am. Chem. Soc.* **2011,** *133,* 8162–8164. doi:10.1021/ja202882q
16. Trnka, T. M.; Grubbs, R. H. *Acc. Chem. Res.* **2001,** *34,* 18–29. doi:10.1021/ar000114f
17. Chauvin, Y. *Angew. Chem., Int. Ed.* **2006,** *45,* 3740–3747. doi:10.1002/anie.200601234
18. Schrock, R. R. *Angew. Chem., Int. Ed.* **2006,** *45,* 3748–3759. doi:10.1002/anie.200600085
19. Fustero, S.; Bello, P.; Miró, J.; Sánchez-Roselló, M.; Haufe, G.; del Pozo, C. *Beilstein J. Org. Chem.* **2013,** *9,* 2688–2695. doi:10.3762/bjoc.9.305
20. Piola, L.; Nahra, F.; Nolan, S. P. *Beilstein J. Org. Chem.* **2015,** *11,* 2038–2055. doi:10.3762/bjoc.11.221
21. Yuan, W.; Wei, Y.; Shi, M. *ChemistryOpen* **2013,** *2,* 63–68. doi:10.1002/open.201300002
22. Leitgeb, A.; Wappel, J.; Slugovc, C. *Polymer* **2010,** *51,* 2927–2946. doi:10.1016/j.polymer.2010.05.002
23. Fouquet, T. *ChemistryOpen* **2014,** *3,* 269–273. doi:10.1002/open.201402048
24. Monsaert, S.; Vila, A. L.; Drozdzak, R.; Van der Voort, P.; Verpoort, F. *Chem. Soc. Rev.* **2009,** *38,* 3360–3372. doi:10.1039/b902345n
25. Vidavsky, Y.; Anaby, A.; Lemcoff, N. G. *Dalton Trans.* **2012,** *41,* 32–43. doi:10.1039/c1dt11404b
26. Ernst, C.; Elsner, C.; Prager, A.; Scheibitz, B.; Buchmeiser, M. R. *J. Appl. Polym. Sci.* **2011,** *121,* 2551–2558. doi:10.1002/app.33972
27. Jakobs, R. T. M.; Sijbesma, R. P. *Organometallics* **2012,** *31,* 2476–2481. doi:10.1021/om300161z
28. Żukowska, K.; Pump, E.; Pazio, A. E.; Woźniak, K.; Cavallo, L.; Slugovc, C. *Beilstein J. Org. Chem.* **2015,** *11,* 1458–1468. doi:10.3762/bjoc.11.158
29. Kozłowska, A.; Dranka, M.; Zachara, J.; Pump, E.; Slugovc, C.; Skowerski, K.; Grela, K. *Chem. – Eur. J.* **2014,** *20,* 14120–14125. doi:10.1002/chem.201403580
30. Tzur, E.; Ivry, E.; Diesendruck, C. E.; Vidavsky, Y.; Goldberg, I.; Lemcoff, N. G. *J. Organomet. Chem.* **2014,** *769,* 24–28. doi:10.1016/j.jorganchem.2014.06.027
31. Poater, A.; Cavallo, L. *Beilstein J. Org. Chem.* **2015,** *11,* 1767–1780. doi:10.3762/bjoc.11.192
32. Vougioukalakis, G. C.; Grubbs, R. H. *Chem. Rev.* **2010,** *110,* 1746–1787. doi:10.1021/cr9002424
33. Leitgeb, A.; Abbas, M.; Fischer, R. C.; Poater, A.; Cavallo, L.; Slugovc, C. *Catal. Sci. Technol.* **2012,** *2,* 1640–1643. doi:10.1039/c2cy20311a
34. Pellicciotta, I.; Marciscano, A. E.; Hardee, M. E.; Francis, D.; Formenti, S.; Barcellos-Hoff, M. H. *Growth Factors* **2015,** *33,* 79–91. doi:10.3109/08977194.2014.999367
35. Hill, J. J.; Davies, M. V.; Pearson, A. A.; Wang, J. H.; Hewick, R. M.; Wolfman, N. M.; Qiu, Y. *J. Biol. Chem.* **2002,** *277,* 40735–40741. doi:10.1074/jbc.M206379200
36. du Toit, J. I.; Jordaan, M.; Huijsmans, C. A. A.; Jordaan, J. H. L.; van Sittert, C. G. C. E.; Vosloo, H. C. M. *Molecules* **2014,** *19,* 5522–5537. doi:10.3390/molecules19055522
37. Phillips, J. P. *Chem. Rev.* **1956,** *56,* 271–297. doi:10.1021/cr50008a003
38. Niedermair, F.; Kwon, O.; Zojer, K.; Kappaun, S.; Trimmel, G.; Mereiter, K.; Slugovc, C. *Dalton Trans.* **2008,** 4006–4014. doi:10.1039/B804832K
39. Kappaun, S.; Sax, S.; Eder, S.; Möller, K. C.; Waich, K.; Niedermair, F.; Saf, R.; Mereiter, K.; Jacob, J.; Müllen, K.; List, E. J. W.; Slugovc, C. *Chem. Mater.* **2007,** *19,* 1209–1211. doi:10.1021/cm062666j
40. Slugovc, C.; Koppitz, A.; Pogantsch, A.; Stelzer, F. *Inorg. Chim. Acta* **2005,** *358,* 2718–2724. doi:10.1016/j.ica.2005.03.042
41. Schmid, T. E.; Modicom, F.; Dumas, A.; Borré, E.; Toupet, L.; Baslé, O.; Mauduit, M. *Beilstein J. Org. Chem.* **2015,** *11,* 1541–1546. doi:10.3762/bjoc.11.169
42. Ryken, S. A.; Schafer, L. L. *Acc. Chem. Res.* **2015,** *48,* 2576–2586. doi:10.1021/acs.accounts.5b00224
43. Samec, J. S. M.; Keitz, B. K.; Grubbs, R. H. *J. Organomet. Chem.* **2010,** *695,* 1831–1837. doi:10.1016/j.jorganchem.2010.04.017
44. Strasser, S.; Pump, E.; Fischer, R. C.; Slugovc, C. *Monatsh. Chem.* **2015,** *146,* 1143–1151. doi:10.1007/s00706-015-1484-x
45. Pump, E.; Leitgeb, A.; Kozłowska, A.; Torvisco, A.; Falivene, L.; Cavallo, L.; Grela, K.; Slugovc, C. *Organometallics* **2015,** *34,* 5438–5453. doi:10.1021/acs.organomet.5b00715
46. Wappel, J.; Urbina-Blanco, C. A.; Abbas, M.; Albering, J. H.; Saf, R.; Nolan, S. P.; Slugovc, C. *Beilstein J. Org. Chem.* **2010,** *6,* 1091–1098. doi:10.3762/bjoc.6.125
47. Burtscher, D.; Lexer, C.; Mereiter, K.; Winde, R.; Karch, R.; Slugovc, C. *J. Polym. Sci., Part A: Polym. Chem.* **2008,** *46,* 4630–4635. doi:10.1002/pola.22763
48. Rmsd is calculated for distances and angles: sn-1 = [∑i = 1→N (CV − EV)2/(N − 1)]1/2, where CV means calculated value, EV means experimental value (X-ray data), and N is the number of distances or angles taken into account.
49. Costas, M.; Ribas, X.; Poater, A.; López Balvuena, J. M.; Xifra, R.; Company, A.; Duran, M.; Solà, M.; Llobet, A.; Corbella, M.; Usón, M. A.; Mahía, J.; Solans, X.; Shan, X.; Benet-Buchholz, J. *Inorg. Chem.* **2006,** *45,* 3569–3581. doi:10.1021/ic051800j
50. Mola, J.; Romero, I.; Rodríguez, M.; Llobet, A.; Parella, T.; Benet-Buchholz, J.; Poater, A.; Duran, M.; Solà, M. *Inorg. Chem.* **2006,** *45,* 10520–10529. doi:10.1021/ic061126l
51. Tawa, G. J.; Topol, I. A.; Burt, S. K.; Caldwell, R. A.; Rashin, A. A. *J. Chem. Phys.* **1998,** *109,* 4852–4963. doi:10.1063/1.477096
52. Martínez, J. P.; Solà, M.; Poater, A. *ChemistryOpen* **2015,** *4,* 774–778. doi:10.1002/open.201500093
53. Leitgeb, A.; Wappel, J.; Urbina-Blanco, C. A.; Strasser, S.; Wappl, C.; Cazin, C. S. J.; Slugovc, C. *Monatsh. Chem.* **2014,** *145,* 1513–1517. doi:10.1007/s00706-014-1249-y
54. Credendino, R.; Poater, A.; Ragone, F.; Cavallo, L. *Catal. Sci. Technol.* **2011,** *1,* 1287–1297. doi:10.1039/c1cy00052g

55. Falivene, L.; Poater, A.; Cazin, C. S. J.; Slugovc, C.; Cavallo, L. *Dalton Trans.* **2013,** *42,* 7312–7317. doi:10.1039/c2dt32277c
56. Bantreil, X.; Poater, A.; Urbina-Blanco, C. A.; Bidal, Y. D.; Falivene, L.; Randall, R. A. M.; Cavallo, L.; Slawin, A. M. Z.; Cazin, C. S. J. *Organometallics* **2012,** *31,* 7415–7426. doi:10.1021/om300703p
57. Szczepaniak, G.; Kosinski, K.; Grela, K. *Green Chem.* **2014,** *16,* 4474–4492. doi:10.1039/C4GC00705K
58. Poater, A.; Ragone, F.; Correa, A.; Cavallo, L. *Dalton Trans.* **2011,** *40,* 11066–11069. doi:10.1039/c1dt10959f
59. Bantreil, X.; Nolan, S. P. *Nat. Protoc.* **2011,** *6,* 69–77. doi:10.1038/nprot.2010.177
60. Poater, A.; Credendino, R.; Slugovc, C.; Cavallo, L. *Dalton Trans.* **2013,** *42,* 7271–7275. doi:10.1039/c3dt32884h
61. Manzini, S.; Urbina-Blanco, C. A.; Poater, A.; Slawin, A. M. Z.; Cavallo, L.; Nolan, S. P. *Angew. Chem., Int. Ed.* **2012,** *51,* 1042–1045. doi:10.1002/anie.201106915
62. Demel, S.; Schoefberger, W.; Slugovc, C.; Stelzer, F. *J. Mol. Catal. A* **2003,** *200,* 11–19. doi:10.1016/S1381-1169(03)00048-7
63. Slugovc, C.; Wappel, J. Olefin Metathesis. WIPO/PCT Patent WO2013/029079 A1, 2013.
64. *Gaussian 09,* Revision D.01; Gaussian, Inc.: Wallingford, CT, U.S.A., 2009.
65. Becke, A. *Phys. Rev. A* **1988,** *38,* 3098–3100. doi:10.1103/PhysRevA.38.3098
66. Perdew, J. P. *Phys. Rev. B* **1986,** *33,* 8822–8824. doi:10.1103/PhysRevB.33.8822
67. Perdew, J. P. *Phys. Rev. B* **1986,** *34,* 7406. doi:10.1103/PhysRevB.34.7406
68. Häusermann, U.; Dolg, M.; Stoll, H.; Preuss, H.; Schwerdtfeger, P.; Pitzer, R. M. *Mol. Phys.* **1993,** *78,* 1211–1224. doi:10.1080/00268979300100801
69. Küchle, W.; Dolg, M.; Stoll, H.; Preuss, H. *J. Chem. Phys.* **1994,** *100,* 7535–7542. doi:10.1063/1.466847
70. Leininger, T.; Nicklass, A.; Stoll, H.; Dolg, M.; Schwerdtfeger, P. *J. Chem. Phys.* **1996,** *105,* 1052–1059. doi:10.1063/1.471950
71. Schäfer, A.; Horn, H.; Ahlrichs, R. *J. Chem. Phys.* **1992,** *97,* 2571–2577. doi:10.1063/1.463096
72. Rappoport, D.; Furche, F. *J. Chem. Phys.* **2010,** *133,* 134105. doi:10.1063/1.3484283
73. Zhao, Y.; Truhlar, D. G. *Theor. Chem. Acc.* **2008,** *120,* 215–241. doi:10.1007/s00214-007-0310-x
74. Barone, V.; Cossi, M. *J. Phys. Chem. A* **1998,** *102,* 1995–2001. doi:10.1021/jp9716997
75. Tomasi, J.; Persico, M. *Chem. Rev.* **1994,** *94,* 2027–2094. doi:10.1021/cr00031a013

License and Terms

BEILSTEIN JOURNAL OF ORGANIC CHEMISTRY

Recent advances in N-heterocyclic carbene (NHC)-catalysed benzoin reactions

Rajeev S. Menon[1], Akkattu T. Biju[2] and Vijay Nair*[3]

Review

Open Access

Address:
[1]Department of Chemistry, Central University of Haryana, Mahendergarh, Haryana-123 029, India, [2]Organic Chemistry Division, National Chemical Laboratory (CSIR), Dr. Homi Bhabha Road, Pune 411 008, India and [3]Organic Chemistry Section, CSIR-National Institute for Interdisciplinary Science and Technology,Trivandrum 695 019, India.; Fax: +91 471 2491712; Tel: +91 471 2490406

Email:
Vijay Nair* - vijaynair_2001@yahoo.com

* Corresponding author

Keywords:
acyloin reaction; benzoin reaction; N-heterocyclic carbenes; organocatalysis; umpolung

Beilstein J. Org. Chem. **2016,** *12,* 444–461.
doi:10.3762/bjoc.12.47

Received: 15 December 2015
Accepted: 24 February 2016
Published: 09 March 2016

This article is part of the Thematic Series "N-Heterocyclic carbenes" and is dedicated to Professor Ron Breslow on the occasion of his 85th birthday.

Guest Editor: S. P. Nolan

Abstract

N-Heterocyclic carbenes (NHCs) have emerged as a powerful class of organocatalysts that mediate a variety of organic transformations. The Benzoin reaction constitutes one of the earliest known carbon–carbon bond-forming reactions catalysed by NHCs. The rapid growth of NHC catalysis in general has resulted in the development of a variety of benzoin and benzoin-type reactions. An overview of such NHC-catalysed benzoin reactions is presented.

Introduction

The benzoin reaction (or condensation) is named after the product it furnishes via a catalytic assembly of two molecules of aromatic aldehydes. One molecule of the aldehyde functions as an acyl anion and the other as a carbonyl electrophile to afford α-hydroxy ketones (benzoins). It is a 100% atom-economic process wherein a new stereocentre is produced. The reaction is sometimes referred to as acyloin condensation to encompass reactions of aliphatic aldehydes. The assembly of two molecules of the same aldehyde is known as homo-benzoin reaction and that of two different aldehydes is known as crossed benzoin reaction. Mechanistically the reaction involves polarity reversal (umpolung) of one aldehyde to generate an acyl anion equivalent and this event is mediated by the catalyst. Alkali metal cyanides and N-heterocyclic carbenes (NHCs) are the two main classes of catalysts that are known to mediate benzoin reactions. This review focuses on the recent advancements made in the area of NHC-catalysed benzoin reactions.

Historically, the first benzoin reaction was reported by Wöhler and Liebig in 1832. They discovered that the cyanide anion can catalyze the union of two molecules of aromatic aldehydes to afford α-hydroxy ketones [1]. More than a century later, a thia-

zolium salt-catalysed benzoin reaction was reported by Ukai [2]. This may be regarded as an early example of organocatalysis using an azolium salt. Breslow postulated in 1958 a mechanistic rationale for the thiazolium salt-catalysed benzoin reaction [3]. He depicted the catalytically active species as a thiazolium zwitterion (the resonance structure of an NHC) and proposed that the reaction proceeds via an enaminol intermediate. The latter is now popularly known as 'Breslow intermediate'. This seminal discovery by Breslow paved the way for further developments in the area of carbene catalysis. Almost three decades later Bertrand and co-workers proved the existence of carbenes as catalytically active species in the benzoin reaction, with the synthesis of a stable phosphinocarbene [4]. Arduengo and co-workers isolated and characterised a stable NHC in 1991 [5]. These two reports on the isolation of NHCs implied that they are more stable and robust than previously considered. Subsequent years witnessed a renewal of interest in NHCs and a flurry of reports, mainly focusing on their catalytic activity, appeared in the literature [6,7].

The original mechanistic proposal by Breslow for the thiazolium salt-catalysed benzoin reaction can be delineated as follows (Scheme 1) [3]. Lapworth had suggested how the cyanide anion functions first as a nucleophile and then as a leaving group in cyanide-catalysed benzoin reactions [8]. Analogously, Breslow invoked the generation of a nucleophilic thiazolylidene species **1** via deprotonation of the thiazolium salt by base. The ylide **1** may also be represented as its resonance structure **1'** (carbene). Nucleophilic addition of **1** to aromatic aldehyde generates the tetrahedral intermediate **2**. The latter then undergoes a proton shift to furnish an enaminol derivative **3**. The aldehyde carbonyl carbon has now transformed into a nucleophilic entity by virtue of conjugation to the nitrogen and sulfur lone pairs. This acyl anion equivalent **3** is known as the "Breslow intermediate". Its reaction with another molecule of aldehyde leads to the formation of an alkoxide intermediate **4**. Proton transfer and subsequent release of thiazolylidene **1** affords the final product, the α-hydroxy ketone **5**. Breslow demonstrated that imidazolium-derived ylides also catalysed benzoin reactions. In most of the cases, the NHC-catalysed formation of benzoin from aldehydes is reversible in nature.

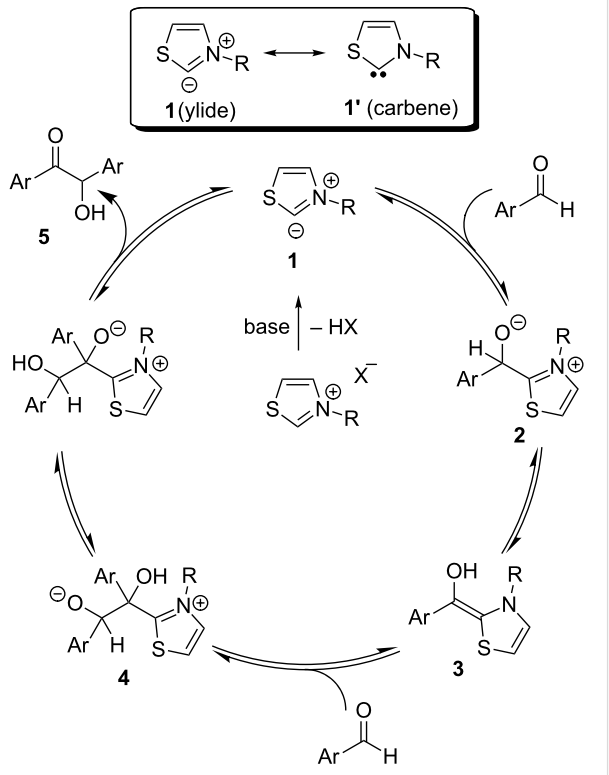

Scheme 1: Breslow's proposal on the mechanism of the benzoin condensation.

In the following sections, detailed discussions on various types of benzoin reactions catalysed by NHCs are presented. In general, thiazolium salt-derived NHCs have found widespread application as catalysts for benzoin reactions, whereas triazolium-derived NHCs have emerged as popular catalysts for enantioselective benzoin transformations.

Review

Homo-benzoin reactions

The homo-benzoin condensation constitutes an overall catalytic dimerization of an aldehyde wherein the acyl anion derived from one molecule adds to another molecule of the aldehyde. (It may be noted that the term 'homo' implies the reaction between two molecules of the same aldehyde. It should not be misconstrued as a 'homologous' benzoin reaction). Benzoin reactions are reversible in basic medium and homo-benzoin products are often isolated as byproducts in other NHC-mediated reactions of aldehydes. The absence of chemoselectivity issues makes homo-benzoin reactions less challenging when compared to the cross-benzoin variant. NHC-mediated aerial oxidation of aldehydes to the corresponding carboxylic acids could compete with homo-benzoin reactions, but can be limited by careful exclusion of oxygen from the reaction mixture. A few recent reports of homo-benzoin reactions are discussed in the following passages.

Stetter's report in 1976 of thiazolium salt-catalysed benzoin reactions may be regarded as the first report of an NHC-catalysed benzoin reaction on a synthetically useful scale [9]. Much later, in 2005, Xu and Xia used *N*-alkyl-substituted imidazolium carbene **6** to efficiently promote benzoin reactions. Although a high catalyst loading (50 mol %) was required, the reactions could be run at mild conditions. It was observed that

neutral and electron rich aromatic aldehydes afford good yields of benzoin products whereas electron deficient aromatic aldehydes and aliphatic aldehydes reacted sluggishly (Scheme 2) [10].

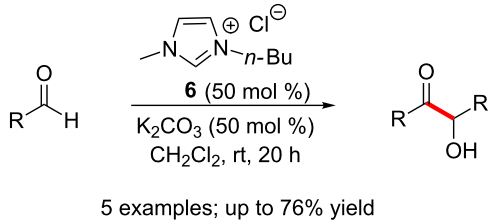

Scheme 2: Imidazolium carbene-catalysed homo-benzoin condensation.

The easily accessible NHC precatalyst **7** endowed with long aliphatic side chains was used by Iwamoto and co-workers for promoting benzoin reactions in aqueous medium. The improved reactivity was attributed to the formation of micelles from the hydrophobic alkyl chains of the catalyst in aqueous medium. The reaction proceeded well with various aromatic and heteroaromatic aldehydes (Scheme 3) [11].

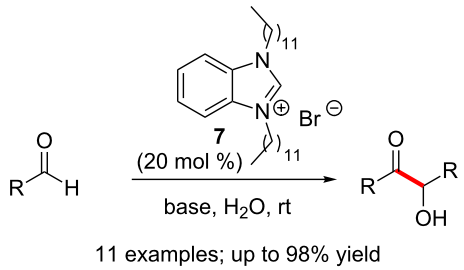

Scheme 3: Homo-benzoin condensation in aqueous medium.

Subsequently, the same group disclosed the application of bis(benzimidazolium) precursor **8** as a more efficient catalyst for the benzoin condensation in aqueous medium. Here, the NHC precatalyst incorporated a long aliphatic bridge between the two imidazolium entities. The aggregation of these units creates a hydrophobic environment in which the two aromatic aldehydes are subjected to catalysis (Scheme 4) [12].

Asymmetric homo-benzoin reactions

Much of the progress in the area of NHC-catalysed asymmetric benzoin reactions has been covered in two excellent reviews [6,7]. Some additional recent examples are discussed below.

A selected list of chiral NHC catalysts that have been explored for mediating asymmetric benzoin reactions is presented in Scheme 5. The bis-triazolium catalyst **9** developed by You promoted asymmetric benzoin reactions in 95% ee [13]. Enders developed the pyroglutamic acid-derived triazolium salt **10** which mediated benzoin reactions in similar enantioselectivities [14].

The chiral triazolium catalyst **11** transfers chiral information to the benzoin products by engaging in hydrogen-bonding interactions [15]. Waser's chiral bifunctional (thio)urea NHC **12** also relies on hydrogen bonding to mediate asymmetric benzoin reactions [16]. A 2-pyrdiyl appendage distinguishes Ukaji's chiral triazolium catalyst **13** from similar salts [17]. Spirocyclic (1*R*)-camphor-derived triazolium salt **14**developed by Rafiński also successfully catalysed asymmetric benzoin condensations [18].

The pentafluorophenyltriazolium catalyst **15** featured in the most efficient asymmetric benzoin reaction reported so far. Inoue and co-workers found that it promotes homocoupling of benzaldehyde at a low loading (4 mol %) to afford benzoin in 90% yield and >99% ee (Scheme 6) [19].

Cross-benzoin reactions

A cross-benzoin reaction unites two different aldehydes wherein one of them functions as the acyl anion equivalent. A total of four products are possible; a pair of homo-benzoin and cross-benzoin adducts each. A substrate-driven selectivity may be observed when one of the aldehydes is significantly less reactive due to electronic or steric reasons. The latter effect may be amplified by employing bulky NHCs. In general, NHC-mediated selective cross-benzoin reactions of electronically and

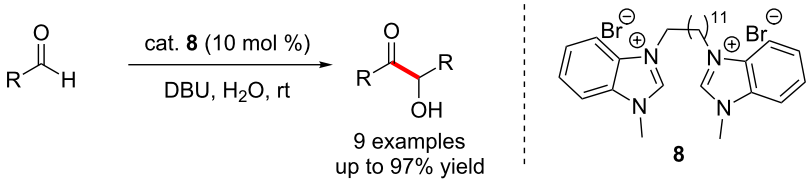

Scheme 4: Homobenzoin condensation catalysed by bis(benzimidazolium) salt **8**.

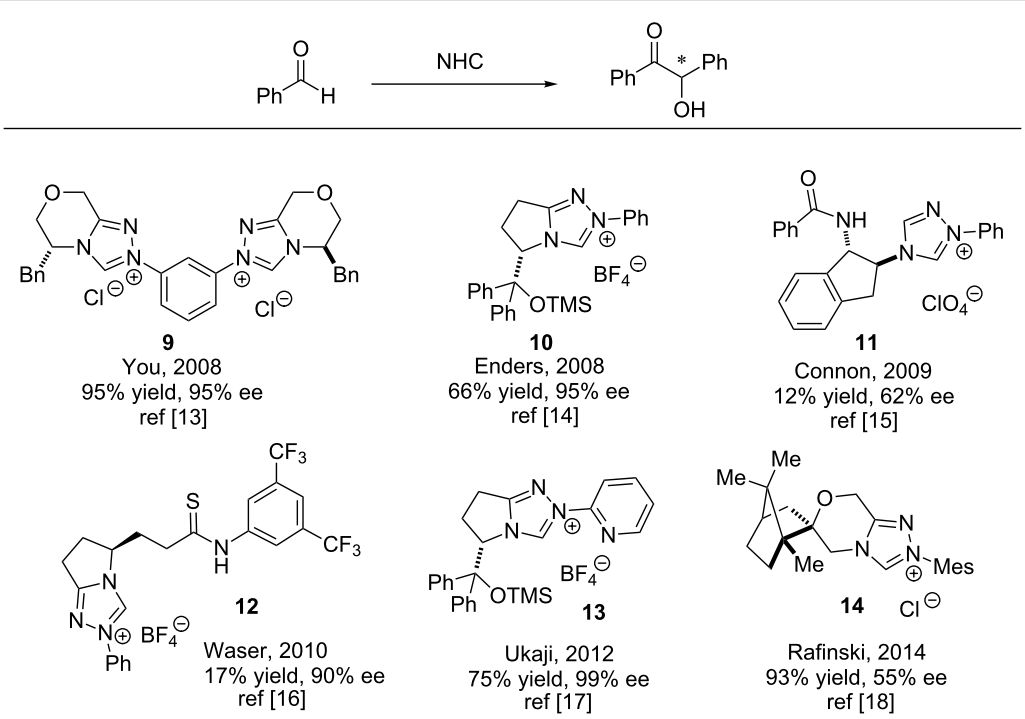

Scheme 5: List of assorted chiral NHC-catalysts used for asymmetric homobenzoin condensation.

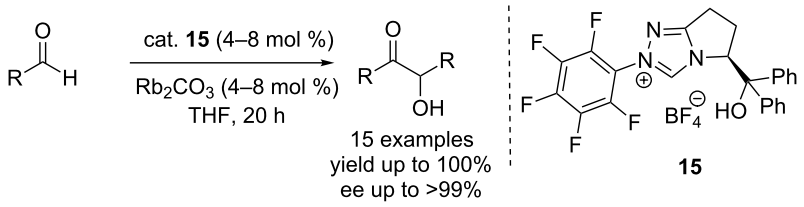

Scheme 6: A rigid bicyclic triazole precatalyst **15** in an efficient enantioselective benzoin reaction.

sterically similar aldehydes remain as a highly challenging transformation.

In 1985, Inoue and co-workers reported the NHC-catalysed selective cross-benzoin reactions of aromatic and aliphatic aldehydes with formaldehyde leading to the formation of α-hydroxy ketones. Although an excellent selectivity was observed for the cross-benzoin product, the yields were low (Scheme 7) [20].

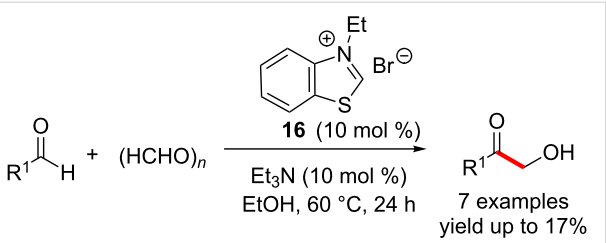

Scheme 7: Inoue's report of cross-benzoin reactions.

Later Kuhl and Glorius employed an NHC generated from the thiazolium salt **17** to synthesise α-hydroxyketones **18** in good yields. This highly selective cross-benzoin reaction has a very broad substrate scope (Scheme 8) [21].

Yang and co-workers developed an intermolecular cross coupling of aromatic aldehydes with acetaldehyde. The reaction showed an interesting divergence in reactivity controlled by the catalysts, viz., the thiazolium salt **19** and triazolium salt **20**. The thiazolium-derived carbene preferentially mediated the formation of the Breslow intermediate from the aromatic aldehyde followed by coupling with acetaldehyde. In contrast, the triazolium-derived carbene prefered to activate acetaldehyde to generate the corresponding acyl anion equivalent followed by coupling with aromatic aldehydes (Scheme 9) [22]. It may be

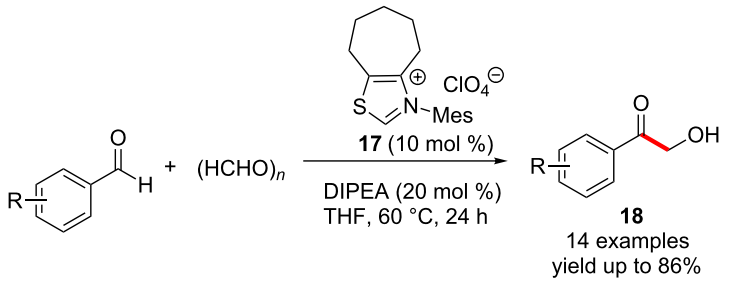

Scheme 8: Cross-benzoin reactions catalysed by thiazolium salt **17**.

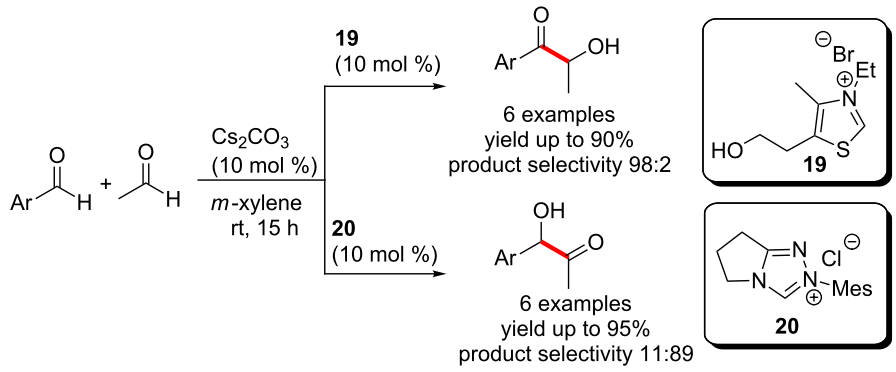

Scheme 9: Catalyst-controlled divergence in cross-benzoin reactions.

mentioned that Connon, Zeitler and co-workers have also reported the use of thiazolium and triazolium precatalysts for selective cross-benzoin reactions [23].

Glorius introduced a number of thiazolium NHC precatalysts endowed with sterically bulky aryl groups on the nitrogen with varying backbone substitution. These NHCs exhibited high levels of reactivity and selectivity in intermolecular cross-benzoin reactions to afford a library of unsymmetrically substituted benzoins [24]. The presence of an *ortho*-substituent on the electrophilic aromatic aldehyde (which presumably hinders the direct addition of NHC to these aldehydes) was necessary for the high levels of selectivity (Scheme 10).

The NHC-catalysed chemoselective intermolecular cross-benzoin condensation reaction of aromatic and aliphatic aldehydes was reported by Yang and co-workers. The chemoselectivity was achieved by using a large excess of the aliphatic aldehyde (molar ratio of 1:15) [25]. Thus, directing groups on the aromatic aldehydes were not a prerequisite for high levels of selectivity in contrast to the earlier example. Consecutive catalytic reactions were utilized in order to reuse the excess of aliphatic aldehydes employed for achieving selectivity. Interestingly, the reaction could be repeated up to five times without affecting the yield of product and chemoselectivity (Scheme 11).

Morpholinone and piperidinone-derived triazolium precatalysts can catalyze highly chemoselectively the cross-benzoin reaction of aliphatic and aromatic aldehydes [26]. Smooth and selective benzoin reactions were observed with a wide variety of linear and branched aliphatic aldehydes as well as aromatic

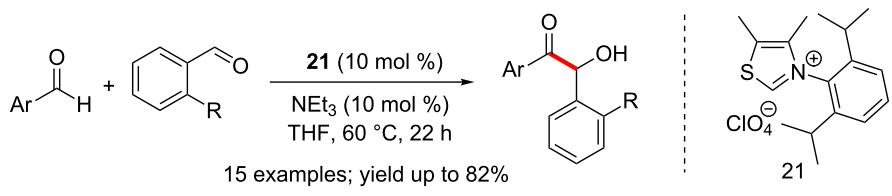

Scheme 10: Chemoselective cross-benzoin reactions catalysed by a bulky NHC.

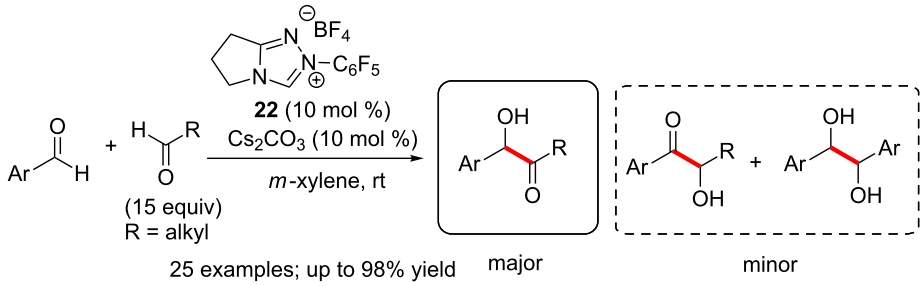

Scheme 11: Selective intermolecular cross-benzoin condensation reactions of aromatic and aliphatic aldehydes.

aldehydes (Scheme 12). Notably, the aliphatic aldehydes functioned as acyl anion equivalents leading to the formation of alkyl ketone (benzoin) products.

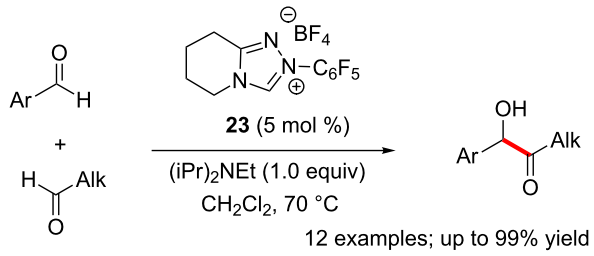

Scheme 12: Chemoselective cross-benzoin reaction of aliphatic and aromatic aldehydes.

Asymmetric cross-benzoin reactions

The development of enantioselective cross-benzoin reactions is an arduous task as both chemoselectivity and stereoselectivity must be controlled by a single catalyst. Unsurprisingly, most of the NHC-catalysed, enantioselective cross-benzoin reactions employ a combination of two distinct carbonyl components to minimize chemoselectivity issues. A selected group of asymmetric cross-benzoin reactions are described in the following section.

An NHC-catalysed union of aryl aldehydes and aryl trifluoromethyl ketones was developed in the laboratory of Enders. This direct intermolecular cross-benzoin reaction proceeded with high yields and chemoselectivity [27]. The reaction furnished excellent yields of α-hydroxy-α-trifluoromethyl ketones **25** possessing a quaternary stereocentre. The homo-benzoin condensation between two aldehydes is reversible under the reaction conditions. This eventually leads to the selective formation of the observed cross-benzoin product. Later, it was found that trifluoromethyl ketimines **26** also function as electrophiles under similar reaction conditions [28]. Although initial attempts of asymmetric transformations were not successful, enantioselective cross-benzoin reactions of heteroaromatic aldehydes (acyl donors) and aryl trifluoromethyl ketones were later developed using the chiral catalyst **27** (Scheme 13) [29].

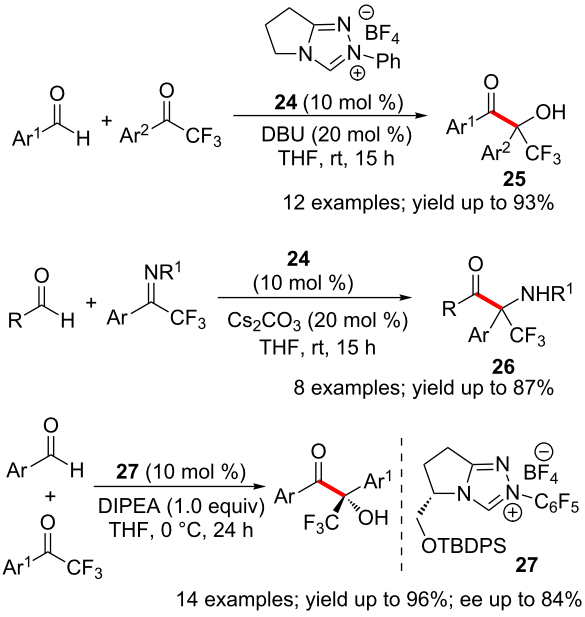

Scheme 13: Cross-benzoin reactions of trifluoromethyl ketones developed by Enders.

The electron-deficient triazolium-derived NHC **23** mediated efficient and chemoselective cross-benzoin reactions of aldehydes and α-ketoesters to produce acyloin products endowed with a quaternary stereocentre [30]. Remarkably, the competing hydroacylation reaction was not observed under these reaction conditions. A variety of aliphatic and aromatic aldehydes functioned as acyl donors, whereas several α-ketoesters could be employed as the electrophilic coupling partner to afford the desired products in moderate to good yields (Scheme 14). Interestingly, preliminary experiments to develop an enantioselective version of this reaction using a chiral NHC returned promising levels of enantioselectivity (76% ee).

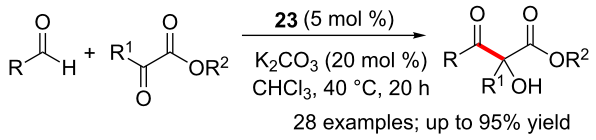

Scheme 14: Cross-benzoin reactions of aldehydes and α-ketoesters.

Subsequently, Gravel and co-workers reported a high yielding chemoselective and enantioselective intermolecular cross-benzoin reaction of aliphatic aldehydes and α-ketoesters. Notably, the reaction affords enantiomerically enriched tertiary alcohols. Excellent levels of enantioselection were obtained by using an electron-deficient valine-derived triazolium salt precatalyst **28** (Scheme 15) [31]. Moreover, diastereoselective reduction of the cross-benzoin products with $NaBH_4$ afforded valuable *syn*-diol products.

Goodman and Johnson disclosed a dynamic kinetic resolution of β-halo-α-ketoesters via NHC-catalysed asymmetric cross-benzoin reaction. Here, the cross-benzoin reaction of aromatic aldehydes with β-stereogenic-α-keto esters afforded fully substituted β-halo-α-glycolic acid derivatives in high diastereoselectivity and enantioselectivity [32]. The NHC generated from the amino indanol-derived chiral triazolium salt **29** provided the best results (Scheme 16). A variety of aromatic aldehydes and a series of β-halo α-ketoesters partake in the reaction to furnish the chiral glycolic acid derivatives.

The enantioselective benzoin reaction between a variety of aldehydes and alkynones is catalysed by the NHC generated from chiral aminoindanol-triazolium salt **29**. The reactions afforded substituted propargylic alcohols in high yields and enantioselectivity (Scheme 17). It is noteworthy that the catalytically generated Breslow intermediates undergo selective 1,2-addition with ynones and the competing Stetter-type reactivity was not observed [33].

Aza-benzoin reactions

In aza-benzoin reactions, the acyl anions generated from aldehydes react with an aza electrophile. Imines possessing an elec-

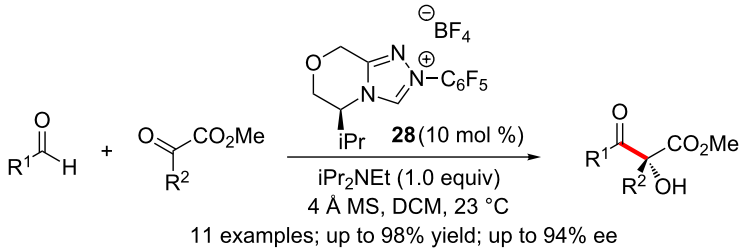

Scheme 15: Enantioselective cross-benzoin reactions of aliphatic aldehydes and α-ketoesters.

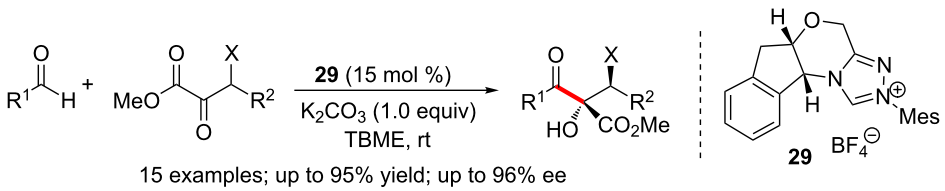

Scheme 16: Dynamic kinetic resolution of β-halo-α-ketoesters via cross-benzoin reaction.

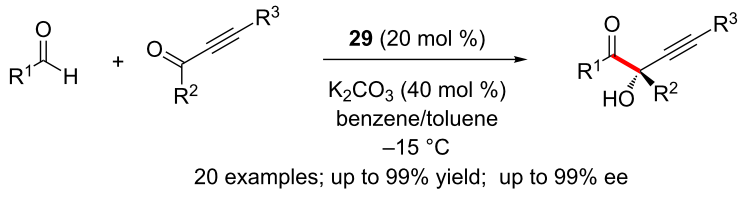

Scheme 17: Enantioselective benzoin reaction of aldehydes and alkynones.

tron-withdrawing N-substituent constitute the most commonly used aza electrophile and the reaction affords an α-aminocarbonyl compound as the product. The NHC-mediated addition of aldehyde-derived acyl anions to nitroso compounds leading to the formation of hydroxamic acid derivatives are also discussed in this section for convenience.

Acylimines function as electrophiles in NHC-catalysed aza-benzoin reaction with aldehydes. The reactive acylimine is generated in situ by the action of base on the sulfonylamide derivative **30** [34]. Meanwhile, the Breslow intermediate is produced from the aldehyde by the thiazolium **31**-derived NHC. The union of these two reactive intermediates furnished α-amidoketones **32** in excellent yields (Scheme 18).

A diastereoselective [4 + 1] annulation of phthalaldehyde with imines leading to the formation of *cis*-2-amino3-hydroxyindanones is catalysed by NHC **31**. The imine electrophile is generated in situ from α-sulfonyl-*N*-Boc amine **33** (Scheme 19). Initial cross-aza-benzoin reaction of one of the aldehyde functionalities with the imine is followed by an intramolecular aldol reaction to furnish the indanone framework [35].

The thiazolium precatalyst **31** can also efficiently mediate cross-aza-benzoin reactions of aromatic and heteroaromatic aldehydes with unactivated aromatic imines **34** (Scheme 20) [36]. A control reaction of the corresponding benzoin (instead of the aldehyde) and imine **34** also afforded the α-amino ketone product **35** in 71% yield. This indicates that the reaction involves reversible formation of aldehyde-homobenzoin adducts.

Enantioselective cross aza-benzoin reaction of aliphatic aldehydes with *N*-Boc-protected imines are promoted efficiently by NHC generated from the chiral triazolium salt **36**. The aldehydes function as the acyl donor and the imines behave as the receptors (Scheme 21). Addition of NHC to the highly electrophilic *N*-Boc imines leads to the formation of corresponding aza-Breslow intermediates; however, it is reversible under the reaction conditions. Importantly, the chirally pure α-amino ketones formed in this reaction are valuable building blocks in organic synthesis [37].

The NHC generated from the bicyclic pentafluoro triazolium salt promoted the chemoselective cross aza-benzoin reaction of

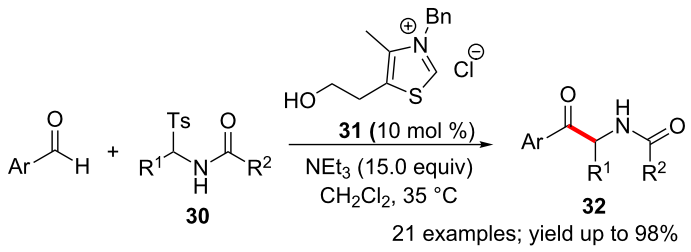

Scheme 18: Aza-benzoin reaction of aldehydes and acylimines.

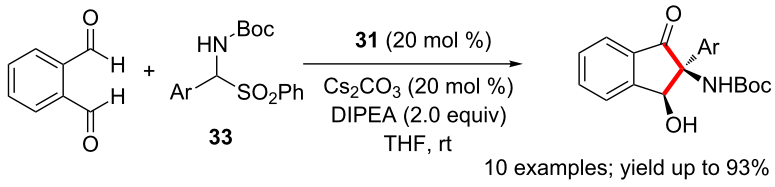

Scheme 19: NHC-catalysed diastereoselective synthesis of *cis*-2-amino 3-hydroxyindanones.

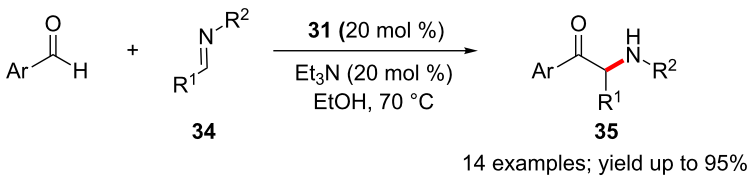

Scheme 20: Cross-aza-benzoin reactions of aldehydes with aromatic imines.

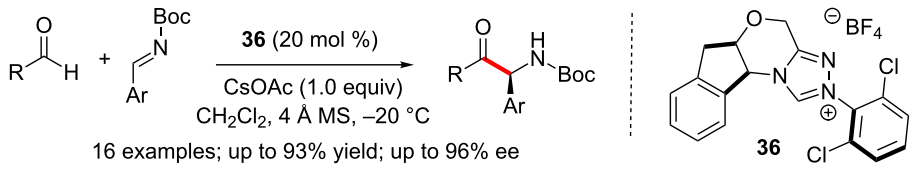

Scheme 21: Enantioselective cross aza-benzoin reaction of aliphatic aldehydes with *N*-Boc-imines.

aldehydes with *N*-PMP-imino esters to afford α-amino-β-keto esters in good yield (Scheme 22) [38]. A range of functional groups are tolerated under the optimised reaction conditions.

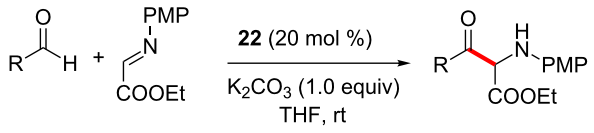

Scheme 22: Chemoselective cross aza-benzoin reaction of aldehydes with *N*-PMP-imino esters.

Mattson and Scheidt developed a catalytic coupling reaction of acylsilanes with imines for the synthesis of aminoketones (Scheme 23). The reaction proceeds through the generation of the Breslow intermediate from the acylsilane followed by a cross-coupling with the imine [39].

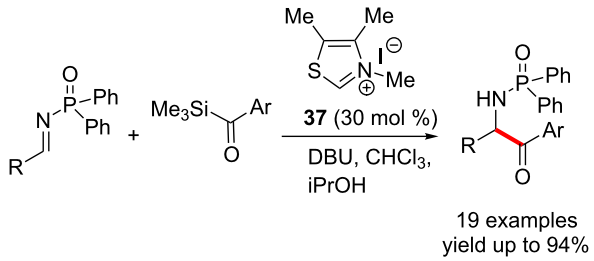

Scheme 23: NHC-catalysed coupling reaction of acylsilanes with imines.

In 2005, Miller and co-workers used the chiral thiazolium salt **38** to catalyse an enantioselective cross-aza-benzoin reaction. Racemisation of the products under the reaction conditions caused erosion of enantioselectivity. This problem was successfully addressed by using a hindered base, pentamethyl piperidine, which was inert towards the products (Scheme 24) [40].

In 2013, Ye disclosed a remarkable NHC-catalysed enantioselective aza-benzoin reaction of enals and activated ketimines leading to the formation of functionalised α-aminoketones **39** in high enantioselectivity [41]. Notably, the homoenolate or enolate reactivity of the NHC-enal adduct was not observed in this case. The presence of a tertiary alcohol functionality and the steric bulk of the NHC-precatalyst **40** were essential for the selective formation of the aza-benzoin adduct. A variety of trifluoromethylated α-aminoketones could be synthesised in enantiomerically pure form using this method (Scheme 25).

Isatin derived ketimines **41** were employed as electrophiles in the NHC-catalysed chemo- and stereoselective cross-aza-benzoin reaction with enals by Chi. The reaction afforded chiral quaternary aminooxindole derivatives. The NHC–enal adduct prefers to react via the acyl anion pathway and the competing homoenolate/enolate reactivity was not observed. The sterically non-congested, electron-deficient NHC-catalyst **42** presumably does not hinder bond formation at the catalyst-bound acyl carbon (Scheme 26) [42].

The aza-benzoin reaction of aldehydes and phosphinoylimines catalysed by the bis(amino)cyclopropenylidene (BAC) carbene **43** was reported recently. The reaction showed excellent selectivity for the aza-benzoin products over the homo-benzoin

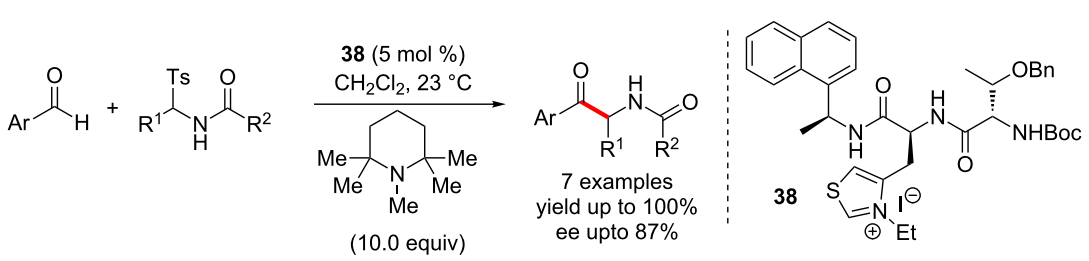

Scheme 24: Thiazolium salt-mediated enantioselective cross-aza-benzoin reaction.

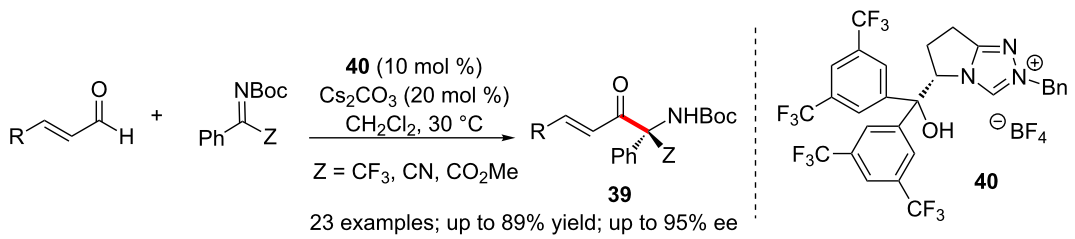

Scheme 25: Aza-benzoin reaction of enals with activated ketimines.

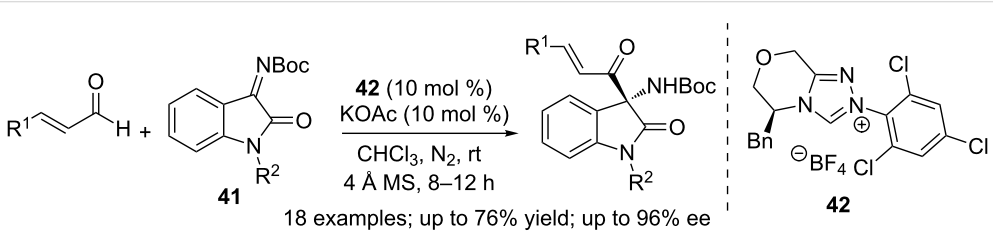

Scheme 26: Isatin derived ketimines as electrophiles in cross aza-benzoin reaction with enals.

adducts. A wide variety of aldehydes react with phosphinoylimines (generated from their sulfinic acid adducts **44**) to afford *N*-phosphinoyl amnioketones (Scheme 27) [43]. The attempted enantioselective version of this reaction using a chiral BAC catalyst was, however, unsuccessful.

As mentioned earlier, nitrosoarenes have been used as the electrophilic component in a few reactions of NHC-bound aldehydes. The addition of acyl anions occur at the nitrogen atom of the nitroso compound. A NHC-catalysed cascade reaction of *o*-vinylarylaldehydes with nitrosoarenes afforded functionalised 2,3-benzoxazin-4-ones **45** [44]. The initial intermolecular aza-benzoin reaction is followed by an intramolecular oxa-Michael reaction to form the observed product (Scheme 28).

Enders reported a cascade reaction which is initiated by an NHC-catalysed aza-benzoin condensation between various aldehydes and nitrosobenzenes to generate the hydroxamic acids **47**. This is followed by a redox esterification of the latter (**47**) with enals. The overall process constitutes a one-pot synthesis of hydroxamic esters **48** [45]. Notably, both steps can be performed using the single NHC catalyst **22** under same reac-

Scheme 27: Aza-benzoin reaction of aldehydes and phosphinoylimines catalysed by the BAC-carbene.

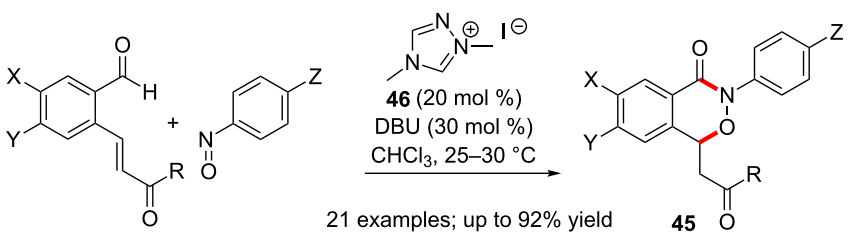

Scheme 28: Nitrosoarenes as the electrophilic component in benzoin-initiated cascade reaction.

tion conditions (Scheme 29). This two-step, one-pot synthesis of formahydroxamic esters constitutes a valuable addition to a thin list of NHC-mediated three-component reactions.

Intramolecular benzoin reactions

One of the earliest reports of an intramolecular benzoin condensation appeared in 1976. Cookson and Lane found that the treatment of anhydrous glutaraldehyde with thiazolium salt **49** and triethylamine resulted in the formation of 2-hydroxycyclopentanone. The latter underwent oxidation to afford 2-hydroxycyclopent-2-en-1-one **50** upon treatment with $Cu(OAc)_2$ (Scheme 30) [46]. Hexanedial furnished the corresponding α-hydroxycyclohexanone under identical reaction conditions.

An intramolecular cross-benzoin condensation between aldehyde and ketone moieties was developed by Suzuki in 2003. The isoxazole-fused cyclohexanone **51** endowed with an aryl aldehyde underwent a smooth cross-benzoin cyclisation in the presence of the thiazolium catalyst **19** and DBU. Although the presence of an isoxazole moiety is not a prerequisite for the success of this annulation, its rigid nature presumably renders the reaction highly stereoselective [47]. This simple and mild method allowed the construction of orthogonally protected polycyclic quinones from readily available starting materials. Later in 2006, they developed the enantioselective version of this reaction using an aminoindanol-derived triazolium salt **52** (Scheme 31) [48].

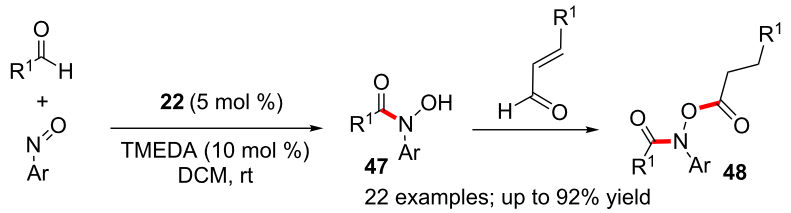

Scheme 29: One-pot synthesis of hydroxamic esters via aza-benzoin reaction.

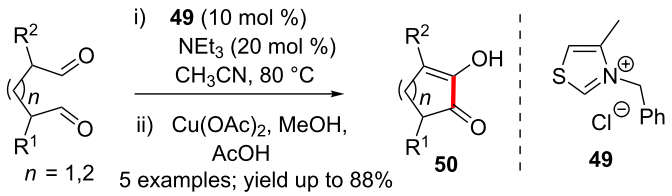

Scheme 30: Cookson and Lane's report of intramolecular benzoin condensation.

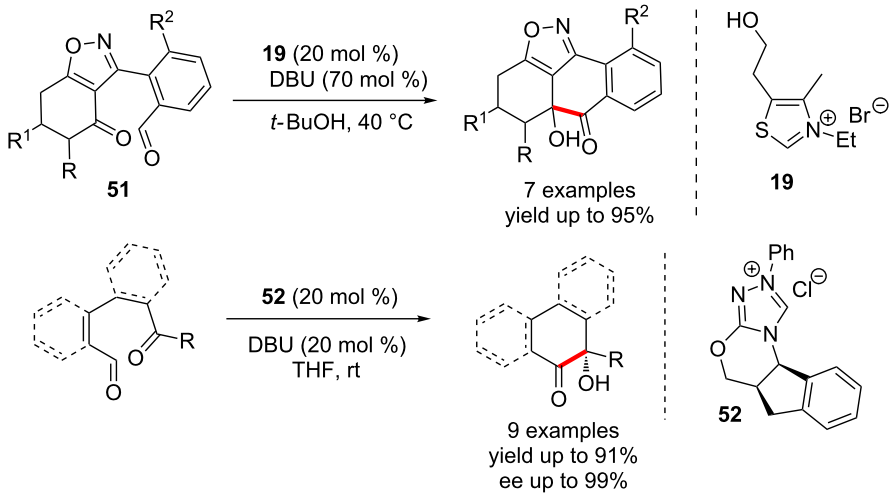

Scheme 31: Intramolecular cross-benzoin condensation between aldehyde and ketone moieties.

Another intramolecular crossed aldehyde-ketone benzoin reaction of simple dicarbonyl systems was developed by Enders (Scheme 32). This method employs commercially available thiazolium salt **19** as precatalyst and affords five- and six-membered cyclic acyloins in good yields [49].

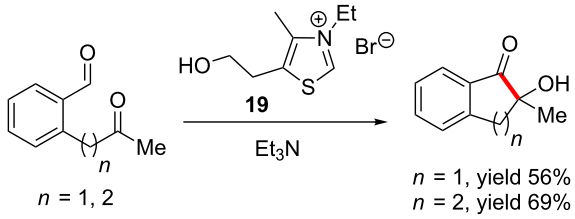

Scheme 32: Intramolecular crossed aldehyde-ketone benzoin reactions.

The enantioselective NHC-catalysed crossed aldehyde-ketone benzoin reaction for the synthesis of five- and six-membered cyclic acyloins was also developed by Enders. NHC generated from the tetracyclic triazolium salt **53** gave the best results [50]. It is noteworthy that the absolute stereochemistry of the α-carbonyl quaternary center of benzo-fused carbocycles and chromanones is installed with excellent control (Scheme 33).

A combination of D-camphor-derived triazolium precatalyst **54** and DBU promoted enantioselective intramolecular cross-benzoin reaction of **55** to afford chromanone **56** in excellent yield and enantioselectivity (Scheme 34). The NHC-precatalyst is conveniently prepared from camphor in 5 steps [51].

NHC generated from the *N*-*tert*-butyl-substituted imidazolium salt **57** catalysed the intramolecular cross-benzoin reaction of chalcones derived from *o*-phthalaldehydes. The reaction proceeded rapidly (20 min) at room temperature to afford good yields (75–94%) of naphthalenone-based tertiary alcohols **58** (Scheme 35) [52].

The synthesis of bicyclic tertiary alcohols possessing two quaternary stereocentres at the bridgehead positions was

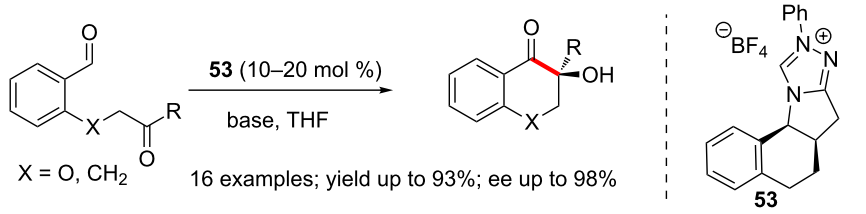

Scheme 33: Enantioselective intramolecular crossed aldehyde-ketone benzoin reaction.

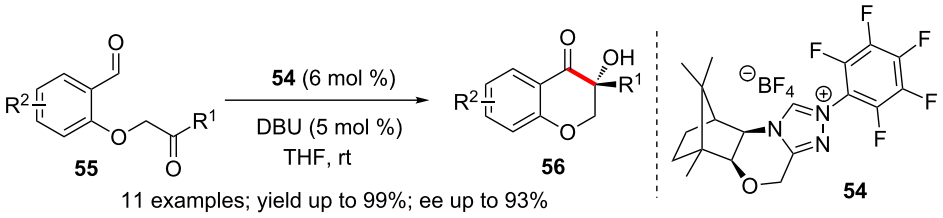

Scheme 34: Chromanone synthesis via enantioselective intramolecular cross-benzoin reaction.

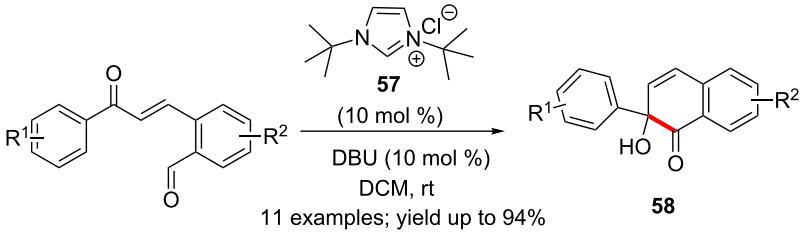

Scheme 35: Intramolecular cross-benzoin reaction of chalcones.

achieved via an asymmetric intramolecular crossed benzoin reaction. A relatively high loading (30 mol %) of the NHC precatalyst **59** was necessary for efficient reactions (Scheme 36) [53].

A multicatalytic Michael–benzoin cascade process for the asymmetric synthesis of functionalised cyclopentanones was disclosed in 2009 by Rovis. The chiral secondary amine **60** catalyzes the initial asymmetric Michael addition of an 1,3-diketone and an enal to afford a δ-ketoaldehyde **61**. Subsequently, a cross-benzoin reaction of the latter promoted by the NHC precatalyst **22**, installs the cyclopentenone system (Scheme 37). It may be noted that the absolute stereochemistry of the process is controlled by the prolinol catalyst **60** and the NHC precatalyst **22** is achiral. Control experiments revealed that the Michael addition is reversible but the NHC catalyst rapidly shuttles the intermediate δ-keto aldehyde **61** to the final product preventing the erosion of enantioselectivity [54]. This cascade reaction constitutes a fine example of symbiotic dual-catalysis wherein both catalysts perform better together in a one-pot reaction than they do independently over two steps.

A conceptually similar enamine-NHC dual-catalytic Michael–benzoin cascade was also developed by Rovis. The reaction proceeds via the generation of an enamine from the enolizable aldehyde **62** in presence of the prolinol catalyst **60** and its subsequent addition to the Michael acceptor **63**. This is followed by NHC-mediated intramolecular cross-benzoin condensation to afford the cyclopentanone **64**. Clear evidence for the co-operative relationship between the catalysts was obtained from control experiments. Chiral triazolium catalyst **65** preferentially converts only one of the diastereomeric Michael adducts into the benzoin product. The prolinol catalyst **60**, on the other hand, mediates the epimerisation of the less reactive diastereomer. This synergy leads to the enrichment of the diastereomeric ratio of the final product **64** (Scheme 38) [55].

Enders developed a closely related iminium-cross-benzoin cascade process involving enals and β-oxo sulfones to generate enantioenriched cyclopentanone derivatives with three contiguous stereocentres. A dual secondary amine/NHC catalytic system comprising of the prolinol **60** and NHC precatalyst **22** was found to give the best results (Scheme 39) [56]. The influence of these catalysts on the diastereoselectivity of the reaction was also studied using NMR techniques.

An NHC-catalysed intramolecular benzoin condensation of carbohydrate-derived dialdehydes has been applied for the construction of carbocyclic sugars. Diastereoselective benzoin reactions of manno- and galacto-configured dialdehydes **66** were promoted by the triazolium carbene precatalyst **22** to produce single inososse stereoisomers **67** in high yields (Scheme 40)

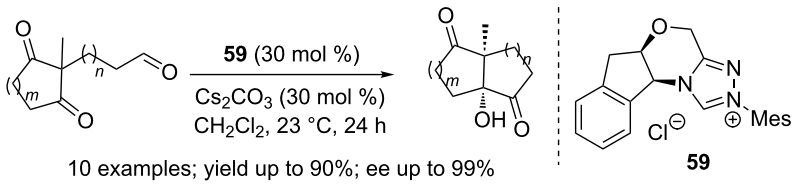

Scheme 36: Synthesis of bicyclic tertiary alcohols by intramolecular benzoin reaction.

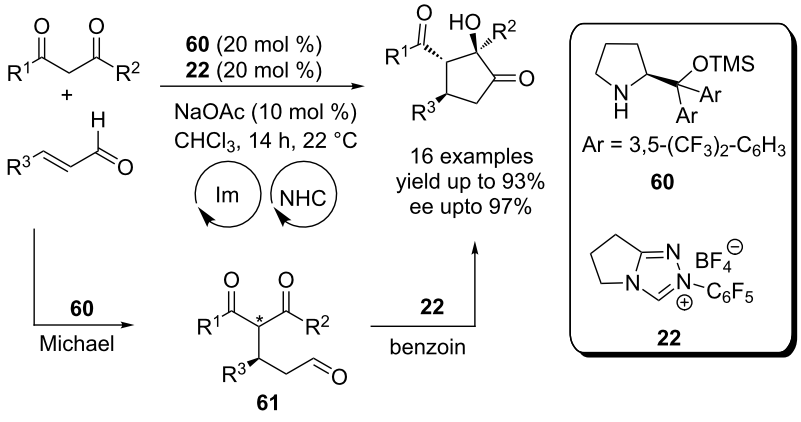

Scheme 37: A multicatalytic Michael–benzoin cascade process for cyclopentanone synthesis.

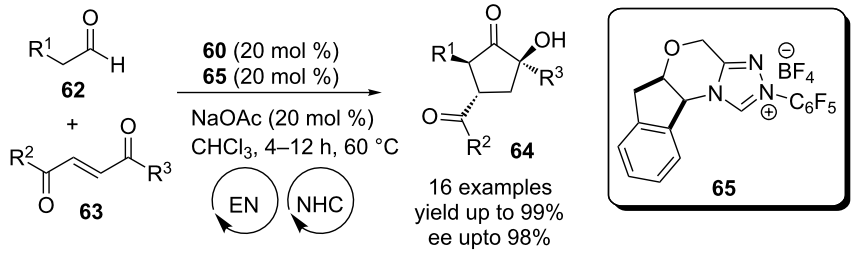

Scheme 38: Enamine-NHC dual-catalytic, Michael–benzoin cascade reaction.

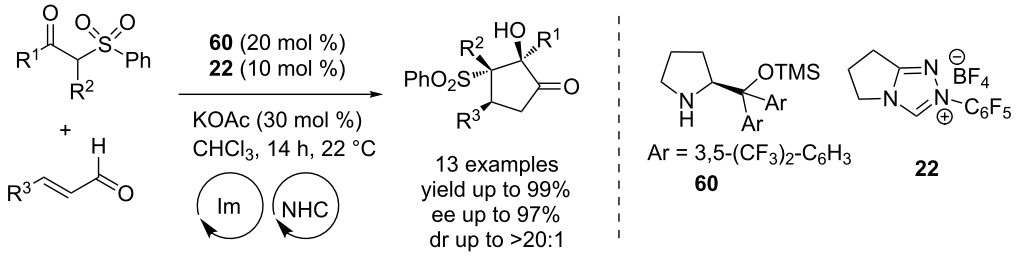

Scheme 39: Iminium-cross-benzoin cascade reaction of enals and β-oxo sulfones.

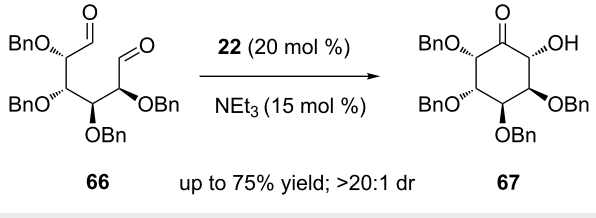

Scheme 40: Intramolecular benzoin condensation of carbohydrate-derived dialdehydes.

[57]. Stereospecific reduction and deprotection of the inosose derivatives furnished *allo*- and *epi*-inositol in good yields.

The camphor-derived triazolium precatalyst **54** promoted enantioselective intramolecular benzoin reactions of *N*-tethered keto-aldehydes effectively. The substrates for the cyclisation are easily accessible and dihydroquinolinone systems possessing a quaternary stereocentre are produced in high yields and enantioselectivities (Scheme 41) [58].

The chiral triazolium salt **68** derived from (1*R*)-camphor has been used in intramolecular cross-benzoin reactions of keto-aldehydes. The former efficiently catalysed stereoselective formation of chromanones **69** bearing quaternary stereocentres (Scheme 42) [59].

Cheng reported that the combination of NHC **24** and a Brønsted base (4-methoxyphenolate) promoted a formal dimerisation of 2-(aroylvinyl)arylaldehydes **70** to afford benzo[*a*]tetrahydrofluorenones **71** [60]. This stereoselective reaction proceeds via a benzoin–Michael–Michael cascade process (Scheme 43).

Further investigations in Cheng's group revealed an intriguing divergent catalytic dimerisation of 2-formylcinnamates **72**.

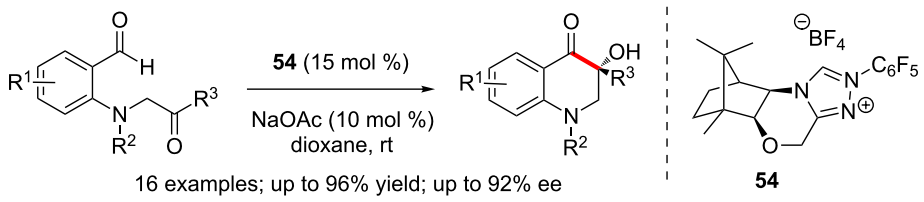

Scheme 41: Enantioselective intramolecular benzoin reactions of *N*-tethered keto-aldehydes.

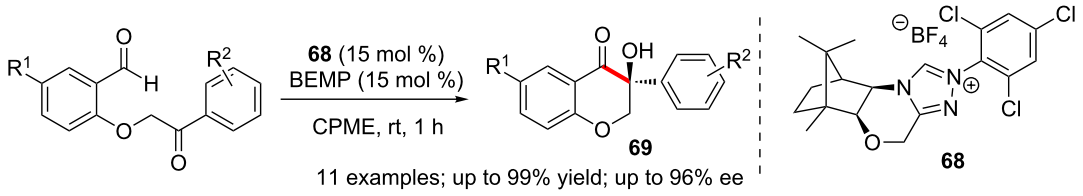

Scheme 42: Asymmetric cross-benzoin reactions promoted by camphor-derived catalysts.

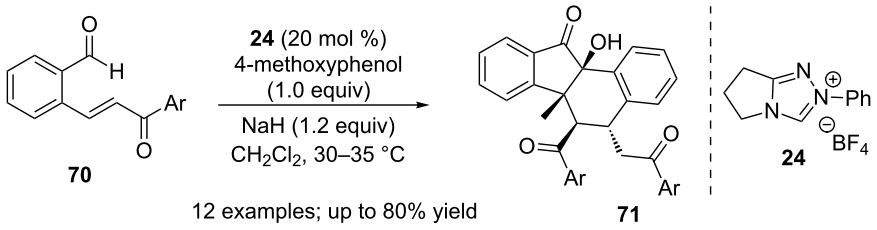

Scheme 43: NHC-Brønsted base co-catalysis in a benzoin–Michael–Michael cascade.

Co-operative catalysis by NHC precatalyst **73** and a Lewis acid (titanium isopropoxide) afforded isochromenone derivatives **74** via a sequence of reactions initiated by a benzoin condensation. Treatment of **72** with the NHC precatalyst **73** alone, on the other hand, afforded isochromeno(4,3-*c*)isochromene derivatives **75** (Scheme 44) [61].

A one-pot multicatalytic reaction for the asymmetric synthesis of complex tetracyclic tetrahydrocarbazole derivatives from readily available precursors was described by Melchiorre. A Diels–Alder reaction of indole-2,3-quinodimethane **76** (generated from **77** and the prolinol catalyst **78**) with the enone **79** affords a tetrahydrocarbazole derivative **80**. The NHC precatalyst **22** then promotes an intramolecular cross-benzoin condensation of the keto-aldehyde to furnish the tetracyclic product **81** (Scheme 45). The yields are moderate; however excellent diastereo- and enantioselectivities were observed for the one-pot reaction [62].

In a similar fashion, an asymmetric multicatalytic cascade reaction involving the dienal **82** and unsaturated cyclic sulfonylimine **83** afforded spiro-fused cycloadducts **84** in good yield and enantioselectivity [63]. Initially, the trienamine **85** is generated by the action of prolinol catalyst **86** on the dienal **82**. The former (**85**) then undergoes a Diels–Alder reaction with the sulfonylimine **83** to generate the keto-aldehyde **87**. Finally, the NHC precatalyst **22** mediates a cross-benzoin reaction of the latter to furnish the spirocyclic product **84** (Scheme 46).

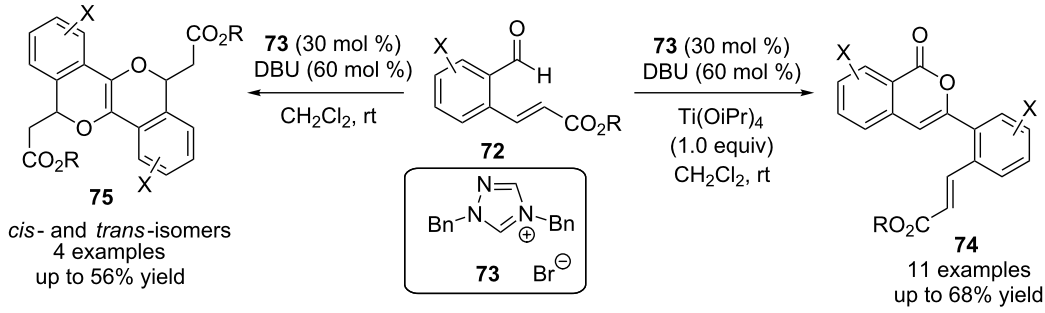

Scheme 44: Divergent catalytic dimerization of 2-formylcinnamates.

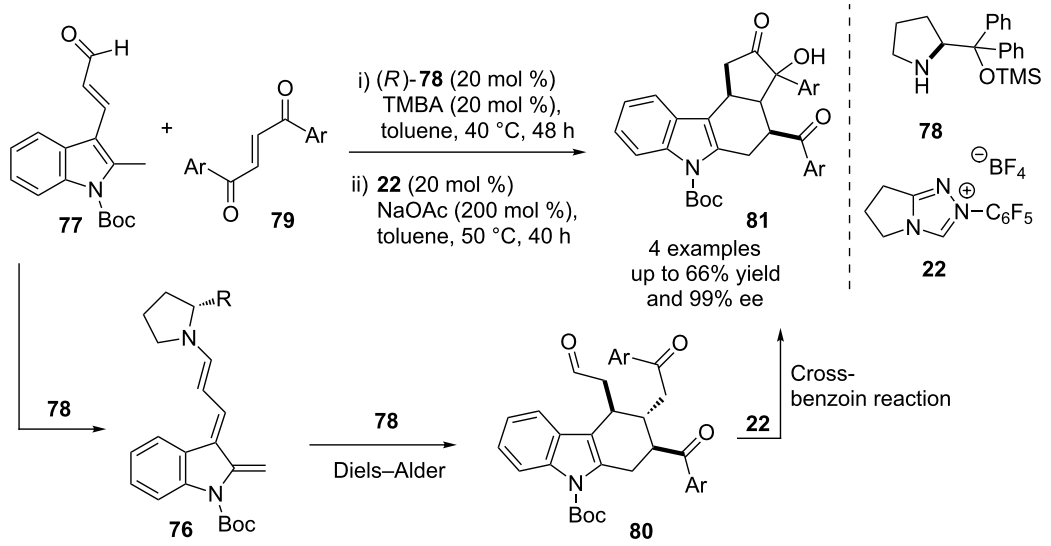

Scheme 45: One-pot, multicatalytic asymmetric synthesis of tetrahydrocarbazole derivatives.

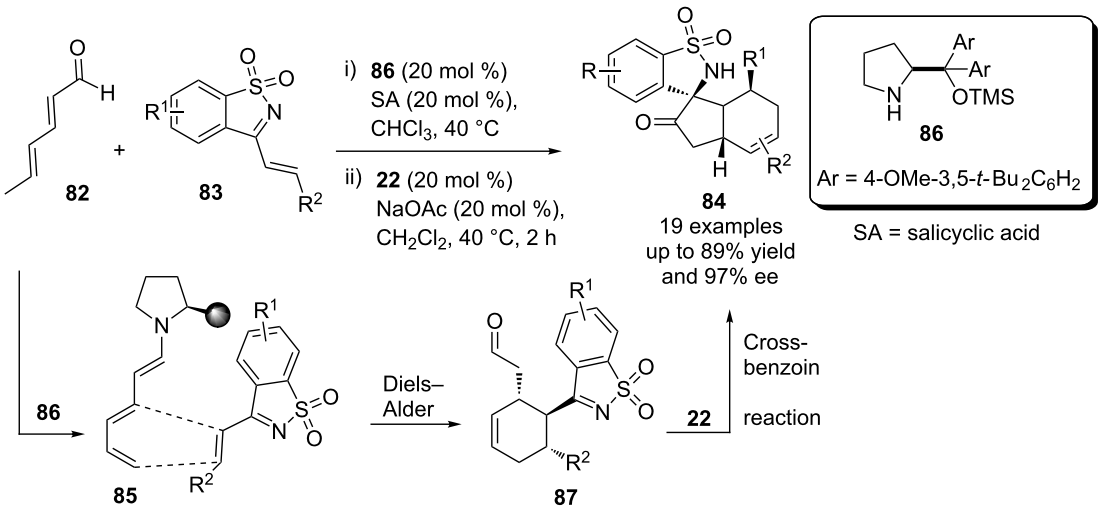

Scheme 46: NHC-chiral secondary amine co-catalysis for the synthesis of complex spirocyclic scaffolds.

Conclusion

The first report of a benzoin reaction by Wöhler and Liebig appeared merely four years after the former disclosed the paradigm-changing urea synthesis. However, detailed investigations of this reaction remained elusive due to a variety of reasons, the toxicity of cyanide catalysts being one of them. Breslow's discovery in 1958 of the thiazolylidene-catalysed benzoin condensation via polarity reversal of aldehydes formed the conceptual basis for the later development of NHC-organocatalysis. The rekindling of interest in NHC-catalysed benzoin reactions coincided with the emergence of N-heterocyclic carbenes in the late twentieth century as non-toxic, readily available and versatile catalysts for a variety of organic transformations. Since then, a number of reports on a variety of benzoin reactions have appeared in the literature. They include homo, crossed, intramolecular and various asymmetric benzoin reactions leading to products that are difficult to access by other means. Aza-benzoin reactions, intramolecular benzoin condensations, use of aldehyde surrogates and use of non-carbonyl electrophiles (nitroso compounds) are some of the developments that revamped the synthetically unattractive, monotonous image of benzoin condensations. The driving force behind this remarkable evolution of benzoin reaction is NHC-catalysis. Benzoin chemistry is well-set to benefit, in the near future, from new developments in the rapidly growing realm of NHC-catalysis.

References

1. Wöhler, F.; Liebig, J. *Ann. Pharm.* **1832,** *3,* 249. doi:10.1002/jlac.18320030302
2. Ukai, T.; Tanaka, R.; Dokawa, T. *J. Pharm. Soc. Jpn.* **1943,** *63,* 296.
3. Breslow, R. *J. Am. Chem. Soc.* **1958,** *80,* 3719. doi:10.1021/ja01547a064
4. Igau, A.; Grutzmacher, H.; Baceiredo, A.; Bertrand, G. *J. Am. Chem. Soc.* **1988,** *110,* 6463. doi:10.1021/ja00227a028
5. Arduengo, A. J., III; Harlow, R. L.; Kline, M. *J. Am. Chem. Soc.* **1991,** *113,* 361. doi:10.1021/ja00001a054
6. Flanigan, D. M.; Romanov-Michailidis, F.; White, N. A.; Rovis, T. *Chem. Rev.* **2015,** *115,* 9307. doi:10.1021/acs.chemrev.5b00060
7. Enders, D.; Niemeir, O.; Henseler, A. *Chem. Rev.* **2007,** *107,* 5606. doi:10.1021/cr068372z
8. Lapworth, A. *J. Chem. Soc., Trans.* **1903,** *83,* 995. doi:10.1039/CT9038300995
9. Stetter, H.; Rämsch, R. Y.; Kuhlmann, H. *Synthesis* **1976,** 733. doi:10.1055/s-1976-24177
10. Xu, L.-W.; Gao, Y.; Yin, J.-J.; Li, L.; Xia, C.-G. *Tetrahedron Lett.* **2005,** *46,* 5317. doi:10.1016/j.tetlet.2005.06.015
11. Iwamoto, K.; Hamaya, M.; Hashimoto, N.; Kimura, H.; Suzuki, Y.; Sato, M. *Tetrahedron Lett.* **2006,** *47,* 7175. doi:10.1016/j.tetlet.2006.07.153
12. Iwamoto, K.; Kimura, H.; Oike, M.; Sato, M. *Org. Biomol. Chem.* **2008,** *6,* 912. doi:10.1039/B719430G
13. Ma, Y.; Wei, S.; Wu, J.; Yang, F.; Liu, B.; Lan, J.; Yang, S.; You, J. *Adv. Synth. Catal.* **2008,** *350,* 2645. doi:10.1002/adsc.200800371
14. Enders, D.; Han, J. *Tetrahedron: Asymmetry* **2008,** *19,* 1367. doi:10.1016/j.tetasy.2008.05.017
15. O'Toole, S. E.; Connon, S. J. *Org. Biomol. Chem.* **2009,** *7,* 3584. doi:10.1039/B908517C
16. Brand, J. P.; Siles, J. I. O.; Waser, J. *Synlett* **2010,** 881. doi:10.1055/s-0029-1219543
17. Soeta, T.; Tabatake, Y.; Inomata, K.; Ukaji, Y. *Tetrahedron* **2012,** *68,* 894. doi:10.1016/j.tet.2011.11.028
18. Rafiński, Z.; Kozakiewicz, A.; Rafińska, K. *Tetrahedron* **2014,** *70,* 5739. doi:10.1016/j.tet.2014.06.066
19. Baragwanath, L.; Rose, C. A.; Zeitler, K.; Connon, S. J. *J. Org. Chem.* **2009,** *74,* 9214. doi:10.1021/jo902018j
20. Matsumoto, T.; Ohishi, M.; Inoue, S. *J. Org. Chem.* **1985,** *50,* 603. doi:10.1021/jo00205a010
21. Kuhl, N.; Glorius, F. *Chem. Commun.* **2011,** *47,* 573. doi:10.1039/C0CC02416C
22. Jin, M. Y.; Kim, S. M.; Han, H.; Ryu, D. H.; Yang, J. W. *Org. Lett.* **2011,** *13,* 880. doi:10.1021/ol102937w
23. Rose, C. A.; Gundala, S.; Connon, S. J.; Zeitler, K. *Synthesis* **2011,** 190. doi:10.1055/s-0030-1258363
24. Piel, I.; Pawelczyk, M. D.; Hirano, K.; Fröhlich, R.; Glorius, F. *Eur. J. Org. Chem.* **2011,** 5475. doi:10.1002/ejoc.201100870
25. Jin, M. Y.; Kim, S. M.; Mao, H.; Ryu, D. H.; Song, C. E.; Yang, J. W. *Org. Biomol. Chem.* **2014,** *12,* 1547. doi:10.1039/C3OB42486C
26. Langdon, S. M.; Wilde, M. M. D.; Thai, K.; Gravel, M. *J. Am. Chem. Soc.* **2014,** *136,* 7539. doi:10.1021/ja501772m
27. Enders, D.; Henseler, A. *Adv. Synth. Catal.* **2009,** *351,* 1749. doi:10.1002/adsc.200900247
28. Enders, D.; Henseler, A.; Lowins, S. *Synthesis* **2009,** 4125. doi:10.1055/s-0029-1217070
29. Enders, D.; Grossmann, A.; Fronert, J.; Raabe, G. *Chem. Commun.* **2010,** *46,* 6282. doi:10.1039/C0CC02013C
30. Rose, C. A.; Gundala, S.; Fagan, C.-L.; Franz, J. F.; Connon, S. J.; Zeitler, K. *Chem. Sci.* **2012,** *3,* 735. doi:10.1039/C2SC00622G
31. Thai, K.; Langdon, S. M.; Bilodeau, F.; Gravel, M. *Org. Lett.* **2013,** *15,* 2214. doi:10.1021/ol400769t
32. Goodman, C. G.; Johnson, J. S. *J. Am. Chem. Soc.* **2014,** *136,* 14698. doi:10.1021/ja508521a
33. Sánchez-Díez, E.; Fernández, M.; Uria, U.; Reyes, E.; Carrillo, L.; Vicario, J. L. *Chem. – Eur. J.* **2015,** *21,* 8384. doi:10.1002/chem.201501044
34. Murry, J. A.; Frantz, D. E.; Soheili, A.; Tillyer, R.; Grabowski, E. J. J.; Reider, P. J. *J. Am. Chem. Soc.* **2001,** *123,* 9696. doi:10.1021/ja0165943
35. Sun, F.-g.; Ye, S. *Org. Biomol. Chem.* **2011,** *9,* 3632. doi:10.1039/C1OB05092C
36. Li, G.-Q.; Dai, L.-X.; You, S.-L. *Chem. Commun.* **2007,** 852. doi:10.1039/B611646A
37. DiRocco, D. A.; Rovis, T. *Angew. Chem., Int. Ed.* **2012,** *51,* 5904. doi:10.1002/anie.201202442
38. Uno, T.; Kobayashi, Y.; Takemoto, Y. *Beilstein J. Org. Chem.* **2012,** *8,* 1499. doi:10.3762/bjoc.8.169
39. Mattson, A. E.; Scheidt, K. A. *Org. Lett.* **2004,** *6,* 4363. doi:10.1021/ol0481129
40. Mennen, S. M.; Gipson, J. D.; Kim, Y. R.; Miller, S. J. *J. Am. Chem. Soc.* **2005,** *127,* 1654. doi:10.1021/ja042650z
41. Sun, L.-H.; Liang, Z.-Q.; Jia, W.-Q.; Ye, S. *Angew. Chem., Int. Ed.* **2013,** *52,* 5803. doi:10.1002/anie.201301304
42. Xu, J.; Mou, C.; Zhu, T.; Song, B.-A.; Chi, Y. R. *Org. Lett.* **2014,** *16,* 3272. doi:10.1021/ol501286e
43. Wilde, M. M. D.; Gravel, M. *Org. Lett.* **2014,** *16,* 5308. doi:10.1021/ol5024807
44. Sun, Z.-X.; Cheng, Y. *Org. Biomol. Chem.* **2012,** *10,* 4088. doi:10.1039/C2OB25137J
45. Song, X.; Ni, Q.; Grossmann, A.; Enders, D. *Chem. – Asian J.* **2013,** *8,* 2965. doi:10.1002/asia.201300938
46. Cookson, R. C.; Lane, R. M. *J. Chem. Soc., Chem. Commun.* **1976,** 804. doi:10.1039/C39760000804
47. Hachisu, Y.; Bode, J. W.; Suzuki, K. *J. Am. Chem. Soc.* **2003,** *125,* 8432. doi:10.1021/ja035308f
48. Takikawa, H.; Hachisu, Y.; Bode, J. W.; Suzuki, K. *Angew. Chem., Int. Ed.* **2006,** *45,* 3492. doi:10.1002/anie.200600268
49. Enders, D.; Niemeir, O. *Synlett* **2004,** 2111. doi:10.1055/s-2004-831306
50. Enders, D.; Niemeir, O.; Balensiefer, T. *Angew. Chem., Int. Ed.* **2006,** *45,* 1463. doi:10.1002/anie.200503885
51. Li, Y.; Feng, Z.; You, S.-L. *Chem. Commun.* **2008,** 2263. doi:10.1039/B801004H
52. Kankala, S.; Edulla, R.; Modem, S.; Vadde, R.; Vasam, C. S. *Tetrahedron Lett.* **2011,** *52,* 3828. doi:10.1016/j.tetlet.2011.05.070
53. Ema, T.; Akihara, K.; Obayashi, R.; Sakai, T. *Adv. Synth. Catal.* **2012,** *354,* 3283. doi:10.1002/adsc.201200499
54. Lathrop, S. P.; Rovis, T. *J. Am. Chem. Soc.* **2009,** *131,* 13628. doi:10.1021/ja905342e
55. Ozboya, K. E.; Rovis, T. *Chem. Sci.* **2011,** *2,* 1835. doi:10.1039/C1SC00175B
56. Enders, D.; Grossmann, A.; Huang, H.; Raabe, G. *Eur. J. Org. Chem.* **2011,** 4298. doi:10.1002/ejoc.201100690
57. Stockton, K. P.; Greatrex, B. W.; Taylor, D. K. *J. Org. Chem.* **2014,** *79,* 5088. doi:10.1021/jo500645z
58. Jia, M.-Q.; You, S.-L. *ACS Catal.* **2013,** *3,* 622. doi:10.1021/cs4000014

59. Rafiński, Z.; Kozakiewicz, A. *J. Org. Chem.* **2015,** *80,* 7468. doi:10.1021/acs.joc.5b01029
60. Tong, Y.-f.; Mao, J.-h.; Wu, S.; Zhao, Y.; Cheng, Y. *J. Org. Chem.* **2014,** *79,* 2075. doi:10.1021/jo4027758
61. Dang, H.-Y.; Wang, Z.-T.; Cheng, Y. *Org. Lett.* **2014,** *16,* 5520. doi:10.1021/ol502791s
62. Liu, Y.; Nappi, M.; Escudero-Adán, E. C.; Melchiorre, P. *Org. Lett.* **2012,** *14,* 1310. doi:10.1021/ol300192p
63. Ma, C.; Gu, J.; Teng, B.; Zhou, Q.-Q.; Li, R.; Chen, Y.-C. *Org. Lett.* **2013,** *15,* 6206. doi:10.1021/ol4030474

License and Terms

BEILSTEIN JOURNAL OF ORGANIC CHEMISTRY

Reactivity studies of pincer bis-protic N-heterocyclic carbene complexes of platinum and palladium under basic conditions

David C. Marelius[1], Curtis E. Moore[2], Arnold L. Rheingold[2] and Douglas B. Grotjahn[*1]

Full Research Paper

Open Access

Address:
[1]Department of Chemistry and Biochemistry, San Diego State University, San Diego, CA 92182-1030, USA and [2]Department of Chemistry and Biochemistry, University of California San Diego, La Jolla, CA 92093-0358, USA

Email:
Douglas B. Grotjahn* - dbgrotjahn@mail.sdsu.edu

* Corresponding author

Keywords:
NHC; ^{15}N NMR spectroscopy; palladium; platinum; protic N-heterocyclic carbene

Beilstein J. Org. Chem. **2016,** *12,* 1334–1339.
doi:10.3762/bjoc.12.126

Received: 07 February 2016
Accepted: 09 June 2016
Published: 28 June 2016

This article is part of the Thematic Series "N-Heterocyclic carbenes".

Guest Editor: S. P. Nolan

Abstract

Bis-protic N-heterocyclic carbene complexes of platinum and palladium (**4**) yield dimeric structures **6** when treated with sodium *tert*-butoxide in CH_2Cl_2. The use of a more polar solvent (THF) and a strong base ($LiN(iPr)_2$) gave the lithium chloride adducts monobasic complex **7** or analogous dibasic complex **8**.

Introduction

N-Heterocyclic carbenes (NHCs) have been extensively researched for a number of purposes since 1991 when Arduengo first isolated free NHCs [1-3]. NHCs as ligands have been known even longer. In 1968, Wanzlick and Öfele separately synthesized mercury(II) and chromium(0) imidazol-2-ylidene complexes [3]. Nearly 50 years of NHC ligand research have demonstrated the importance of the electronic and steric effects that can be modified by altering the alkyl or aryl groups on each nitrogen atom. Less common are protic imidazol-2-ylidene (PNHC) ligands with a hydrogen atom on one or both of the stabilizing nitrogens. The synthesis of PNHC complexes has proven to be a challenge, which has limited studies of their reactivity [4-8].

Protic imidazol-2-ylidene ligands (e.g., **1**) have been shown to form an imidazolyl ligand (e.g., **2**) after deprotonation with a basic proton-accepting nitrogen (Figure 1). We are unaware of reports on an experimentally determined pK_a value of a PNHC imidazolidene complex, but looking at related derivatives, Isobe showed that a 2-palladated pyridine was 3.57 pK_a units more basic than pyridine [9,10]. Considering reactions other than simple proton transfer, imidazol-2-yl complexes have recently been used to bind to a second transition metal [11]. Additionally, Cp*Ir complexes from our group [12] demonstrated heterolysis of the H–H bond of H_2 and of the C–H bond of acetylene. The same ligand in CpRu complexes **2** and **3** showed heterolysis of dihydrogen [13]. **1** had a much faster ligand exchange

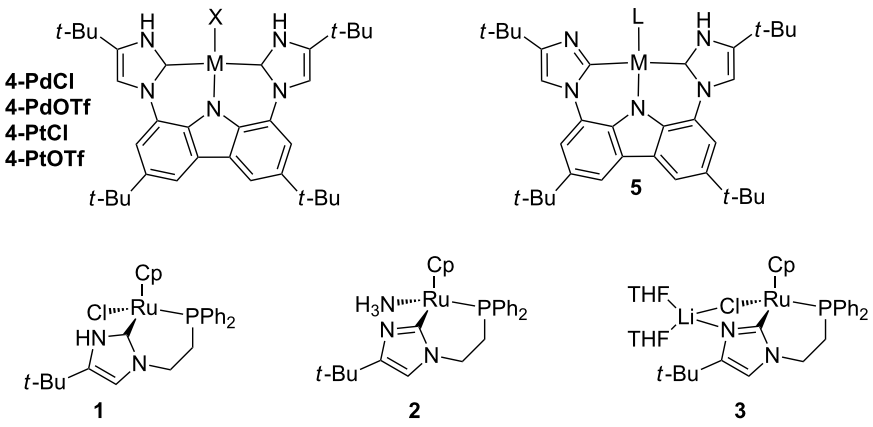

Figure 1: Previously reported PNHC complexes of interest for this work, along with the targeted complex **5**.

rate after ionization as compared to the Cp*Ir analog (ethylene bound in 5 min at rt (CpRu) instead of 16 h at 70 °C (Cp*Ir)). Species **1** could be converted in situ to the hydride and isolated, or generated in situ and used as a transfer hydrogenation catalyst. Interestingly, the ligand substitution rate of ethylene and the heterolysis of dihydrogen was much greater for **3** than for **2**. With only a few papers exploring the utility of these imidazol-2-yl complexes, we aim to extend this to our recently reported pincer bis PNHC complexes **4-PdCl** and **4-PtCl** and their triflato analogs [14]. The design of these complexes was inspired by studies of Kunz et al. on aprotic analogs [15,16].

Results and Discussion

The loss of one NH proton from the bis-PNHC complex **4** could lead to structure **5**, a complex concurrently containing a PNHC proton donor and a bond activating imidazol-2-yl unit. In an attempt to form **5**, **4-PdCl** was dissolved in CD_2Cl_2, and the solution was saturated with ethylene, followed by the addition of sodium *tert*-butoxide. After 2 h at room temperature, an NMR spectrum was acquired that showed a new, unsymmetrical species, as expected for **5**. Crystals were grown by vapor diffusion of pentanes into benzene and analyzed. Surprisingly, the data showed that the dimer **6-Pd** had formed such that the open site was not filled with ethylene, but rather was occupied by an imidazolyl nitrogen from a second complex (Figure 2). The palladium and platinum dimer complexes, **6-Pd** and **6-Pt**, could be formed by addition of sodium *tert*-butoxide to the chloride analogs (Scheme 1), and isolated in 50–56% yields.

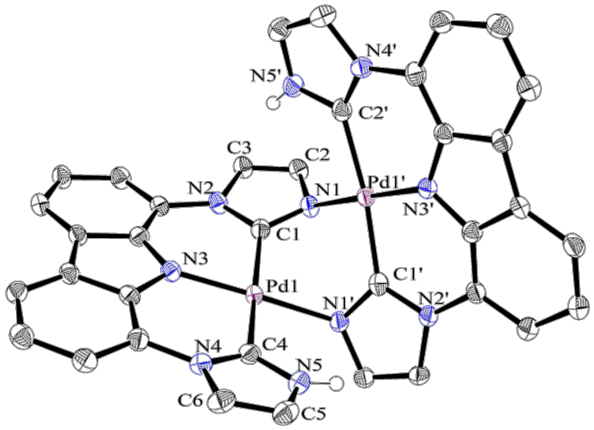

Figure 2: Crystal structure of **6-Pd**. The atoms of the *tert*-butyl groups, C–H bonds, and the solvent have been omitted for clarity.

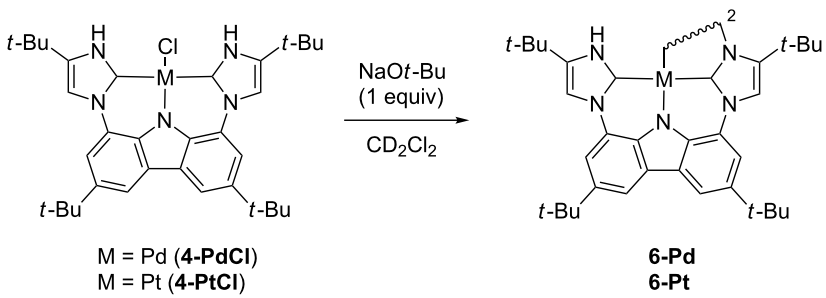

Scheme 1: Formation of dimers **6-Pd** and **6-Pt** by addition of NaO*t*-Bu.

The examination of the dimer crystal structure (see Figure 2 for **6-Pd**) shows strain in the Pd1–N1' (and Pd1'–N1) bond. This is due to the metal that remains in the plane defined by the three coordinating atoms of the tridentate ligand (i.e., C1, N3, and C4). The fourth donor atom from the other has to bend out of the plane with the N1' imidazole ring because of the adjacent sterics of the *tert*-butyl groups on the imidazole. The strain can be quantified by examining how far the metal is from the N1 (or N1')-bound imidazole plane (C1–C2–C3–N1–N2 plane and the symmetry-equivalent atoms): for **6-Pd,** 1.241 Å and, for **6-Pt**, 1.094 Å (Table 1). Further evidence is given by the dihedral angles: Pd1–C1–N1–Pd1' = −40.4(4)° and 36.5(3)° for **6-Pd** and **6-Pt**, respectively, C1–Pd1–N1'–C1' = 72.4(3)° and 67.3(2)° for **6-Pd** and **6-Pt**, respectively.

The NMR results are completely consistent with persistence of the dimers in solution. For monomeric species such as **4-PdCl** and **4-PtCl**, the NH proton resonance is typically downfield shifted with a chemical shift of ca. 11 ppm, whereas this signal is strongly shifted upfield to 8.03 (**6-Pd**) or 8.19 ppm (**6-Pt**). The crystal structures for both **6-Pd** and **6-Pt** show that the NH is located above the pi system of one imidazole ring of the other half of the dimer, which would be expected to shield the NH and cause a significant upfield chemical shift. Moreover, a ROESY experiment on **6-Pt** (Figure S6, Supporting Information File 1) confirms that the NH (N5', Figure 2) has a through-space interaction with the proton on the imidazole ring (C3, Figure 2), a situation that would not be possible for a monomeric structure.

Attempts to synthesize **5** using sodium alkoxide bases led to the formation of dimer structures **6** with presumed loss of NaCl. Therefore, lithium chloride adducts **7** were targeted because LiCl adduct **3** was isolable yet highly reactive. As demonstrated by NMR spectroscopy, the dissolution of **4-PdCl** in a mixture of THF (0.7 mL) and C_6D_6 (0.1 mL) followed by the addition of one equivalent of $LiN(iPr)_2$ deprotonates one of the PNHC complexes. This gives **7-Pd**, without evidence of dimer formation (Scheme 2). The addition of a second equivalent of $LiN(iPr)_2$ deprotonates the second PNHC complex, giving **8-Pd**. The ^{1}H NMR spectrum for compound **7-Pt** consists of a single NH peak at 10.90 ppm and six aromatic peaks, which all integrate to one proton. The asymmetry is also observed in the ^{13}C NMR spectrum, which consists of 18 peaks between 100 and 170 ppm. As for **8-Pt**, the ^{1}H NMR spectrum has no peak where the NH peak typically is located, and in the aromatic

Table 1: Key bond lengths (Å) and angles (°) of dimers **6** compared to parent compounds **4**.

	4-PdCl	6-Pd	4-PtCl	6-Pt
M–N1	–	2.092(3)	–	2.079(3)
M–N3	1.961(3)	1.962(3)	1.9627(19)	1.969(3)
M–C4	2.006(4), 1.998(4)	2.034(4)	2.007(2), 2.014(2)	2.014(3)
M–C1	–	1.984(4)	–	1.996(3)
N3–M–X	178.09(10)	176.3(1)	179.85(6)	175.6(1)
C1–M–C4	175.43(17)	167.9(2)	176.29(9)	168.3(1)
M out plane[a]	–	1.241	–	1.094

[a]The metal-to-plane distance defined by the five corresponding N-coordinated imidazole atoms; this value would be near zero in the absence of strain.

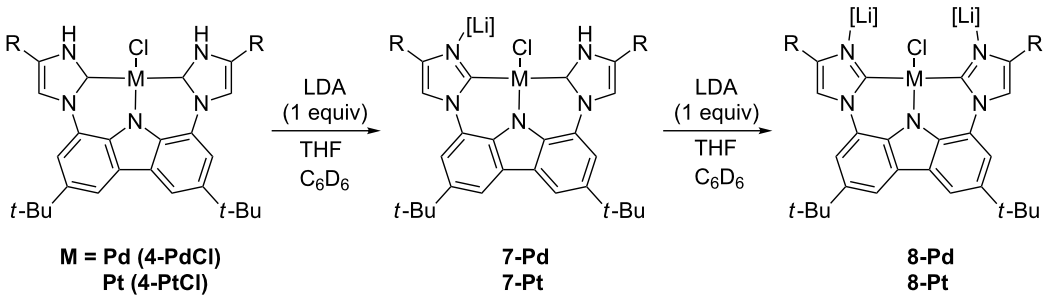

Scheme 2: Formation of **7** and **8** by addition of $LiN(iPr)_2$ (1 or 2 equiv) (R = *tert*-butyl).

region there are three peaks. The ^{13}C NMR spectrum thus consists of 9 peaks between 100 and 170 ppm, showing the reappearance of symmetry.

^{15}N chemical shift data give structural insight (Table 2), as exemplified by **1**–**3** [10]. The $\Delta_{\mathbf{x}}$ (difference in ^{15}N shifts for compound **x**) is near zero for a PNHC (**1**), maximum for the imidazolyl conjugate base **2**, and slightly less for an imidazolyl lithium chloride adduct **3**. The δ_N for the aprotic nitrogen incapable of acid base chemistry (N2) hardly changes, whereas for the protic (N1), the changes depend on its environment. In the following discussion, **1** and **4-PtCl** are considered the reference starting material complexes because they are both neutral PNHC species with M–Cl moieties. Their Δ_x values are named as Δ_{ref}. For **1**, $\Delta_{ref} = 1.5$, whereas for **4-PdCl**, $\Delta_{ref} = -13.1$. This difference is likely due to a variety of factors related to the electronics of the nonprotic substituent of the PNHC and/or the ring size of the chelates, which is beyond the scope of this paper. For a given metal center and mono- or bis-NHC framework, we want to diagnose the effects of chemical changes at N1. For this purpose, we introduce the quantity $\Delta\Delta = \Delta_{\mathbf{x}} - \Delta_{ref}$ to account for the change in $\Delta_{\mathbf{x}}$ that accompanies a chemical change from the reference compound to the new species **x**. Looking at complex **6-Pt**, ΔΔ for the NH nitrogen is only 0.3 ppm and only −4.4 ppm for the NM nitrogen. The ΔΔ values for both nitrogens are relatively unchanged as the carbene character of the ligand is still intact. Interestingly, **6-Pd** shows a similar small ΔΔ value for the NH (2.6) but a greater ΔΔ for the NM of 17.4 ppm. This is possibly a result of the differing ring strain in the Pt case (M out of plane 1.094 Å for **6-Pt** vs 1.241 for **6-Pd**) and/or smaller M–N distance (2.079(3) Å for **6-Pt** vs 2.092(3) Å for **6-Pd**, Table 1). Turning now to **7-Pt** and **8-Pt**, we note that the deprotonated nitrogens of **7-Pt** and **8-Pt** show large values of ΔΔ = 80.5 ppm and 77.8 ppm, respective-

Table 2: ^{15}N chemical shift values (ppm) of complexes in this paper.[a]

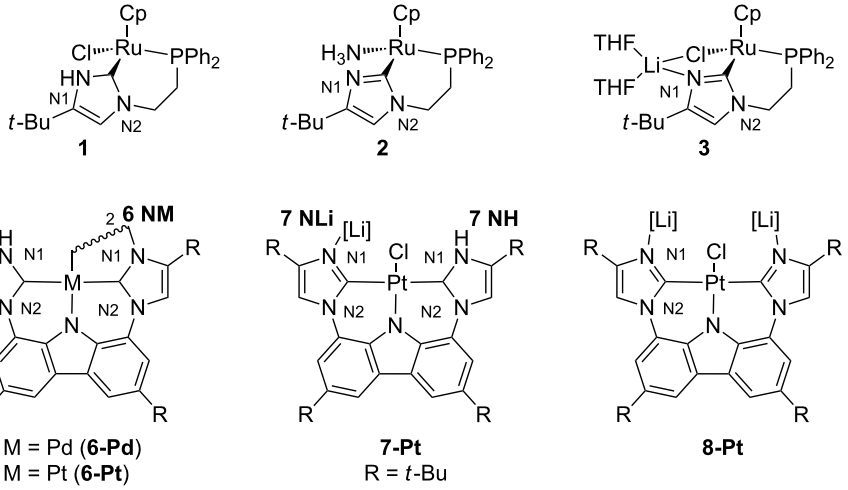

Complex	N1[b]	N2[c]	Δ_x[d]	ΔΔ[e]
1	−197.1	−198.6	1.5	0 (defined)
2	−110.4	−199.9	89.5	88.0
3	−122.1	−196.8	74.7	73.2
4-PtCl	−211.0	−197.9	−13.1	0 (defined)
7-Pt NH	−212.7	−198.4	−14.4	−1.3
7-Pt Li	−129.9	−197.3	67.4	80.5
8-Pt	−127.4	−192.0	64.7	77.8
6-Pt NH	−209.9	−197.0	−12.9	0.3
6-Pt NPd	−215.3	−197.8	−17.5	−4.4
6-Pd NH	−208.3	−192.6	−15.7	2.6
6-Pd NPt	−193.5	−195.8	2.3	17.4

[a]Determined using ^1H,^{15}N gHMBC on natural abundance material in THF (0.7 mL) and benzene-d_6 (0.1 mL) (**4-PtCl**, **7**, **8**), or CD_2Cl_2 (**6**). [b]N1 = either NH or derivative of PNHC. [c]N2 = aprotic nitrogen incapable of acid base chemistry. [d]$\Delta_{\mathbf{x}}$ = N1 − N2. [e]$\Delta\Delta = \Delta x - \Delta_{ref}$ where $\Delta_{ref} = -13.1$ for type-**1** compounds and 1.5 for type-**4** compounds.

ly. This resembles the results for the CpRu species **2** and **3** (ΔΔ = 88.0 ppm and 73.2 ppm, respectively). The values of ΔΔ for the deprotonated nitrogens (that bear a Pt or Pd) in the crystallographically characterized dimers **6-Pt** and **6-Pd** are much smaller (17.4, −4.4). The large ΔΔ values for the deprotonated nitrogens of **7-Pt** and **8-Pt** could be due to either structural formulation as a LiCl adduct or free imidazolyl species. However, the dependence of the stability of **7** and **8** on the presence of chloride (see below) argues strongly for a chloride ligand on the central metal. This leads us to assign structures **7-Pt** and **8-Pt** as LiCl-imidazolyl adducts. All attempts at characterization by crystallography have been unsuccessful due to the very water-sensitive nature of **7** and **8**. Therefore, the environment of the lithium and chloride is unknown but it is assumed to be similar to that of **3**, which is formed under very similar conditions. The ^{15}N chemical shift data give structural insight that is unavailable by any other means regarding the absence of solid-state structures or meaningfully diagnostic ^{7}Li chemical shifts.

An indication of the reactivity of imidazolyl complexes was deduced after bubbling H_2 through a solution of **7-Pt** for 16 h in THF/C_6D_6, where only a small amount of **4-PtCl** was regenerated, likely from adventitious water. The addition of AgOTf did not facilitate H_2 heterolysis, but formed the dimer **6-Pt** (Figure S7, Supporting Information File 1). Bubbling ethylene through a solution of **7-Pt** gave some **4-PtCl**, again likely from adventitious water (Figure S8, Supporting Information File 1). The rigorously dried substrate 1-heptene (20 equiv) was added to **8-Pt**, where no reaction was observed even after heating at 70 °C for 4 h (Figure S9, Supporting Information File 1).

Unlike imidazolyl complex **3**, **7-Pt** showed no tendency to lose LiCl. One possible route to a more labile LiOTf adduct was to deprotonate **4-PtOTf**, but the action of $LiN(iPr)_2$ yielded mostly the dimer **6-Pt** (Figure S10, Supporting Information File 1). Alternatively, the deprotonation of $[\mathbf{4\text{-}Pt(CH_3CN)}]^+$ $\mathbf{OTf}^-$ by $LiN(iPr)_2$ (1 equiv) gave an analog of **5**, where L = CH_3CN. However in practice, this typically yielded a number of species (Figure S11, Supporting Information File 1). It appears that the LiCl-imidazolyl adduct complexes **7-Pt** and **8-Pt** have a much slower ligand exchange rate compared to complex **3**. This was expected given the change from ruthenium to platinum [17].

To see if the faster ligand exchange would lead to LiCl loss with palladium, **7-Pd** was synthesized. Unfortunately, similar results were observed with the platinum analog where 1-heptene did not react with **7-Pd** (which was then converted to **8-Pd** by addition of $LiN(iPr)_2$). Then AgOTf was added to **8-Pd**, which formed a deprotonated dimer complex. Even with palladium, the loss of the chloride ligand seemed to be too slow.

Conclusion

In conclusion, attempts at forming an imidazolyl complex from **4-MCl** using sodium alkoxides led to strained dimers **6**. However, **4-MCl** could be deprotonated with either 1 or 2 equiv of $LiN(iPr)_2$ to give **7**, an intriguing species with one PNHC ligand and one Li-imidazolyl adduct, or **8**, a bis imidazolyl complex. Unfortunately, substrates could not displace the chloride ligand without formation of dimer **6**, and the deprotonated complexes were water sensitive. The attempts at deprotonating the more labile triflate complex **4-PtOTf** led to the formation of dimer **6-Pt**. To increase the lability of the chloride ligand, species **4-PdCl** and **4-PdOTf** were examined but gave dimer **6-Pd**. In summary, the reactivity of bis-PNHC complexes **4** and bases appears to be dominated by the formation of the dimeric structures. Studies to reduce dimer formation by various means, such as increasing steric hindrance at the imidazolyl nitrogens, will be reported in due course.

Supporting Information

The Supporting Information contains details on syntheses of **6-Pd** and **6-Pt**, NMR data for **4-PtCl**, **6-Pd**, **6-Pt**, **7-Pt**, and **8-Pt** and Figues S6–S12.

Supporting Information File 1

Experimental information and NMR spectroscopy figures.
[http://www.beilstein-journals.org/bjoc/content/supplementary/1860-5397-12-126-S1.pdf]

Acknowledgements

We would like to thank Dr. LeRoy Lafferty for his expert NMR assistance and NSF CHE 1464781 for partial support.

References

1. Hermann, W. A. *Angew. Chem., Int. Ed.* **2002,** *41,* 1290. doi:10.1002/1521-3773(20020415)41:8<1290::AID-ANIE1290>3.0.CO;2-Y
2. Díez-González, S.; Marion, N.; Nolan, S. P. *Chem. Rev.* **2009,** *109,* 3612. doi:10.1021/cr900074m
3. Hopkinson, M. N.; Richter, C.; Schedler, M.; Glorius, F. *Nature* **2014,** *510,* 485. doi:10.1038/nature13384
4. Kuwata, S.; Ikariya, T. *Chem. – Eur. J.* **2011,** *17,* 3542. doi:10.1002/chem.201003296
5. Hahn, F. E. *ChemCatChem* **2013,** *5,* 419. doi:10.1002/cctc.201200567
6. Zhao, B.; Han, Z.; Ding, K. *Angew. Chem., Int. Ed.* **2013,** *52,* 4744. doi:10.1002/anie.201204921
7. Kuwata, S.; Ikariya, T. *Chem. Commun.* **2014,** *50,* 14290. doi:10.1039/C4CC04457F
8. Jahnke, M. C.; Hahn, F. E. *Coord. Chem. Rev.* **2015,** *293–294,* 95. doi:10.1016/j.ccr.2015.01.014

9. Isobe, K.; Kai, E.; Nakamura, Y.; Nishimoto, K.; Miwa, T.; Kawaguchi, S.; Kinoshita, K.; Nakatsu, K. *J. Am. Chem. Soc.* **1980,** *102,* 2475. doi:10.1021/ja00527a065
10. Isobe, K.; Kawaguchi, S. *Heterocycles* **1981,** *16,* 1603. doi:10.3987/R-1981-09-1603
11. Flowers, S. E.; Cossairt, B. M. *Organometallics* **2014,** *33,* 4341. doi:10.1021/om500592u
12. Miranda-Soto, V.; Grotjahn, D. B.; DiPasquale, A. G.; Rheingold, A. L. *J. Am. Chem. Soc.* **2008,** *130,* 13200. doi:10.1021/ja804713u
13. Miranda-Soto, V.; Grotjahn, D. B.; Cooksy, A. L.; Golen, J. A.; Moore, C. E.; Rheingold, A. L. *Angew. Chem., Int. Ed.* **2011,** *50,* 631. doi:10.1002/anie.201005100
14. Marelius, D. C.; Darrow, E. H.; Moore, C. E.; Golen, J. A.; Rheingold, A. L.; Grotjahn, D. B. *Chem. – Eur. J.* **2015,** *21,* 10988. doi:10.1002/chem.201501945
15. Seyboldt, A.; Wucher, B.; Hohnstein, S.; Eichele, K.; Rominger, F.; Törnroos, K. W.; Kunz, D. *Organometallics* **2015,** *34,* 2717. doi:10.1021/om500836m
16. Moser, M.; Wucher, B.; Kunz, D.; Rominger, F. *Organometallics* **2007,** *26,* 1024. doi:10.1021/om060952z
17. Helm, L.; Merbach, A. E. *Chem. Rev.* **2005,** *105,* 1923. doi:10.1021/cr030726o

License and Terms